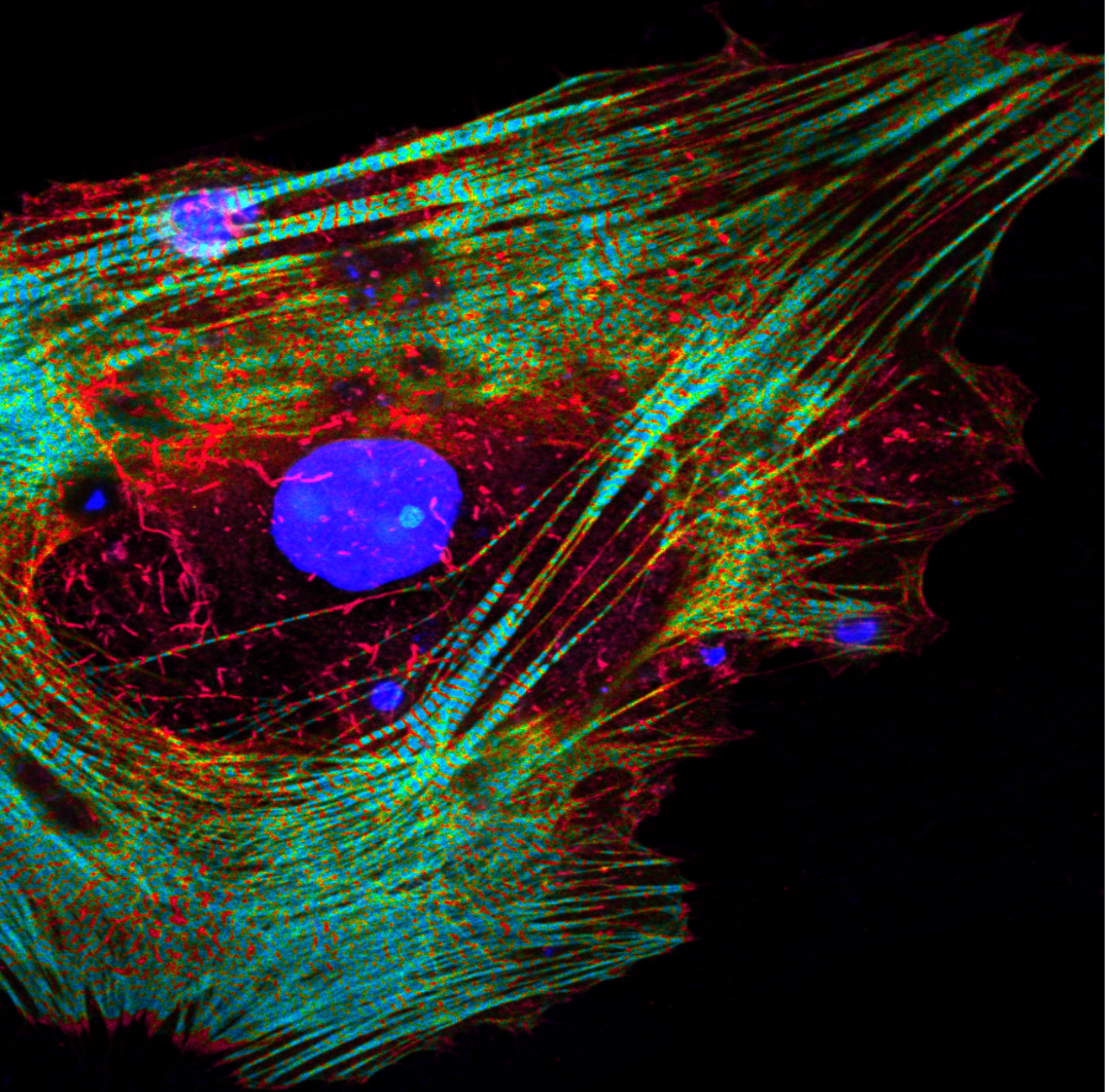


To repair the infarcted heart



Marijn C Peters

TO REPAIR THE INFARCTED HEART

Marijn C. Peters

To repair the infarcted heart

© Marijn C. Peters

ISBN: 978-94-6416-766-5

Printing: *Ridderprint* (www.ridderprint.nl)

Cover 'hypoxic iPSC cardiomyocyte sarcomeric troponin and actinin stain'

The research in this thesis was conducted at the University Medical Center Utrecht, Utrecht University and the Regenerative Medicine Center in Utrecht, The Netherlands and Stanford University, California, United States of America

The research described in this thesis was supported by a grant of the Dutch Heart Foundation (CVON REMAIN 2014B027).

Financial support by the Dutch Heart Foundation for the publication of this thesis is gratefully acknowledged. Additionally financial contribution for publication of this thesis by Guerbet Nederland B.V. and Angiocare is greatly appreciated.

Copyright © Marijn Peters 2021. All rights reserved. No parts of this thesis may be reproduced, stored in a retrieval system of any nature, or transmitted in any form or by any means, without prior written consent of the author. The copyright of the articles that have been published has been transferred to the respective journals.

TO REPAIR THE INFARCTED HEART

Het herstellen van een hartinfarct
(met een samenvatting in het Nederlands)

Proefschrift

ter verkrijging van de graad van doctor aan de Universiteit Utrecht
op gezag van de rector magnificus, prof.dr. H.R.B.M. Kummeling,
ingevolge het besluit van het college voor promoties
in het openbaar te verdedigen op

donderdag 25 november 2021
des middags te 2.15 uur

door

Maria Catharina Peters
geboren op 28 augustus 1993
te Nijmegen

Promotoren:

Prof. dr. J.P.G. Sluiter

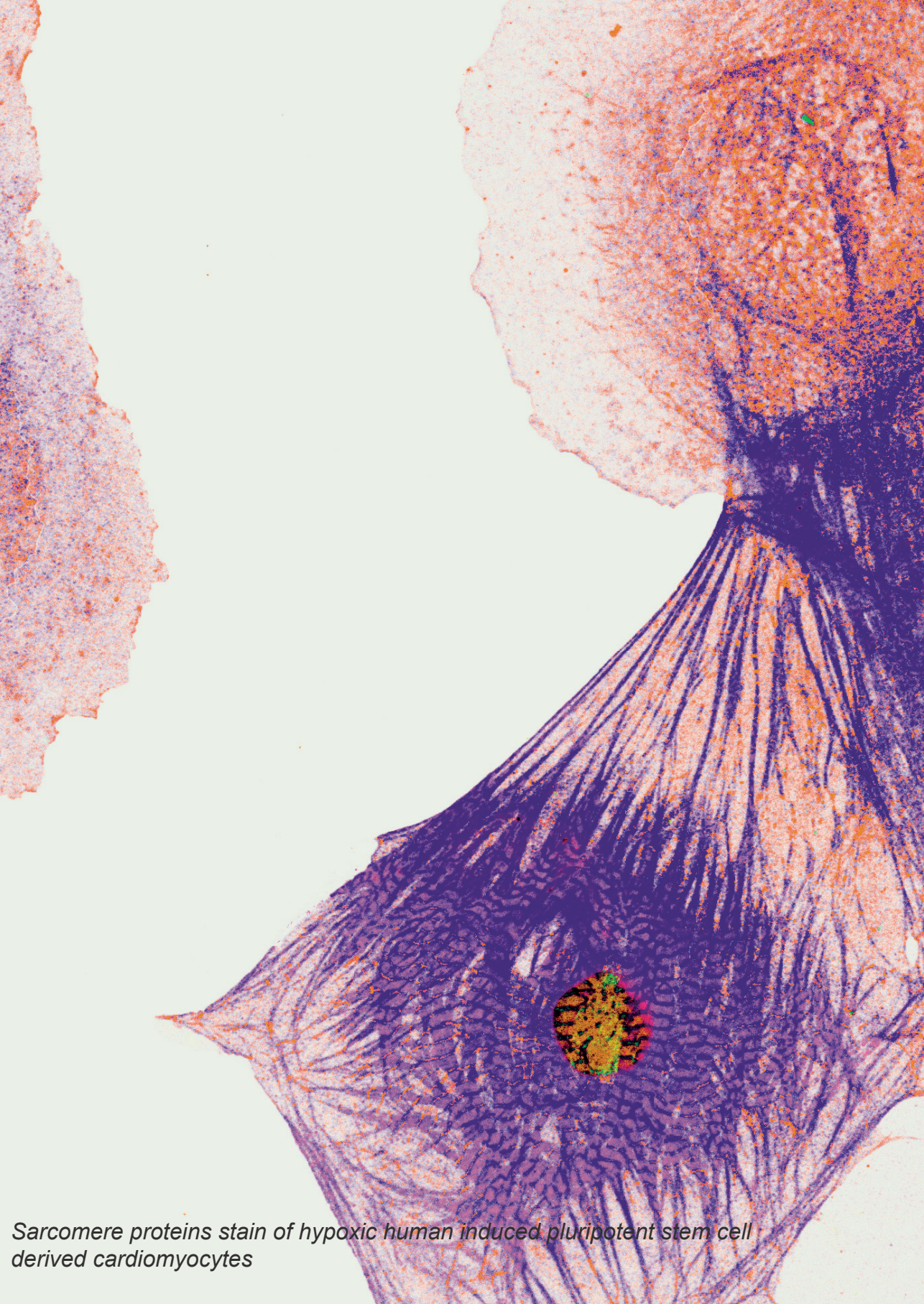
Prof. dr. S.A.J. Chamuleau

Copromotor:

Dr. K. Neef

CONTENTS

Chapter 1	Introduction	7
Part I Cardioprotection and limiting ischemia/reperfusion injury		
Chapter 2	A novel receptor-interacting protein-1 (RIP1) inhibitor (GSK'547) protects human cardiac cells from ischemia/reperfusion-triggered necroptotic cell death	25
Chapter 3	Metabolic maturation increases human iPSC-derived cardiomyocyte susceptibility to hypoxic injury	51
Part II Cardiomyocyte proliferation to regenerate the heart		
Chapter 4	Induction of cardiomyocyte proliferation, a new way forward for true myocardial regeneration?	73
Chapter 5	Follistatin-like 1 in cardiovascular disease and inflammation	85
Chapter 6	Follistatin-like 1 promotes proliferation of matured human hypoxic iPSC-cardiomyocytes and is secreted by human cardiac fibroblasts	113
Part III Local and sustained delivery of non-coding RNAs to repair the heart		
Chapter 7	Non-coding RNAs in endothelial cell signalling and hypoxia during cardiac regeneration	143
Chapter 8	A novel method to quantify retention of multi-functional supramolecular hydrogels for heart regenerative drug release	175
Part IV General discussion		
Chapter 9	Summary and general discussion	203
	Addendum	223
	Nederlandse samenvatting	
	Acknowledgements	
	List of publications	
	Curriculum vitae	



Sarcomere proteins stain of hypoxic human induced pluripotent stem cell derived cardiomyocytes

Chapter 1

HOW TO REPAIR THE INFARCTED HEART

Introduction and outline of this thesis

Marijn C. Peters^{1,2}

¹ Department of Cardiology, Laboratory of Experimental Cardiology, Division of Heart and Lungs, University Medical Centre Utrecht, The Netherlands.

² Regenerative Medicine Centre Utrecht, University Medical Centre Utrecht, The Netherlands.

INTRODUCTION

Cardiovascular diseases remain the leading cause of death worldwide with 17,9 million deaths annually¹. Primarily, ischemic heart disease (IHD) is a major cause of mortality with >9 million annual deaths. In IHD, occlusion of a coronary artery leads to decreased oxygen and nutrient supply to the contractile myocardium causing cardiomyocyte cell death. Occlusion is mainly caused by atherosclerosis: the progressive accumulation of lipids and inflammatory cells causing lesion development in the arterial wall². Current therapies for myocardial infarction include reperfusion therapy via percutaneous coronary intervention or coronary artery bypass grafts and pharmaceutical interventions to lower blood pressure¹. With 2 million reperfusion procedures per year in Europe alone to open the occluded vessel and re-oxygenate the ischemic myocardium, the acute mortality of IHD has decreased substantially^{3,4}. However, current therapies treat the symptoms of a myocardial infarction and relieve the increased pressure on the injured heart but do not repair the vast number of cardiomyocytes lost during an ischemic episode^{1,3-5}. When investigating the loss of cardiomyocytes following ischemic injury, a burst of cardiomyocyte cell death occurs over the first 6 to 24 hours of ischemia and reperfusion⁶. The rapid loss of cells causes an inflammatory response in which monocytes and neutrophils infiltrate the injured tissue to clear cellular debris and initiate the formation of granulation tissue^{6,7}. Fibroblasts proliferate in the infarct area to produce extracellular matrix and replace the injured cardiomyocytes with a fibrous network preventing loss of myocardial structure and acute cardiac rupture. The loss of cardiomyocytes as a result of ischemia drives ventricular remodeling to maintain cardiac output⁸, including hypertrophy of cardiomyocytes in the remote areas and scar maturation to maintain myocardial structural integrity. However, myocardial remodelling also gradually causes increased cardiac workload via ventricular dilatation, decreased oxygenation and myocardial stiffness capable of causing heart failure⁸. Studying the mechanisms underlying cardiomyocyte cell death after

ischemic injury and during the post-reperfusion phase could provide insights into how excessive cell death can be prevented.

MECHANISMS OF CELL DEATH IN THE INFARCTED HEART

The surge of cardiomyocyte cell death directly after the cessation of blood supply is followed by a more gradual increase in cell death in the borderzone of the infarct as a result of residual ischemia and a cumulative increase in apoptosis in the remote area in failing hearts⁶. The initial damage in patients after an ischemic insult cannot only be attributed to direct ischemia exposure due to the loss of oxygen and nutrient supply, but also to injury as a result of the applied reperfusion strategy, so called acute ischemia/reperfusion (I/R) injury. I/R injury can account for up to 50% of the infarct size as the sudden increase in oxygenation during reperfusion generates reactive oxygen species (ROS) that damage intracellular molecules and stimulate cell death pathways^{9,10}. Both apoptotic and necrotic cell death have been reported to play a part in ischemia and I/R related damage⁶. Apoptotic cell death is a regulated form of cell death characterised by nuclear fragmentation, cell shrinkage and vesicle formation to encapsule cellular content and enable phagocytosis by neighbouring cells without causing inflammation¹¹. In contrast to apoptotic cell death, necrotic cell death does lead to an inflammatory response as membrane integrity is lost and cellular content is released into the extracellular environment¹². Necrotic cell death was long believed to be unregulated but recent evidence shows distinct cellular pathways that initiate necrotic cell death, so called necroptosis, regulated by receptor-interacting protein kinases (RIP)¹³. Necroptosis has been studied in depth over the past century and it has been identified as a main mode of cell death mediating myocardial I/R injury^{14–17}.

TREATING ISCHEMIC HEART FAILURE

To improve the prognosis of patients with heart failure, approaches that address

the loss of cardiac tissue have become a main interest of cardiovascular research. Multiple reparative methods have been investigated: inhibiting cell death¹⁸, activating cell protective mechanisms¹⁹, stimulating angiogenesis²⁰ or stimulating the renewal of cardiomyocytes²¹. Stimulating cardiomyocyte renewal has been attempted using stem cells from different sources believed to be capable of differentiating into viable myocardium. Given the severity of heart failure, clinical trials using stem or progenitor cell therapies with autologous mononuclear bone marrow cells, myoblasts, and mesenchymal stem cells were quickly initiated with the aim to recover functional myocardium^{22–24}. Although cell therapies led to some functional recovery in heart failure patients, the long-term effects were limited and cell retention was low as cells were rapidly removed after injection^{25,26}. Furthermore, it was found injected cells do not exert their protective effect via differentiation into cardiomyocytes but via paracrine effects^{27–29}. The discovery of embryonic stem cells (ESC) first enabled the generation of vast numbers of human cardiomyocytes that could potentially repopulate the infarct area³⁰. However, using embryonic stem cells came with ethical concerns³¹. In recent years, other methods to stimulate renewal of cardiomyocytes are being tested in preclinical trials via the implantation of cardiomyocytes differentiated from human induced pluripotent stem cells (hiPSC). Although this method provides promising results, the connection of implanted cells with the native myocardium and prevention of arrhythmias remains challenging³².

Next to the exogenous supplementation of cells to renew the myocardium, activation of the cardiomyocyte cell cycle of autologous cells has received increased interest. Assessment of nuclear bomb test derived ¹⁴C in genomic DNA of human hearts indicated that human cardiomyocytes maintained a proliferative capacity, even though only at a degree of <1%³³. The additional finding that the zebrafish heart is capable of complete regeneration after cardiac injury via proliferation of pre-existing cardiomyocytes emphasized the feasibility of this approach^{34–36}.

MECHANISMS OF CARDIAC REGENERATION

This newly discovered innate reparative capacity of zebrafish hearts led to questions on whether human adult cardiomyocytes were terminally differentiated or could be stimulated to proliferate. To answer the question whether the regenerative capacity of the zebrafish heart is evolutionary conserved, the response to cardiac injury in mammalian neonatal hearts was assessed. This showed that murine neonatal hearts could completely repair itself up to 7 days after birth through the proliferation of pre-existing cardiomyocytes³⁵. Similarly in neonatal and zebrafish hearts, proliferation of cardiomyocytes following injury was characterised by hypoxia signaling^{34,37}, fast revascularisation^{38,39} and regulation of ECM deposition to prevent scar maturation^{40,41}. At 7 days, an increase in extracellular matrix stiffness⁴², altered DNA methylation⁴², and the increased expression of Meis1 and cofactor Hoxb13 was found to induce cardiomyocyte cell cycle arrest and thereby to prevent full cardiac repair post-injury^{43,44}. Furthermore, the postnatal shift in the cardiomyocyte energy metabolism from anaerobic glycolysis to oxidative phosphorylation of fatty acids to increase energy efficiency also increased the generation of mitochondrial ROS that stimulate cardiomyocyte cell cycle arrest^{45,46}. Analysis of cardiomyocyte proliferation in human hearts was in line with these findings as cardiomyocyte proliferation was found to contribute to heart growth in infants and similarly as in the murine heart, cardiomyocyte proliferation transiently decreased to very low levels by 20 years of age⁴⁷. However, as the regenerative response of cardiomyocyte proliferation following cardiac injury was found to be evolutionary conserved from zebrafish to young human hearts, diseases might be curable by stimulating this innate regenerative mechanism. Learning from this natural phenomenon and stimulating the innate reparative capacity of the heart by targeting cardiomyocyte proliferation has become a key focus in the field⁴⁸⁻⁵².

MODELLING THE HUMAN HEART

Exploring the mechanisms that control cardiomyocyte cell cycle arrest or enable cardiomyocyte proliferation can provide scope to regenerate the human heart. However, differences between animal hearts and the human heart are a major reason why successful regenerative therapies in preclinical studies have failed in their clinical translation⁵³⁻⁵⁹. To start, zebrafish and neonatal hearts contain approximately one-hundred-thousand cardiomyocytes while for human hearts an ischemic episode alone can lead to the loss of billions of cardiomyocytes^{59,60}. Therefore, repairing this vast number of cardiomyocytes lost during an ischemic episode requires a more extensive proliferative response than a small animal heart requires. Furthermore, the electrophysiology and beating rate of murine cardiomyocytes (350 beats/minute) is dramatically different than that of human cardiomyocytes (70 beats/minute)^{59,61,62}. Hearts of large animals (e.g. porcine, canine) have a more similar physiology of its coronary circulation and size but differences are still present in anatomy and conductivity⁶³⁻⁶⁵. Furthermore, spontaneous long-term development of atherosclerotic lesions, as found in humans as a prevalent cause of IHD, rarely occurs in animals. In pigs, a commonly used large animal model for cardiovascular diseases, only modelling of early atherosclerotic lesions is possible with a hyperlipidaemic diet⁶⁶. Moreover, differences in gene expression and enzyme activity between animal and human cells have been reported that could affect drug responsiveness^{56,67}.

These differences emphasize the strong need for the development of human models to assess mechanisms of cardiac regeneration before advancing to clinical trials. The discovery of hiPSC technology, in which differentiated human cells (e.g. skin fibroblasts) could be reprogrammed into multipotent stem cells and subsequently be differentiated into another differentiated cell type, enabled the derivation of large numbers of human cells and *in vitro* modelling of human diseases^{68,69}. Furthermore, this technology enabled the generation of patient-specific disease modelling to study pathophysiology mechanisms as found in patients with specific

gene mutations. For cardiovascular diseases, hiPSC-derived cardiomyocytes have been generated for many cardiomyopathies^{70,71}. Furthermore, studies have also attempted to model IHD using hiPSC-derived cardiomyocytes⁷²⁻⁷⁴. Even though the field of hiPSC technology to model human cardiovascular diseases is very promising, the immaturity of the generated hiPSC-cardiomyocytes remains an issue for true representation of adult human cardiomyocytes^{75,76}. The hiPSC-derived cardiomyocytes were found to be in a foetal-like morphology, electrophysiology, gene expression profile and metabolism⁷⁷⁻⁷⁹. To increase the maturity of hiPSC-cardiomyocytes, multiple studies focused on improving physiological and metabolic maturation profiles^{80,81}. Combining these improved hiPSC-cardiomyocytes with ischemic disease modelling could enable the identification and development of reparative therapies that can be translated into patients.

RNA THERAPY

In translating preclinical research, finding the right clinical target in the complex process of cardiomyocyte proliferation remains challenging as cellular behaviour is under tight regulation by multiple pathways. A powerful new level of regulation, also present in the post-ischemic processes in the heart, are families of non-coding RNAs^{82,83}. Unlike messenger RNA that is translated into protein to exert its biological function, non-coding RNAs are not translated but function as RNA directly by regulating transcription, translation and epigenetic gene expression^{84,85}. Non-coding RNAs can be subdivided into several classes, including long non-coding RNAs, circular RNAs and microRNAs (miRNAs). One non-coding RNA can target multiple genes and regulate multiple processes, making them interesting powerful tools to alter the complex mechanism of cardiac repair. Targeting non-coding RNAs has recently emerged as a promising therapeutic approach due to their regulatory function in cardiac disease. Non-coding RNAs have been linked to processes of cardiac regeneration in the zebrafish and neonatal heart^{86,87}, whereas a group of miRNAs

targets YAP-Hippo signalling and thereby modulates the actin network to mediate cardiomyocyte proliferation^{49,88}. miRNAs that positively regulate cardiomyocyte proliferation were found to be decreased in expression after birth⁸⁵. Furthermore, while some miRNAs could stimulate cardiomyocyte proliferation, modulation of the miRNA target gene was not always sufficient to produce the same cellular outcome due to complex transcriptional regulation⁸⁵. Since miRNA function appears to be a cell specific phenomenon, optimizing cell-specific delivery of miRNAs or miRNA inhibitors could be a better strategy to promote cardiomyocyte proliferation.

DELIVERY OF REGENERATIVE THERAPIES

One of the main challenges for regenerative therapies or RNA therapy is controlled delivery and RNA stability. Previous studies have attempted to inject large cells into the heart but discovered an immediate flush-out via the dense microvascular venous network of the heart²⁶. Furthermore, retaining RNA in the inflammatory ischemic microenvironment to effectively modulate the behaviour of cells is equally challenging due to the presence of ribonucleases that degrade free RNA⁸⁹. To increase the retention of therapeutics into the heart, injectable slow-release hydrogels have been developed. Injectable hydrogels are liquid before injection and form cross-link bonds after injection to a gel-phase to retain injected factors in a protected water-rich environment, similar to human tissue⁹⁰. Gel cross-linking can be mediated via different means and is depending on the chemistry of the gel, e.g. UV light⁹¹, shear stress^{92,93}, temperature⁹⁴ or pH changes⁹⁵. Combining the hydrogel with a cholesterol-modified miRNA could enable uptake of the miRNA over the plasma membrane of the target cell via cell fusion or endosomal internalization through the hydrophobic nature of cholesterol^{93,96}. Recent studies reporting delivery of cholesterol-modified miRNA or insulin-growth factor (IGF) using shear-thinning or pH-responsive injectable hydrogels, respectively, could improve the functional

benefit of the therapy in a porcine animal model^{93,97}. Interestingly, hydrogels could be fine-tuned and would be able to release the drug over a period of weeks to provide a sustained regenerative signal rather than a single pulse of drug release at the moment of injection⁹⁸. A shear-thinning mesoporous hydrogel containing silica nanoparticles was found to enable the delivery of an angiogenic miRNA in a pig infarct model and limit infarct size⁹⁹. Despite the extensive research into the development of injectable hydrogels^{90,100–102}, the readouts are often focussed on functional effect of hydrogel-mediated delivery instead of the degree of hydrogel retention at the target site. This leaves the question unanswered whether hydrogels are better retained in the beating heart or whether there is accumulation of injected hydrogel at remote locations.

THESIS OUTLINE

Many advances have been made in moving towards repairing the infarcted ischemic heart, but clinical translation remains challenging. It is unlikely that the solution of repairing the heart lies in a single factor targeting a single process. The main objective of the research in this thesis is to explore methods to protect the heart from ischemic and I/R injury and stimulate the innate reparative capacity of the heart to renew damaged myocardium. To provide scope to achieve these complex tasks, we subdivided the research into answering three consecutive questions:

1. How can we protect human cardiac cells from I/R injury?
2. How can we stimulate human cardiomyocytes to generate new functional cardiomyocytes to repair injured tissue?
3. If we have a protective and reparative therapy available, how can we deliver it safely and effectively to the right location in the heart?

Chapter 2 focusses on the first step towards cardiac repair: limiting the damage inflicted during an ischemic event and reperfusion, the current golden standard

of therapy. In this chapter we introduce a novel therapeutic factor that efficiently targets necroptotic cell death, a major form of cell death determining I/R injury.

In **Chapter 3**, we develop a hiPSC-cardiomyocyte based platform to model human IHD. To do this, we assessed the role of metabolic maturation on susceptibility of hiPSC-cardiomyocytes to hypoxic damage.

Chapter 4 discusses the potential of stimulating cardiomyocyte proliferation to regenerate the heart by focussing on the role of miRNA-128 in cardiac regeneration.

Chapter 5 introduces the glycoprotein Follistatin-like 1 as a potential therapeutic tool to prevent cardiomyocyte cell death, increase vascularisation in the infarcted area and stimulate cardiomyocyte renewal.

In **Chapter 6**, we used our model developed in chapter 3 to test the potential of Follistatin-like 1 as a therapeutic factor to treat human IHD.

In **Chapter 7**, we discuss the role of non-coding RNAs in cardiac regeneration and vascularisation and how to provide localized and sustained delivery of non-coding RNAs to the infarcted region.

Chapter 8 describes a new method we developed to assess the retention of injected hydrogels after cardiac injection using real-time tracking with radioactively labelled hydrogel subunits.

Chapter 9 provides a summary and general discussion of the work presented in this thesis and discusses future directions.

REFERENCES

1. Virani SS, Alonso A, Benjamin EJ, et al. Heart Disease and Stroke Statistics—2020 Update: A Report from the American Heart Association.; 2020.
2. Libby P, Ridker PM, Maseri A. Inflammation and atherosclerosis. *Circulation*. 2002;105(9):1135-1143.
3. Mozaffarian D, Benjamin EJ, Go AS, et al. Executive summary: Heart disease and stroke statistics-2016 update: A Report from the American Heart Association. *Circulation*. 2016;133(4):447-454.
4. Townsend N, Wilson L, Bhatnagar P, Wickramasinghe K, Rayner M, Nichols M. Cardiovascular disease in Europe: Epidemiological update 2016. *Eur Heart J*. 2016;37(42):3232-3245.
5. Mozaffarian D, Benjamin EJ, Go AS, et al. Heart Disease and Stroke Statistics — 2016 Update A Report From the American Heart Association. *AHA Stat Updat*. 2016:38-360.
6. Konstantinidis K, Whelan RS, Kitsis RN. Mechanisms of cell death in heart disease. *Arterioscler Thromb Vasc Biol*. 2012;32(7):1552-1562.
7. Van Der Laan AM, Nahrendorf M, Piek JJ. Healing and adverse remodelling after acute myocardial infarction: Role of the cellular immune response. *Heart*. 2012;98(18):1384-1390.
8. Cokkinos D V., Pantos C. Myocardial remodeling, an overview. *Heart Fail Rev*. 2011;16(1):1-4.
9. Yellon DM, Hausenloy DJ. Myocardial reperfusion injury. *N Engl J Med*. 2007;357:1121-1135.
10. Ferrari R, Geconi C, Curello S, et al. Role of oxygen free radicals in ischemic and reperfused myocardium. *Am J Clin Nutr*. 1991;53
11. Dorn GW. Apoptotic and non-apoptotic programmed cardiomyocyte death in ventricular remodelling. *Cardiovasc Res*. 2009;81(3):465-473.
12. Khoury MK, Gupta K, Franco SR, Liu B. Necroptosis in the Pathophysiology of Disease. *Am J Pathol*. 2020;190(2):272-285.
13. Zhe-wei S, Li-sha G, Yue-chun L. The Role of Necroptosis in Cardiovascular Disease. *Front Pharmacol*. 2018;721(9):1-9.
14. Szobi A, Gonçalvesová E, Varga Z, et al. Analysis of necroptotic proteins in failing human hearts. *J Transl Med*. 2017;15(1):1-7.
15. Linkermann A, Hackl MJ, Kunzendorf U. Necroptosis in Immunity and Ischemia-Reperfusion Injury. *Am J Transplant*. 2013;1:2797-2804.
16. Ying L, Benjanuwattra J, Chattipakorn SC, Chattipakorn N. The role of RIPK3-regulated cell death pathways and necroptosis in the pathogenesis of cardiac

- ischaemia-reperfusion injury. *Acta Physiol.* 2021;231(2).
17. Zhang T, Zhang Y, Cui M, et al. CaMKII is a RIP3 substrate mediating ischemia- and oxidative stress – induced myocardial necroptosis. *Nat Med.* 2016;22(2).
 18. Oerlemans MIFJ, Liu J, Arslan F. Inhibition of RIP1-dependent necrosis prevents adverse cardiac remodeling after myocardial ischemia – reperfusion in vivo. *Basic Res Cardiol.* 2012; 107 (4).
 19. Oh H, Wang SC, Prahash A, et al. Telomere attrition and Chk2 activation in human heart failure. *Proc Natl Acad Sci.* 2003;100(9):5378-5383.
 20. Tirziu D, Simons M. Angiogenesis in the human heart: Gene and cell therapy. *Angiogenesis.* 2005;8(3):241-251.
 21. Dimmeler S, Zeiher AM, Schneider MD. Unchain my heart: The scientific foundations of cardiac repair. *J Clin Invest.* 2005;115(3):572-583.
 22. Menasché P, Hagège AA, Scorsin M, et al. Myoblast transplantation for heart failure. *Lancet.* 2001;357(9252):279-280.
 23. Strauer BE, Brehm M, Zeus T, et al. Repair of infarcted myocardium by autologous intracoronary mononuclear bone marrow cell transplantation in humans. *Circulation.* 2002;106(15):1913-1918.
 24. Assmus B, Schächinger V, Teupe C, et al. Transplantation of progenitor cells and regeneration enhancement in acute myocardial infarction (TOPCARE-AMI). *Circulation.* 2002;106(24):3009-3017.
 25. Hofmann M, Wollert KC, Meyer GP, et al. Monitoring of bone marrow cell homing into the infarcted human myocardium. *Circulation.* 2005;111(17):2198-2202.
 26. Feyen DAM, Van Den Hoogen P, Van Laake LW, et al. Intramyocardial stem cell injection: Go(ne) with the flow. *Eur Heart J.* 2017;38(3):184-186.
 27. Murry CE, Soonpaa MH, Reinecke H, et al. Haematopoietic stem cells do not transdifferentiate into cardiac myocytes in myocardial infarcts. *Nature.* 2004;428(6983):664-668.
 28. Balsam LB, Wagers AJ, Christensen JL, Kofidis T, Weissmann IL, Robbins RC. Haematopoietic stem cells adopt mature haematopoietic fates in ischaemic myocardium. *Nature.* 2004;428(6983):668-673.
 29. Fazel S, Cimini M, Chen L, et al. Cardioprotective c-kit+ cells are from the bone marrow and regulate the myocardial balance of angiogenic cytokines. *J Clin Invest.* 2006;116(7):1865-1877.
 30. Evans MJ, Kaufman MH. Establishment in culture of pluripotential cells from mouse embryos. *Nature.*
 31. McLaren A. Ethical and social considerations of stem cell research. *Nature.* 2001;414(6859):129-131.
 32. Shiba Y, Gomibuchi T, Seto T, et al. Allogeneic transplantation of iPS cell-derived

- cardiomyocytes regenerates primate hearts. *Nature*. 2016;538(7625):388-391.
33. Bergmann O, Bhardwaj RD, Bernard S, et al. Evidence for Cardiomyocyte Renewal in Humans. *Science*. 2009;324:98-102.
 34. Jopling C, Suñé G, Faucherre A, Fabregat C, Izpisua Belmonte JC. Hypoxia induces myocardial regeneration in zebrafish. *Circulation*. 2012;126(25):3017-3027.
 35. Porrello ER, Mahmoud AI, Simpson E, et al. Transient Regenerative Potential of the Neonatal Mouse Heart. *Science*. 2011;331:1078-1081.
 36. Jopling C, Sleep E, Raya M, Martí M, Raya A, Belmonte JCI. Zebrafish heart regeneration occurs by cardiomyocyte dedifferentiation and proliferation. *Nature*. 2010;464(7288):606-609.
 37. Kimura W, Xiao F, Canseco DC, et al. Hypoxia fate mapping identifies cycling cardiomyocytes in the adult heart. *Nature*. 2015;523(7559):226-230.
 38. Juni RP, Abreu RC, Diseases C, Sciences L, Surgery C, Martins C. Regulation of microvascularization in heart failure - The close relationship between endothelial cells, non-coding RNAs, and exosomes. *Non-coding RNA Res*. 2017;2(1):45-55.
 39. Smart N. Prospects for Improving Neovascularisation of the Ischaemic Heart: Lessons from Development. *Microcirculation*. 2016;44(0).
 40. Münch J, Grivas D, González-Rajal Á, Torregrosa-Carrión R, de la Pompa JL. Notch signalling restricts inflammation and *Serpine1* expression in the dynamic endocardium of the regenerating zebrafish heart. *Dev*. 2017;144(8):1425-1440.
 41. Sánchez-Iranzo H, Galardi-Castilla M, Sanz-Morejón A, et al. Transient fibrosis resolves via fibroblast inactivation in the regenerating zebrafish heart. *Proc Natl Acad Sci*. 2018;115(16):4188-4193.
 42. Notari M, Ventura-Rubio A, Bedford-Guaus SJ, et al. The local microenvironment limits the regenerative potential of the mouse neonatal heart. *Sci Adv*. 2018;4(5).
 43. Mahmoud AI, Kocabas F, Muralidhar SA, et al. *Meis1* regulates postnatal cardiomyocyte cell cycle arrest. *Nature*. 2013;497(7448):249-253.
 44. Nguyen NUN, Canseco DC, Xiao F, et al. A calcineurin–*Hoxb13* axis regulates growth mode of mammalian cardiomyocytes. *Nature*. 2020;582(7811):271-276.
 45. Puente BN, Kimura W, Muralidhar SA, et al. The oxygen-rich postnatal environment induces cardiomyocyte cell-cycle arrest through DNA damage response. *Cell*. 2014;157(3):565-579.
 46. Cardoso Alisson C., Lam NT, Savla JJ, et al. Mitochondrial Substrate Utilization Regulates Cardiomyocyte Cell Cycle Progression. *Nat Metab*. 2020;2(2):167-178.
 47. Mollova M, Bersell K, Walsh S, et al. Cardiomyocyte proliferation contributes to heart growth in young humans. *Proc Natl Acad Sci U S A*. 2013;110(4):1446-1451.
 48. D'Uva G, Aharonov A, Lauriola M, et al. ERBB2 triggers mammalian heart regeneration by promoting cardiomyocyte dedifferentiation and proliferation. *Nat Cell*

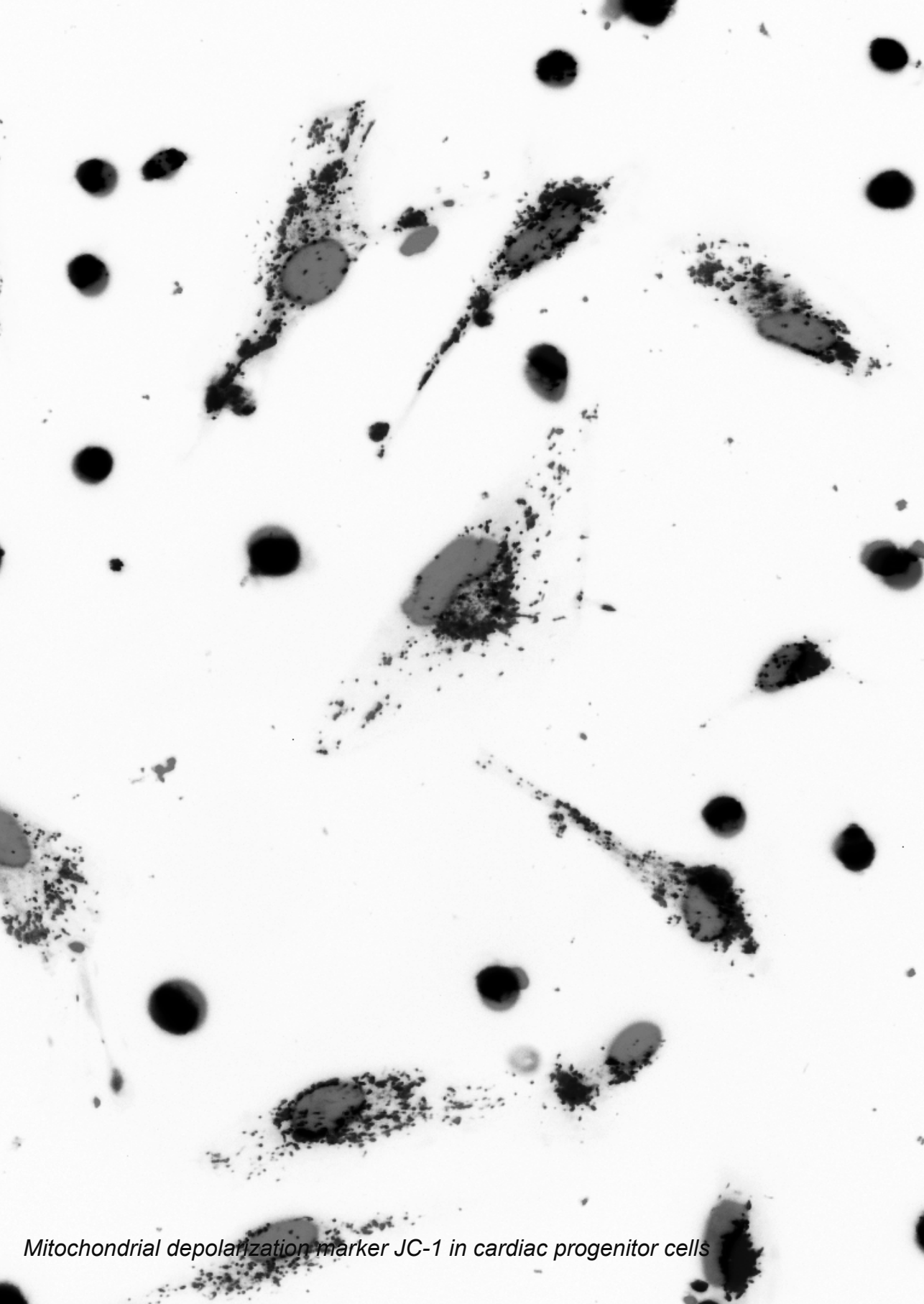
Biol. 2015;17(5):627-638.

49. Diez-Cuñado M, Wei K, Bushway PJ, et al. miRNAs that Induce Human Cardiomyocyte Proliferation Converge on the Hippo Pathway. *Cell Rep.* 2018;23(7):2168-2174.
50. Wei K, Serpooshan V, Hurtado C, et al. Epicardial FSTL1 reconstitution
51. Lei Z, Peters M, Sluijter JPG. Induction of cardiomyocyte proliferation, a new way forward for true myocardial regeneration? *Non-coding RNA Investig.* 2018;2(7):46-46.
52. Nguyen PD, Bakker DEM De, Bakkers J. Cardiac regenerative capacity : an evolutionary afterthought ? *Cell Mol Life Sci.* 2021;(Mi).
53. Ge Z, Lal S, Le TYL, dos Remedios C, Chong JJH. Cardiac stem cells: translation to human studies. *Biophys Rev.* 2015;7(1):127-139.
54. Rehman J. Bone marrow tinctures for cardiovascular disease: Lost in translation. *Circulation.* 2013;127(19):1935-1937.
55. Kooij V, Venkatraman V, Tra J, et al. Sizing up models of heart failure: Proteomics from flies to humans. *Proteomics - Clin Appl.* 2014;8:653-664.
56. Siller R, Greenhough S, Park I-H, J. Sullivan G. Modelling Human Disease with Pluripotent Stem Cells. *Curr Gene Ther.* 2013;13(2):99-110.
57. Rog-Zielinska EA, Kong CHT, Zgierski-Johnston CM, et al. Species differences in the morphology of transverse tubule openings in cardiomyocytes. *Europace.* 2018;20:120-124.
58. Naqvi N, Li M, Calvert JW, et al. A proliferative burst during preadolescence establishes the final cardiomyocyte number. *Cell.* 2014;157(4):795-807.
59. Sadek H, Olson EN. Toward the Goal of Human Heart Regeneration. *Cell Stem Cell.* 2020;26(1):7-16.
60. Milani-Nejad N, Janssen PML. Small and Large Animal Models in Cardiac Contraction Research: Advantages and Disadvantages. *Pharmacol Ther.* 2014;141(3):1-5.
61. Hamlin RL, Altschuld RA. Extrapolation from mouse to man. *Circ Cardiovasc Imaging.* 2011;4(1):2-4.
62. Kaese S, Verheule S. Cardiac electrophysiology in mice: A matter of size. *Front Physiol.* 2012;3:1-19.
63. Bhagat K. Endothelial function and myocardial infarction. 1998;39:312-317.
64. Lelovas PP, Kostomitsopoulos NG, Xanthos TT. A comparative anatomic and physiologic overview of the porcine heart. *J Am Assoc Lab Anim Sci.* 2014;53(5):432-438.
65. Crick SJ, Sheppard MN, Ho SY, Gebstein L, Anderson RH. Anatomy of the pig heart:

- comparisons with normal human cardiac structure. *J Anat.* 1998;193(1):105-119.
66. Artinger S, Deiner C, Loddenkemper C, Schwimmbeck PL, Schultheiss HP, Pels K. Complex porcine model of atherosclerosis: Induction of early coronary lesions after long-term hyperlipidemia without sustained hyperglycemia. *Can J Cardiol.* 2009;25(4):109-114.
67. Kobayashi Y, Fukami T, Nakajima A, Watanabe A, Nakajima M. Species Differences in Tissue Distribution and Enzyme Activities of Arylacetamide Deacetylase in Human, Rat, and Mouse. *Drug Metab Dispos.* 2012;40(4):671-679.
68. Takahashi K, Yamanaka S. Induction of Pluripotent Stem Cells from Mouse Embryonic and Adult Fibroblast Cultures by Defined Factors. *Cell.* 2006;126(4):663-676.
69. Shi Y, Inoue H, Wu JC, Yamanaka S. Induced pluripotent stem cell technology: a decade of progress. *Nat Rev Drug Discov.* 2017;16(2):115-130.
70. Ceholski DK, Turnbull IC, Kong C, et al. Functional and Transcriptomic Insights into Pathogenesis of R9C Phospholamban Mutation using Human Induced Pluripotent Stem Cell-Derived Cardiomyocytes. *J Mol Cell Cardiol.* 2018;119:147-154.
71. van Mil A, Balk GM, Neef K, et al. Modelling inherited cardiac disease using human induced pluripotent stem cell-derived cardiomyocytes: Progress, pitfalls, and potential. *Cardiovasc Res.* 2018;114(14):1828-1842.
72. Häkli M, Kreutzer J, Mäki AJ, et al. Human induced pluripotent stem cell-based platform for modeling cardiac ischemia. *Sci Rep.* 2021;11(1):1-13.
73. Sebastião MJ, Gomes-Alves P, Reis I, et al. Bioreactor-based 3D human myocardial ischemia/reperfusion in vitro model: a novel tool to unveil key paracrine factors upon acute myocardial infarction. *Transl Res.* 2020;215:57-74.
74. Wei H, Wang C, Guo R, Takahashi K, Naruse K. Development of a model of ischemic heart disease using cardiomyocytes differentiated from human induced pluripotent stem cells. *Biochem Biophys Res Commun.* 2019;520(3):600-605.
75. Koivumäki JT, Naumenko N, Tuomainen T, et al. Structural immaturity of human iPSC-derived cardiomyocytes: In silico investigation of effects on function and disease modeling. *Front Physiol.* 2018;9:1-17.
76. Goversen B, van der Heyden MAG, van Veen TAB, de Boer TP. The immature electrophysiological phenotype of iPSC-CMs still hampers in vitro drug screening: Special focus on IK1. *Pharmacol Ther.* 2018;183:127-136.
77. Van Den Berg CW, Okawa S, Chuva De Sousa Lopes SM, et al. Transcriptome of human foetal heart compared with cardiomyocytes from pluripotent stem cells. *Dev.* 2015;142(18):3231-3238.
78. Deicher A, Seeger T. Human Induced Pluripotent Stem Cells as a Disease Model System for Heart Failure. *Curr Heart Fail Rep.* 2021;18(1):1-11.
79. Sacchetto C, Vitiello L, de Windt LJ, Rampazzo A, Calore M. Modeling

- cardiovascular diseases with hipsc-derived cardiomyocytes in 2d and 3d cultures. *Int J Mol Sci.* 2020;21(9).
80. Feyen DAM, McKeithan WL, Bruyneel AAN, et al. Metabolic Maturation Media Improve Physiological Function of Human iPSC-Derived Cardiomyocytes. *Cell Rep.* 2020;32(3).
 81. Horikoshi Y, Yan Y, Terashvili M, et al. Fatty acid-treated induced pluripotent stem cell-derived human cardiomyocytes exhibit adult cardiomyocyte-like energy metabolism phenotypes. *Cells.* 2019;8(1095):1-21.
 82. Archer K, Broskova Z, Bayoumi AS, et al. Long non-coding RNAs as master regulators in cardiovascular diseases. *Int J Mol Sci.* 2015;16(10):23651-23667.
 83. Tao L, Bei Y, Zhou Y, Xiao J, Li X. Non-coding RNAs in cardiac regeneration. *Oncotarget.* 2015;6(40):42613-42622.
 84. Greco CM, Condorelli G. Epigenetic modifications and noncoding RNAs in cardiac hypertrophy and failure. *Nat Rev Cardiol.* 2015;12(8):488-497.
 85. Abbas N, Perbellini F, Thum T. Non-coding RNAs: emerging players in cardiomyocyte proliferation and cardiac regeneration. *Basic Res Cardiol.* 2020;115(5):1-20.
 86. Yin VP, Lepilina A, Smith A, Poss KD. Regulation of zebrafish heart regeneration by miR-133. *Dev Biol.* 2012;365(2):319-327.
 87. Adamowicz M, Morgan CC, Haubner BJ, et al. Functionally Conserved Noncoding Regulators of Cardiomyocyte Proliferation and Regeneration in Mouse and Human. *Circ Genomic Precis Med.* 2018;11(2):1-13.
 88. Eulalio A, Mano M, Ferro MD, et al. Functional screening identifies miRNAs inducing cardiac regeneration. *Nature.* 2012;492(7429):376-381.
 89. Jo J ichiro, Gao JQ, Tabata Y. Biomaterial-based delivery systems of nucleic acid for regenerative research and regenerative therapy. *Regen Ther.* 2019;11:123-
 90. Hasan A, Khattab A, Islam MA, et al. Injectable Hydrogels for Cardiac Tissue Repair after Myocardial Infarction. *Adv Sci.* 2015;2(11):1-18.
 91. Wang G, Cao X, Dong H, Zeng L, Yu C, Chen X. A hyaluronic acid based injectable hydrogel formed via photo-crosslinking reaction and thermal-induced diels-alder reaction for cartilage tissue engineering. *Polymers (Basel).* 2018;10(9).
 92. Uman S, Dhand A, Burdick JA. Recent advances in shear-thinning and self-healing hydrogels for biomedical applications. *J Appl Polym Sci.* 2020;137(25):1-20.
 93. Wang LL, Liu Y, Chung JJ, et al. Local and sustained miRNA delivery from an injectable hydrogel promotes cardiomyocyte proliferation and functional regeneration after ischemic injury. *Nat Biomed Eng.* 2018;1:983-992.
 94. Lu WN, Lü SH, Wang H Bin, et al. Functional improvement of infarcted heart by co-injection of embryonic stem cells with temperature-responsive chitosan hydrogel.

- Tissue Eng - Part A. 2009;15(6):1437-1447.
95. Bastings MMC, Koudstaal S, Kieltyka RE, et al. A fast pH-switchable and self-healing supramolecular hydrogel carrier for guided, local catheter injection in the infarcted myocardium. *Adv Healthc Mater.* 2014;3(1):70-78.
 96. Schroeder A, Levins CG, Cortez C, Langer R, Anderson DG. Lipid-based nanotherapeutics for siRNA delivery. *J Intern Med.* 2010;267(1):9-21.
 97. Koudstaal S, Bastings MMC, Feyen DAM, et al. Sustained delivery of insulin-like growth factor-1/hepatocyte growth factor stimulates endogenous cardiac repair in the chronic infarcted pig heart. *J Cardiovasc Transl Res.* 2014;7(2):232-241.
 98. Garbern JC, Minami E, Stayton PS, Murry CE. Delivery of basic fibroblast growth factor with a pH-responsive, injectable hydrogel to improve angiogenesis in infarcted myocardium. *Biomaterials.* 2011;32(9):2407-2416.
 99. Li Y, Chen X, Jin R, et al. Injectable hydrogel with MSNs/microRNA-21-5p delivery enables both immunomodification and enhanced angiogenesis for myocardial infarction therapy in pigs. *Sci Adv.* 2021;7(9):1-20.
 100. Roche ET, Hastings CL, Lewin SA, et al. Comparison of biomaterial delivery vehicles for improving acute retention of stem cells in the infarcted heart. *Biomaterials.* 2014;35(25):6850-6858.
 101. Bakker MH, Tseng CCS, Keizer HM, et al. MRI Visualization of Injectable Ureidopyrimidinone Hydrogelators by Supramolecular Contrast Agent Labeling. *Adv Healthc Mater.* 2018;7(11):1-8.
 102. Pape ACH, Bakker MH, Tseng CCS, et al. An injectable and drug-loaded supramolecular hydrogel for local catheter injection into the pig heart. *J Vis Exp.* 2015;2015(100):1-8.



Mitochondrial depolarization marker JC-1 in cardiac progenitor cells

Chapter 2

A NOVEL RECEPTOR-INTERACTING PROTEIN-1 (RIP1) INHIBITOR (GSK'547) PROTECTS HUMAN CARDIAC CELLS FROM ISCHEMIA/REPERFUSION-TRIGGERED NECROPTOTIC CELL DEATH

in preparation

Marijn M.C. Peters^{1,2*}, Klaus Neef^{1,2}, Angela Markovska^{1,2,3}, Marish I.F.J. Oerlemans^{1,2}, Steven A.J. Chamuleau^{3, 4}, Joost P.G. Sluijter^{1,2}

¹ Department of Cardiology, Laboratory of Experimental Cardiology, Division of Heart and Lungs, University Medical Centre Utrecht, The Netherlands.

² Regenerative Medicine Centre Utrecht, University Medical Centre Utrecht, The Netherlands.

³ Utrecht University, Utrecht, The Netherlands

⁴ Amsterdam UMC Heart Center, Department of Cardiology, Amsterdam, The Netherlands

ABSTRACT

Coronary reperfusion therapy to treat myocardial infarction can lead to a second wave of cardiomyocyte cell death through the release of reactive oxygen species (ROS) known as myocardial ischemia-reperfusion injury (I/R). RIP1 phosphorylation and the execution of necroptosis is a major pathway activated during myocardial I/R injury, which was previously inhibited by the use of the non-selective inhibitor necrostatin-1 (Nec-1). We therefore studied the potential of a novel and specific RIP1 kinase inhibitor, called GSK'547, to prevent myocardial injury in a human *in vitro* model for I/R. In order to simulate I/R injury *in vitro*, human cardiac progenitor cells (hCPCs) were stimulated with hydrogen peroxide (H_2O_2) in the absence or presence of RIP1 inhibitor GSK'547. Upon H_2O_2 stimulation, a dose-dependent increase in DAPI⁺ (necroptotic) cell population and not the AnV⁺ DAPI⁻ (apoptotic) population was observed, as shown by flow cytometric analysis. Specific prevention of apoptosis did not save hCPCs from oxidative stress-induced cell death. Treatment with physiologically low concentrations of GSK'547 was shown to decrease necroptotic cell death and protected hCPCs from H_2O_2 -induced damage to a similar extent as treatment with 1000-fold higher concentrations of the previously reported inhibitor Nec1. While necrosome component mRNA levels remained similar, treatment with GSK'547 decreased the protein phosphorylation of MLKL, RIP1, and RIP3 and prevented the oxidative stress-induced loss of nuclear RIP1 and RIP3 localisation. Remarkably, GSK'547 also decreased H_2O_2 -induced mitochondrial depolarization and expression and activation of CAMKII, a protein mediating mitochondria-dependent cell death. Here, we reported GSK'547 as a novel cardioprotective tool to prevent oxidative stress-induced cardiac cell death. This provides scope to prevent myocardial I/R.

INTRODUCTION

Coronary angioplasty is performed around 2 million times each year in Europe to restore perfusion in patients after myocardial infarction¹⁻³. Although this treatment is highly efficient to prevent excessive damage from myocardial ischemia, it paradoxically can cause additional myocardial damage through the release of reactive oxygen species (ROS)^{2,4,5}. The loss of cardiomyocytes as a result of ischemia and ischemia/reperfusion (I/R) injury is an important predicting factor in the progression towards heart failure⁶⁻⁸. For many years, myocyte loss through apoptosis was considered the only regulated and thereby therapeutically targetable form of cell death after an ischemic event^{9,10}. However, studies attempting to prevent I/R damage with anti-apoptotic therapies remain inconclusive¹¹. Over the past two decades, the role of myocardial damage through necrosis has come to light^{10,12,13}. Necrosis was long considered to be a non-regulated process caused by exposure to insurmountable stress and therefore not considered a potential therapeutic target to treat cardiac I/R injury. This concept was challenged upon revealing the presence of regulated mechanisms of necrotic cell death, called necroptosis, which could be activated by ligands of cell death receptors and required the activation of specific cell death pathways^{11,13}. Necroptosis is now considered to be an important mediator of myocardial damage^{12,14}, via opening of the mitochondrial permeability transition pore (mPTP) and via complexation of the kinases receptor-interacting protein-1 (RIP1), RIP3, and mixed lineage kinase domain-like protein (MLKL). It remains unclear, however, whether this mitochondrially-dependent mechanism and RIP1-RIP3-MLKL-dependent necroptotic pathway function separately in disease^{15,16}. Pharmacological inhibition of either cyclophilin-D dependent mPTP opening or RIP1 activity prevented oxidative-stress induced cell death emphasizing the important role of necroptosis in I/R injury^{12,17-19}. Previously, we have shown in human cardiac progenitor cells (hCPCs)²⁰, and in murine and porcine models of myocardial I/R injury prevention of necroptosis using RIP1 inhibitor Nec1

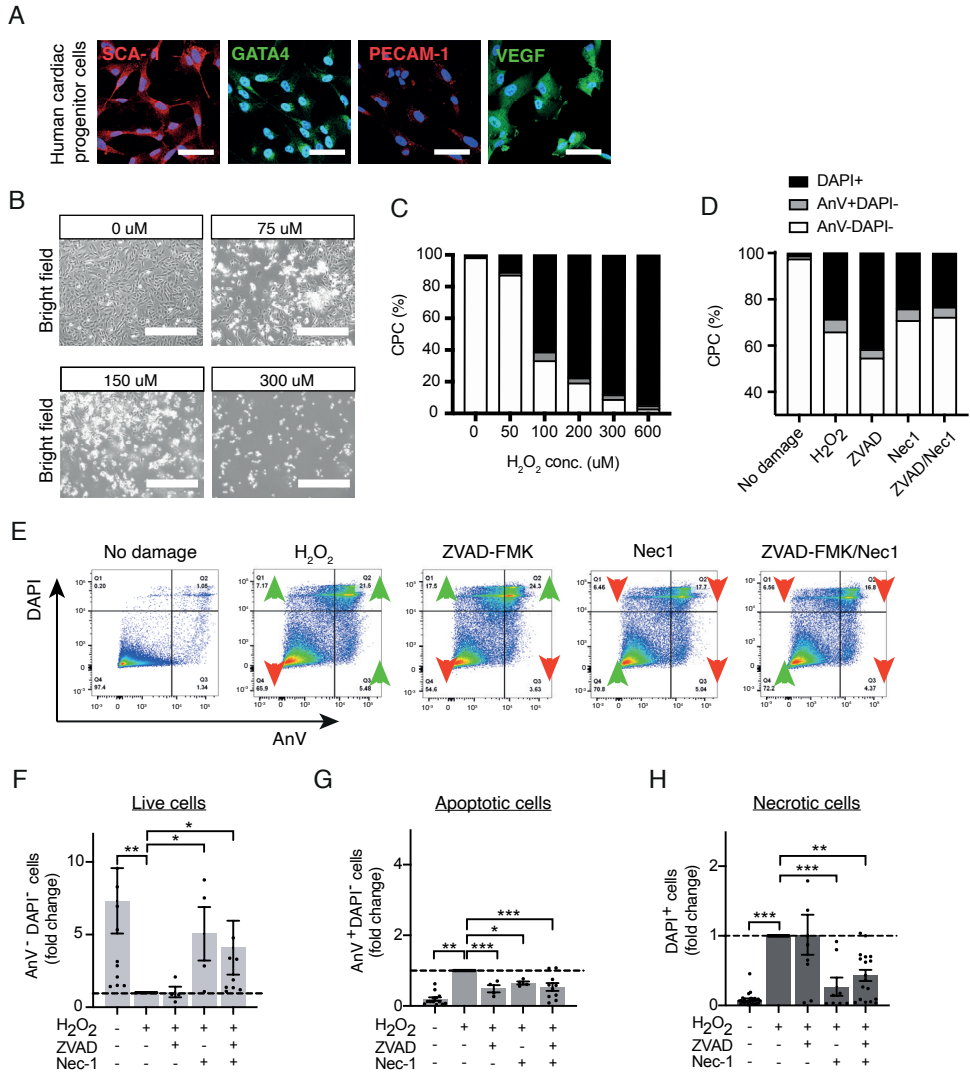


Figure 1. Hydrogen peroxide treatment primarily leads to necrotic cell death in human cardiac progenitor cells

A. Marker expression of hCPCs detected by immunofluorescence. Scale bar: 50 μ m. **B.** Bright-field imaging of hCPCs after stimulation with 0, 75, 150, 300 μ M hydrogen peroxide (H_2O_2). Scale bar: 200 μ m. **C.** Dose-dependent effect of H_2O_2 treatment on cell death as detected by AnV/DAPI flow cytometry. **D.** Contributions of apoptosis and necrosis to H_2O_2 -induced cell death. **E.** AnV/DAPI flow cytometry representation of cell death populations after pre-conditioning with ZVAD-FMK (20 μ M) or Necrostatin-1 (Nec1)(60 μ M) and stimulation with H_2O_2 (75 μ M). **F-H.** Quantification of live cells (AnV-DAPI-) (**F**), apoptotic cells (AnV+DAPI-) (**G**) and necroptotic cells (DAPI+) (**H**). n=4-10 experiments, data was analysed using one-way ANOVA and Dunnett multiple comparison. *P<0,05, **P<0,01, *** P<0,001. Data represented as mean \pm SEM.

stimulated cell survival, reduced infarct size, prevented adverse remodelling and preserved left ventricular function^{19,21}. Although promising to prevent myocardial I/R injury, progression to clinical use of RIP1 inhibitor Nec1 has been hampered by constraints regarding specificity and activity and valorisation protection²²⁻²⁴.

In the present study, we tested a novel small molecule GSK3540547A (GSK'547), selected as the most potent and specific RIP1 binding candidate in a kinase inhibitor screen²⁵, as a potential therapeutic agent to prevent myocardial I/R injury in a human cardiac *in vitro* model. We show GSK'547 efficiently suppresses hydrogen-peroxide induced necroptotic cell death in hCPCs and prevents additional mitochondrial dysfunction, mediated via the RIP1-RIP3-MLKL pathway and the RIP3-CAMKII-mPTP pathway.

RESULTS

Hydrogen peroxide leads to necrotic cell death

We previously established a human I/R injury *in vitro* model system, using hCPCs²⁶ capable of differentiating into cardiomyocytes²⁶, that had predictive mechanistic results on necroptosis inhibition for our animal follow-up studies^{19,21,27}. We therefore considered this human cell model to be a good predictive model to study basic cardiac cell mechanisms of cell death.

In line with previous characterisation²⁶, hCPCs were positive for Sca-1-like epitope and expressed GATA4, PECAM-1, and VEGF (**Figure 1a**). To determine modes of cell death upon oxidative stress-induced cardiac damage, we performed flow cytometric analysis using dual labeling with annexin V (AnV) and DAPI. Stimulation with hydrogen peroxide increased cell death and cellular detachment dose-dependently, increasing the DAPI⁺ (necrotic/necroptotic) cell population (**Figure 1b, c**). To discriminate necroptotic and apoptotic cell death by AnV/DAPI, we preconditioned

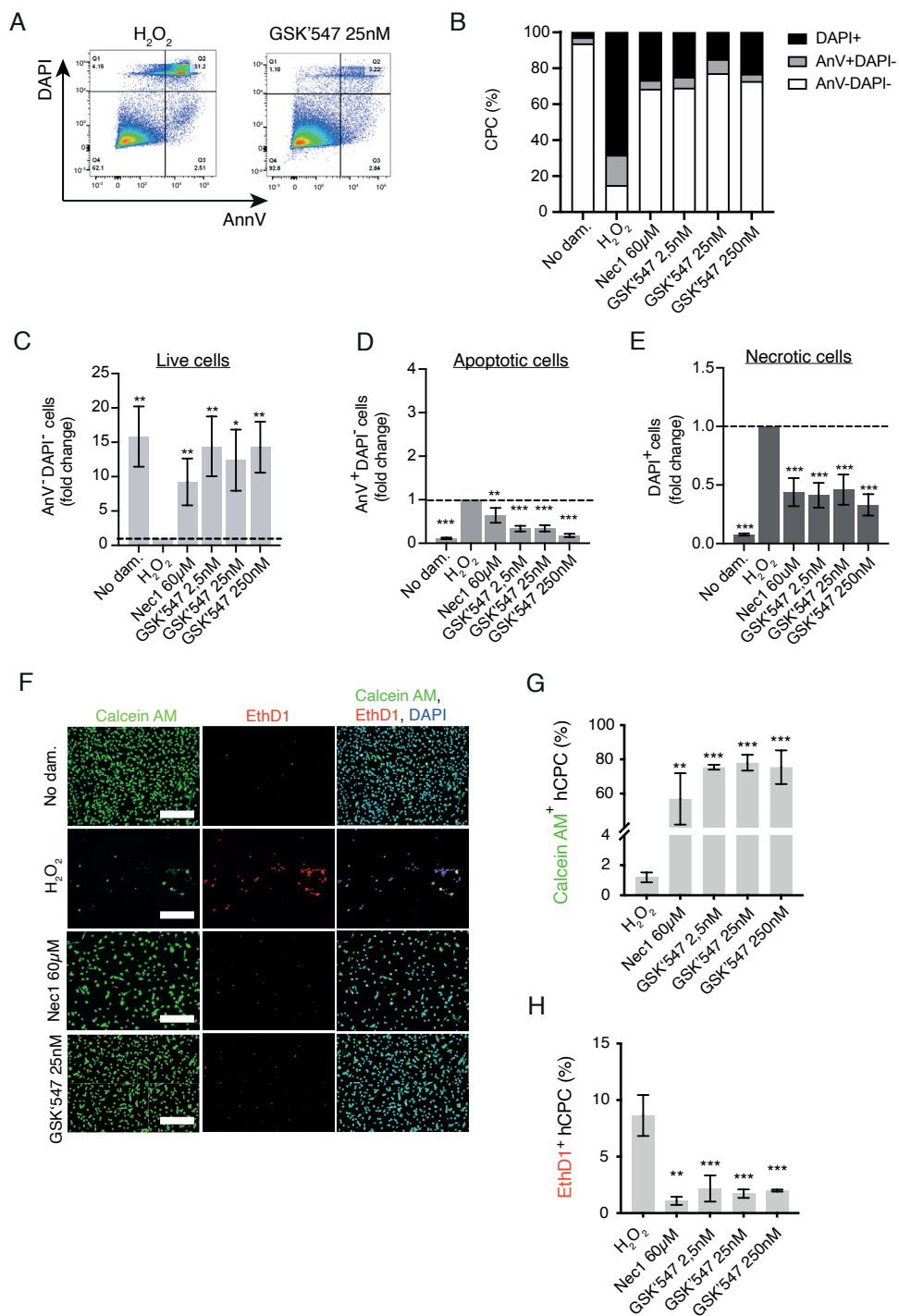


Figure 2. GSK'547 increases survival of hCPCs during oxidative stress

A. AnV/DAPI flow cytometry representations of cell death populations after preconditioning with Nec1 (60 μ M) or GSK'547 (2.5nM, 25nM or 250nM) and stimulation with H₂O₂ (75 μ M). **B.** Contribution of necroptosis and apoptosis to GSK'547 mediated cardioprotection. **C-E.** Quantification of living cells (AnV-DAPI-) (**C**), apoptotic cells (AnV+DAPI-) (**D**), and necrotic cells (DAPI+) (**E**). **F.** Representative images of Calcein A/EthD1 viability stain. Scale bar: 200 μ m. **G, H.** Quantification of **F**. n=5 experiments, data was analysed using one-way ANOVA and Dunnett multiple comparison. *P<0,05, ** P<0,01, *** P<0,001. Data represented as mean \pm SEM.

the cells with an apoptosis inhibitor (ZVAD-FMK) or a necroptosis inhibitor (Nec1). While only a small portion of cells had an apoptotic signature (13,7 \pm 3,6% [AnV+DAPI⁻] vs 29,5 \pm 4,4% [DAPI⁺], **Figure 1d, e**), preconditioning with caspase 8 inhibitor ZVAD-FMK increased the DAPI⁺ cell population without affecting the live cell population (fold change, 0,49 \pm 0,10 [AnV+DAPI⁻]; 1,14 \pm 5,2 [DAPI⁺], 1,04 \pm 0,37[AnV-DAPI⁻], **Figure 1f-h**). Preconditioning with Nec1 decreased the DAPI⁺ (necrotic/necroptotic) and AnV+DAPI⁻ (apoptotic) cell population and increased the live cell population (fold change, 0,65 \pm 0,04 [AnV+DAPI⁻]; 0,27 \pm 0,13 [DAPI⁺], 5,05 \pm 1,8 [AnV-DAPI⁻], *P*<0,05, **Supplemental figure 1**).

GSK'547 protects against oxidative stress-induced cell death

Next, we assessed whether our novel RIP1 inhibitor, GSK'547, could prevent necroptosis at low concentrations. Although at a 1 \times 10⁴ fold lower concentration than nec-1, GSK'547 prevented oxidative stress induced cell death to the same extent, decreasing both the DAPI⁺ (necroptotic) and AnV⁺ DAPI⁻ (apoptotic) cell population (0,41 \pm 0,11 fold [DAPI⁺]; 0,34 \pm 0,07 fold [AnV+DAPI⁻], 14,4 \pm 4,36 fold [AnV-DAPI⁻], *P*<0,01, **Figure 2a-e**). Furthermore, live/dead staining confirmed GSK'547 increased calcein AM⁺ cells (live) (1,2 \pm 0,33% [H₂O₂] vs 75,4 \pm 1,4% [GSK'547], *P*<0,001) and decreased ethidium homodimer-1⁺ cells (dead) (8,6 \pm 1,8% [H₂O₂] vs 2,2 \pm 1,2% [GSK'547], *P*<0,01, **Figure 2f-h**). Hereby, we show GSK'547 is a potent inhibitor

of necroptotic cell death, since it was very effective at low concentrations without having further effects upon increasing dosage to 250nM, and promoted cell survival.

GSK'547 prevents oxidative stress induced necroptosis by targeting RIP1, RIP3 and MLKL phosphorylation

Necroptosis is regulated by RIP1 autophosphorylation followed by RIP1-dependent phosphorylation of RIP3, and translocation of consecutively phosphorylated MLKL to the plasma membrane²⁸⁻³⁰. Treatment with GSK'547 decreased RIP1, RIP3 and MLKL phosphorylation while there were no changes in total protein levels or mRNA levels (**Figure 3, Supplemental figure 2**).

Next to the kinase dependent role of RIP1 and RIP3, the subcellular localization of RIP1 has also been reported to contribute to the regulation of necroptosis via the activation of e.g. PARP1³⁰⁻³². To investigate changes in subcellular localization upon hydrogen peroxide exposure, we performed immunofluorescence staining and subcellular fractionation. While MLKL localization remained unaffected by hydrogen peroxide exposure (**Figure 4a, b, e**), RIP1 and RIP3 expression, found both in the cytoplasm and nucleus, disappeared in the nucleus following hydrogen peroxide exposure (**Figure 4a-d**). Prevention of RIP1 activation via GSK'547 could maintain the presence of nuclear RIP1 and RIP3 localization. Next to immunofluorescent localization, cellular fractioning confirmed this shift of both RIP1 as RIP3 from the nucleus upon hydrogen peroxide exposure, and their return after both Nec1 as GSK'547 treatment (**Figure 4f-h**). These results validate the protective effect of RIP1-inhibitor GSK'547 via the regulation of phosphorylated RIP1-RIP3-MLKL-mediated necroptosis and suggest a role of the cellular localization of both RIP1 and RIP3 in oxidative stress-induced necroptosis.

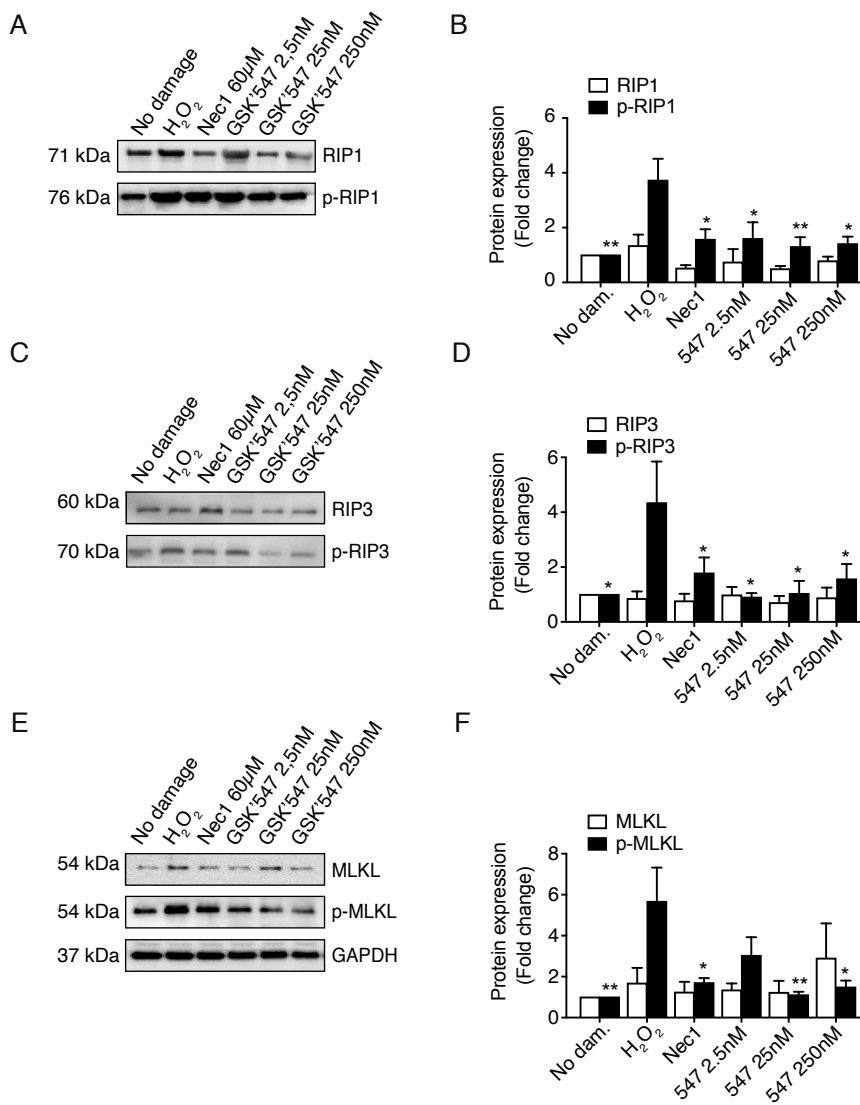


Figure 3. GSK'547 abolishes H₂O₂-induced hCPC necroptosis by preventing RIP1, RIP3, and MLKL phosphorylation

A. RIP1 protein expression levels detected by Western blot. **B.** Quantification of **A.** **C.** RIP3 protein expression levels detected by Western blot. **D.** Quantification of **C.** **E.** MLKL protein expression levels detected by Western blot. **F.** Quantification of **E.** n=4 experiments, data was analysed using one-way ANOVA and Dunnett multiple comparison and significance is measured compared to H₂O₂. *P<0,05, ** P<0,01, *** P<0,001. Data represented as mean ±SEM

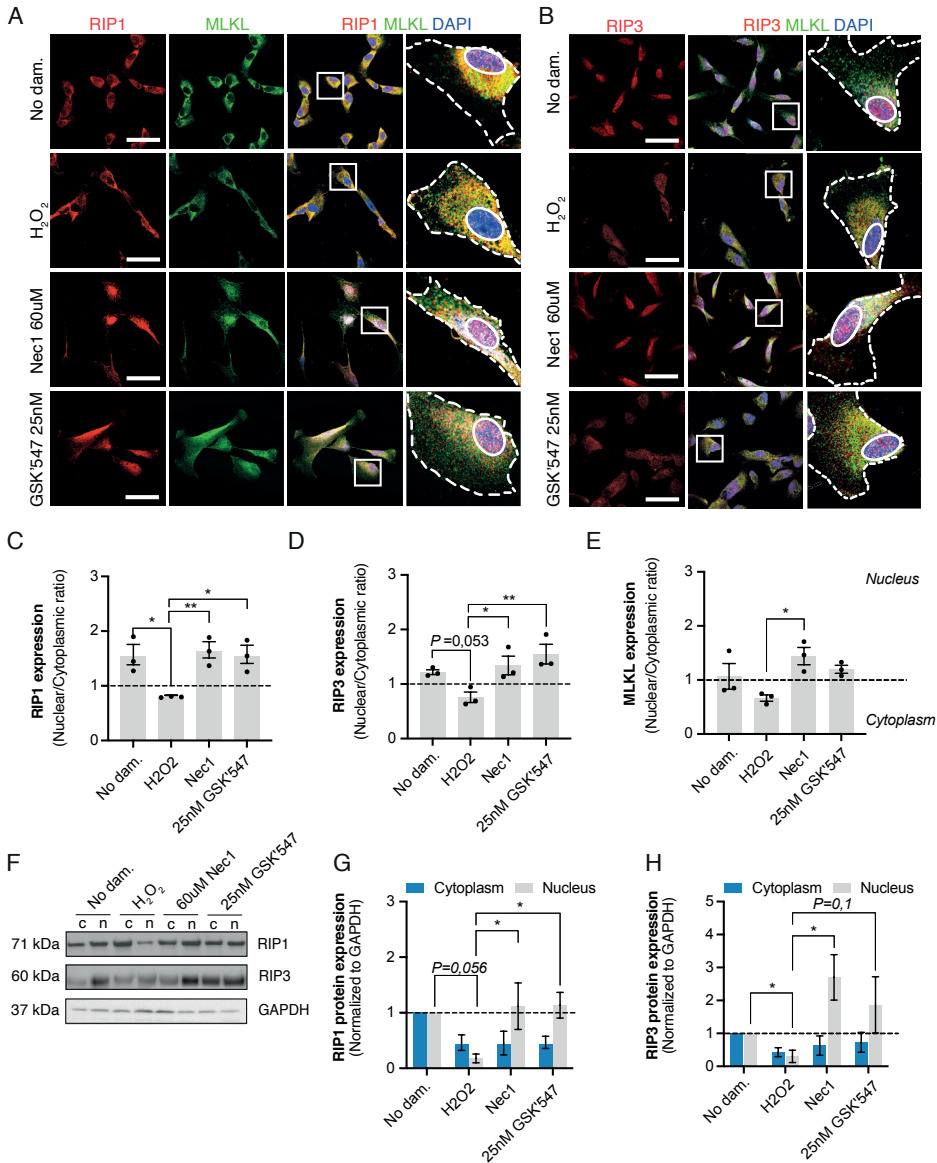


Figure 4. GSK'547 prevents H₂O₂-induced decreased nuclear localization of RIP1 and RIP3

A. RIP1 and MLKL protein localization detected by immunofluorescence imaging. **B, C.** Quantification of **A.** **C.** RIP3 and MLKL protein localization detected by immunofluorescence imaging. **D-E.** Quantification of **C.** **F.** RIP1 protein levels in the cytosolic (c) or nuclear (n) subcellular fraction as confirmed by Western blot. Lamin B1 protein levels were assessed to confirm the purity of the nuclear fraction. Quantification of **E.** n=3 experiments, data was analysed using one-way ANOVA and Dunnett multiple comparison and significance is measured compared to H₂O₂. Scale bar: 400µm. *P<0,05, ** P<0,01, *** P<0,001. Data represented as mean ± SEM.

GSK'547 prevents hydrogen peroxide induced mitochondrial dysfunction

Next to activation of the RIP3-MLKL necroptosis pathway, RIP1 is also an activator of Ca²⁺/calmodulin-dependent protein kinase (CaMKII) via RIP3 phosphorylation^{14,15,33}. CaMKII activation and subsequent opening of the mitochondrial permeability mPore and protein transition pore has been reported as an important mediator of cardiac I/R^{14,34}. Hydrogen peroxide induced loss of mitochondrial membrane potential to a similar degree as our positive control, a chemical inhibitor of oxidative phosphorylation (carbonyl cyanide m-chlorophenyl hydrazone (CCCP)) (**Figure 5a, b**). GSK'547 was able to prevent expression of phosphorylated CaMKII (**Figure 5c-e**). This shows that GSK'547 inhibits hydrogen peroxide induced loss of mitochondrial membrane potential ($\Delta\Psi_m$) similarly as the 1×10^4 fold higher concentration of nec-1 as visualized by a loss of J-aggregates (red) and an increase in JC-1 monomers (green) (**Figure 5a, b**). Furthermore, GSK'547 prevented the hydrogen peroxide induced increase in CaMKII mRNA expression and expression of phosphorylated CaMKII (**Figure 5c-e**). This shows that GSK'547 inhibits necroptosis by both targeting the RIP1-RIP3-MLKL- and the RIP3-CAMKII-mPore-axis (**Supplemental figure 3**).

DISCUSSION

Damage caused by reperfusion of the ischemic myocardium can lead to irreversible damage via the release of ROS and can account for up to 50% of the myocardial infarct size³⁵. In previous studies, we have shown inhibition of necroptotic cell death via nec-1 administration to mice and pigs could prevent reperfusion injury and limit myocardial cell death^{11,21}. Also, in hCPCs we observed nec-1 to be effective in preventing hydrogen peroxide induced cell death²⁰. As clinical translation of nec-1 is hindered by low potency (78,8% protein binding)²³, rapid plasma clearance in females (<60 minutes)²³, low bioavailability (54,4%)³⁶, poor *in vivo* pharmacokinetic properties³⁷, but mainly due to poor intellectual property protection, targeting the

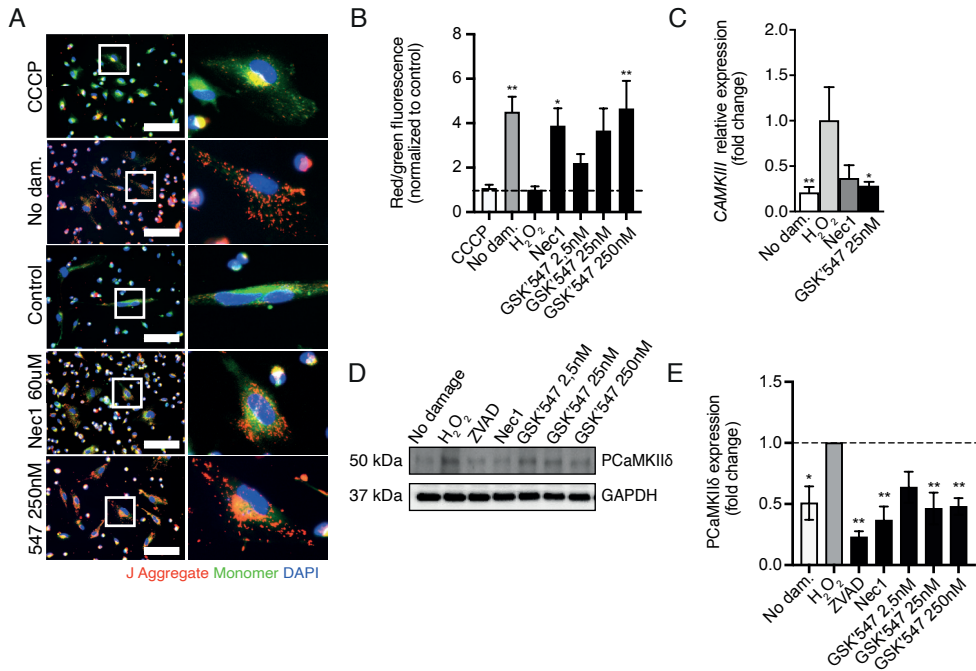


Figure 5. GSK'547 prevents H₂O₂-induced mitochondrial damage

A. JC-1 staining analysed by confocal microscopy. CCCP; positive control of mitochondrial membrane depolarization. **B.** Quantification of red/green ratio (**A**). **C.** CaMKII mRNA expression levels normalized to tata binding protein (TBP) expression as detected by RT-qPCR. **D.** PCaMKII δ protein levels as detected by Western blot. **E.** Quantification of **D**. Scale bar: 400 μ m, n=3 experiments, data was analysed using one-way ANOVA and Dunnett multiple comparison and significance is measured compared to H₂O₂. *P<0,05, ** P<0,01, *** P<0,001. Data represented as mean \pm SEM. CCCP; Carbonyl cyanide m-chloroperyl hydrazone.

necroptosis to prevent I/R via nec-1 in patients with ischemic injury remains impossible.

With the selection and development of a potent RIP1 inhibitor with good pharmacokinetic properties, a close derivative of GSK'547, GSK2982772 successfully completed a phase 1 clinical trial in psoriasis, rheumatoid arthritis, and ulcerative colitis patients²⁵. Here, GSK'547 was further developed from GSK2982772, to maintain potency in humans and animal models. In our study, we could confirm potent inhibition of RIP1 activation and necroptosis. Moreover, we observed altered intracellular localization of RIP1 and RIP3 after hydrogen peroxide stimulation and

A novel receptor-interacting protein-1 (RIP1) inhibitor (GSK'547) protects human cardiac cells from ischemia/reperfusion-triggered necroptotic cell death

ability of GSK'547 to prevent loss of nuclear RIP1 and RIP3 expression. Our findings demonstrate that GSK'547 potently inhibits activation of RIP1 and prevents necroptosis of human cardiac cells upon hydrogen peroxide exposure. By prevention of RIP1 activation both MLKL mediated necroptosis and CAMKII-mPTP mediated necroptosis was inhibited, increasing cellular viability upon oxidative stress.

Previous studies on the role of apoptosis upon myocardial I/R injury often used TUNEL stainings or analyses of DNA fragmentation³⁸, which, without the use of additional controls (staining for active caspase-3³⁹), could also point to necroptotic cell death⁴⁰⁻⁴³. Also, dual staining with AnV and DAPI to differentiate between modes of cell death has been challenged, as AnV+DAPI⁻ cells could also indicate primary necrotic cells responsive to nec-1⁴⁴. This is in line with our findings where we measured a decrease in AnV+DAPI⁻ cells after preconditioning hCPCs with nec-1 or GSK'547. Therefore, we recommend the use of specific controls such as necrostatin-1 and ZVAD-FMK to distinguish between different modes of cell death.

It is important to note, next to apoptosis and necroptosis, ferroptosis has also been implicated as an important contributor to cardiac I/R injury⁴⁵. In ferroptosis, cell death is primarily induced by oxidative damage to the mitochondria and lipid peroxidation through mitochondrial iron accumulation. Previous studies have shown that preservation of mitochondrial membrane integrity could prevent ferroptosis in neuronal dysfunction^{46,47}. Since multiple cell death pathways contribute to cell loss in disease conditions, it is likely that cell death pathways bisect to activate the same proteins to mediate cell death¹⁶. Furthermore, the presence of several stimuli (e.g. ROS, TNF α) in the infarcted region could stimulate multiple pathways after I/R injury. Although the present study does not include other ligands that can potentially induce necroptotic cell death during I/R injury, hydrogen peroxide has been identified as the main active ROS in cardiomyocytes and considered the primary inducer of cardiac I/R injury⁴⁸. Furthermore, exogenous administration of hydrogen peroxide

is considered a physiologically relevant model of endogenous ROS release in cardiovascular disease⁴⁹.

Previous studies have shown changes in subcellular localization of necrosome components play a role in necroptosis regulation^{30,32,50–53} and prevention of nuclear export of RIP1 and RIP3 reduces TNF α -induced necroptosis⁵⁰. Interestingly, a kinase independent role of nuclear RIP1 during oxidative stress in murine embryonic fibroblasts was also reported in regulating PARP1 mediated necroptosis^{32,57}. As we show decreased nuclear RIP1 levels upon oxidative stress and necroptosis mechanisms have been shown to exhibit cell type specific profiles^{29,32}, it is unlikely that PARP1-mediated necroptosis plays a major role in oxidative stress mediated cell death of cardiac cells. Previous research did show nec-1 prevented necroptosis in hippocampal neurons while also preventing RIP3 nuclear translocation⁵⁴. Whether there was a causal relationship between the prevention of RIP3 nuclear export and nec-1 mediated necroptosis inhibition remains unknown. This is the first report showing inhibition of RIP1 activation can alter subcellular localisation of both RIP1 and RIP3 in cardiac cells. The mechanisms through which nec1 and GSK'547 prevent loss of nuclear RIP1 and RIP3 localization after oxidative stress remain to be elucidated. Previous research showed cytoplasmic RIP1 and RIP3 lead to necroptotic cell death via MLKL mediated necrosome formation²⁸. Nuclear RIP1 and RIP3 have been shown to contribute to necroptotic cell death via nuclear export indicating nuclear-cytoplasm shuttling as a mechanism of necroptosis regulation^{55,56}.

Taken together, we have shown that a novel RIP1 inhibitor, GSK'547, can efficiently block necroptotic cell death in human cardiac cells at very low concentrations by targeting RIP3 and MLKL phosphorylation and mitochondrial dysfunction. This highly selective and potent inhibitor for necroptosis-induced cell death is therefore a novel candidate to block I/R-induced injury upon myocardial infarction.

METHODS

Cell Culture. Human foetal cardiac progenitor cells (hCPC) were isolated and cultured as previously described²⁶. Briefly, hCPCs were obtained from human foetal heart tissue after elective abortion using anti-Sca1-coupled magnetic beads. Subsequently, hCPCs were cultured on 0,1% gelatin coated plates in M199 (Gibco)/EGM-2 (Lonza) (3:1) media supplemented with 10% FBS (Gibco), 1% MEM non-essential amino acids (NEAA) (Gibco) and 1% penicillin/streptomycin (Gibco). To use human foetal tissue, permission by informed consent and approval of the ethics committee of the University Medical Centre Utrecht was obtained.

Experimental procedure. Cells were pre-incubated with 20uM ZVAD-FMK (Promega), 60uM Necrostatin-1 (Abcam) or 2,5nM, 25nM, 250nM GSK'547 6 hours prior to exposure to 75uM tert-butyl hydrogen peroxide (Sigma) for 16-20 hours.

Immunostaining. Cells were fixed in 4% paraformaldehyde for 30 minutes and permeabilized with 0.1% triton-X100 (Sigma Aldrich) in PBS. Following 1 hour blocking in 10% normal goat serum (Vector Laboratories) in 1% bovine serum albumin (BSA) (Millipore Sigma), cells were stained with primary antibodies RIP1 (Invitrogen 1:200), RIP3 (Invitrogen 1:200) and MLKL (Sigma Aldrich 1:200) overnight at 4°C. For primary antibody detection, cells were incubated with fluorescent secondary antibodies (Invitrogen Alexa 1:200) and 4',6-diamidino-2-phenylindole (DAPI) (Vector laboratories) used as nuclear marker. Visualisation and documentation were performed by confocal microscopy (Sp8x, Leica). ImageJ software (ImageJ 1.51a)⁵⁸ was used for image analysis. For protein localization quantification, mean pixel intensity in the nucleus was compared to mean pixel intensity of the cytoplasm per cell to exclude differences between images in pixel intensity and differences in area size. The images were taken at a magnification of 63x and the mean pixel intensity of 5 cells per image were quantified with 5 images per condition per experiment for 3 experiments to give an indication of subcellular protein localization. To confirm

quantitatively, protein levels were also determined on gel electrophoresis.

Cell death analysis. Cells were stained with calcein AM and ethidium homodimer-1 (Invitrogen LIVE/DEAD™ Viability/Cytotoxicity Kit L3224) to determine the live-dead ratio. Images were obtained using the Evos Fluid Cell Imaging station (ThermoFischer Scientific) and analysed using ImageJ software. For quantitative cell death analysis, cells were dissociated (Miltenyi Biotec Multi tissue dissociation kit 130-110-204) and stained with AnV-conjugated FITC (Invitrogen V13242) and DAPI. Staining was analysed by flow cytometry (BD FACSCanto Cell Analyzer (BD Bioscience)) using BD FACSDiva software (BD bioscience) and FlowJo 10.6.1 software (Becton, Dickinson & Company).

Quantitative real-time PCR. RNA was isolated using Tripure (Roche 11667165001) and reverse transcribed to cDNA using qScript cDNA synthesis kit (Quantabio 95047-100), both according to manufacturer's manuals. Total RNA levels were determined using NanoDrop (Denovix DS-11) and gene transcript levels were quantified using Perfecta SYBR green super mix (Quantabio) and gene specific primers in a CFX96 qPCR instrument (BioRad).

Cell fractioning. After exposure to hydrogen peroxide, cells were harvested and nuclear and cytoplasmic fractions were isolated using the cell fractionation kit (Abcam). After dissociation with 0,05% trypsin/EDTA (Gibco), cells were centrifuged at 300g and resuspended in buffer A. After cell count determination, cells were resuspended in buffer B (1000-fold dilution of detergent 1), incubated on a rotator and centrifuged at 5000g to extract the cytoplasmic fraction. The nuclear fraction was isolated after incubation in buffer C (25-fold dilution of detergent 2) and consecutive centrifugation steps at 5000g and 10000g. The purity of the nuclear fraction was determined by western blotting for nuclear protein Lamin B1.

Western blotting. Total protein was extracted using RIPA lysis buffer (Thermo

A novel receptor-interacting protein-1 (RIP1) inhibitor (GSK'547) protects human cardiac cells from ischemia/reperfusion-triggered necroptotic cell death

Scientific 89901) supplemented with phosphatase inhibitors (PhosSTOP, Roche) and protease inhibitors (cOmplete, Roche). Protein concentrations were quantified using Pierce BCA protein assay kit (Thermo Scientific). Samples were prepared for sodium dodecyl-sulfate polyacrylamide gel electrophoresis (SDS-PAGE) using NuPAGE reducing agent (Thermo Scientific) and NuPAGE LDS sample buffer (Thermo Scientific) and run in a 4–15% acrylamide Mini-Protean TGX gel (BioRad). Transfer of the proteins to the polyvinylidene fluoride (PDVF) membrane was mediated by the Transblot Turbo system (BioRad). After blocking with 5% BSA in TBST, the membrane was incubated with primary antibodies against RIP1 (Novus Biologicals), p-RIP1 (Cell signaling), RIP3 (Invitrogen), p-RIP3 (Abcam), MLKL (Invitrogen), p-MLKL (Cell signaling), CaMKII δ (Thermo Scientific) at 1:1000. Secondary HRPO labelled antibodies were used 1:2000 for detection with oxidizing reagent and enhanced luminol reagent (Western Lightning Plus ECL) and samples were scanned using BioRad ChemiDoc™ Imager system.

Mitochondrial membrane potential. Cells were stained with JC-1 dye (ThermoFisher Scientific, #T3168 3,2 $\mu\text{g/ml}$) as a mitochondrial membrane potential probe. As a positive control of mitochondrial depolarization, cells were treated with 25 μM carbonyl cyanide 3-chlorophenylhydrazone (CCCP) (Sigma Aldrich). Nuclei were stained with Hoechst 33342. Images were obtained with the Evos Flouid microscope and red (~590 nm)/green (~525 nm) fluorescence intensity ratio was quantified by measuring the mean gray value of the separate channels (ImageJ) normalized to the CCCP control.

Statistical analysis. The n number indicates biological replicates (the number of experiments performed with multiple cell batches or passages) and is logged in the text and in the figures. Statistical analysis was performed using Prism 8 (GraphPad) software and data represents mean \pm SEM. To test for normality, a Shapiro-Wilk test was performed. For comparison of the expression, one-way ANOVA with Dunnett

multiple comparisons was used to determine statistically significant ($P < 0.05$) results.

ACKNOWLEDGEMENTS

The authors thank Jean-Luc Tran and Allison Beal from GlaxoSmithKline for providing the GSK'547 compound.

SOURCES OF FUNDING

Marijn M.C. Peters is supported by a Netherlands Cardiovascular Research Initiative (CVON) grant (REMAIN 2014B27). Joost P.G. Sluiter is supported by the PLN foundation, and Horizon2020 ERC-2016-COG-EVICARE [725229] and BRAVE (grant number 874827).

SUPPLEMENTARY INFORMATION

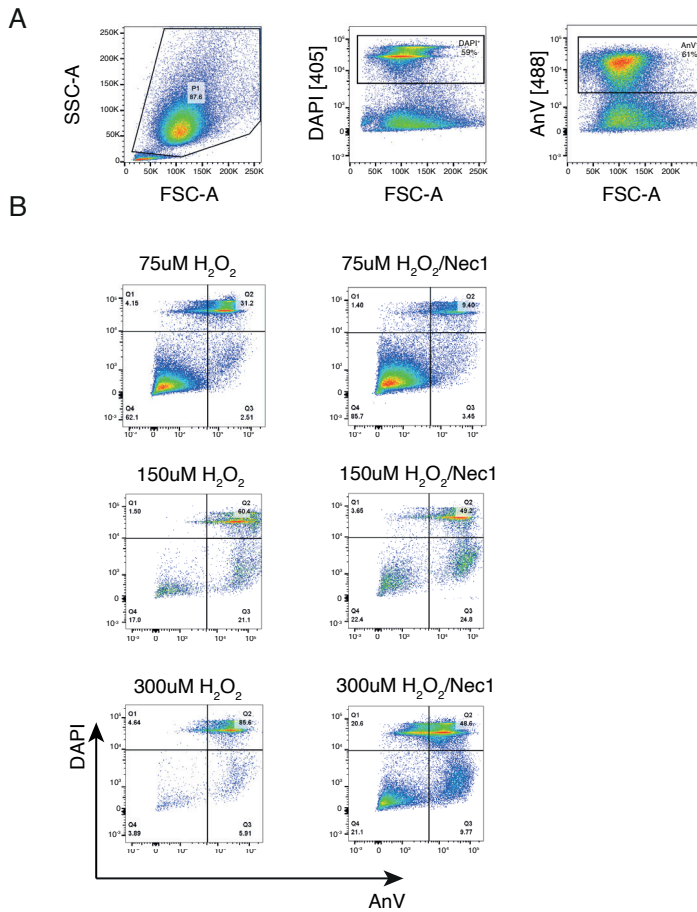


Figure S1. Hydrogen peroxide induces dose-dependent cell death in cardiac progenitor cells
A. FACS gating strategy of hCPCs after stimulation with H_2O_2 (75 μM). **B.** Increasing H_2O_2 concentration limits the protective potential of Nec-1. Representative density plots are shown.

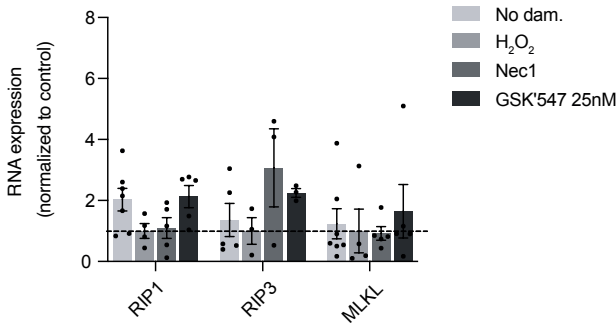


Figure S2. Necroptosis inhibition does not influence RIP1, RIP3, and MLKL RNA expression
RNA expression normalized to H₂O₂ treated hCPCs and GAPDH housekeeping gene expression.

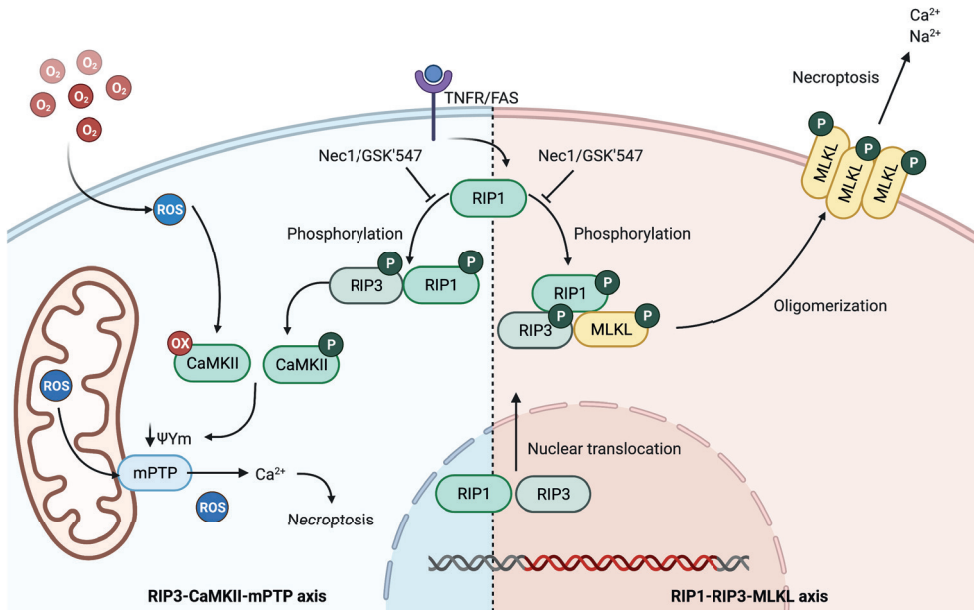


Figure S3. Schematic illustration of necroptosis signalling in the oxidative stress response of human cardiac cells

REFERENCES

1. Rotter M, Pfiffner D, Maier W, Zeiher AM, Meier B. Interventional cardiology in Europe 1999. *Eur Heart J.* 2003;24(12):1164-1170.
2. Antman EM, Hand M, Armstrong PW, et al. 2007 Focused update of the ACC/AHA 2004 guidelines for the management of patients with ST-elevation myocardial infarction: A report of the American College of Cardiology/American Heart Association task force on practice guidelines. *Circulation.* 2008;117(2):296-329.
3. Van de Werf F, Chair, Ardissino D, et al. Management of acute myocardial infarction in patients presenting with ST-segment elevation. *Eur Heart J.* 2003;24(1):28-66.
4. Ferrari R, Ceconi C, Curello S, et al. Role of oxygen free radicals in ischemic and reperfused myocardium. *Am J Clin Nutr.* 1991;53
5. Perrelli MG, Pagliaro P, Penna C. Ischemia/Reperfusion Injury and Cardioprotective Mechanisms: Role of Mitochondria and Reactive Oxygen Species. *World J Cardiol.* 2011;3(6):186-200.
6. Takemura G, Fujiwara H. Role of apoptosis in remodeling after myocardial infarction. *Pharmacol Ther.* 2004;104(1):1-16.
7. Luedde M, Lutz M, Carter N, et al. RIP3, a kinase promoting necroptotic cell death, mediates adverse remodeling after myocardial infarction. *Cardiovasc Res.* 2014;103(2):206-216.
8. Szobi A, Gonçalvesová E, Varga Z V, et al. Analysis of necroptotic proteins in failing human hearts. *J Transl Med.* 2017:1-7.
9. Gottlieb RA. Mitochondria – a matter of life and death Mitochondrial signaling in apoptosis : Mitochondrial daggers to the breaking heart. *Basic Res Cardiol.* 2003;98:242-249.
10. Whelan RS, Kaplinskiy V, Kitsis RN. Cell Death in the Pathogenesis of Heart Disease : Mechanisms and Significance. *Annu Rev Physiol.* 2010;72:19-44.
11. Oerlemans MIFJ, Koudstaal S, Chamuleau SA, De Kleijn DP, Doevendans PA, Sluijter JPG. Targeting cell death in the reperfused heart: Pharmacological approaches for cardioprotection. *Int J Cardiol.* 2013;165(3):410-422.
12. Kung G, Konstantinidis K, Kitsis RN. Programmed Necrosis, Not Apoptosis, in the Heart. *Circ Res.* 2011; 108 (8):1017-1036.
13. Zhu H, Sun A. Programmed necrosis in heart disease : Molecular mechanisms and

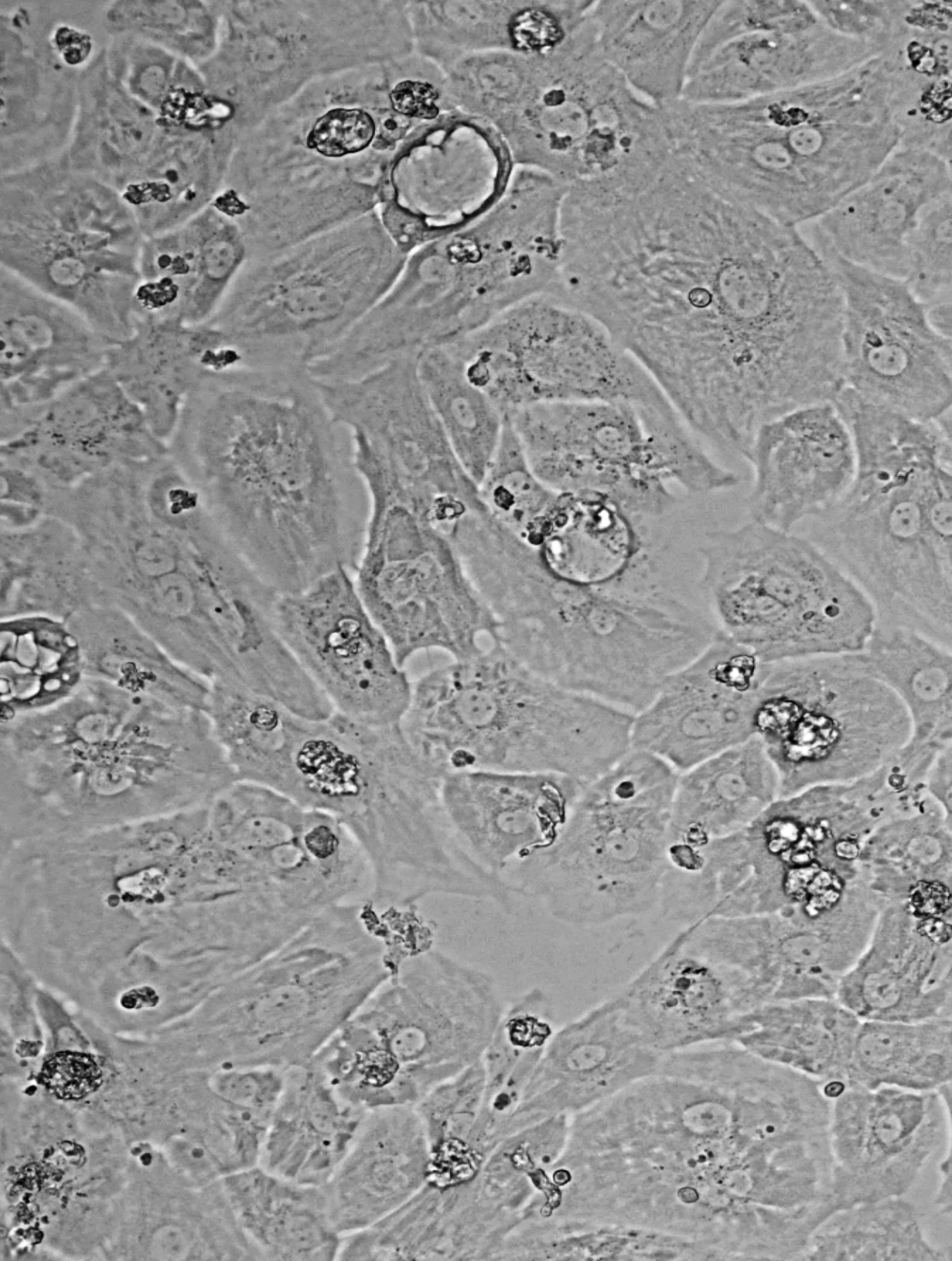
- clinical implications. *Journal of Molecular and Cellular Cardiology*. 2018;116:125-134.
14. Zhang T, Zhang Y, Cui M, et al. CaMKII is a RIP3 substrate mediating ischemia- and oxidative stress – induced myocardial necroptosis. *Nature Med*. 2016;22(2).
 15. Ye YC, Wang HJ, Yu L, Tashiro SI, Onodera S, Ikejima T. RIP1-mediated mitochondrial dysfunction and ROS production contributed to tumor necrosis factor alpha-induced L929 cell necroptosis and autophagy. *Int Immunopharmacol*. 2012;14(4):674-682.
 16. Marshall KD, Baines CP. Necroptosis: Is there a role for mitochondria? *Front Physiol*. 2014;5:1-5.
 17. Baines CP, Kaiser RA, Purcell NH, et al. Loss of cyclophilin D reveals a critical role for mitochondrial permeability transition in cell death. 2005;434:626-629.
 18. Nakagawa T, Shimizu S, Watanabe T. Cyclophilin D-dependent mitochondrial permeability transition regulates some necrotic but not apoptotic cell death. *Nature*. 2005;434 (7033):752-658.
 19. Oerlemans MIFJ, Liu J, Arslan F. Inhibition of RIP1-dependent necrosis prevents adverse cardiac remodeling after myocardial ischemia – reperfusion in vivo. *Basic Res Cardiol*. 2012: 107 (4).
 20. Feyen D, Gaetani R, Liu J, et al. Increasing short-term cardiomyocyte progenitor cell (CMPC) survival by necrostatin-1 did not further preserve cardiac function. *Cardiovascular Research*. 2018:83-91.
 21. Koudstaal S, Oerlemans MIFJ, Spoel TIG Van Der, Janssen AWF. Necrostatin-1 alleviates reperfusion injury following acute myocardial infarction in pigs. *Eur J Clin Invest*. 2014;1:150-159.
 22. Takahashi N, Duprez L, Grootjans S, et al. Necrostatin-1 analogues : critical issues on the specificity, activity and in vivo use in experimental disease models. *Cell Death Dis*. 2012:1-10.
 23. Degtrev A, Maki JL, Yuan J. Activity and specificity of necrostatin-1, small-molecule inhibitor of RIP1 kinase. 2013:9047.
 24. Teng X, Degtrev A, Jagtap P, et al. Structure-activity relationship study of novel necroptosis inhibitors. *Bioorganic Med Chem Lett*. 2005;15(22):5039-5044.
 25. Harris PA, Berger SB, Jeong JU, et al. Discovery of a First-in-Class Receptor Interacting Protein 1 (RIP1) Kinase Specific Clinical Candidate (GSK2982772) for

the Treatment of Inflammatory Diseases.1:1-42.

26. Smits AM, Vliet P Van, Metz CH, Korfage T, Sluijter JPG, Doevendans PA. Human cardiomyocyte progenitor cells differentiate into functional mature cardiomyocytes : an in vitro model for studying human cardiac physiology and pathophysiology. *Nat Prot.* 2009; 4 (2): 232-243.
27. Liu J, Mil A Van, Vrijssen K, et al. MicroRNA-155 prevents necrotic cell death in human cardiomyocyte progenitor cells via targeting RIP1 Quantitative RT-PCR CMPC isolation and culture Luciferase experiments. *J Cell Mol Med.* 2011;15(7):1474-1482.
28. Sun L, Wang H, Wang Z, et al. Mixed lineage kinase domain-like protein mediates necrosis signaling downstream of RIP3 kinase. *Cell.* 2012;148(1-2):213-227.
29. Vandenabeele P, Galluzzi L, Vanden Berghe T, Kroemer G. Molecular mechanisms of necroptosis: An ordered cellular explosion. *Nat Rev Mol Cell Biol.* 2010;11(10):700-714.
30. Samson AL, Zhang Y, Geoghegan ND, et al. MLKL trafficking and accumulation at the plasma membrane control the kinetics and threshold for necroptosis. *Nat Commun.* 2020;11(1):1-17.
31. Yoon S, Bogdanov K, Kovalenko A, Wallach D. Necroptosis is preceded by nuclear translocation of the signaling proteins that induce it. *Cell Death Differ.* 2016;23(2):253-260.
32. Jang KH, Jang T, Son E, Choi S, Kim E. Kinase-independent role of nuclear RIPK1 in regulating parthanatos through physical interaction with PARP1 upon oxidative stress. *Biochim Biophys Acta - Mol Cell Res.* 2018;1865(1):132-141.
33. Zhe-wei S, Li-sha G, Yue-chun L. The Role of Necroptosis in Cardiovascular Disease. 2018;9:1-9.
34. Kuznetsov A V., Javadov S, Margreiter R, Grimm M, Hagenbuchner J, Ausserlechner MJ. The role of mitochondria in the mechanisms of cardiac ischemia-reperfusion injury. *Antioxidants.* 2019;8(10).
35. Yellon DM, Hausenloy DJ. Myocardial reperfusion injury. *N Engl J Med.* 2007;1121-1135.
36. Geng F, Yin H, Li Z, et al. Quantitative analysis of necrostatin-1, a necroptosis inhibitor by LC-MS/MS and the study of its pharmacokinetics and bioavailability. *Biomed Pharmacother.* 2017;95:1479-1485.

37. Ting AT. Programmed Necrosis Methods and Protocols. *Methods in Molecular Biology*. 2018:1857.
38. Gottlieb RA, Burleson KO, Kloner RA, Babior BM, Engler RL. Reperfusion injury induces apoptosis in rabbit cardiomyocytes. *J Clin Invest*. 1994;94(4):1621-1628.
39. Vanden Berghe T, Grootjans S, Goossens V, et al. Determination of apoptotic and necrotic cell death in vitro and in vivo. *Methods*. 2013;61(2):117-129.
40. Zhu Y, Cui H, Lv J, et al. Angiotensin II triggers RIPK3-MLKL-mediated necroptosis by activating the Fas/FasL signaling pathway in renal tubular cells. *PLoS One*. 2020;15(3):1-19.
41. Galluzzi L, Aaronson SA, Abrams J, et al. Guidelines for the use and interpretation of assays for monitoring cell death in higher eukaryotes. *Cell Death Differ*. 2009;16(8):1093-1107.
42. Wen S, Ling Y, Yang W, et al. Necroptosis is a key mediator of enterocytes loss in intestinal ischaemia/reperfusion injury. *J Cell Mol Med*. 2017;21(3):432-443.
43. Wu W, Liu P, Li J. Necroptosis: An emerging form of programmed cell death. *Crit Rev Oncol Hematol*. 2012;82(3):249-258.
44. Sawai H, Domae N. Discrimination between primary necrosis and apoptosis by necrostatin-1 in Annexin V-positive/propidium iodide-negative cells. *Biochem Biophys Res Commun*. 2011;411(3):569-573.
45. Fang X, Wang H, Han D, et al. Ferroptosis as a target for protection against cardiomyopathy. *Proc Natl Acad Sci U S A*. 2019;116(7):2672-2680.
46. Neiteimeier S, Jelinek A, Laino V, et al. BID links ferroptosis to mitochondrial cell death pathways. *Redox Biol*. 2017;12:558-570.
47. Jelinek A, Heyder L, Daude M, et al. Mitochondrial rescue prevents glutathione peroxidase-dependent ferroptosis. *Free Radic Biol Med*. 2018;117:45-57.
48. Bae S, Park M, Kang C, Dilmen S, Kang TH, Kang DG. Hydrogen Peroxide-Responsive Nanoparticle Reduces Myocardial Ischemia/Reperfusion Injury. *J Am Heart Assoc*. 2016:1-11.
49. Schröder E, Eaton P. Hydrogen peroxide as an endogenous mediator and exogenous tool in cardiovascular research: issues and considerations. *Curr Opin Pharmacol*. 2008;8(2):153-159.
50. Weber K, Roelandt R, Bruggeman I, Estornes Y, Vandenabeele P. Nuclear RIPK3

- and MLKL contribute to cytosolic necrosome formation and necroptosis. *Commun Biol.* 2018;1(1):1-13.
51. Rodriguez DA, Weinlich R, Brown S, et al. Characterization of RIPK3-mediated phosphorylation of the activation loop of MLKL during necroptosis. *Cell Death Differ.* 2016;23(1):76-88.
 52. Yoon S, Bogdanov K, Kovalenko A, Wallach D. Necroptosis is preceded by nuclear translocation of the signaling proteins that induce it. 2016:253-260.
 53. Cai Z, Jitkaew S, Zhao J, et al. Plasma membrane translocation of trimerized MLKL protein is required for TNF-induced necroptosis. *Nat Cell Biol.* 2014;16(1):55-65.
 54. Yin B, Xu Y, Wei RL, He F, Luo BY, Wang JY. Inhibition of receptor-interacting protein 3 upregulation and nuclear translocation involved in Necrostatin-1 protection against hippocampal neuronal programmed necrosis induced by ischemia/reperfusion injury. *Brain Res.* 2015;1609(1):63-71.
 55. Weber K. Nuclear RIPK3 and MLKL contribute to cytosolic necrosome formation and necroptosis. *Commun Biol.* (2018):1-13.
 56. Yang Y, Ma J, Chen Y, Wu M. Nucleocytoplasmic shuttling of receptor-interacting protein 3 (RIP3): Identification of novel nuclear export and import signals in RIP3. *J Biol Chem.* 2004;279(37):38820-38829.
 57. Sosna J, Voigt S, Mathieu S, et al. TNF-induced necroptosis and PARP-1-mediated necrosis represent distinct routes to programmed necrotic cell death. *Cell Mol Life Sci.* 2014;71(2):331-348.
 58. Abramoff MD, Magalhães PJ, Ram SJ. Image processing with imageJ. *Biophotonics Int.* 2004;11(7):36-41.



*Human induced pluripotent stem cell derived cardiomyocytes
CVI-273 P35 d40*

Chapter 3

METABOLIC MATURATION INCREASES HUMAN IPSC-DERIVED CARDIOMYOCYTE SUSCEPTIBILITY TO HYPOXIC INJURY

Submitted

*Marijn M.C. Peters*¹, Renee G.C. Maas¹, Iris van Adrichem¹, Pieter A.M. Doevendans¹, Mark Mercola², Tomo Šarić³, Steven A.J. Chamuleau^{1,4}, Joost P.G. Sluijter¹, Anna P. Hnatiuk^{2*}, and Klaus Neef^{1*}

¹ Department of Cardiology, Laboratory of Experimental Cardiology, Regenerative Medicine Centre Utrecht, University Medical Centre Utrecht, University Utrecht, Utrecht, the Netherlands

² Cardiovascular Institute and Department of Medicine, Stanford University, Stanford, CA 94305, USA

³ Center for Physiology and Pathophysiology, Institute for Neurophysiology, Faculty of Medicine and University Hospital Cologne, University of Cologne, Cologne, Germany

⁴ Amsterdam UMC Heart Center, Department of Cardiology, Amsterdam, the Netherlands

* Equal contribution

ABSTRACT

Development of new cardioprotective approaches by using *in vivo* models of human ischemic heart disease remains challenging because the physiology of the human heart differs significantly from rodent animal hearts. Human induced pluripotent stem cell-derived cardiomyocytes (hiPSC-CMs) have been considered a very promising tool for translational studies. However, their immature nature remains a roadblock for human cardiac disease modelling. To overcome this roadblock, media that improve maturation of hiPSC-CMs have recently been developed. Here, we test the effect of metabolic maturation on hypoxia susceptibility in hiPSC-CMs. hiPSCs were differentiated into CMs and matured either in RPMI/B27 medium or in previously defined maturation medium (MM). We induced hypoxia by exposure to 5% or 1% oxygen in nutrient-rich or nutrient-deprived media. CMs matured in RPMI/B27 medium did not show a significant increase in cell death during hypoxia, independent of media glucose or serum content (dead/live ratio: $0,02 \pm 0,004$ [24h 21% O₂]; $0,11 \pm 0,04$ [24h 1% O₂], $p > 0,05$). CMs matured in MM, however, did show an increase in cell death with increased duration of hypoxia ($0,58 \pm 0,06$ [0h]; $1,1 \pm 0,09$ [24h 1%]). Furthermore, only metabolically-matured CMs showed increased TUNEL+ CMs ($7,5\% \pm 1,3\%$ [control]; $42,2\% \pm 11,0\%$, $p < 0,001$ [24h 1% O₂]) and decreased viability, as measured by flow cytometry ($90,8\% \pm 0,71\%$ [control]; $76,3\% \pm 2,2\%$ [24h 1% O₂], $p < 0,01$) compared to immature CMs ($84,5\% \pm 2,0\%$ [control]; $73,7\% \pm 3,4\%$ [24h 1% O₂], $p > 0,05$). Furthermore, mitochondrial respiration was significantly inhibited in MM-matured hiPSC-CMs when exposed to 1% hypoxia for both 4 and 24 hours, compared to control media. Taken together, we show that hiPSC-CMs at higher level of maturation have increased susceptibility to hypoxia and are, therefore, more suitable to mimic ischemic heart disease *in vitro*. It would be of interest to further investigate the underlying metabolic mechanisms that influence the susceptibility to cardiac hypoxia.

INTRODUCTION

Ischemic heart disease is a major cause of death worldwide¹. The decrease in oxygen and nutrient availability in the myocardium leads to cardiomyocyte (CM) death and therefore loss of cardiac contractile force². Current clinical therapies focus on early reperfusion of the ischemic tissue, thereby decreasing the tissue damage which occurs after myocardial infarctions but also resulting in additional myocardial injury through the generation of reactive oxygen species (ROS)^{3,4}, referred to as ischemia/reperfusion (I/R) injury. To develop improved therapeutic approaches to protect the heart from I/R injury, both animal models and *in vitro* disease modelling platforms are often used. Although cardioprotective factors have shown promising therapeutic effects in *in vitro* cell models and in animal experiments, they failed in showing clear beneficial effects in clinical trials⁵. The role of comorbidities, ageing, and the use of medication, which are not included in preclinical models, are brought forward as explanation for this translational failure. On top of these considerations, it is likely that the used models are also not completely predictable for human CM behaviour through the considerable difference between CMs in the human heart and those in animal hearts⁶, including calcium handling⁷, electrophysiology⁷, myofilament composition^{8,9}, maturation expression profile¹⁰, and metabolism¹¹. The development of human induced pluripotent stem cell (hiPSC) technology¹² and their differentiation into cardiomyocytes (CMs)¹³ opened doors for more suitable human-based cardiac disease modelling by the generation of patient-specific CMs and pre-clinical screening of therapeutics¹¹. Although offering clear advantages by having a human basis, hiPSC-CMs derived from a 20-day differentiation protocol have a foetal rather than adult CM phenotype^{14,15}. Adult human CMs generate 90% of their energy from mitochondrial oxidative phosphorylation while neonatal rat CMs and hiPSC-CMs use glycolysis as their main energy source, as reflected in a lower expression of fatty acid β -oxidation markers^{16,17}. Especially for disease processes governed by increased anaerobic glycolysis, increased basal glycolysis and absence of glucose

oxidation, immature hiPSC-CMs could limit efficient disease modelling and clinical predictability^{16,18}. Deprivation of oxygen and nutrients in adult CMs leads to cellular damage due to the high reliance of adult CMs on oxygen-dependent β -oxidation¹⁹. This makes modelling of ischemic heart disease in immature CMs challenging. Several studies focussed on increasing the maturation of hiPSC-CMs by stimulating the post-natal shift from anaerobic glycolysis-dependent metabolism to aerobic β -oxidation^{20–23}. In this study, we test whether immature hiPSC-CMs can be sensitized to oxygen deprivation and if metabolic maturation of hiPSC-CMs improves the susceptibility of the CMs to oxygen and nutrient deprivation. Furthermore, we assess the effect of short- and long-term hypoxia and the effect of the reintroduction of oxygen and nutrients that can model I/R damage.

RESULTS

Immature hiPSC-CMs are not sensitive to hypoxia

To develop an *in vitro* ischemia and I/R model, we differentiated hiPSCs to CMs using the well-established RPMI/B27-based differentiation protocol²⁴. In the differentiation process, we included two purification and two replating steps to generate a high-purity cardiomyocyte population (ACTN⁺: 83,3 \pm 1,3; **Figure 1a-c**). The CMs resembled an immature CM phenotype with a basal proliferative rate (5,9% \pm 0,8%; Ki67-positive cells **Figure 1d**), similar to reported values in neonatal mice and young infant hearts^{25,26}.

To test the sensitivity of hiPSC-CMs to oxygen and nutrient deprivation, we exposed the cells to hypoxia in media of variable nutrient compositions (**Supplementary table 1**). In short, three different media were included: a) lipid-poor and glucose-rich media (DMEM/10% knockout serum replacement and RPMI/B27 medium), b) low-glucose media (RPMI no glucose/B27 medium) and c) lipid-rich low-glucose

Metabolic maturation increases human iPSC-derived cardiomyocyte susceptibility to hypoxic injury

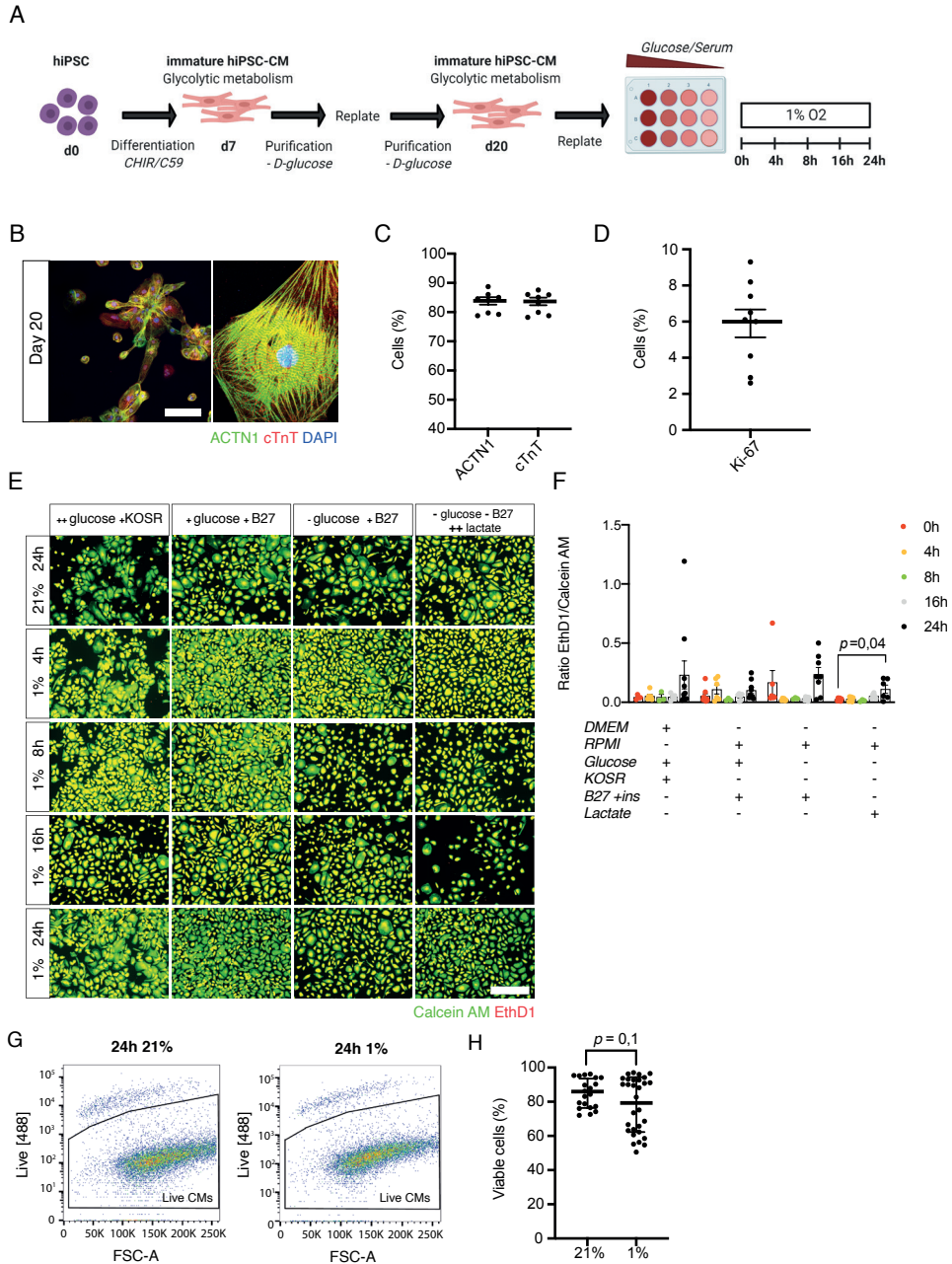


Figure 1. Oxygen deprivation does not induce reproducible damage in immature hiPSC-cardiomyocytes

A. Schematic representation of experimental set-up. **B, C.** ACTN1 and cTnT expression of day 20 hiPSC-cardiomyocytes (CMs) in immunofluorescence microscope images (**B**) and flow cytometry (**C**). **D.** Ki-67 positivity of day 20 hiPSC-CMs. **E.** Calcein AM/ethidium homodimer-1 staining of day 20 hiPSC-

Figure 1 continued

CM cultured in media with indicated nutrient compositions (++glucose++serum: 10%KOSR/DMEM/B27; +glucose+serum: RMP/B27; glucose+serum: RPMIpur/B27; -glucose-serum+lactate: RPMI/pur/lactate) exposed to 21% oxygen for 24h or 1% oxygen for 4, 8, 16, 24h and quantification (**F**). **G**. Flow cytometry analysis of viability of day 20 CMs cultured for 24h in 21% or 1% oxygen and quantification (**H**). Data were analysed using one-way ANOVA and Dunnett multiple comparison. * $P < 0,05$. Scale bar: 200 μ m. Data are shown as mean \pm SEM.

medium (RPMI no glucose/lactate/lipid) to test whether glucose, serum and lipid media-content would increase susceptibility to hypoxia. Incubation in 1% oxygen did not lead to increased cell death of 20-days old lactate-purified CMs in the presence of glucose compared to normal culture at 21% oxygen ($0,05 \pm 0,02$ [21%]; $0,1 \pm 0,03$ [24h 1%], $P > 0,05$; **Figure 1e, f**). In the absence of glucose, the exposure of 20-days old CMs for 24h to lactate medium, slightly increased the percentage of dead cells, as shown by a significant increase in ethidium homodimer-1/calcein AM ratio ($0,02 \pm 0,005$ [21%]; $0,11 \pm 0,004$ [24h 1%], $\alpha = 0,04$). To more accurately quantify the effect of the long-term (24h) oxygen deprivation on CM viability, we assessed the degree of membrane disruption with an amine-reactive dye by flow cytometry. Although in 12 out of 30 experiments a small reduction in cell viability was observed, the overall viability in the used cell lines remained statistically unchanged ($85 \pm 1,9$ [21%]; $78,3 \pm 3,0$ [24h 1%], $P = 0,1$; **Figure 1g, h**).

Metabolically matured hiPSC-CMs are sensitive to hypoxia

To investigate whether further stimulation towards more metabolic mature CMs (e.g. lower resting membrane potential, rapid depolarization, increased Ca^{2+} dependence, sarcomere organization and force generation) would increase the susceptibility of the CMs to hypoxia, we used prolonged cultivation in our previously described metabolic maturation medium²⁰ (**Figure 2a**). Compared to the immature 20 days-old CMs, maturation medium increased the purity of CMs at day 40 of differentiation as

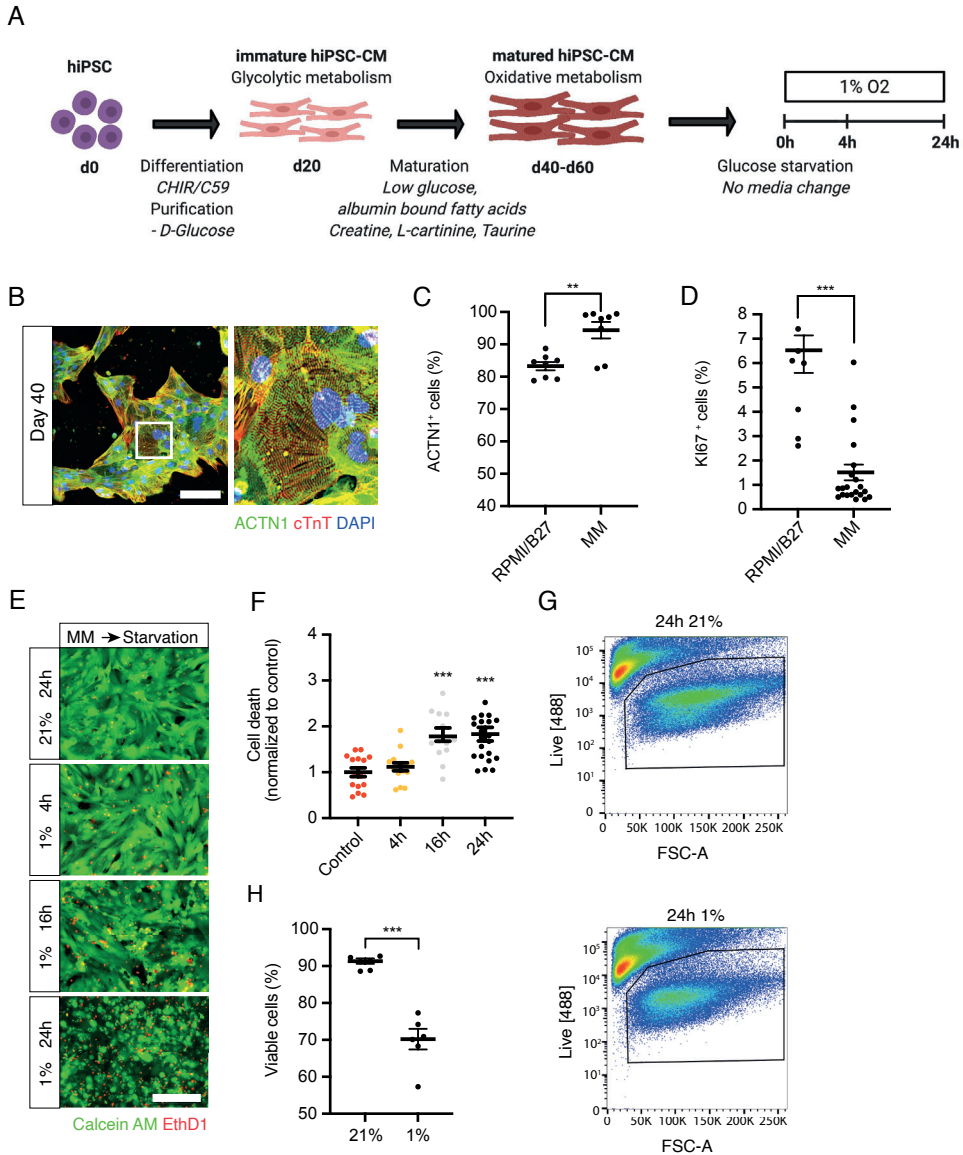


Figure 2. Oxygen deprivation induces cell death of mature hiPSC-CMs

A. Schematic representation of experimental set-up. **B, C.** ACTN1 and cTnT expression of day 40 metabolically matured hiPSC-cardiomyocytes (CMs) in immunofluorescence microscope images (B) and flow cytometric analysis of ACTN1 expression (C). **D.** Ki-67 positivity of day 40 matured hiPSC-CMs compared to day 20 hiPSC-CMs. **E.** Calcein AM/ethidium homodimer-1 staining of day 40 matured hiPSC-CMs exposed to 21% oxygen for 24h or 1% oxygen for 4, 8, 16, or 24h and quantification (F). **G, H.** Flow cytometry analysis day 40 matured hiPSC-CMs viability after 24h in 21% or 1% oxygen and quantification (H). Data were analysed using one-way ANOVA and Dunnett multiple comparison. * $P < 0,05$, ** $P < 0,01$, *** $P < 0,001$, Scale bar: 200µm. Data are shown as mean \pm SEM.

seen by ACTN1 immunoreactivity ($83,3 \pm 1,3\%$ [RPMI/B27] vs $94,4 \pm 2,6\%$ [MM], $P < 0,01$, **Figure 2b, c**) and decreased Ki-67 positivity, as described previously²⁰ ($5,9 \pm 0,77$ [RPMI/B27] vs $1,4 \pm 0,32$ [MM], $P < 0,01$; **Figure 2d**). In contrast to immature 20-days-old CMs, metabolically matured 40-days-old CMs showed significantly increased cell death after 16h and 24h of hypoxia when normalized to atmospheric oxygen level controls ($1,78 \pm 0,14$ fold [16h 1%]; $1,83 \pm 0,15$ fold [24h 1%]; **Figure 2e, f**). Sensitivity to hypoxia was further confirmed by a reduction in cell viability as determined by flow cytometry ($90,8 \pm 0,71\%$ [21%] vs $70,0 \pm 3,6\%$ [24h 1%], $P < 0,001$; **Figure 2g, h**).

We further extended our analyses in metabolically-matured CMs, by including a more tissue-like physiological normoxia condition of 5% oxygen (**Figure 3a**)²⁷. Although matured CMs showed stable α -actinin expression ($92,7 \pm 3,35\%$ [24h 21%]; vs $93,8 \pm 1,7\%$, $P = 0,74$ [24h 1%]; **Supplemental figure 1**) as measured by flow cytometry, both incubation in 5% and 1% oxygen decreased defined myofibrillar organization as seen by α -actinin and cardiac troponin T (cTnT) immunoreactivity (**Figure 3b, c**).

Furthermore, an increased number of TUNEL⁺ CMs was observed after short (4h) periods of hypoxia of 5% ($25,5 \pm 1,2\%$) and 1% ($23,7 \pm 1,6\%$) oxygen compared to atmospheric oxygen concentration ($15,4 \pm 0,83\%$) in metabolically matured CMs ($p < 0,05$; **Figure 3d, e**). Increased duration of hypoxia, elevated the percentage of TUNEL⁺ CMs from $12,0 \pm 1,5\%$ in the control group to $41,5 \pm 4,5\%$ and $37,6 \pm 3,5\%$ in the 5% and 1% oxygen group, respectively ($p < 0,001$; **Figure 3d, e**). We did not observe a significant difference in the number of TUNEL⁺ nuclei between 5% and 1% oxygen, both after short (4h) or long-term (24h) hypoxia.

To determine whether oxygen saturation affects the CM glucose consumption and lactate production, we collected conditioned media after exposure to 4h or 24h hypoxia and measured glucose, lactate and lactate dehydrogenase concentrations. Glucose consumption in matured CMs cultures at 1% for 4h ($2,08 \pm 0,37$ mM) did

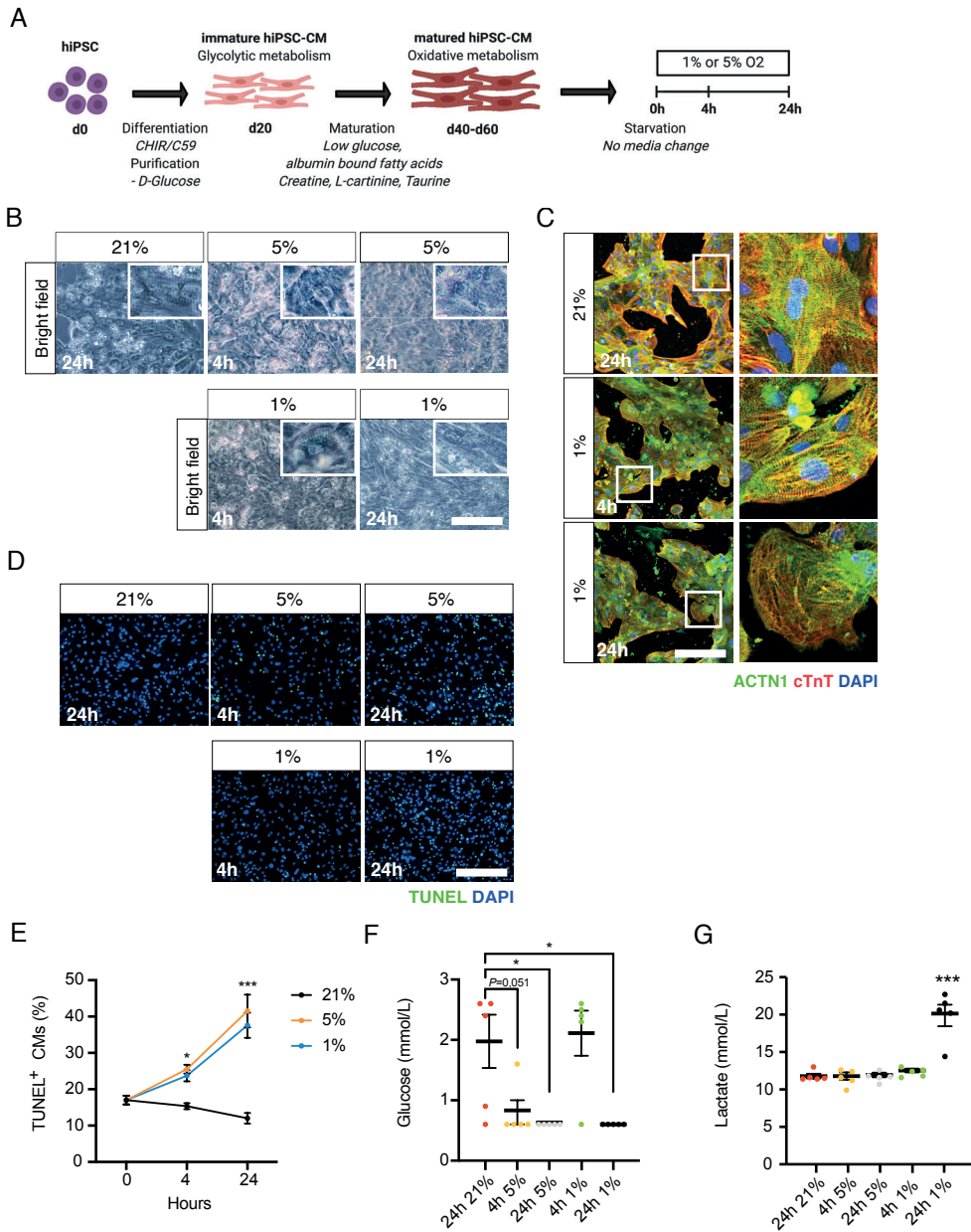


Figure 3. Oxygen saturation of 5% is sufficient to induce cell death of matured hiPSC-cardiomyocytes

A. Schematic representation of experimental set-up. **B.** Bright-field images of cardiomyocytes exposed to 21%, 5% or 1% oxygen for 4 or 24h in nutrient starvation. **C.** Representative microscopic images of ACTN1 and cTnT staining. Square indicates area of close-up. **D.** Representative microscopic images of TUNEL-stained cardiomyocyte nuclei. **E.** Quantification of TUNEL staining. **F-H.** Media glucose (**F**), lactate (**G**) levels after 4 to 24h incubation in 21%, 5% or 1% oxygen. Data were analysed using one-

Figure 3 continued

way ANOVA and Dunnett multiple comparison. * $P < 0,05$, ** $P < 0,01$, *** $P < 0,001$, Scale bar: 200 μm . Data are shown as mean \pm SEM.

not significantly differ from that in control CMs kept at 21% oxygen for 24h ($1,82 \pm 0,44\text{mM}$, $P > 0,05$, **Figure 3f**). However, CMs cultured in 5% oxygen for 4h consumed a significantly higher amount of glucose thus reducing its concentration in the medium ($0,8 \pm 0,2 \text{ mM}$, $P = 0,05$). 24h of cultivation at both 5 and 1% oxygen significantly increased glucose consumption by matured CMs, thereby reducing glucose levels below the reference value of 0,6 mM. Lactate concentrations in the medium increased only when CMs were incubated for 24h in 1% oxygen and not in 5% oxygen (from $11,8 \pm 0,31\text{mM}$ [21%], $11,7 \pm 0,3\text{mM}$ [5%] to $19,9 \pm 1,4 \text{ mM}$ [1%], $P < 0,001$, **Figure 3g**).

Metabolic profiling of immature and matured hypoxic hiPSC-CM

Even though hypoxia did not increase cell death in immature CMs, lack of oxygen might still inhibit mitochondrial function. To determine the effect of hypoxia on oxidative mitochondrial respiration in 20-day-old immature and 40-day-old mature CMs, we assessed their oxygen consumption rate under atmospheric as well as under and short-term (4h) and long-term (24h) hypoxia. Irrespective of whether they were cultured in glucose-rich or glucose-deprived media, immature CMs were less sensitive to short- and long-term hypoxia compared to matured CMs (**Figure 4a-c**). In matured CMs, the basal respiration, ATP production, proton leak, maximal respiration, and spare respiratory capacity were significantly decreased upon both short and long-term hypoxia. The non-mitochondrial respiration capacity was significantly reduced only upon long-term hypoxia. All together, these results provide further support for our findings that more-mature hiPSC-CMs are metabolically reliant on oxidative phosphorylation and are significantly more sensitive to hypoxia compared to younger CMs cultured in glucose-or lactate-rich media. Comparative

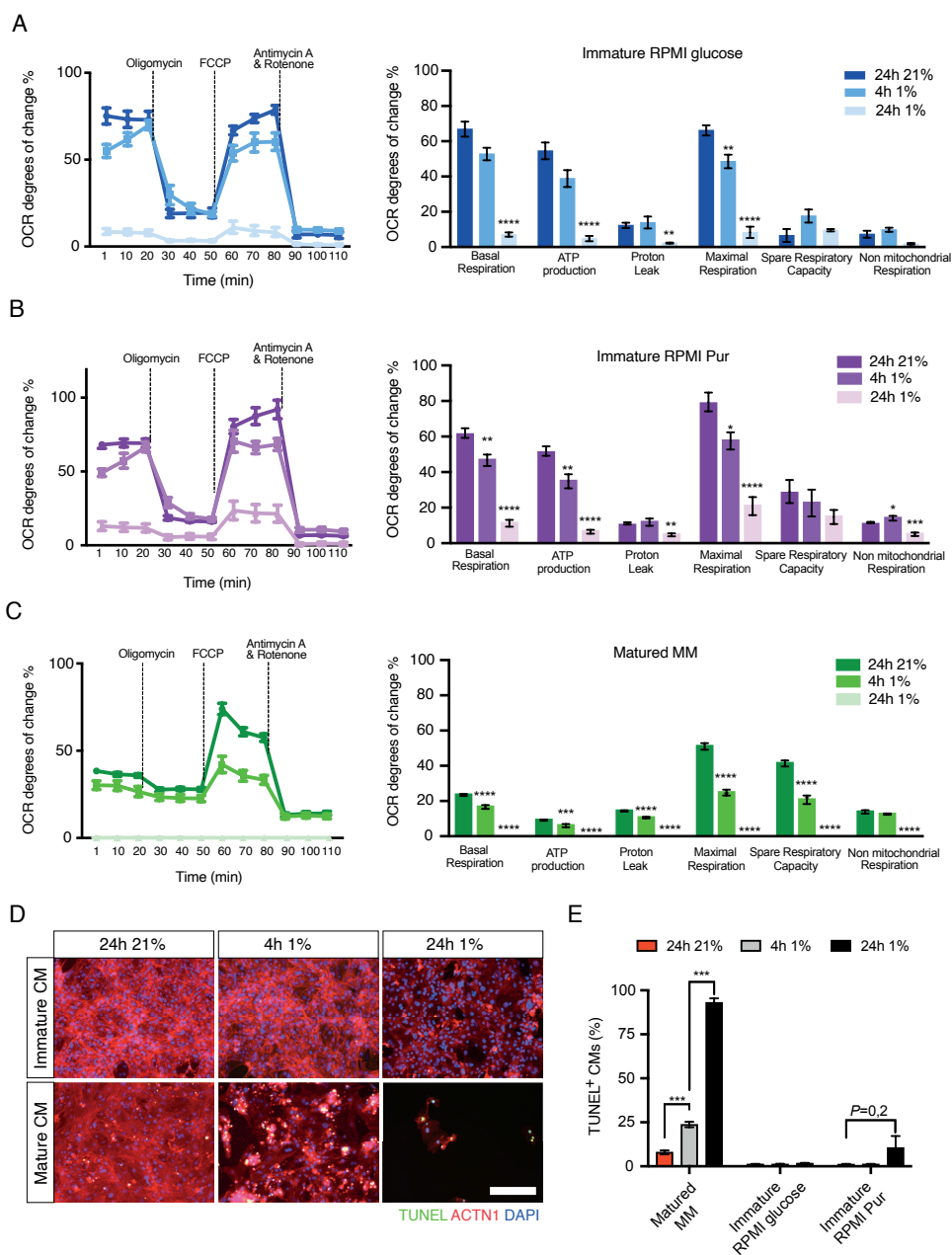


Figure 4. Metabolic profiling of hypoxic immature and mature hiPSC-CMs

A-C. Normalized real-time oxygen consumption rate (OCR) of immature hiPSC-CMs in RPMI/B27 glucose media (**A**), RPMI/B27 no glucose (purification) media (**B**) and metabolically matured hiPSC-CMs (**C**) in normoxia (21% 24h), short-term hypoxia (1% 4h), or long-term hypoxia (1% 24h) as measured by Seahorse extracellular flux analyser. Cells were treated with oligomycin, FCCP, and antimycin A and rotenone to measure mitochondrial respiration. Data are normalized to highest OCR in group. **D.** Co comparative images of TUNEL staining of cardiomyocytes used in metabolic profiling. **E.** Quantification of

Figure 4 continued

TUNEL stain. Graphs **A-C** represent data from 1-2 replicated experiments and 1-2 cardiac differentiations (n=5). Scale bar: 200µm. Data were analysed using one-way ANOVA and Dunnett multiple comparison. *P<0,05, ** P<0,01, ***P<0,001, ****P<0,0001. Scale bar: 200µm. Data are shown as mean ± SEM.

analysis demonstrated that cultivation at 1% oxygen increased the fraction of TUNEL⁺ apoptotic cells in the population of mature CMs from $7,92 \pm 1,09\%$ in the control group to $23,8 \pm 1,5\%$ in short-term hypoxia and $93,0 \pm 2,4\%$ in long-term hypoxia (P<0,001) without increasing TUNEL-positivity in immature CMs ($1,1 \pm 0,23\%$ [24h 21%], $1,18 \pm 0,2\%$ [4h 1%], $10,6 \pm 6,6\%$ [24h 1%], P>0,05; **Figure 4d, e**). These results strongly suggest that CMs, cultured in the presence of glucose, resemble the immature embryonic CM phenotype with respect to their energy substrate utilization, active metabolic pathways, and survival upon low oxygen exposure. In contrast, hiPSC-CMs cultured for longer time in the presence of fatty acids as the primary energy source, more closely resemble adult CMs, consistent with previous reports²⁰. Interestingly, we found that matured-CMs are more sensitive to the low oxygen environment, leading to an ultra-low mitochondrial function, DNA fragmentation, and ultimately apoptosis.

DISCUSSION

In the present study, we observed that the conventional method of hiPSC differentiation and maturation in RPMI/B27-based media generates CMs that are insensitive to ischemic cell death. Furthermore, we show metabolic maturation of hiPSC-CMs increases susceptibility to ischemic cell death. The ability of immature hiPSC-CMs to increase the glycolytic flux in anaerobic conditions is in line with the characteristics of foetal CMs that have a lower threshold to reach oxygen insufficiency²⁸⁻³⁰. During development, arterial blood oxygen saturation fluctuates around 3% but this would be considered hypoxia in the adult heart based on the activation of hypoxia-induced gene

expression²⁹. Foetal CMs develop under low oxygen conditions and use anaerobic energy pathways for cardiac growth. The low oxygen saturation stabilizes hypoxia-inducible factor 1 α (HIF1 α) in foetal CMs thereby enhances glycolytic metabolism via LDH-A regulation in the compact myocardium and preventing CM maturation^{23,30,31}. Also in hiPSC-CMs, inhibition of HIF1 α has been related to CM maturation and shifting metabolism from aerobic glycolysis towards oxidative phosphorylation²³. High glucose-containing cell culture media, having concentrations \sim 15 mmol/L do not represent the metabolic cues in the human *in vivo* situation, where concentrations range around \sim 3 mmol/L nor support effective CM maturation³². Furthermore, a four-fold postnatal increase in circulating fatty acids contributes to the increased fatty acid β -oxidation in adult cardiomyocytes^{32,33}. Despite their main use of aerobic glycolysis, we did observe a decrease in mitochondrial respiration rate in immature hiPSC-CMs following hypoxia. This could be related to the reoxygenation step required for Seahorse analysis. Reperfusion-related damage is caused by the release of reactive oxygen species upon the sudden increase in oxygen availability⁴. Hypoxia and reoxygenation have previously been shown to induce only limited damage, lacking an increase in HIF1 α expression, while prolonged hypoxia alone did not affect the beating frequency in immature hiPSC-CMs²⁸. A previously observed limited effect of hypoxia compared to reperfusion injury on calcium overload in immature hiPSC-CMs³⁴, potentially explains the effect measured in our seahorse assay. During maturation, the glycolytic metabolism is insufficient to generate adequate ATP levels for cardiac contractions³¹. The increased oxygen availability around birth decreases HIF1 α , which mediates the mitochondrial shift towards more energy-efficient oxidative phosphorylation-based metabolism^{30,35}. With this increased availability of ATP, CMs mature with a concomitant increase in ploidy, myofibrillar organization, and the number of mitochondria that support cardiac contractility³¹. However, these changes and the increased contractile demand might functionally limit metabolic flexibility. In contrast to immature hiPSC-CMs, we observed that metabolically matured

hiPSC-CMs were sensitive to hypoxia-induced cell death and showed decreased mitochondrial respiration after 4 hours of hypoxia. Additionally, lactate production as a result of anaerobic glycolysis was not observed in normoxic conditions or in short-term hypoxia but did increase in prolonged hypoxia, indicating that only after longer hypoxic conditions the metabolically matured hiPSC-CMs shift towards anaerobic glycolysis. This observation was in line with the drop in glucose levels in these conditions. Interestingly, we showed that 5% oxygen, considered physiologically normoxia in most tissue²⁷, induced a similar degree of cell death as 1% oxygen in metabolically matured hiPSC-CMs. This underscores the idea that hypoxia-induced cell death pathways are already induced at a decrease from 21% to 5% oxygen, although previous studies suggested oxygen concentrations between 0,5 and 2% to be cellular hypoxia³⁴. This difference in tissue-like physiological normoxia and cell culture normoxia is an important factor to take into account when modelling hypoxia-related diseases in *in vitro* models.

In summary, we have shown that metabolically matured hiPSC-CMs are more sensitive to ischemic injury and are therefore more suitable to model human ischemic heart disease *in vitro*. With this model, we show that CM apoptosis is increased after 4h exposure to 5% or 1% oxygen, which can be used to test cardioprotective and regenerative approaches in translation to clinical therapy.

METHODS

Cell culture. The female hiPSC line CVI-273 was kindly provided by Joseph Wu, Stanford University (CVI-273, Sendai virus reprogrammed). The female hiPSC line NP0141-31B (UKKi032-C) was generated in the Šarić group from peripheral blood mononuclear cells using the Sendai virus-based reprogramming method as previously described^{36,37}. This line is deposited at the European Bank for induced Pluripotent Stem Cells (EBiSC, <https://ebisc.org/>) and is registered in the online

registry (hPSCreg (<https://hpsreg.eu/>). hiPSCs were grown in Essential 8™ medium (Gibco A1517001). When reaching 80-90% confluency, differentiation to CMs was initiated by changing medium to RPMI 1640 (ThermoFisher Scientific 11875085) supplemented with 2% B27 minus insulin (ThermoFisher Scientific A1895601) (B27- medium) and 7uM CHIR99021 (Selleck Chemicals S2924). After 3 days, cells were supplemented with B27-medium and 2 uM Wnt-C59 (R&D systems 5148) to inhibit canonical Wnt signaling. On day 7, the medium was changed to RPMI 1640 and 2% B27 plus insulin supplement (ThermoFisher Scientific, 17504001) (B27+ medium) followed by purification in no glucose RPMI 1640 (ThermoFisher Scientific, 118979020) and 2% B27 plus insulin supplement on day 9. On day 11 of differentiation, cells were re-plated in B27+ medium supplemented with 10% KnockOut™ serum replacement (KOSR, ThermoFisher Scientific, 108280028) and 10 μM selective Rock-1 inhibitor Y-27632 (Selleck Chemicals, S1049). After the second purification on day 14 for two days in no glucose RPMI 1640, the medium was changed to B27+ medium. On day 20, the purification medium was changed to maturation medium²⁰ or cells were kept in B27+ medium. Cells were matured in maturation medium for 3 weeks before re-plating with medium changes every four days.

Damage induction. Before hypoxia, the medium was changed to medium containing variable nutrient compositions (**Supplementary table 1**). Ischemia was induced by incubation in a 5% hypoxia incubator (NuAire) or 1% oxygen using BD GasPak™ EZ Pouch system.

Immunofluorescent staining. After fixation in 4% paraformaldehyde for 30 minutes, cells were permeabilized in 0,1% Triton-X100 before blocking in 10% normal goat serum/1% BSA (Millipore Sigma). Primary antibodies used were: α-actinin (Sigma-Aldrich A7811, 1:00), cardiac troponin T (Abcam ab45932, 1:100), Ki-67 (Abcam ab8330, 1:200), pH3 (Cell Signaling Technology #9701 1:200), and aurora b kinase

(Abcam ab2254, 1:100). Detection was mediated by incubation with Alexa Fluor® antibody conjugates (ThermoFisher Scientific) and nuclei were visualised using DAPI. Mounting was performed using Fluoromount-G™ mounting medium (ThermoFisher Scientific). For apoptotic cell death analysis, TUNEL assays (Roche) were performed according to the manufacturer's instructions. Imaging was performed on a confocal microscope (Leica Sp8x) and image analysis using ImageJ.

Flow cytometry. Cells were gently dissociated with multi tissue dissociation kit (Miltenyi Biotec) and incubated with LIVE/DEAD™ fixable green dead cell stain kit (ThermoFisher Scientific). This kit contains a fixable fluorescent dye that binds to amines. In living cells, this amine-reactive dye can only bind amines on the cell surface as opposed to dead cells in which the dye can additionally bind exposed amines on the interior of the cell due to membrane disruption leading to a higher fluorescent labeling of dead cells. After live dead staining, cells were fixed in inside fix solution (Miltenyi Biotec) and stained with primary antibodies diluted in inside perm solution (Miltenyi Biotec). α -actinin-VioBlue (Miltenyi Biotec, 1:10) and cardiac troponin-t VioBlue (Miltenyi Biotec, 1:10) were used as conjugated antibodies. As a control, universal isotype control antibodies (REA Miltenyi Biotec) were used. Media and washes were collected to obtain a complete representation of cell loss. The samples were analysed using FACS Canto system (BD Bioscience) and FlowJo software.

Seahorse analysis. Mitochondrial respiration was measured using a XF24 Extracellular Flux Analyzer (Seahorse Bioscience, Billerica, MA) to assess the effect of hypoxia on the electron transport chain complexes. XF24 plates were used and coated with 0.1 mg/mL matrigel before cells were seeded at a density of 1.0×10^5 cells per well. 24h or 4h before Seahorse analysis, plates were placed in a BD GasPak™ EZ Pouch system to induce hypoxia. 1 hour before plate measurement, cell culture media were removed and cells were washed with Seahorse XF DMEM

Basal Medium (Agilent) supplemented with 2% B27 (Gibco), 4mM glutamine (Gibco), 10mM glucose, and 1% chemically defined lipid concentrate (Gibco) three times. During the measurements, stress test inhibitors were added: oligomycin (2,5mM), carbonyl cyanide-p-trifluoromethoxyphenyl-hydrazone (FCCP) (2,5mM), rotenone and antimycin A (2,5mM). At the end of measurement, the oxygen consumption rate (OCR) values were normalized to cell nuclei per well by Hoechst staining and 20x magnification imaging using the Evos Flويد microscope and ImageJ. Baseline respiration was calculated by subtracting the OCR after rotenone and antimycin A addition from the respiration as measured at the first time point. ATP production was calculated as the OCR at the first time point minus the OCR after oligomycin infusion. The proton leak was determined by subtracting the OCR after FCCP infusion from the value after oligomycin infusion. Maximal OCR was calculated as the difference between the OCR after FCCP infusion and after rotenone and antimycin A infusion. Respiratory capacity was calculated by subtracting the difference between the OCR before the addition of inhibitors and after rotenone and antimycin A infusion from the OCR after FCCP infusion. Lastly, non-mitochondrial respiration was defined as the OCR after rotenone and antimycin A infusion. The highest rates per plate were normalized to 100% rate per well. The experiment was done in 1-2 biological replicates, with each replicate consisting of 5 technical repeats per condition (Mean \pm SEM, n=3 counts/well).

Statistical analysis. hiPSC lines from two donors were used and the number (n) depicted in individual figures represents the number of independent experiments performed. Each experiment was performed with both cell lines to confirm reproducibility. Statistical analysis was performed using Prism 8 (GraphPad) software and quantifications were represented as mean \pm SEM. To compare the expression of 2 groups a normality test was performed followed by a Student's t-test. For >2 groups, one-way ANOVA was used after confirmation of normal distribution with a Shapiro-Wilk test. Post-hoc analysis was done with Dunnett multiple comparisons to

determine statistically significant ($P < 0,05$) results.

ACKNOWLEDGEMENTS

The authors would like to acknowledge Joseph Wu for providing the CVI-273 hiPS cell line. Maïke Kreutzenbeck and Rebecca Dieterich, University of Cologne, for their technical support with the generation and characterisation of the NP0141-31B pluripotent stem cells. *Funding:* M.M.C.P. is supported by a Netherlands Cardiovascular Research Initiative (CVON) grant (REMAIN 2014B27), M.M. is supported by the National Institutes Health (5P01HL141084 and 1R01HL152055) and Foundation Leducq (CUREPLaN), and J.P.G.S and R.G.C.M are supported by the PLN foundation, J.P.G.S is supported by Horizon2020 ERC-2016-COG-EVICARE [725229] and BRAVE (grant number 874827). The UKKi032-C hiPSC line was generated in the project “European Bank for induced Pluripotent Stem Cells (EBiSC)”, which was supported by the Innovative Medicine Initiative Joint Undertaking (IMI-JU) funded by the European Commission and the European Federation of Pharmaceutical Industries and Associations (EFPIA, grant agreement No. 115582).

SUPPLEMENTAL FIGURES

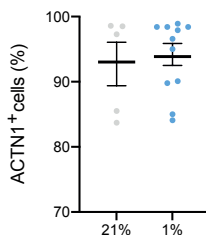


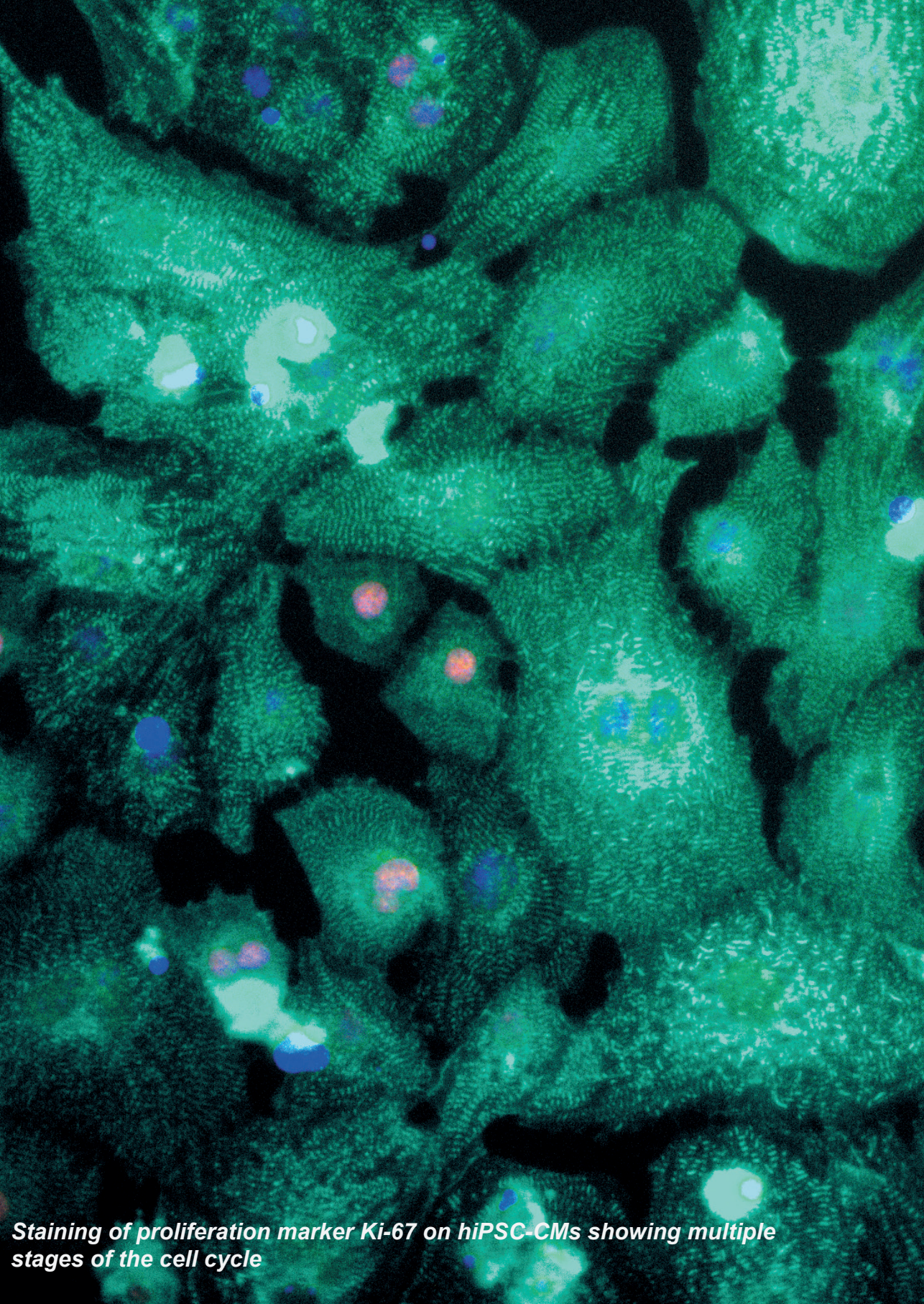
Figure S1. Oxygen deprivation does not lead to decreased ACTN1 positivity in mature hiPSC-CMs
Flow cytometry analysis of CMs after 24h in 21% oxygen or 1% oxygen. Data were analysed using one-way ANOVA and Dunnett multiple comparison. Data are shown as mean \pm SEM.

REFERENCES

1. Virani SS, Alonso A, Benjamin EJ, et al. *Heart Disease and Stroke Statistics—2020 Update: A Report from the American Heart Association.*; 2020.
2. Oerlemans MIFJ, Koudstaal S, Chamuleau SA, De Kleijn DP, Doevendans PA, Sluijter JPG. Targeting cell death in the reperfused heart: Pharmacological approaches for cardioprotection. *Int J Cardiol.* 2013;165(3):410-422.
3. Antman EM, Hand M, Armstrong PW, et al. 2007 Focused update of the ACC/AHA 2004 guidelines for the management of patients with ST-elevation myocardial infarction: A report of the American College of Cardiology/American Heart Association task force on practice guidelines. *Circulation.* 2008;117(2):296-329.
4. Ferrari R, Ceconi C, Curello S, et al. Role of oxygen free radicals in ischemic and reperfused myocardium. *Am J Clin Nutr.* 1991;53
5. Hausenloy DJ, Garcia-Dorado D, Bøtker HE, et al. Novel targets and future strategies for acute cardioprotection: Position Paper of the European Society of Cardiology Working Group on Cellular Biology of the Heart. *Cardiovasc Res.* 2017;113(6):564-585.
6. Milani-Nejad N, Janssen PML. Small and Large Animal Models in Cardiac Contraction Research: Advantages and Disadvantages. *Pharmacol Ther.* 2014;141(3):1-5.
7. Pond AL, Scheve BK, Benedict AT, et al. Expression of distinct ERG proteins in rat, mouse, and human heart. Relation to functional I(Kr) channels. *J Biol Chem.* 2000;275(8):5997-6006.
8. Swynghedauw B. Developmental and functional adaptation of contractile proteins in cardiac and skeletal muscles. *Physiol Rev.* 1986;66(3):710-771.
9. Marian AJ. On mice, rabbits and human heart failure. *Circulation.* 2005;111(18):2276-2279.
10. Uosaki H, Taguchi Y h. Comparative Gene Expression Analysis of Mouse and Human Cardiac Maturation. *Genomics, Proteomics Bioinforma.* 2016;14(4):207-215.
11. Karakikes I, Ameen M, Termglinchan V, Wu JC. Human Induced Pluripotent Stem Cell-Derived Cardiomyocytes: Insights into Molecular, Cellular, and Functional Phenotypes. *Circ Res.* 2015;117(1):80-88.
12. Takahashi K, Tanabe K, Ohnuki M, et al. Induction of Pluripotent Stem Cells from Adult Human Fibroblasts by Defined Factors. *Cell.* 2007;131(5):861-872.
13. Burridge PW, Keller G, Gold JD, Wu JC. Production of de novo cardiomyocytes: Human pluripotent stem cell differentiation and direct reprogramming. *Cell Stem Cell.* 2012;10(1):16-28.
14. Robertson C, Tran DD, George SC. Concise review: Maturation phases of human pluripotent stem cell-derived cardiomyocytes. *Stem Cells.* 2013;31(5):829-837.
15. Herron TJ. Calcium and voltage mapping in hiPSC-CM monolayers. *Cell Calcium.* 2016;59(2-3):84-90.
16. Ulmer BM, Eschenhagen T. Human pluripotent stem cell-derived cardiomyocytes for studying energy metabolism. *Biochim Biophys Acta - Mol Cell Res.* 2020;1867(3):118471.

17. Tohyama S, Hattori F, Sano M, et al. Distinct metabolic flow enables large-scale purification of mouse and human pluripotent stem cell-derived cardiomyocytes. *Cell Stem Cell*. 2013;12(1):127-137.
18. Fillmore N, Levasseur JL, Fukushima A, et al. Uncoupling of glycolysis from glucose oxidation accompanies the development of heart failure with preserved ejection fraction. 2018:1-12.
19. Hidalgo A, Glass N, Ovchinnikov D, et al. Modelling ischemia-reperfusion injury (IRI) in vitro using metabolically matured induced pluripotent stem cell-derived cardiomyocytes. *APL Bioeng*. 2018;2(2).
20. Feyen DAM, McKeithan WL, Bruyneel AAN, et al. Metabolic Maturation Media Improve Physiological Function of Human iPSC-Derived Cardiomyocytes. *Cell Rep*. 2020;32(3).
21. Ulmer BM, Stoehr A, Schulze ML, et al. Contractile Work Contributes to Maturation of Energy Metabolism in hiPSC-Derived Cardiomyocytes. *Stem Cell Reports*. 2018;10(3):834-847.
22. Horikoshi Y, Yan Y, Terashvili M, et al. Fatty acid-treated induced pluripotent stem cell-derived human cardiomyocytes exhibit adult cardiomyocyte-like energy metabolism phenotypes. *Cells*. 2019;8(1095):1-21.
23. Hu D, Linders A, Yamak A, et al. Metabolic maturation of human pluripotent stem cell-derived cardiomyocytes by inhibition of HIF1 α and LDHA. *Circ Res*. 2018;123(9):1066-1079.
24. Li Y, Chen X, Jin R, et al. Injectable hydrogel with MSNs/microRNA-21-5p delivery enables both immunomodification and enhanced angiogenesis for myocardial infarction therapy in pigs. *Sci Adv*. 2021;7(9):1-20.
25. Ye L, Qiu L, Zhang H, et al. Cardiomyocytes in Young Infants with Congenital Heart Disease: A Three-Month Window of Proliferation. *Sci Rep*. 2016;6(February):1-9.
26. Kretzschmar K, Post Y, Bannier-Hélaouët M, et al. Profiling proliferative cells and their progeny in damaged murine hearts. *Proc Natl Acad Sci U S A*. 2018;115(52):E12245-E12254.
27. Carreau A, Hafny-Rahbi B El, Matejuk A, Grillon C, Kieda C. Why is the partial oxygen pressure of human tissues a crucial parameter? Small molecules and hypoxia. *J Cell Mol Med*. 2011;15(6):1239-1253.
28. Häkli M, Kreutzer J, Mäki AJ, et al. Human induced pluripotent stem cell-based platform for modeling cardiac ischemia. *Sci Rep*. 2021;11(1):1-13.
29. J. Patterson A, Zhang L. Hypoxia and Fetal Heart Development. *Curr Mol Med*. 2010;10(7):653-666.
30. Ascutto RJ, Ross-Ascutto NT. Substrate metabolism in the developing heart. *Semin Perinatol*. 1996;20(6):542-563.
31. Menendez-Montes I, Escobar B, Palacios B, et al. Myocardial VHL-HIF Signaling Controls an Embryonic Metabolic Switch Essential for Cardiac Maturation. *Dev Cell*. 2016;39(6):724-739.
32. Slaats RH, Schwach V, Passier R. Metabolic environment in vivo as a blueprint for

- differentiation and maturation of human stem cell-derived cardiomyocytes. *Biochim Biophys Acta - Mol Basis Dis.* 2020;1866(10):165881.
33. Lopaschuk GD, Jaswal JS. Energy metabolic phenotype of the cardiomyocyte during development, differentiation, and postnatal maturation. *J Cardiovasc Pharmacol.* 2010;56(2):130-140.
 34. Wei W, Liu Y, Zhang Q, Wang Y, Zhang X, Zhang H. Danshen-Enhanced Cardioprotective Effect of Cardioplegia on Ischemia Reperfusion Injury in a Human-Induced Pluripotent Stem Cell-Derived Cardiomyocytes Model. *Artif Organs.* 2017;41(5):452-460.
 35. Neary MT, Ng KE, Ludtmann MHR, et al. Hypoxia signaling controls postnatal changes in cardiac mitochondrial morphology and function. *J Mol Cell Cardiol.* 2014;74:340-352.
 36. Matsa E, Burridge PW, Yu KH, et al. Transcriptome Profiling of Patient-Specific Human iPSC-Cardiomyocytes Predicts Individual Drug Safety and Efficacy Responses In Vitro. *Cell Stem Cell.* 2016;19(3):311-325.
 37. Hamad S, Derichsweiler D, Papadopoulos S, et al. Generation of human induced pluripotent stem cell-derived cardiomyocytes in 2D monolayer and scalable 3D suspension bioreactor cultures with reduced batch-to-batch variations. *Theranostics.* 2019;9(24):7222-7238.



Staining of proliferation marker Ki-67 on hiPSC-CMs showing multiple stages of the cell cycle

Chapter 4

INDUCTION OF CARDIOMYOCYTE PROLIFERATION, A NEW WAY FORWARD FOR TRUE MYOCARDIAL REGENERATION?

Adapted from:

Non-coding RNA Investigation. 2018, 2; 1-5. doi: 10.21037/ncri.2018.07.04

Published on 1 August 2018

Zhiyong Lei^{1,*}, *Marijn M.C. Peters*^{1,2,*}, and Joost P.G. Sluiter^{1,2}

¹ Department of Cardiology, Laboratory of Experimental Cardiology, University Medical Centre Utrecht, University Utrecht, Utrecht, the Netherlands

² UMC Utrecht Regenerative Medicine Centre, University Medical Centre Utrecht, the Netherlands

* Equal contribution

HEART FAILURE AND CURRENT THERAPIES

Ischemic heart disease (IHD) and heart failure (HF) are major causes of morbidity and mortality worldwide and although acute treatment during myocardial infarction has improved significantly, chronic burden of the disease gained much attention recent years^{1,2}. The major cause of the failing hearts, the loss of contractile cardiomyocytes, is currently still a problem to overcome. The only treatment modalities that are nowadays available for contractile dysfunction includes left ventricle assist devices (LVAD) and heart transplantation. Both are well accepted therapies but with different draw-backs for large patient groups, thereby pointing to the lack of enough donor hearts and the need for endured medication use³. Regenerative medicine is a direction in which the loss of contractile tissue is aimed to be recovered by the exogenous addition of progenitor or stem cells. Although originally having high expectations, which was implicated by scientific progress in preclinical models, and long-term, randomized clinical trials with good safety profiles for delivery of cells to the myocardium, regenerative therapy for cardiovascular disease had been inconsistent and shown modest efficacy thus far. Recent reviews have nicely illustrated current drawback and the need for improvements for these strategies, using cells or cell-derived products⁴⁻⁶. Due to the lack of major steps forward, other directions have been explored, boosted by the observations of Bergmann and his colleagues that cardiomyocytes from the human heart have a certain degree of renewal capacity⁷. This, in combination with the work of Poss which demonstrated the potential of cardiomyocytes to divide, has pushed new regenerative strategies forward⁸.

CARDIOMYOCYTES RENEWAL AND THE CELL CYCLE

The cardiac regenerative capacity mainly depends on the ability of cardiomyocytes to proliferate after injury^{9,10}. Adult amphibian hearts can completely regenerate after apex resection through cell cycle re-entry of pre-existing cardiomyocytes in the infarct borderzone^{9,11}. In the mammalian heart, cardiomyocytes proliferate prenatally and

withdraw from the cell cycle 7 days after birth¹². At 3 days after birth, cardiomyocytes retain a constant cell volume and are primarily mononucleated¹³. This is in contrast to the abundance of multinucleated cardiomyocytes through DNA replication in the absence of cytokinesis 1–2 weeks after birth^{13,14}. Under basal conditions in the adult mammalian heart, proliferation of cardiomyocyte replaces the cardiomyocytes that die due to apoptosis at a rate of 0.5–1% a year⁷. Although after cardiac injury the cardiomyocyte proliferation rate increases, it remains insufficient to regenerate the heart¹⁵. The endogenous repair mechanisms that occur after injury in the neonatal and the amphibian heart do lead to complete restoration of the myocardium. Stimulating the same endogenous repair mechanism in the adult mammalian heart, through the proliferation of pre-existing cardiomyocytes, can currently be considered the most feasible method to regenerate the heart in a clinical setting. The program that regulates cardiomyocyte cell cycle withdrawal remains largely unknown but is hypothesized to result from the relative hypoxia and the postnatal metabolic shift from anaerobic glycolysis to oxidative phosphorylation¹⁶. This is in line with studies demonstrating that in amphibian hearts, cardiac regeneration depends on hypoxia signaling¹⁷. Furthermore, the rare population of cycling cardiomyocytes in the adult mammalian heart were found to be located in hypoxic niches¹⁸. Even though it might seem contradictory to the role of hypoxia in regeneration, the infarcted myocardium requires sufficient revascularization for functional regeneration to occur. The neonatal and zebrafish heart are heavily vascularized after cardiac injury and without vascularisation of the infarct area, regeneration ends prematurely^{12,19}. To investigate the regulators of cardiac regeneration, studies have analysed the changes in expression of coding and non-coding genes at p7 when the mammalian heart loses its capacity to regenerate. Analysis of the non-coding transcriptome in cardiac disease indicated the essential role of non-coding RNAs in cardiac biology and in epigenetic control of gene expression in the diseased heart^{20,21}. miRNAs regulate the expression of target mRNA by binding to the 3'UTR and hereby either

preventing the translation of the mRNA or aiding in its degradation. LncRNAs (>200 nucleotides) can regulate epigenetic gene silencing, bind to miRNAs, and function as protein scaffolds²². Exploring the expression at P1, P3, P5, P7, and P10 showed differential expression of the 413 miRNAs and 545 lncRNAs in both endothelial cells and cardiomyocytes²³. A marked transition between P3 and P5 was found of 240 miRNAs including the increase in expression of miR-451, miR-195, and miR-22 and a decrease in expression of miR-6240. miR-451 was previously reported to protect erythrocytes against oxidative stress which could also be a potential explanation of its upregulation in cardiac development towards relative hyperoxia²⁴. miR-195 is member of the miR-15 family which has been described to be upregulated in the postnatal mammalian heart and contribute to cardiomyocyte cell cycle withdrawal²⁵. miR-22 induces cardiac senescence by preventing cardiomyocyte proliferation and by activating cardiac fibroblasts²⁶. Other miRNAs that have been associated with the induction of cardiomyocyte proliferation include miR-590, miR199a²⁷, miR-210²⁸, and miR-133²⁹. Recent evidence identified 96 miRNAs to be able to induce cardiomyocyte proliferation in human induced pluripotent stem cell derived cardiomyocytes³⁰. Sixty-seven of these miRNAs targeted the Hippo pathway through the repression of Hippo and the activation of Yap, suggesting this pathway might be a promising target for cardiac regenerative therapy.

MIRNA-128, A NEW PLAYER THAT PROMOTES CARDIOMYOCYTE PROLIFERATION

Recently in Nature Communications, Huang and colleagues reported a new player, microRNA-128 (miRNA-128), which is upregulated in cardiomyocytes during the postnatal switch from proliferation to terminal differentiation³¹. miR-128 is an intronic miRNA, encoded by two isoforms; miR-128-1 and miR-128-2³². The pri-miR-128-1 gene resides within the R3H domain containing protein 1 gene (R3HDM1) and pri-miR-128-2 lies within the cAMP-regulated phosphoprotein, 21 kDa gene (ARPP21,

also known as regulator of calmodulin signaling, RCS). This organization is conserved in human, rat, and mouse genomes³². Early studies pointed to a role of miR-128 as a tumour suppressor, but others found a role in neural and brain development and in behaviour disorders³³⁻³⁵. In the myocardium, however, the expression of miR-128 is low during early developmental stages but is increased during postnatal heart growth. The cardiac-specific overexpression of miR-128, via a tet-off transgenic mouse system, impaired cardiac homeostasis by inducing a progressive increase of heart mass and thereby to increased heart-to-body weight ratios. Detailed analyses suggested that cardiomyocytes increased in size (a hypertrophic response) and thereby to reduced fractional shortening and ejection fraction. More detailed analyses displayed that cardiomyocyte proliferation was reduced upon overexpression of miR-128, with no effect on apoptosis rates, thereby suggesting an early cell cycle exit for cardiomyocytes. Interestingly, the cardiac-specific deletion of miR-128 in both *in vitro* cultured neonatal cardiomyocytes as *in vivo* mouse hearts resulted in an increased dedifferentiation of cardiomyocytes and increased proliferation rates. Interestingly, although the number of cardiomyocytes was larger, being smaller in size, the mice developed normally and exhibited no cardiac dysfunctions. Confirmatory, the overexpression of miR-128 in neonatal mice at P1 inhibited cardiac regeneration upon myocardial apex resection, whereas deletion of miR-128 in adult mice promoted cardiac regeneration upon ischemic injury. The authors further explored putative targets and suggest a role for Suz12, affecting histone modifications and p27, promoting cardiomyocytes into the S-phase to divide.

POTENTIAL IMPACT AND FUTURE DIRECTIONS

miR-128 was previously being reported as a neuronal enriched miRNA, but also involved in cardiac repair of lower vertebrates such as the newt³⁶. In these species, however, the observed effects of miR-128 inhibition were mainly attributed to proliferation of non-cardiomyocyte populations and alteration of extracellular matrix

deposition. Although the authors suggest this might be due to differences in complex of the heart cell types between the species, it also points towards some concerns for translation of these findings regarding miRNA therapeutics for patient care if we cannot control potential off-target cell effects³¹. In the past few years, several types of miRNA inhibitors have been developed such as antagomiRs, antimiRs and LNAs which have been shown to be very effective in inhibiting their specific targets. We and many others labs have shown that these microRNA inhibitors demonstrate much longer effects than conventional pharmaceuticals³⁷. This long-lasting effect will definitely increase the possibility of side-effects, especially in this case of miR-128, which is a potent cell cycle regulator with known effects in other cell types and organs. For these reasons, there is a strong need to develop new methods to increase miRNA therapeutic delivery, prevent off-target cellular uptake and, in the case of miR-128, increase cardiac-specific uptake. Our lab has further developed a local delivery technology called ultrasound-triggered microbubble destruction (UTMD) for microRNA delivery. In this technology, positive charged gas-filled microbubbles can be loaded with negative charged microRNA inhibitors, antimiR or antagomirs. By locally applying ultrasound, gas-filled microbubbles can be destructed and thereby deliver their cargo to the targeted area³⁸. Using this technology, we have been able to significantly increase local delivery of antagomir to the healthy heart with minimum side-effects. Interestingly, similar results were also observed in a myocardial infarction and reperfusion model, even without ultrasound treatment. This is probably caused by the fact that the inhibitors can be enriched in the infarcted region through local injury-induced vascular leakage, which is a possible mechanism how ultrasound triggered microbubble destruction delivers its cargo too³⁹. Another possible strategy to achieve targeted delivery will be nanovectors which are armed with cardiac homing peptide. Inspired by the observation that post myocardial infarction AT1 levels are increased, Xue et al. have developed a nanovector with AT1 targeting peptides on the surface. Armed with miR-1 inhibitors, this nanovector can significantly inhibit

miR-1 induced apoptosis in the infarcted region⁴⁰. Although only a few cases have been successful to specific delivery of miRNAs into the myocardium, we believe with the continuous efforts to develop new delivery vehicles such as polymers, lipid nanoparticles, and extracellular vesicles with difference formulations in combination with difference targeting strategies, it is possible to take full advantage of microRNA therapeutics while minimize their potential side-effect.

CONCLUSIONS

The growing burden of chronically diseased cardiovascular patients that develop heart failure needs new treatment modalities to restore contractile properties of the myocardium. Although attempts to minimize the damage to the cardiac tissue in acute settings is successful, still new approaches are needed to prevent chronic disease. Cardiac regenerative medicine offers potential inspiring strategies, including the use of endogenous or exogenous injection of progenitor cell population. Since the simple injection of cell types is hampered by retention of high cell numbers, other options are explored as well, including the stimulation of post-natal cardiomyocyte proliferation. These novel approaches are extremely exciting, especially by the use of miRNA therapeutics, which can lead to long-lasting and potent effects. The future directions of these approaches are aiming to further explore the potential of the identified molecules and improve local targeting and timed exposure of the therapeutics to reduce costs and toxic effects and, maybe of most importance for the stimulation of cell division, prevent off-target effects in other cell types.

ACKNOWLEDGEMENTS

Funding: This work was supported by Horizon2020 ERC-2016-COG EVICARE (725229), Technobeat (668724), and the Netherlands CardioVascular Research Initiative (CVON), PPS grant: TOP-EVs (the Nederland Heart Foundation), CAS-NWO Program: Cardiac cell therapy in a preclinical animal model for hereditary

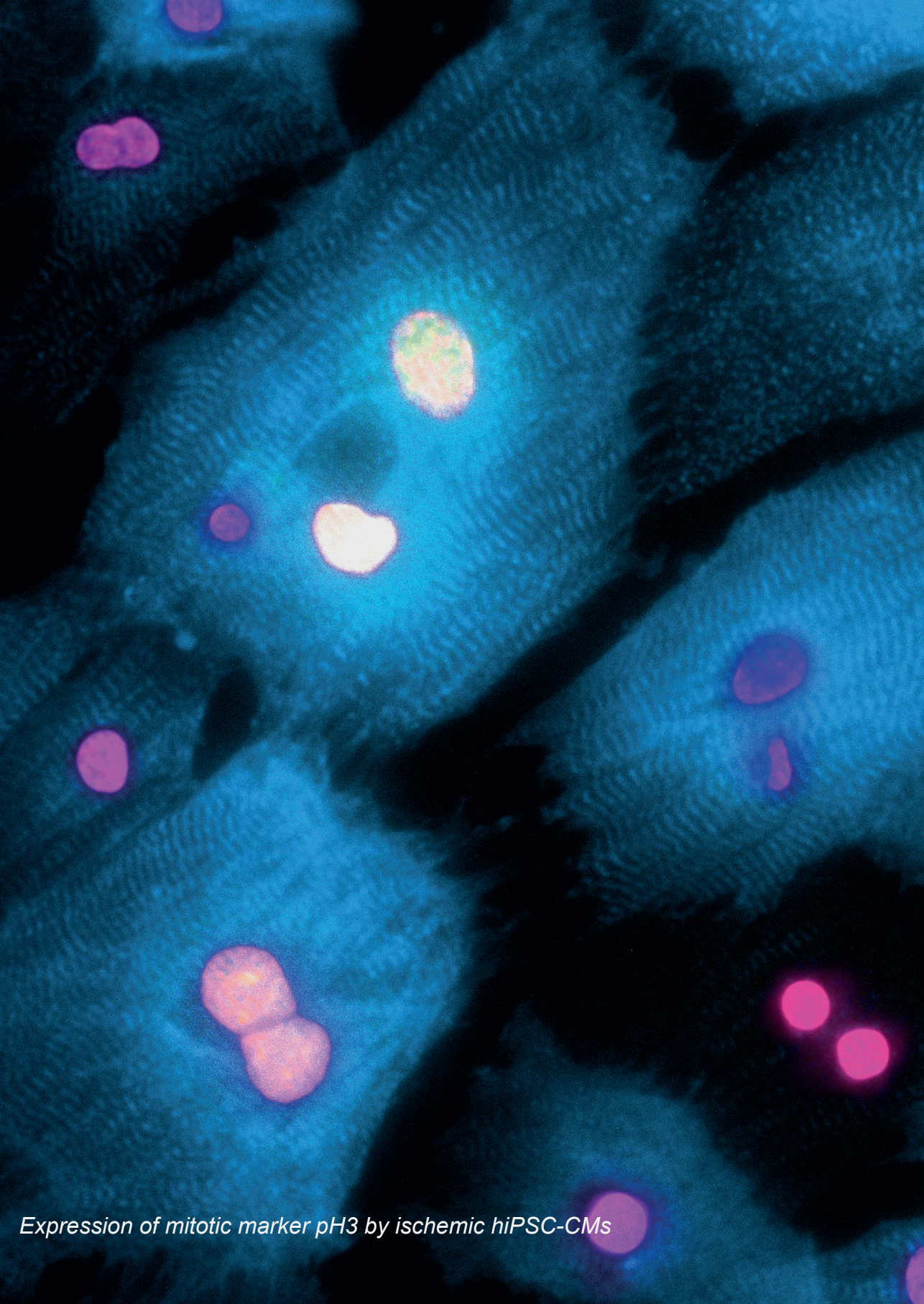
cardiomyopathy the Dutch Heart Foundation, Dutch Federations of University Medical Centres, the Netherlands Organization for Health Research and Development, and the Royal Netherlands Academy of Sciences (REMAIN).

REFERENCES

1. Townsend N, Wilson L, Bhatnagar P, Wickramasinghe K, Rayner M, Nichols M. Cardiovascular disease in Europe: Epidemiological update 2016. *Eur Heart J.* 2016;37(42):3232-3245.
2. Mozaffarian D, Benjamin EJ, Go AS, et al. Executive summary: Heart disease and stroke statistics-2016 update: A Report from the American Heart Association. *Circulation.* 2016;133(4):447-454.
3. Ponikowski P, Voors A. 2016 Esc guidelines for the diagnosis and treatment of acute and chronic heart failure: The Task Force for the diagnosis and treatment of acute and chronic heart failure of the European society of cardiology (ESC): Developed with the special contribution of the heart failure association (HFA) of the ESC. *Russ J Cardiol.* 2017;141(1):7-81.
4. Madonna R, Van Laake LW, Davidson SM, et al. Position Paper of the European Society of Cardiology Working Group Cellular Biology of the Heart: Cell-based therapies for myocardial repair and regeneration in ischemic heart disease and heart failure. *Eur Heart J.* 2016;37(23):1789-1798.
5. Fernández-Avilés F, Sanz-Ruiz R, Climent AM, et al. Global position paper on cardiovascular regenerative medicine. *Eur Heart J.* 2017;38(33):2532-2546.
6. Sluijter JPG, Davidson SM, Boulanger CM, et al. Extracellular vesicles in diagnostics and therapy of the ischaemic heart: Position Paper from the Working Group on Cellular Biology of the Heart of the European Society of Cardiology. *Cardiovasc Res.* 2018;114(1):19-34. doi:10.1093/cvr/cvx211
7. Bergmann O, Bhardwaj RD, Bernard S, et al. Evidence for Cardiomyocyte Renewal in Humans. *Science.* 2009;324:98-102.
8. Tzahor E, Poss KD. Cardiac regeneration strategies: Staying young at heart. *Science (80-).* 2017;356(6342):1035-1039.
9. Jopling C, Sleep E, Raya M, Martí M, Raya A, Belmonte JCI. Zebrafish heart regeneration occurs by cardiomyocyte dedifferentiation and proliferation. *Nature.* 2010;464(7288):606-609.
10. Aguirre A, Sancho-Martinez I, Izpisua Belmonte JC. Reprogramming toward heart regeneration: Stem cells and beyond. *Cell Stem Cell.* 2013;12(3):275-284.
11. Poss KD, Wilson LG, Keating MT. Heart Regeneration in Zebrafish. 2002;298:2188-2191.
12. Porrello ER, Mahmoud AI, Simpson E, et al. Transient Regenerative Potential of the Neonatal Mouse Heart. *Science (80-).* 2011;331:1078-1081
13. Li F, Wang X, Capasso JM, Gerdes AM. Rapid transition of cardiac myocytes from hyperplasia to hypertrophy during postnatal development. *J Mol Cell Cardiol.* 1996;28(8):1737-1746.
14. Ahuja P, Sdek P, MacLellan WR. Cardiac myocyte cell cycle control in development, disease, and regeneration. *Physiol Rev.* 2007;87(2):521-544.
15. D'Uva G, Aharonov A, Lauriola M, et al. ERBB2 triggers mammalian heart regeneration by promoting cardiomyocyte dedifferentiation and proliferation. *Nat Cell*

- Biol. 2015;17(5):627-638.
16. Puente BN, Kimura W, Muralidhar SA, et al. The oxygen-rich postnatal environment induces cardiomyocyte cell-cycle arrest through DNA damage response. *Cell*. 2014;157(3):565-579.
 17. Jopling C, Suñé G, Faucherre A, Fabregat C, Izpisua Belmonte JC. Hypoxia induces myocardial regeneration in zebrafish. *Circulation*. 2012;126(25):3017-3027.
 18. Kimura W, Xiao F, Canseco DC, et al. Hypoxia fate mapping identifies cycling cardiomyocytes in the adult heart. *Nature*. 2015;523(7559):226-230.
 19. Lepilina A, Coon AN, Kikuchi K, et al. A Dynamic Epicardial Injury Response Supports Progenitor Cell Activity during Zebrafish Heart Regeneration. *Cell*. 2006;127(3):607-619.
 20. Grote P, Witterl L, Hendrix D, et al. The Tissue-Specific lncRNA Fendrr Is an Essential Regulator of Heart and Body Wall Development in the Mouse. *Dev Cell*. 2013;24(2):206-214.
 21. Archer K, Broskova Z, Bayoumi AS, et al. Long non-coding RNAs as master regulators in cardiovascular diseases. *Int J Mol Sci*. 2015;16(10):23651-23667.
 22. Juni RP, Abreu RC, Diseases C, Sciences L, Surgery C, Martins C. Regulation of microvascularization in heart failure - The close relationship between endothelial cells, non-coding RNAs, and exosomes. *Non-coding RNA Res*. 2017;2(1):45-55.
 23. Adamowicz M, Morgan CC, Haubner BJ, et al. Functionally Conserved Noncoding Regulators of Cardiomyocyte Proliferation and Regeneration in Mouse and Human. *Circ Genom Precis Med*. 2018;11(2):e001805.
 24. Yu D, Dos Santos CO, Zhao G, et al. miR-451 protects against erythroid oxidant stress by repressing 14-3-3 ζ . *Genes Dev*. 2010;24(15):1620-1633.
 25. Porrello ER, Mahmoud AI, Simpson E, et al. Regulation of neonatal and adult mammalian heart regeneration by the miR-15 family. *Proc Natl Acad Sci*. 2013;110(1):187-192.
 26. Jazbutyte V, Fiedler J, Kneitz S, et al. MicroRNA-22 increases senescence and activates cardiac fibroblasts in the aging heart. *Age*. 2013;35(3):747-762.
 27. Eulalio A, Mano M, Ferro MD, et al. Functional screening identifies miRNAs inducing cardiac regeneration. *Nature*. 2012;492(7429):376-381.
 28. Arif M, Pandey R, Alam P, et al. MicroRNA-210-mediated proliferation, survival, and angiogenesis promote cardiac repair post myocardial infarction in rodents. *J Mol Med*. 2017;95(12):1369-1385.
 29. Yin VP, Lepilina A, Smith A, Poss KD. Regulation of zebrafish heart regeneration by miR-133. *Dev Biol*. 2012;365(2):319-327.
 30. Diez-Cuñado M, Wei K, Bushway PJ, et al. miRNAs that Induce Human Cardiomyocyte Proliferation Converge on the Hippo Pathway. *Cell Rep*. 2018;23(7):2168-2174.
 31. Huang W, Feng Y, Liang J, et al. Loss of microRNA-128 promotes cardiomyocyte proliferation and heart regeneration. *Nat Commun*. 2018;9(1).
 32. Megraw M, Sethupathy P, Gumireddy K, Jensen ST, Huang Q, Hatzigeorgiou AG.

- Isoform specific gene auto-regulation via miRNAs: A case study on miR-128b and ARPP-21. *Theor Chem Acc.* 2010;125(3-6):593-598.
33. Weiss GJ, Bemis LT, Nakajima E, et al. EGFR regulation by microRNA in lung cancer: Correlation with clinical response and survival to gefitinib and EGFR expression in cell lines. *Ann Oncol.* 2008;19(6):1053-1059.
 34. Krichevsky AM, King KS, Donahue CP, Khrapko K, Kosik KS. Erratum: A microRNA array reveals extensive regulation of microRNAs during brain development (*RNA* (2003) 9 (1274-1281)). *Rna.* 2004;10(3):551.
 35. Ching AS, Ahmad-Annuar A. A perspective on the role of microRNA-128 regulation in mental and behavioral disorders. *Front Cell Neurosci.* 2015;9:1-8.
 36. Witman N, Heigwer J, Thaler B, Lui WO, Morrison JI. MiR-128 regulates non-myocyte hyperplasia, deposition of extracellular matrix and Islet1 expression during newt cardiac regeneration. *Dev Biol.* 2013;383(2):253-263.
 37. Kwekkeboom RFJ, Lei Z, Doevendans PA, Musters RJP, Sluijter JPG. Targeted delivery of miRNA therapeutics for cardiovascular diseases: Opportunities and challenges. *Clin Sci.* 2014;127(6):351-365.
 38. Kwekkeboom RFJ, Lei Z, Bogaards SJP, et al. Ultrasound and Microbubble-Induced Local Delivery of MicroRNA-Based Therapeutics. *Ultrasound Med Biol.* 2015;41(1):163-176.
 39. Kwekkeboom RFJ, Sluijter JPG, Van Middelaar BJ, et al. Increased local delivery of antagomir therapeutics to the rodent myocardium using ultrasound and microbubbles. *J Control Release.* 2016;222:18-31.
 40. Xue X, Shi X, Dong H, et al. Delivery of microRNA-1 inhibitor by dendrimer-based nanovector: An early targeting therapy for myocardial infarction in mice. *Nanomedicine Nanotechnology, Biol Med.* 2018;14(2):619-631.



Expression of mitotic marker pH3 by ischemic hiPSC-CMs

Chapter 5

FOLLISTATIN-LIKE 1 IN CARDIOVASCULAR DISEASE AND INFLAMMATION

Adapted from:

Mini-reviews in Medicinal Chemistry. 2019, 19 (6), 1379 - 1389 doi: 10.2174/1389557519666190312161551

Published online 6 March 2019

Marijn M.C. Peters^{1*}, Timion A. Meijs^{1*}, Wouter Gathier¹, Pieter A.M. Doevendans¹, Joost P.G. Sluijter¹, Steven A.J. Chamuleau¹ and Klaus Neef¹

¹ Department of Cardiology, Laboratory of Experimental Cardiology, Regenerative Medicine Centre Utrecht, University Medical Centre Utrecht, University Utrecht, Utrecht, the Netherlands

* Equal contribution

ABSTRACT

Follistatin-like 1 (FSTL1), a secreted glycoprotein, has been shown to participate in regulating developmental processes and to be involved in states of disease and injury. Spatiotemporal regulation and posttranslational modifications contribute to its specific functions and make it an intriguing candidate to study disease mechanisms and potentially develop new therapies. With cardiovascular diseases as the primary cause of death worldwide, clarification of mechanisms underlying cardiac regeneration and revascularization remains essential. Recent findings on FSTL1 in both acute coronary syndrome and heart failure emphasize its potential as a target for cardiac regenerative therapy. With this review, we aim to shed light on the role of FSTL1 specifically in cardiovascular disease and inflammation.

1. INTRODUCTION

Follistatin-like 1 (FSTL1), also known as TSC-36 and follistatin-related protein (FRP), was first discovered in an osteoblastic cell line as a gene induced by transforming growth factor (TGF) β 1 expression¹. This 308 amino acid extracellular glycoprotein is a member of the SPARC (secreted protein acidic rich in cysteine) family of proteins^{2,3} and has a molecular mass ranging from 37 to 55 kDa^{4,5}. Analysis in mice indicated it to be most abundantly expressed in the lungs⁶, the heart⁷, skeletal muscle⁸, smooth muscle⁹, and vascular endothelium⁹. Multiple effects of FSTL1 have been reported, including a regulatory role in embryogenesis¹⁰, inhibition of proliferation in cancer cells¹¹, and modulation of inflammatory responses⁶. Mechanistically, these various roles of FSTL1 are mediated through different pathways targeting BMP for developmental processes, AKT/AMPK in the context of cardiac disease and CD14/TLR4 for immunological processes¹².

1.1. Cardiokines as potential therapeutic targets for heart failure

Heart failure represents a significant health burden within the spectrum of cardiovascular diseases affecting approximately 26 million people worldwide¹³. The treatment options are limited which leads to a poor prognosis with a five-year survival rate of 51.5%¹⁴. Over the last years, cardiovascular research on heart failure has focused on methods to repair the heart. The use of stem cells in the context of cardiac regeneration has been studied extensively. However, the results of (pre-)clinical trials using stem cell therapy are inconsistent¹⁵. The main obstacles that are encountered are the complex molecular mechanisms underlying cardiac repair, but also the delivery method¹⁵, low cellular retention¹⁶ and functional integration¹⁷. Furthermore, the focus on repair of the injured myocardium is accompanied by undervalued importance of the restoration of the microvasculature of the heart and the functional integration of the injected cells within the host myocardium and the extracellular matrix¹⁸. The use of extracellular vesicles has also received interest as the vesicles can mediate

paracrine effects and multiple reparative functions, including stimulating angiogenesis and cardiomyocyte proliferation¹⁹. There is increasing evidence suggesting that endogenous factors secreted from cardiac tissue, referred to as cardiokines, play an essential role in regulating cellular mechanisms in the heart²⁰. They can function through autocrine, paracrine, and endocrine signaling and are involved in responses to injury, cardiac remodeling, and inter-cellular and inter-organ communication^{21–25}.

1.2. FSTL1 IN CARDIAC DISEASE

A protective effect of FSTL1 has been reported in various cardiac diseases (**Figure 1**) and development²⁶. In transaortic constricted hearts, FSTL1 reduces cardiomyocyte apoptosis via phosphorylated AMPK signaling²⁰. Furthermore, the loss of FSTL1 in transaortic constricted hearts is associated with more severe myocardial hypertrophy and loss of ventricular function, emphasizing a role for FSTL1 in maintaining cardiac function²⁷. Similarly, in infarcted hearts FSTL1 protects from apoptosis and induces angiogenesis via phosphorylated AKT signaling^{7,28,29}. For the stimulation of angiogenesis, phosphorylated AKT signaling is dependent on the interaction between FSTL1 and transmembrane protein DIP2A, which functions as a receptor for FSTL1. A 22% increase in the secretion of FSTL1 by skeletal muscle fibres during exercise could also be the underlying mechanism of cardioprotection acquired through exercise⁸. The capacity to modulate cardiovascular diseases via both cardiac secreted FSTL1 and skeletal muscle secreted FSTL1 indicates the potential role of FSTL1 in myocardial repair after injury.

1.3. FSTL1 MAY ENHANCE CARDIAC FUNCTION FOLLOWING I/R INJURY

1.3.1. Cardioprotection

FSTL1 has been described as an active modulator of cellular responses in various cardiac conditions and may have the capacity to generate both cardioprotective and regenerative responses. Previous studies showed that FSTL1 acts as a cardiopro

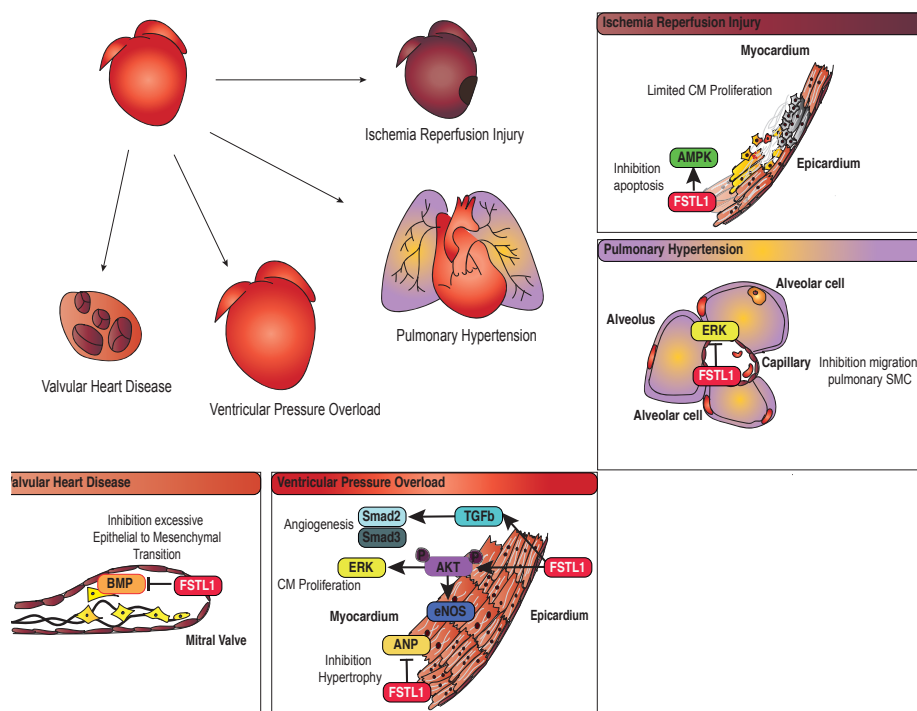


Figure 1. The role of FSTL1 in cardiovascular diseases.

In the injured heart, FSTL1 can influence multiple processes through the interplay with distinct molecular pathways in multiple cardiac cell types. In the healthy and the hypertrophied heart, the epicardial cells secrete FSTL1 inhibiting hypertrophy, stimulating cardiomyocyte proliferation and inducing angiogenesis. Epicardial FSTL1 expression is abolished during ischemia reperfusion injury. Myocardial FSTL1 can inhibit cardiomyocyte apoptosis. In valvular heart disease FSTL1 regulates epithelial to mesenchymal transition. In pulmonary hypertension, FSTL1 inhibits the migration of pulmonary smooth muscle cells (SMC).

protective factor after ischemia/reperfusion (I/R) injury. FSTL1 overexpression attenuated apoptosis in neonatal rat cardiomyocytes after exposure to hypoxia and reoxygenation. Additionally, systemic administration of recombinant FSTL1 after myocardial infarction in mice significantly reduced the rate of cardiomyocyte apoptosis and the size of the infarct³⁰. Similarly, anti-apoptotic effects of FSTL1 have been shown *in vitro* and in murine and porcine I/R models³⁰. Upregulation of endogenous FSTL1, as a response to exercise, attenuated cardiac fibrosis, while intraperitoneal administration of FSTL1 was associated with increased systolic function in a rat model of myocardial infarction³¹. There is increasing evidence suggesting that these cardioprotective

properties may be mediated by activation of AMP-activated protein kinase signaling^{30,32}. Furthermore, a recent study shows FSTL1 expression is suppressed by miRNA-9-5p, a non-coding RNA which is upregulated after ischemic injury³³. Antagomir mediated inhibition of miRNA-9-5p in a murine acute MI model attenuated fibrosis and inflammation and preserved cardiac function.

1.3.2. Proliferative responses

Recently, FSTL1 was found to act as a regenerative factor by promoting proliferation of mouse embryonic stem cell-derived cardiomyocytes *in vitro*³⁴ raising hopes to stimulate the limited endogenous regenerative capacity of the adult human heart³⁵ beyond the reported 0.8% of cardiomyocytes dividing annually to maintain homeostasis³⁶. This baseline proliferation rate can be increased to some extent, for instance by signaling from cellular damage induced by the increased concentration of reactive oxygen species (ROS) in response to ischemia/reperfusion injury³⁷, via the Nrg1/ErbB2 pathway³⁸ and via the Hippo-YAP pathway³⁹, but stimulation of cardiomyocyte proliferation to allow for substantial restoration of the myocardium was considered illusive until recently. Analysis in a mouse model of MI revealed a switch in FSTL1 expression from epicardial to myocardial cells going along with a switch in posttranslational modification from the hypoglycosylated to a hyperglycosylated isoform³⁴. Since this isoform has been shown *in vitro* to be cardioprotective (anti-apoptotic) but not regenerative (proliferative), reconstitution of hypoglycosylated FSTL1 expression was mediated by surgical application of a FSTL1-loaded collagen-based patch to the epicardium immediately after the induction of myocardial infarction. Restoring epicardial FSTL1 expression significantly reduced scarring, stimulated cardiomyocyte proliferation, and enhanced cardiac function following ischemic injury in murine and porcine models³⁴. FSTL1 induced increase of GDF-15 expression and activation of TGF β -Smad2/3 signaling seems to be a potential pathway for induction of cardiomyocyte proliferation^{31,40}. These results indicate that the decrease of

epicardial FSTL1 is likely an adverse reaction to ischemic stress and that reconstitution comprises a promising method to preserve cardiac function and attenuate cardiac remodeling. However, a recent study found no evidence of epicardial FSTL1 expression in a *Fstl1*-eGFP reporter mouse, but could confirm FSTL1 dependent activation of cardiac fibroblasts preventing post-myocardial-infarction ventricular wall rupture⁴¹.

1.3.3. Stimulatory effects on revascularization

Besides inhibiting apoptosis and stimulating proliferation of cardiomyocytes, FSTL1 may also attenuate ischemia/reperfusion injury by inducing revascularization. Recent studies have demonstrated that FSTL1 promotes angiogenesis during ischemic stress through activation of Akt-eNOS-dependent signaling⁴², and TGF β -Smad2/3 after myocardial infarction³¹. Epicardial injection of FSTL1 following myocardial infarction resulted in increased vascularization of the myocardium, particularly in the border zone of the infarcted area³⁴. Furthermore, there is evidence suggesting that FSTL1 enhances endothelial cell function and survival⁴² and plays a role in vascular remodeling following arterial injury by preventing neointimal hyperplasia⁴³.

1.4. FSTL1 AS BIOMARKER

FSTL1 is strongly expressed under cardiac hypoxic conditions and has been proposed to be a potential diagnostic biomarker in acute coronary syndrome (ACS) and heart failure. Patients with ACS showed serum concentrations of FSTL1 increased by 88% compared to healthy controls⁴⁰. Upregulation of FSTL1 in ACS patients was independently correlated with an increased incidence of diabetes mellitus, increased N-terminal pro-B-type natriuretic peptide (NT-proBNP) and c-reactive protein (CRP) levels. Serum FSTL1 levels above the median were associated with reduced survival one year after ACS compared to those below the median [P < 0.019]. In a cohort of 106 ACS patients, patients were 3.7 times more likely to die from a cardiovascular

cause when their serum FSTL1 concentration was within the top quartile compared to patients with levels in the three lower quartiles [$P < 0.001$]. The prognostic value of FSTL1 in ACS showed similar discriminatory potential as traditional markers CRP and NT-proBNP⁴⁰. Furthermore, GDF-15, which is induced by FSTL1, has strong prognostic value for patients with non-ST-elevation ACS⁴⁴. FSTL1 concentrations are increased in patients with ischemic and dilating cardiomyopathy with a left ventricular ejection fraction of less than 40%. In these systolic heart failure patients, serum FSTL1 levels were elevated by 56% compared to matched controls and associated with increased left ventricular mass, left ventricular posterior wall thickness, and increased brain natriuretic peptide levels⁴⁵. Moreover, significantly elevated serum FSTL1 levels have been found in patients with end-stage heart failure with a left ventricular assist device implantation⁹ and in patients with heart failure with preserved ejection fraction (HFpEF)⁴⁶. A recent study showed that the upregulation of FSTL1 expression in heart failure could be accurately detected using gold nanoparticles. According to the authors, advantages of this technique are the low costs and rapid execution compared to current methods to diagnose heart failure, e.g. NT-proBNP and echocardiography⁴⁷.

The efficacy of FSTL1 as a biomarker, especially in relation to established clinical biomarkers and the association with cardiovascular events and mortality, shows promise, but still requires additional research. The increased circulation of FSTL1 in heart failure might suggest further increasing circulating FSTL1 would not improve cardiac function. Contrary to this hypothesis, a recent study showed acute or chronic FSTL1 infusion normalized cardiac metabolism and improved diastolic and contractile function⁴⁸.

1.5. ATTENUATION OF CARDIAC HYPERTROPHY

FSTL1 has been identified as an active modulator of cardiac ventricular hypertrophy. In a mouse model of ventricular pressure overload induced by transverse aortic

constriction (TAC), cardiomyocyte-specific knock-out of FSTL1 resulted in excessive hypertrophy and deterioration of systolic ventricular function²⁷. In contrast, transgenic mice overexpressing FSTL1, both conditionally and constitutively, were refractory to developing cardiac hypertrophy in this model. Moreover, systemic administration of FSTL1 decreased the hypertrophic response, enhanced systolic function, and attenuated left ventricular dimensions in both wildtype and FSTL1-knockout (FSTL1-KO) mice. TAC resulted in a 2.2-fold increase of FSTL1 serum levels and this increase was attenuated in the myocyte-specific FSTL1-KO mice, suggesting that cardiomyocytes are the main source of FSTL1 in mice subjected to TAC²⁷.

The ability of FSTL1 to prevent hypertrophic responses has also been demonstrated *in vitro* using adult rat ventricular cardiomyocytes⁴⁶. Supplementation of FSTL1 to cell culture attenuated cardiomyocyte hypertrophy by d-aldosterone induced *in vitro* and reduced expression of atrial natriuretic peptide (ANP), a marker of cardiomyocyte hypertrophy. This was confirmed *in vivo* showing that increased systemic levels of FSTL1 from transgenic overexpression were associated with reduced cardiac hypertrophy and improved diastolic function in a mouse model of heart failure with preserved ejection fraction (HFpEF)⁴⁶.

1.6. PROTECTION FROM PULMONARY HYPERTENSION

Recent evidence suggests that FSTL1 also plays a role in attenuating pulmonary hypertension⁴⁹. During pulmonary hypertension, high blood pressure in the arteries of the lungs increases the workload of the heart and can lead to right ventricular heart failure. In patients with pulmonary hypertension due to chronic obstructive pulmonary disease FSTL1 serum levels are elevated. When comparing heterozygous FSTL1+/- knock-out mice with wild type FSTL1+/+ mice, in a state of hypoxia induced pulmonary hypertension, the heterozygous mice with decreased FSTL1 expression showed higher right systolic ventricular pressures and increased right ventricular hypertrophy. Systemic administration of FSTL1 improved right-sided

systolic pressures⁴⁹. Additionally, endothelium-derived FSTL1 appears to regulate the development and remodeling of the pulmonary vasculature and loss of this type of FSTL1 may result in a reduction of right ventricular function⁵⁰.

1.7. FSTL1 AND VALVULAR HEART DISEASE

Limited evidence is available regarding the potential association of FSTL1 and valvular heart disease. Recently, it has been described that endocardial and endothelial deletion of FSTL1 resulted in severe deformation of the mitral valve in a mouse model⁵¹. FSTL1 is normally expressed in both mitral valve leaflets and inhibits bone morphogenetic protein (BMP) signaling to prevent excessive proliferation of valve cells. Echocardiography of a conditional FSTL1 knockout mouse showed mitral regurgitation and progressive left ventricular dysfunction, eventually leading to cardiovascular death⁵¹.

FSTL1 is associated with cardiomyocyte and endothelial cell function, and its pleiotropic function renders its potential to modulate specific processes, including cardiomyocyte survival, cardiomyocyte proliferation and angiogenesis. Additionally, modulation of FSTL1 expression can improve or worsen cardiac function in multiple cardiac diseases. Therefore, FSTL1 has the potential to serve as a therapeutic target to treat I/R injury, pulmonary hypertension, cardiomyocyte hypertrophy, and valvular heart disease.

1.8. INFLAMMATION IN CARDIAC DISEASES

An increasing body of evidence supports the essential role of inflammation in both the development and the progression of cardiovascular diseases⁵². Acute myocardial infarction is often caused by the formation of a thrombus on atherosclerotic plaques in coronary arteries, a process involving the activation of platelets, the accumulation of immune cells and systemic and local inflammatory events⁵³. In the

ischemic myocardium, injured myocytes release their intracellular content resulting in a well-orchestrated signaling cascade of neutrophil and monocyte infiltration. Reperfusion of the infarcted area leads to I/R injury mediated by the release of ROS, inducing leukocyte chemokine upregulation. The infiltration of immune cells mediates the secretion of pro-inflammatory cytokines tumour necrosis factor (TNF), IL-1 β , and IL-6. The knockdown of TNF ameliorated myocardial I/R injury indicating the role of inflammation in the pathogenesis of I/R injury⁵⁴. But the inflammatory response in the heart after ischemia is not only detrimental for cardiac function: extensive evidence suggests the involvement of inflammatory mechanisms in post-infarction cardiac repair through the clearance of dead cells⁵⁵ and also mediating regeneration by macrophages in the neonatal heart⁵⁶. Furthermore, in a mouse model of cardiac pressure overload due to TAC, hypertrophy and myocardial inflammation preceding fibrosis was observed⁵⁷. Additionally, Inflammation plays a role in the pathogenesis of pulmonary hypertension where endothelial dysfunction is accompanied by the upregulation of pro-inflammatory cytokines IL-1, MCP-1 and IL-6⁵⁸.

1.9. FSTL1 IN INFLAMMATION

The identification of FSTL1 as an autoantigen in the synovium of patients with rheumatoid arthritis (RA)⁴ led to increased interest to study FSTL1 in inflammatory diseases. Follow-up studies identified both pro-inflammatory and anti-inflammatory effects of FSTL1 (**Figure 2**). In multiple inflammatory diseases (e.g. RA^{59,60}, Sjögrens syndrome, ulcerative colitis, systemic lupus erythematosus, systemic sclerosis, and dermatomyositis/polymyositis, asthma⁶¹) FSTL1 levels were found to be increased and associated with disease progression. Expression of FSTL1 was found to be specifically increased in mesenchymal lineage cells and not in the hematopoietic lineage in patients with RA. The plasma levels of FSTL1 were increased in acute Kawasaki disease compared to healthy controls, and a relation was found between increased FSTL1 levels and the likelihood to develop coronary aneurysms⁶². Also,

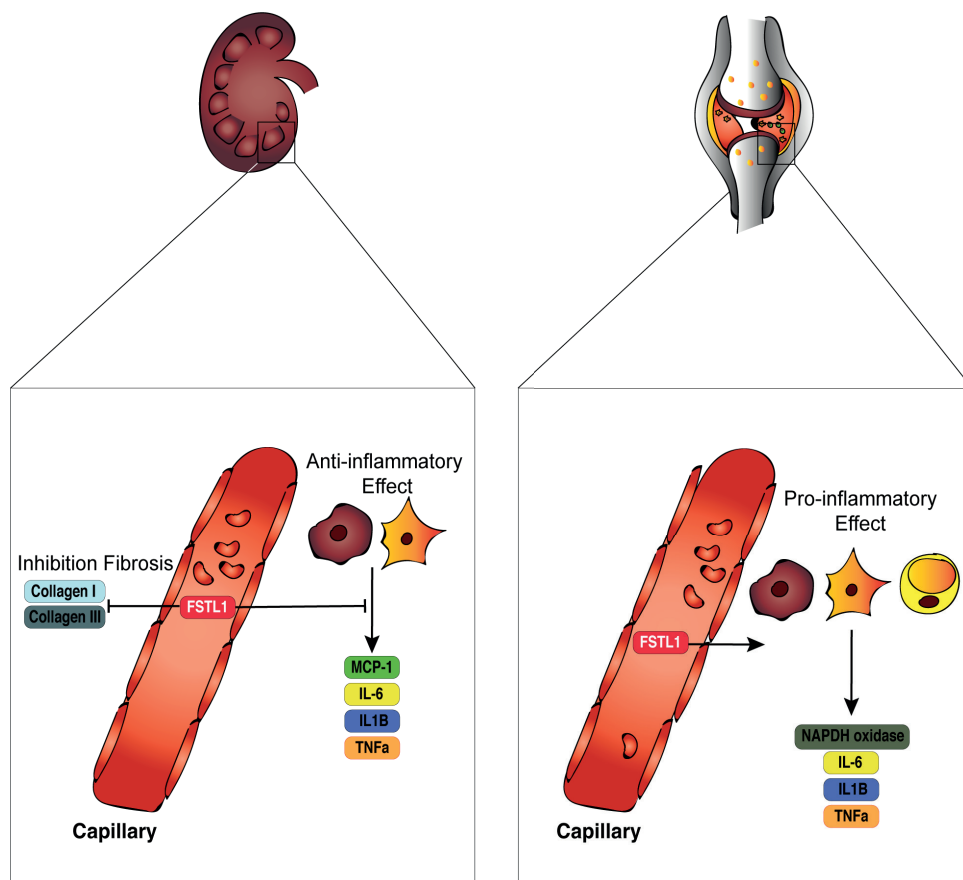


Figure 2. The bifunctional role of FSTL1 in inflammation

In the kidney, FSTL1 has an anti-inflammatory effect by inhibiting fibrosis and macrophage and fibroblast cytokine secretion. In joints, FSTL1 can mediate the secretion of pro-inflammatory cytokines by macrophages, fibroblasts and adipocytes.

in patients with obesity (BMI ≥ 25 kg/m²), serum FSTL1 levels were significantly elevated compared to control patients. Furthermore, elevated FSTL1 mRNA levels were seen in subcutaneous and epididymal adipose tissue in a mouse model of obesity⁶³. The pro-inflammatory capacity of FSTL1 is mediated by the expression of pro-inflammatory cytokines IL-6, IL-1 β , TNF α , IFN γ -related genes⁶⁴, MCP-1⁶⁵ and NF- κ B signaling⁶⁶. FSTL1 promotes IL-1 β secretion by regulating the activity of the NLRP3 inflammasome both *in vitro* and *in vivo*⁶⁷. The injection of FSTL1 in the paws

of wild type mice caused swelling only in the presence of IFN- γ ⁶⁴. Not only exogenously administered FSTL1, but also endogenously expressed FSTL1 has a pro-inflammatory effect as shown in a mouse model of CIA treated with anti-FSTL1 antibodies. Here, amelioration of arthritis and reduced mRNA levels for IL-1 β , IFN- γ , and CXCL10, which is a mediator in bone erosion in CIA, were observed^{64,68}. It appears most of the pro-inflammatory effects of FSTL1 are associated with its effect on arthritis. It is unclear whether this will also have implications for the therapeutic application of FSTL1 as a regenerative factor. Other studies report the anti-inflammatory capacity of FSTL1. An ameliorating effect of recombinant human FSTL1 on arthritis in a mouse model of CIA has been described⁶⁹. Treatment with FSTL1 prevented swelling of footpads and reduced the clinical score used to assess arthritis severity. Furthermore, FSTL1 was able to prevent cartilage breakdown and bone erosion by down regulating expression of c-fos, ets-2, Il-6, MMP-3, and MMP-9, genes that are involved in destructive joint inflammation⁶⁹⁻⁷³. In an *in vitro* model of neural inflammation in mouse astrocytes, FSTL1 attenuated the upregulation of pro-inflammatory cytokines after LPS treatment by suppressing the MAPK/p-ERK1/2 pathway⁷⁴. Intravenous administration of FSTL1 in mice 4 weeks after subtotal nephrectomy ameliorated fibrosis and mice that received FSTL1 showed smaller glomerular area and fewer intraglomerular cells⁷⁵. Lower mRNA levels of TNF- α , IL-6, IL-1 β , MCP-1, NADPH oxidase components, connective tissue growth factor, TGF- β 1, collagen I, and collagen III were found in the remaining kidney tissue of FSTL1 treated mice. Mechanistically, the dual role of FSTL1 has been linked to pro-inflammatory processes via CD14 and TLR4 and to inhibition of tissue destruction via the downregulation of matrix metalloproteinase (MMPs) regulated via DIP2A, pAKT and up-regulation of FOS⁷⁶. Thus, the capacity of FSTL1 to play either a pro- or anti-inflammatory role might stem from the various pathways through which FSTL1 is able to act. As the inflammatory response is also important in multiple cardiac diseases and FSTL1 has been reported to have cardioprotective and regenerative effects, it is important to

study whether FSTL1 treatment might have a pro-inflammatory effect in the heart. Still, the role of FSTL1 in cardiac inflammation remains largely unknown. Analysis of the expression of pro-inflammatory cytokines after FSTL1 in a mouse and pig model of I/R injury showed decreased levels of TNF- α and IL-6³⁰. Also, in cultured neonatal rat cardiomyocytes, lipopolysaccharide (LPS) stimulated expression of pro-inflammatory cytokines was decreased after FSTL1 treatment. FSTL1 supplementation to macrophages, which are abundantly present in the myocardium after cardiac I/R injury led to an AMPK-dependent decrease in TNF- α and IL-6 expression after LPS or BMP-4 stimulation³⁰.

Furthermore, the effect of cardiac myocyte-derived FSTL1 on chronic kidney disease (CKD) was studied in a mouse model of subtotal nephrectomy comparing healthy mice to cardiac-specific FSTL1 knockout mice⁷⁵. Significantly higher levels of pro-inflammatory cytokines TNF- α , IL-6, IL-1 β , MCP-1, and NADPH oxidase components were expressed in FSTL1 knockout mice compared to control mice. It has been suggested that FSTL1 exerts anti-inflammatory effects via the inhibition of BMP-4 dependent inflammatory pathways³⁰ and pro-inflammatory effects via the activation of TLR4/MyD88/NF- κ B and MAPK signaling pathways⁷⁷. Thus, the capacity of FSTL1 to play either a pro- or anti-inflammatory role might stem from the various pathways through which FSTL1 is able to act. Another intriguing explanation of the ambiguous role of FSTL1 in inflammation and inflammatory diseases could be post-translational modification of FSTL1².

2.1. INFLUENCE OF POST-TRANSLATIONAL MODIFICATION ON FSTL1 FUNCTION

Healthy epicardium expresses FSTL1, which is ceased after myocardial injury. As mentioned, FSTL1 can attenuate detrimental effects from myocardial injury by inducing cardiomyocyte proliferation, reducing apoptosis and inflammation, and promoting revascularization^{34,41}. However, increasing FSTL1 circulating levels after

myocardial infarction with FSTL1 from myocardial origin did not induce cardiomyocyte proliferation. Only FSTL1 from epicardial origin was found to be capable to induce a regenerative response³⁴. Analysing and comparing biochemical properties of epicardial and myocardial FSTL1 revealed slower migration of myocardial FSTL1 in SDS polyacrylamide gel electrophoresis, representing increased molecular weight, potentially from post-translational modifications. Application of tunicamycin, an inhibitor and catalyst of reversion of N-linked glycosylation, abolished this difference in migration, suggesting hyperglycosylation as a cause of the observed high molecular weight of the FSTL1 myocardial isoform. Thus, it seems plausible that glycosylation and potentially other post-translational modifications play a role in modulating the abilities of FSTL1 to generate cardioprotective and regenerative responses.

In previous studies multiple glycosylated isoforms of FSTL1 with varying molecular weights have been detected^{2,4,5}. Bacterially expressed recombinant FSTL1, primarily produced in *Escherichia coli*, is a hypoglycosylated isoform, whereas FSTL1 expressed in mammalian cells is extensively glycosylated. Glycosylated FSTL1 protected mouse embryonic stem cell-derived cardiomyocytes (mESC-CMs) from apoptosis following H₂O₂ application, although no effect on proliferation, indicating potential regenerative properties, was observed. In contrast, bacterially produced FSTL1 did stimulate proliferation of mESC-CMs but failed to attenuate H₂O₂-induced apoptosis³⁴. FSTL1 produced in insect cells also inhibited apoptosis and inflammatory responses following ischemia/reperfusion injury, as shown in mouse and pig models³⁰. However, when comparing FSTL1 expressed in mammalian cells, insect cells, and bacterial cells, no differences were found in the stimulation of fibroblast mobility, despite significant variations in the extent of glycosylation⁷⁸. A recent study analysed whether ablation of the N glycosylation of the FSTL1 expressed in mammalian cells could increase the regenerative capacity of the human FSTL1⁷⁹. This study showed that a mutation in a single N glycosylation site (N180Q) of FSTL1 could trigger cardiomyocyte proliferation and cardiac regeneration in a mouse MI model. Based on

Table 1. Specifications of recombinant FSTL1 used in research on cardiac disease

Parameter	Study	Origin Fstl1	Expression system	Tag	Supplier	In vivo/vitro	Main findings	
Cardio protection	Gorgens, 2013	Human	E.Coli	6His at N-terminus	Aviscera Bioscience	<i>In vitro</i>	No alteration of Akt phosphorylation following insulin stimulation	
		Human	E. Coli	His at N-terminus	GenWay			
	Maruyama, 2016	Human	HEK293	-	-	Proteos Inc.	<i>In vitro</i>	Promotion of cardiac fibroblast mobility, no significant differences between the isoforms
		Human	E. Coli	6His at N-terminus	6His at N-terminus	Aviscera Bioscience		
		Mouse	Mouse cell line	6His at C-terminus	6His at C-terminus	R&D Systems		
		Mouse	Insect Sf9 cell	FLAG at C-terminus	FLAG at C-terminus	Walsh Laboratory		
	Ogura, 2012	Human	Insect Sf9 cell	FLAG at C-terminus	-	-	<i>In vitro/vivo</i>	Inhibition of apoptosis and inflammatory responses following cardiac I/R injury
	Oshima, 2008	Mouse	HEK293	V5 epitope at C-terminus	-	-	<i>n vitro/vivo</i>	Reduction of apoptosis in neonatal rat CMs after I/R injury by upregulation of AKT and ERK signalling, reduction of myocardial infarct size and apoptosis following MI in mice

Table 1 continued

Cardio protection	Ouchi, 2010	Mouse	Insect Sf9 cell	FLAG at C-terminus	-	<i>In vitro</i>	Enhanced survival, mobility and differentiation into network structures in ECs, reduced I/R induced apoptosis and AKT phosphorylation in CM, effects attenuated by DIP2A
	Zhang, 201	Human	Mouse myeloma cell line, NS0 derived	-	R&D Systems	<i>In vivo</i>	Decreased RV systolic pressure and hypertrophy index in mice with hypoxia-induced pulmonary hypertension
Modulating cardiac hypertrophy	Tanaka, 2016	Human	Insect Sf9 cell	FLAG at C-terminus	-	<i>In vivo</i>	Decrease aldosteron-induced CM hypertrophy and diastolic dysfunction in mice with HFpEF
	Wei, 2015	Human	E.Coli	6His at C-terminus	Aviscera Bioscience	<i>in vitro/vivo</i>	CM proliferation, not protection from H2O2-induced apoptosis in hESC-CM and murine and swine I/R
Cardiorenal communication	Haya-kawa, 2015	Human	Mouse myeloma cell line	ASP and 10His at C-terminus	R&D Systems	<i>In vitro</i>	Inhibited H2O2-induced apoptosis in hESC-CM not proliferation inducing.
		Human	Insect Sf9 cell	FLAG at C-terminus	-	<i>In vitro</i>	Decrease inflammatory cytokines, phosphorylation AMP-activated protein kinase in human mesangial cells

Table 1 continued

Parameter	Study	Origin Fstl1	Expression system	Tag	Supplier	In vivo/vitro	Main findings
EC and revascularisation	Miyabe, 2014	Human	Insect Sf9 cell	FLAG at C-terminus	-	In vitro	Decreased proliferation of aortic SMCs
	Wu, 2015	Human	Mouse myeloma cell line	ASP10His at C-terminus	R&D Systems	In vitro	attenuated hemin-induced differentiation and survival of erythroid cells, regulated TGFβ and BMP
	Xi, 2016	Human	E.Coli	21His at N-terminus	ProSpec	In vivo	angiogenesis and improved systolic cardiac function after MI in rats
Biomarker	Widera, 2012	Mouse	Insect Sf9 cell	-	-	In vitro	Increased GDF-15 production in adult mouse CMs
	Widera, 2009	Human	Mouse cell line	-	R&D Systems	In vitro	Used for calculation serum Fstl1 concentrations
Chemical properties	Hambrook 2004	Mouse	HEK293	His-Myc at N-terminus	-	In vitro	No structural changes following calcium alteration
	Li, 2013	Mouse	Drosophila S2	6His at C-terminus	-	In vitro	Inhibition of BMP4-induced phosphorylation of Smad1/5/8 in MV1Lu cells
	Tanaka, 2010	Human	COS-7 cells	FLAG	-	In vitro	DIP2A as Fstl1 receptor, Fstl1 binds CD14 and other members TGFβ-family

I/R; Ischemia/reperfusion, MI; myocardial infarction, CM; cardiomyocyte, EC; endothelial cell, RV; right ventricular, HFpEF; heart failure with preserved ejection fraction, hESC-CM; human embryonic stem cell derived cardiomyocyte, SMC; smooth muscle cell

these results, it is plausible that the upregulation of myocardial and downregulation of epicardial FSTL1 expression following MI alters distribution and ratios of hyper- and hypoglycosylated FSTL1 in the damaged heart. Since several different isoforms and sources of FSTL1 have been used in previous studies and therefore results are difficult to compare across studies, **Table 1** provides an overview of the specifications of previously used recombinant FSTL1 and the main results found with each of these forms. However, precise mechanistic cues of post-translational modifications leading to either cardioprotective or regenerative capacities of FSTL1 still remain to be elucidated.

2.2. METHOD OF DELIVERY TO THE INJURED HEART

Previously described cardioprotective properties of FSTL1 *in vitro* and in small animal models are considered promising and raise the question which application method would be most suitable for FSTL1 to exhibit its effects in large animals and in humans. Systemic administration of FSTL1 is a conceivable option, however it is unlikely that it will have considerable beneficial effect as FSTL1 is already upregulated in response to various cardiac conditions, including ACS, ischemic cardiomyopathy, end-stage heart failure, and HFpEF. Intramyocardial injections with regenerative factors at the site of injury may potentially induce a cardiac regenerative response⁷⁹⁻⁸⁵.

In summary, FSTL1 expression and function has been shown to be closely linked to cardiac disease, both as a marker, and increasingly as a potential therapeutic compound or target. It is important to determine the mechanism and extent of the specific pro- and anti-inflammatory effects when FSTL1 is considered as a potential therapeutic agent or target to treat cardiovascular diseases. Finally, the method of application of FSTL1 in the context of cardiovascular disease will also very likely play a role on how inflammatory responses turn out. Characterization of the effect of FSTL1 on inflammatory cell infiltration and activation in the heart is essential before

therapeutic application can be considered.

CONCLUSION

FSTL1 is a cardiokine with multiple implications in cellular processes in the heart, particularly in response to cardiac injury. An increasing body of evidence indicates that FSTL1 may attenuate I/R injury by inhibiting cardiomyocyte apoptosis and stimulating cardiomyocyte proliferation and revascularization, suggesting a potential role in regenerative therapy for heart failure patients. Furthermore, a protective role of FSTL1 has been described in cardiac hypertrophy and pulmonary hypertension. Effects and function of FSTL1 in the context of inflammation remain ambiguous and require further research, especially in acute and chronic cardiovascular disease. The spatio-temporal organization of FSTL1 expression, its localization and onset after induction of damage, as well as post-translational modifications of FSTL1, mostly in terms of glycosylation, have been shown to be critical parameters of activity. The hypoglycosylated epicardial FSTL1, diminished upon myocardial injury, holds most potential in exerting cardioprotective and regenerative effects. To achieve this, epicardial reconstitution of FSTL1 following I/R injury may be preferred, despite the risks associated with a potentially invasive procedure.

In conclusion, FSTL1 exhibits regenerative and tissue-protective features making it a promising candidate for novel approaches to treat cardiovascular disease, while mechanistic details need further research before advancing to therapeutic applications.

ACKNOWLEDGEMENTS

Marijn Peters is supported by a Netherlands CardioVascular Research Initiative (CVON) grant (REMAIN 2014B027). Joost Sluijter is supported by Horizon2020 ERC-2016-COG EVICARE [725229].

REFERENCES

1. Shibanuma M, Mashimo J, Mita A, Kuroki T, Nose K. Cloning from a mouse osteoblastic cell line of a set of transforming-growth-factor- β -regulated genes, one of which seems to encode a follistatin-related polypeptide. *Eur J Biochem.* 1993;217:13-19.
2. Hambrock HO, Kaufmann B, Müller S, et al. Structural characterization of TSC-36/Flik: Analysis of two charge isoforms. *J Biol Chem.* 2004;279(12):11727-11735.
3. Widera C, Horn-Wichmann R, Kempf T, et al. Circulating concentrations of follistatin-like 1 in healthy individuals and patients with acute coronary syndrome as assessed by an immunoluminometric sandwich assay. *Clin Chem.* 2009;55(10):1794-1800.
4. Tanaka M, Ozaki S, Osakada F, Mori K, Okubo M, Nakao K. Cloning of follistatin-related protein as a novel autoantigen in systemic rheumatic diseases. *Int Immunol.* 1998;10(9):1305-1314.
5. Zwijsen A, Blockx H, Van Arnhem W, et al. Characterization of a Rat C6 Glioma-Secreted Follistatin-Related Protein (FRP): Cloning and Sequence of the Human Homologue. *Eur J Biochem.* 1994;225(3):937-946.
6. Miyamae T, Marinov AD, Sowders D, et al. Follistatin-Like Protein-1 Is a Novel Proinflammatory Molecule. *J Immunol.* 2006;177(7):4758-4762.
7. Oshima Y, Ouchi N, Sato K, Izumiya Y, Pimentel DR, Walsh K. Follistatin-like 1 is an Akt-regulated cardioprotective factor that is secreted by the heart. *Circulation.* 2008;117(24):3099-3108.
8. Görgens SW, Raschke S, Holven KB, Jensen J, Eckardt K, Eckel J. Regulation of follistatin-like protein 1 expression and secretion in primary human skeletal muscle cells. *Arch Physiol Biochem.* 2013;119(2):75-80.
9. Lara-Pezzi E, Felkin LE, Birks EJ, et al. Expression of follistatin-related genes is altered in heart failure. *Endocrinology.* 2008;149(11):5822-5827.
10. Adams D, Larman B, Oxburgh L. Developmental expression of mouse Follistatin-like 1 (Fstl1): Dynamic regulation during organogenesis of the kidney and lung. *Gene Expr Patterns.* 2007;7(4):491-500.
11. Sumitomo K, Kurisaki A, Yamakawa N, et al. Expression of a TGF- β 1 inducible gene, TSC-36, causes growth inhibition in human lung cancer cell lines. *Cancer Lett.* 2000;155(1):37-46.
12. Sylva M, Moorman AFM, Van den Hoff MJB. Follistatin-like 1 in vertebrate development. *Birth Defects Res Part C - Embryo Today Rev.* 2013;99(1):61-69.
13. Ambrosy AP, Fonarow GC, Butler J, et al. The global health and economic burden of hospitalizations for heart failure: Lessons learned from hospitalized heart failure registries. *J Am Coll Cardiol.* 2014;63(12):1123-1133.
14. Taylor CJ, Ryan R, Nichols L, Gale N, Richard Hobbs FD, Marshall T. Survival following a diagnosis of heart failure in primary care. *Fam Pract.* 2017;34(2):161-

168.

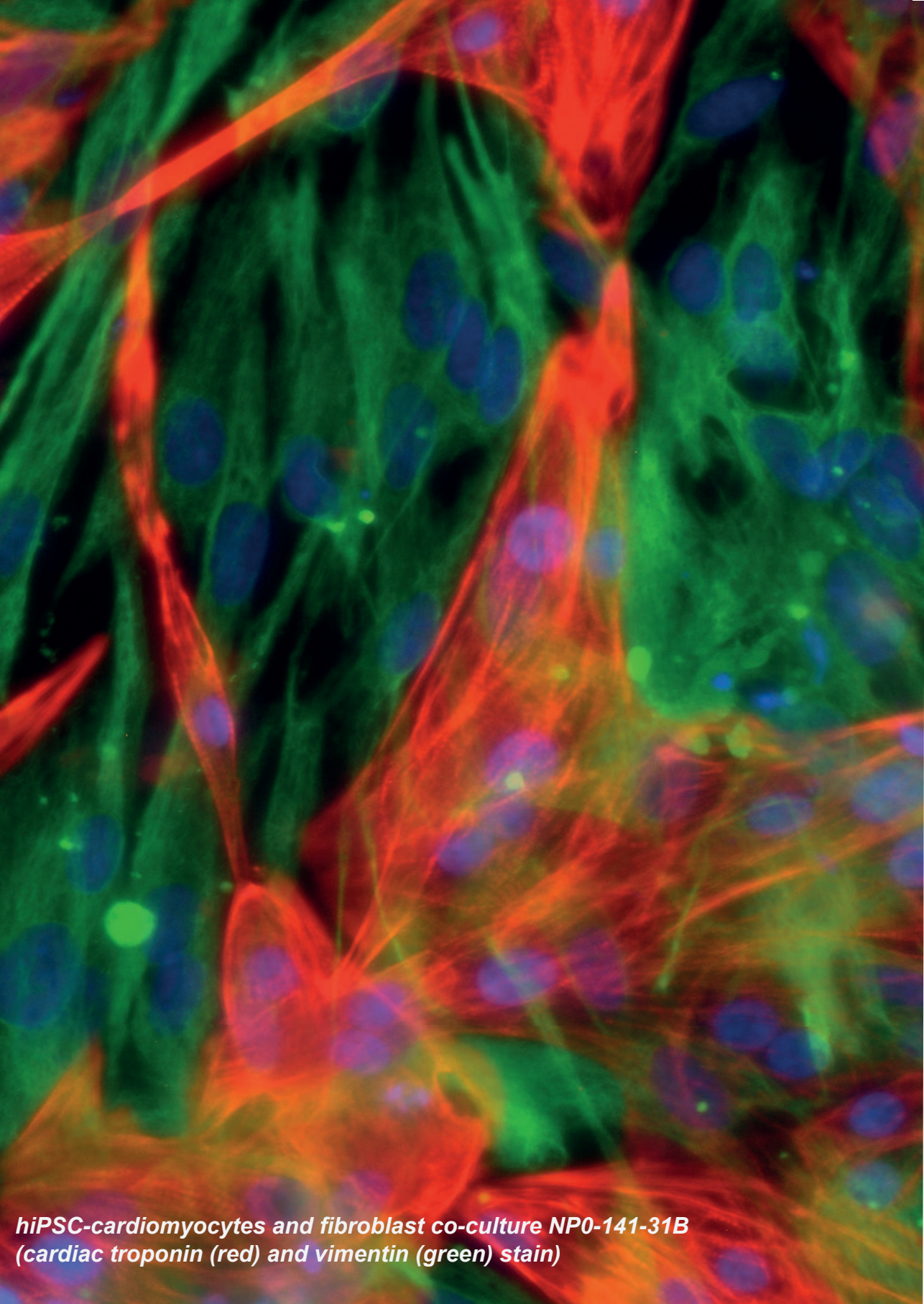
15. Fisher SA, Zhang H, Doree C, Mathur A, Martin-Rendon E. Stem cell treatment for acute myocardial infarction. *Cochrane Database Syst Rev.* 2015;2015(9).
16. Feyen DAM, Van Den Hoogen P, Van Laake LW, et al. Intramyocardial stem cell injection: Go(ne) with the flow. *Eur Heart J.* 2017;38(3):184-186.
17. Madonna R, Van Laake LW, Davidson SM, et al. Position Paper of the European Society of Cardiology Working Group Cellular Biology of the Heart: Cell-based therapies for myocardial repair and regeneration in ischemic heart disease and heart failure. *Eur Heart J.* 2016;37(23):1789-1798.
18. Fernández-Avilés F, Sanz-Ruiz R, Climent AM, et al. Global position paper on cardiovascular regenerative medicine. *Eur Heart J.* 2017;38(33):2532-2546.
19. Sluijter JPG, Davidson SM, Boulanger CM, et al. Extracellular vesicles in diagnostics and therapy of the ischaemic heart: Position Paper from the Working Group on Cellular Biology of the Heart of the European Society of Cardiology. *Cardiovasc Res.* 2018;114(1):19-34.
20. Shimano M, Ouchi N, Walsh K. Cardiokines: Recent progress in elucidating the cardiac secretome. *Circulation.* 2012;126(21). doi:10.1161/
21. Deddens JC, Vrijzen KR, Girao H, Doevendans PA, Sluijter JPG. Cardiac-released extracellular vesicles can activate endothelial cells. *Ann Transl Med.* 2017;5(3):4-6.
22. Doroudgar S, Glembotski CC. The cardiokine story unfolds: Ischemic stress-induced protein secretion in the heart. *Trends Mol Med.* 2011;17(4):207-214.
23. Jahng JWS, Song E, Sweeney G. Crosstalk between the heart and peripheral organs in heart failure. *Exp Mol Med.* 2016;48(3):1-11.
24. Walsh K. Adipokines, myokines and cardiovascular disease. *Circ J.* 2009;73(1):13-18.
25. Chiba A, Watanabe-Takano H, Miyazaki T, Mochizuki N. Cardiomyokines from the heart. *Cell Mol Life Sci.* 2018;75(8):1349-1362.
26. Mattiotti A, Prakash S, Barnett P, van den Hoff MJB. Follistatin-like 1 in development and human diseases. *Cell Mol Life Sci.* 2018;75(13):2339-2354.
27. Shimano M, Ouchi N, Nakamura K, et al. Cardiac myocyte follistatin-like 1 functions to attenuate hypertrophy following pressure overload. *Proc Natl Acad Sci U S A.* 2011;108(43):899-906.
28. Ouchi N, Asami Y, Ohashi K, et al. DIP2A functions as a FSTL1 receptor. *J Biol Chem.* 2010;285(10):7127-7134.
29. Liu S, Wang L, Wang W, et al. TSC-36/FRP inhibits vascular smooth muscle cell proliferation and migration. *Exp Mol Pathol.* 2006;80(2):132-140.
30. Ogura Y, Ouchi N, Ohashi K, et al. Therapeutic impact of follistatin-like 1 on myocardial ischemic injury in preclinical models. *Circulation.* 2012;126(14):1728-

- 1738.
31. Xi Y, Gong DW, Tian Z. FSTL1 as a Potential Mediator of Exercise-Induced Cardioprotection in Post-Myocardial Infarction Rats. *Sci Rep.* 2016;6(August):1-11.
 32. Beauloye C, Bertrand L, Horman S, Hue L. AMPK activation, a preventive therapeutic target in the transition from cardiac injury to heart failure. *Cardiovasc Res.* 2011;90(2):224-233.
 33. Xiao Y, Zhang Y, Chen Y, et al. Inhibition of MicroRNA-9-5p protects against cardiac remodeling following myocardial infarction in mice. *Hum Gene Ther.* 2019;30(3):286-301.
 34. Wei K, Serpooshan V, Hurtado C, et al. Epicardial FSTL1 reconstitution regenerates the adult mammalian heart. *Nature.* 2015;525(7570):479-485.
 35. Rooij E Van. Cardiac Repair after Myocardial Infarction. *N Engl J Med.* 2016:85-87.
 36. Bergmann O, Zdunek S, Felker A, et al. Dynamics of Cell Generation and Turnover in the Human Heart. *Cell.* 2015;161(7):1566-1575.
 37. Buggisch M, Ateghang B, Ruhe C, et al. Stimulation of ES-cell-derived cardiomyogenesis and neonatal cardiac cell proliferation by reactive oxygen species and NADPH oxidase. *J Cell Sci.* 2007;120(5):885-894.
 38. D'Uva G, Aharonov A, Lauriola M, et al. ERBB2 triggers mammalian heart regeneration by promoting cardiomyocyte dedifferentiation and proliferation. *Nat Cell Biol.* 2015;17(5):627-638.
 39. Heallen T, Zhang M, Wang J, et al. Hippo Pathway Inhibits Wnt Signaling to Restrain Cardiomyocyte Proliferation and Heart Size. *Science.* 2011;332:458-461.
 40. Widera C, Giannitsis E, Kempf T, et al. Identification of follistatin-like 1 by expression cloning as an activator of the growth differentiation factor 15 gene and a prognostic biomarker in acute coronary syndrome. *Clin Chem.* 2012;58(8):1233-1241.
 41. Kretzschmar K, Post Y, Bannier-Hélaouët M, et al. Profiling proliferative cells and their progeny in damaged murine hearts. *Proc Natl Acad Sci U S A.* 2018;115(52):E12245-E12254.
 42. Ouchi N, Oshima Y, Ohashi K, et al. Follistatin-like 1, a secreted muscle protein, promotes endothelial cell function and revascularization in ischemic tissue through a nitric-oxide synthase-dependent mechanism. *J Biol Chem.* 2008;283(47):32802-32811.
 43. Miyabe M, Ohashi K, Shibata R, et al. Muscle-derived follistatin-like 1 functions to reduce neointimal formation after vascular injury. *Cardiovasc Res.* 2014;103(1):111-120.
 44. Wollert KC, Kempf T, Peter T, et al. Prognostic value of growth-differentiation factor-15 in patients with non-ST-elevation acute coronary syndrome. *Circulation.* 2007;115(8):962-971.
 45. El-Armouche A, Ouchi N, Tanaka K, et al. Follistatin-like 1 in chronic systolic heart

- failure a marker of left ventricular remodeling. *Circ Hear Fail.* 2011;4(5):621-627.
46. Tanaka K, Valero-Muñoz M, Wilson RM, et al. Follistatin-Like 1 Regulates Hypertrophy in Heart Failure With Preserved Ejection Fraction. *JACC Basic to Transl Sci.* 2016;1(4):207-221. doi:10.1016/j.jacbts.2016.04.002
 47. Namdari M, Negahdari B, Cheraghi M, Aiyelabegan HT, Eatmadi A. Cardiac failure detection in 30 minutes: new approach based on gold nanoparticles. *J Microencapsul.* 2017;34(2):132-139.
 48. Seki M, Powers JC, Maruyama S, et al. Acute and chronic increases of circulating FSTL1 normalize energy substrate metabolism in pacing-induced heart failure. *Circ Hear Fail.* 2018;11(1):1-12.
 49. Zhang W, Wang W, Liu J, et al. Follistatin-like 1 protects against hypoxia-induced pulmonary hypertension in mice. *Sci Rep.* 2017;7:1-14.
 50. Tania NP, Maarsingh H, Bos IST, et al. Endothelial follistatin-like-1 regulates the postnatal development of the pulmonary vasculature by modulating BMP/Smad signaling. *Pulm Circ.* 2017;7(1):219-231.
 51. Prakash S, Borreguero LJJ, Sylva M, et al. Deletion of Fstl1 (Follistatin-Like 1) from the Endocardial/Endothelial Lineage Causes Mitral Valve Disease. *Arterioscler Thromb Vasc Biol.* 2017;37(9):e116-e130.
 52. Ruparelina N, Chai JT, Fisher EA, Choudhury RP. Inflammatory processes in cardiovascular disease: A route to targeted therapies. *Nat Rev Cardiol.* 2017;14(3):133-144.
 53. Mullenix PS, Andersen CA, Starnes BW. Atherosclerosis as inflammation. *Ann Vasc Surg.* 2005;19(1):130-138.
 54. Maekawa N, Wada H, Kanda T, et al. Improved myocardial ischemia/reperfusion injury in mice lacking tumor necrosis factor- α . *J Am Coll Cardiol.* 2002;39(7):1229-1235.
 55. Jiang B, Liao R. The paradoxical role of inflammation in cardiac repair and regeneration. *J Cardiovasc Transl Res.* 2010;3(4):410-416.
 56. Aurora AB, Porrello ER, Tan W, et al. Macrophages are required for neonatal heart regeneration. *J Clin Invest.* 2014;124(3):1382-1392.
 57. Xia Y, Lee K, Li N, Corbett D, Mendoza L, Frangogiannis NG. Characterization of the inflammatory and fibrotic response in a mouse model of cardiac pressure overload. *Histochem Cell Biol.* 2009;131(4):471-481.
 58. Humbert M, Monti G, Brenot F, et al. Increased interleukin-1 and interleukin-6 serum concentrations in severe primary pulmonary hypertension. *Am J Respir Crit Care Med.* 1995;151:1628-1631.
 59. Li D, Wang Y, Xu N, et al. Follistatin-like protein 1 is elevated in systemic autoimmune diseases and correlated with disease activity in patients with rheumatoid arthritis. *Arthritis Res Ther.* 2011;13(1):1-12.

60. Wilson DC, Marinov AD, Blair HC, et al. Follistatin-like protein 1 is a mesenchyme-derived inflammatory protein and may represent a biomarker for systemic-onset juvenile rheumatoid arthritis. *Arthritis Rheum.* 2010;62(8):2510-2516.
61. Miller M, Beppu A, Rosenthal P, et al. Fstl1 Promotes Asthmatic Airway Remodeling by Inducing Oncostatin M. *J Immunol.* 2015;195(8):3546-3556.
62. Gorelik M, Wilson DC, Cloonan YK, Shulman ST, Hirsch R. Plasma follistatin-like protein 1 is elevated in Kawasaki disease and may predict coronary artery aneurysm formation. *J Pediatr.* 2012;161(1):116-119.
63. Fan N, Sun H, Wang Y, et al. Follistatin-like 1: A potential mediator of inflammation in obesity. *Mediators Inflamm.* 2013;2013.
64. Clutter SD, Wilson DC, Marinov AD, Hirsch R. Follistatin-Like Protein 1 Promotes Arthritis by Up-Regulating IFN- γ . *J Immunol.* 2009;182(1):234-239. , Oxburgh L, Bushnell DS, Hirsch R. FSTL1 promotes arthritis in mice by enhancing inflammatory cytokine/chemokine expression. *Arthritis Rheum.* 2012;64(4):1082-1088.
66. Ni S, Miao K, Zhou X, et al. The involvement of follistatin-like protein 1 in osteoarthritis by elevating NF- κ B-mediated inflammatory cytokines and enhancing fibroblast like synoviocyte proliferation. *Arthritis Res Ther.* 2015;17(1):1-10.
67. Chaly Y, Fu Y, Marinov A, et al. Follistatin-like protein 1 enhances NLRP3 inflammasome-mediated IL-1 β secretion from monocytes and macrophages. *Eur J Immunol.* 2014;44(5):1467-1479.
68. Kwak HB, Ha H, Kim HN, et al. Reciprocal cross-talk between RANKL and interferon- γ -inducible protein 10 is responsible for bone-erosive experimental arthritis. *Arthritis Rheum.* 2008;58(5):1332-1342.
69. Kawabata D, Tanaka M, Fujii T, et al. Ameliorative Effects of Follistatin-Related Protein/TSC-36/FSTL1 on Joint Inflammation in a Mouse Model of Arthritis. *Arthritis Rheum.* 2004;50(2):660-668.
70. Conway JG, Wakefield JA, Brown RH, et al. Inhibition of cartilage and bone destruction in adjuvant arthritis in the rat by a matrix metalloproteinase inhibitor. *J Exp Med.* 1995;182(2):449-457.
71. Dooley S, Herlitzka I, Hanselmann R, et al. Constitutive expression of c-fos and c-jun, overexpression of ets-2, and reduced expression of metastasis suppressor gene nm23-H1 in rheumatoid arthritis. *Ann Rheum Dis.* 1996;55(5):298-304.
72. Shiozawa S, Shimizu K, Tanaka K, Hino K. Studies on the contribution of c-fos/AP-1 to arthritic joint destruction. *J Clin Invest.* 1997;99(6):1210-1216.
73. Tamura T, Udagawa N, Takahashi N, et al. Soluble interleukin-6 receptor triggers osteoclast formation by interleukin 6. *Proc Natl Acad Sci U S A.* 1993;90(24):11924-11928.
74. Cheng KY, Liu Y, Han YG, et al. Follistatin-like protein 1 suppressed pro-inflammatory cytokines expression during neuroinflammation induced by

- lipopolysaccharide. *J Mol Histol*. 2017;48(2):63-72.
75. Hayakawa S, Ohashi K, Shibata R, et al. Cardiac myocyte-derived follistatin-like 1 prevents renal injury in a subtotal nephrectomy model. *J Am Soc Nephrol*. 2015;26(3):636-646.
 76. Murakami K, Tanaka M, Usui T, et al. Follistatin-related protein/follistatin-like 1 evokes an innate immune response via CD14 and toll-like receptor 4. *FEBS Lett*. 2012;586(4):319-324.
 77. Guo J, Liang W, Li J, Long J. Knockdown of FSTL1 inhibits oxLDL-induced inflammation responses through the TLR4/MyD88/NF- κ B and MAPK pathway. *Biochem Biophys Res Commun*. 2016;478(4):1528-1533.
 78. Maruyama S, Nakamura K, Papanicolaou KN, et al. Follistatin-like 1 promotes cardiac fibroblast activation and protects the heart from rupture. *EMBO Mol Med*. 2016;8(8):949-966.
 79. Magadum A, Singh N, Kurian AA, Sharkar MTK, Chepurko E, Zangi L. Ablation of a Single N-Glycosylation Site in Human FSTL 1 Induces Cardiomyocyte Proliferation and Cardiac Regeneration. *Mol Ther - Nucleic Acids*. 2018;13(December):133-143.



*hiPSC-cardiomyocytes and fibroblast co-culture NP0-141-31B
(cardiac troponin (red) and vimentin (green) stain)*

Chapter 6

FOLLISTATIN-LIKE 1 PROMOTES PROLIFERATION OF MATURED HYPOXIC HUMAN IPSC-CARDIOMYOCYTES AND IS SECRETED BY HUMAN CARDIAC FIBROBLASTS

Submitted

*Marijn M.C. Peters*¹, *Sofia Di Martino*¹, *Thomas Boelens*¹, *Pieter A. Doevendans*¹,
Steven A.J. Chamuleau^{1,2}, *Joost P.G. Sluijter*^{1*}, and *Klaus Neef*^{1*}

¹ Department of Cardiology, Laboratory of Experimental Cardiology, Regenerative Medicine Centre Utrecht, University Medical Centre Utrecht, University Utrecht, Utrecht, the Netherlands

² Amsterdam UMC Heart Centre, Department of Cardiology, Amsterdam, the Netherlands

ABSTRACT

The human heart has limited regenerative capacity. Therefore, patients often progress to heart failure after ischemic injury, despite advances in reperfusion therapies generally decreasing mortality. Follistatin-like 1 (FSTL1) has been shown to increase cardiomyocyte (CM) proliferation, decrease CM apoptosis and prevent cardiac rupture in animal models of ischemic heart disease depending on its glycosylation state. To explore its therapeutic potential, we used a human *in vitro* model of cardiac ischemic injury using human induced pluripotent stem cell-derived CMs (iPSC-CMs) and assessed potential regenerative and protective effects of two differently glycosylated variants of human FSTL1. Furthermore, we investigated the interplay between cardiac fibroblasts (cFBs) and iPSC-CMs after ischemic damage with respect to FSTL1 expression. Both FSTL1 variants increased viability, while only hypo-glycosylated FSTL1 increased CM proliferation post-ischemia. Human foetal and iPSC derived cFBs expressed and secreted FSTL1 under normoxic conditions, while FSTL1 secretion increased by iPSC derived cFBs upon ischemia but decreased in CMs. Co-culture with CMs and cFBs increased FSTL1 secretion compared to secretion in cFB monoculture. Taken together, we have shown FSTL1 induces CM proliferation in a human model of cardiac ischemic injury by using iPSC-CM. Furthermore, this is the first report of FSTL1 secretion by human cFBs.

INTRODUCTION

The human heart has limited regenerative capacity and repairs itself poorly after injury. After ischemic injury, patients often progress to heart failure despite the decrease in direct mortality by reperfusion therapies^{1,2}. In contrast to the adult human heart, neonatal vertebrate and invertebrate hearts can substantially regenerate from injury or disease via induced proliferation of cardiomyocytes (CMs) *in situ*^{3,4}. Since damaged adult CMs in the human heart show upregulation of genes involved in heart development and invertebrate heart regeneration, a rudimentary cardiac regeneration mechanism seems to exist, yet inefficient to cope with massive CM damage or loss, as inflicted by ischemic insult from myocardial infarction⁵⁻⁹. Thus, stimulation of the CM cell cycle to potentially re-establish regenerative capacity in the adult human heart has become a key focus in the field of advanced cardiac therapies. Induction of CM proliferation in regenerating hearts has been linked to paracrine signalling, often attributed to secretion from the epicardium¹⁰⁻¹⁴. Furthermore, efficient cardiac regeneration has been shown to be accompanied by revascularisation induced by epicardial derived endothelial and smooth muscle cells¹⁵. These cellular responses to tissue damage rely on intercellular communication via soluble paracrine factors¹⁶ and the close proximity of endothelial cells, cardiac fibroblasts (cFBs) and CMs^{17,18}. Changes in the cellular composition after an ischemic insult, as the number of cFBs increase and the number of CMs and endothelial cells decrease, alters paracrine signalling and cross-talk between cardiac cells and thus effects damage response^{16,19}. The epicardium has been identified to be instrumental in mediating cardiac regeneration initially in the zebrafish heart, and later epicardial Follistatin like-1 (FSTL1) has been confirmed to act as myogenic cardiokine in murine and porcine cardiac injury models²⁰. Furthermore, cardioprotective and angiogenic effects of Fstl1 have been reported²¹⁻²⁸. FSTL1 is a 308 amino acid glycoprotein of the SPARC protein family, with three N-glycosylation sites^{27, 29-31}, with one (N180) being critically linked to the role of FSTL1 in cardiac regeneration³¹. Additionally, an increase in secretion

of FSTL1 with higher molecular weight, likely due to protein glycosylation, could be observed in mouse serum and myocardium after myocardial infarction^{20,28}. All this strongly suggests, that regulation of FSTL1 expression and glycosylation after myocardial infarction could guide approaches on exploiting its regenerative potential for the heart. Besides its role in CM renewal, the expression of FSTL1 by cFBs in the infarct area was found to be essential to prevent cardiac rupture^{32,33}.

As indicated, so far animal studies have shed some light on FSTL1 as a potential therapeutic agent to induce cardiac regeneration by stimulating both CM proliferation, protection from apoptosis, revascularisation and stabilizing the infarct scar. However, these findings have yet to be confirmed in a human setting. The development of CMs derived from human induced pluripotent stem cells (iPSC-CMs) has become a new promising way to model the complex cellular physiology of human cardiac cells, while taking into account the usually relatively immature phenotype of iPSC-CMs³⁴. Using methods to stimulate metabolic maturation of iPSC-CMs and stimulate oxidative phosphorylation-based energy metabolism³⁵ could improve their susceptibility to ischemic damage and enable their use as a model of ischemic heart disease.

In this study, we sought to assess the cardiac regenerative capacity of FSTL1 and its' glycosylation state using a human iPSC-CM-based *in vitro* ischemia model, and exploring a potential role of cardiac fibroblasts.

RESULTS

Hypo- and hyperglycosylated FSTL1 variants exert cardioprotective effects

We analysed cardioprotective effects of FSTL1 and the effect of FSTL1 glycosylation by treating CMs with bacterially produced hFSTL1(low-glycosylated; gly^{low}-FSTL1) or mammalian produced hFSTL1 (glycosylated; gly^{high}-FSTL1) at the onset of 24h hypoxia (**Figure 1a**). The increased molecular weight of gly^{high}-FSTL1 was confirmed

Follistatin-like 1 promotes proliferation of matured hypoxic human iPSC-cardiomyocytes and is secreted by human cardiac fibroblasts

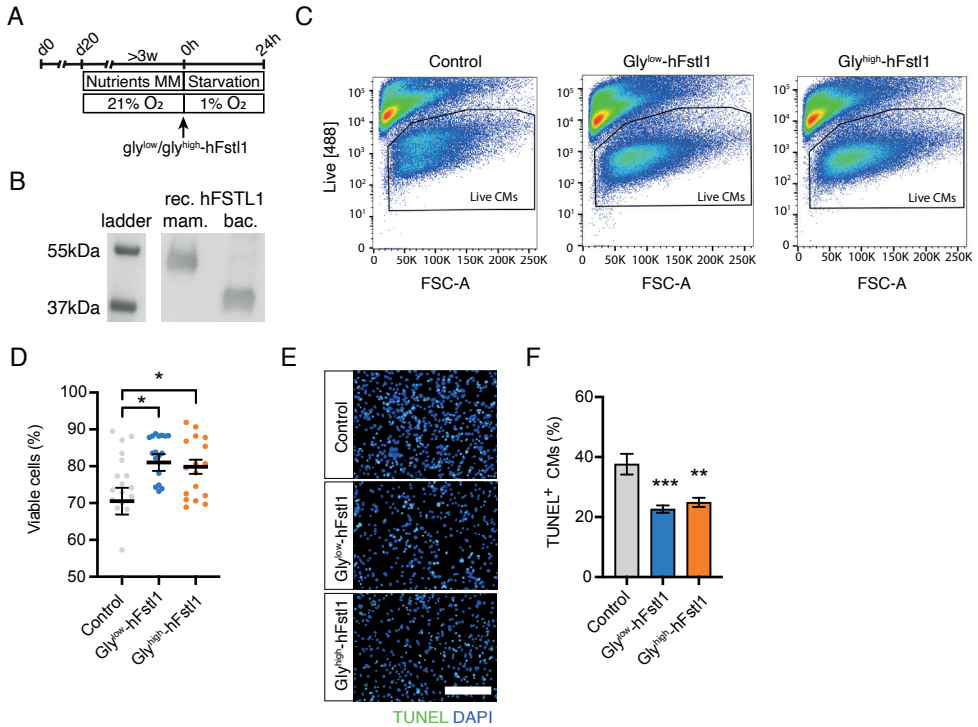


Figure 1. FSTL1 increases survival of hypoxic matured iPSC cardiomyocytes

A. Schematic representation of experimental set-up. **B.** Western blot analysis of bacterial and mammalian produced hFSTL1. **C.** Flow cytometry analysis of live dead staining. **D.** Quantification of **C.** **E.** Microscopic images of TUNEL stained CM nuclei. **F.** Quantification of **E.** n=3 experiments. Data was analysed using one-way ANOVA and Dunnett multiple comparison. * $P < 0,05$, ** $P < 0,01$, *** $P < 0,001$. Scale bar: 200 μ m. Data represented as mean \pm SEM.

by Western blot (50 kDa vs 37 kDa gly^{low}-FSTL1) (**Figure 1b**). Flow cytometric analysis showed a significant increase in viability after treatment with either glycosylation variant compared to control (from 70 \pm 3,6% [Control] to 81 \pm 2,3% [gly^{low}-FSTL1] or 79,4 \pm 1,9% [gly^{high}-FSTL1], $P < 0,05$; **Figure 1c, d**). Furthermore, both glycosylation variants of FSTL1 decreased the number of TUNEL+ CMs (from 37,6 \pm 3,5% [Control] to 22,6 \pm 1,2% [gly^{low}-FSTL1] or 24,9 \pm 1,5% [gly^{high}-FSTL1], $P < 0,01$; **Figure 1e, f**).

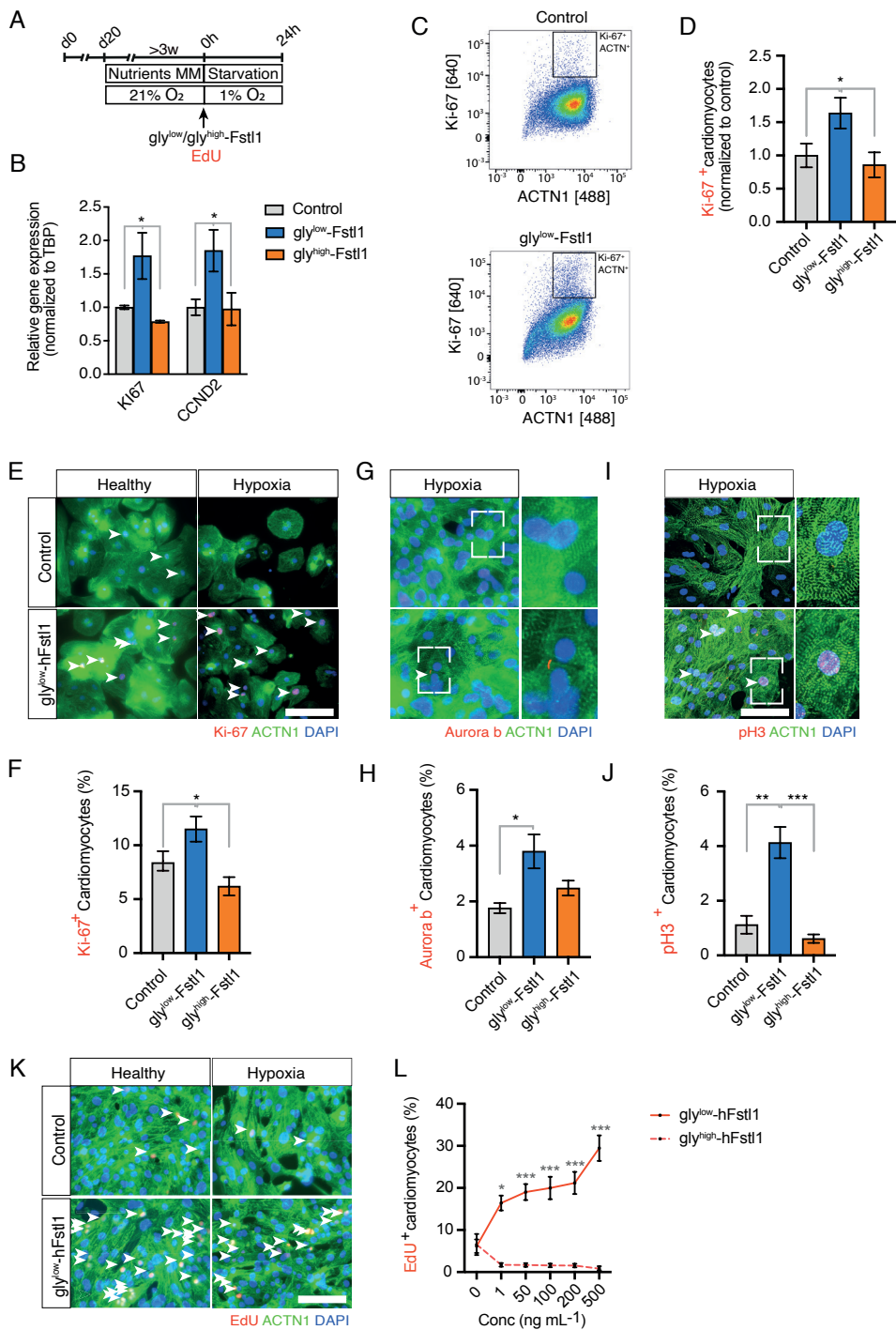


Figure 2. Gly^{low}-FSTL1 treatment induces proliferation in healthy and hypoxic matured iPSC-CMs

A. Schematic representation of experimental set-up. **B.** mRNA expression of cell cycle genes Ki-67 and CNND2 (CYCLIN D2) normalized to TATA binding protein (TBP) expression. **C.** Flow cytometry analysis of Ki-67-positive CMs (**C**) and quantification (**D**). **E-J.** Representative images and quantification of Ki-67 (**E, F**), pH3 (**G, H**), and aurora b kinase (**I, J**). **K, L.** Microscopic images of EdU, ACTN1 staining (**K**) and quantification (**L**). Arrowheads indicate EdU+ CMs. n=3 experiments for staining and n=6 experiments for flow cytometry. Data was analysed using one-way ANOVA and Dunnett multiple comparison.*P<0,05, **P<0,01, ***P<0,001. Scale bar: 200µm. Data represented as mean ± SEM.

Hypoglycosylated FSTL1 increases proliferation of hypoxic mature iPSC-CMs

To determine whether FSTL1 could promote proliferation in 40-days metabolic matured iPSC-CMs, we exposed the cells to FSTL1 at the onset of 24h hypoxia (**Figure 2a**). Gly^{low}-FSTL1 treatment prior to 24h ischemia increased the mRNA expression of proliferation marker Ki-67 compared to control ($1,77 \pm 0,35$ fold [gly^{low}-FSTL1]), $P < 0,05$) and G1/S cell cycle marker CYCLIN D2 compared to control ($1,82 \pm 0,28$ fold [gly^{low}-FSTL1]), $P < 0,05$; **Figure 2b**). Expression of proliferation marker Ki-67 was increased after gly^{low}-FSTL1 treatment as confirmed by flow cytometry ($1,64 \pm 0,23\%$ [gly^{low}-FSTL1]), $P < 0,05$; **Figure 2c, d**) and immunocytochemistry (**Figure 2e, f**) from 8,4% to 11,5% Ki-67⁺-CMs while treatment with gly^{high}-FSTL1 did not increase Ki-67 expression (6,2% Ki-67⁺ CMs). Similarly, only gly^{low}-FSTL1 treatment increased expression of cytokinesis marker aurora b kinase (from $1,76 \pm 0,18\%$ [control] to $3,8 \pm 0,61\%$ [gly^{low}-FSTL1]), $P < 0,05$; **Figure 2g, h**) and mitotic marker pH3 (from $1,12 \pm 0,33\%$ [control] to $4,13 \pm 0,57\%$ [gly^{low}-FSTL1]), $P < 0,01$; **Figure 2i, j**).

To further validate if FSTL1 can increase CM proliferation, iPSC-CMs were incubated with 5-ethynyl-20-deoxyuridine (EdU) at the moment of the FSTL1 administration at the onset of 24h hypoxia to analyse DNA synthesis. gly^{low}-FSTL1 dose-dependently increased EdU incorporation in hypoxic CMs while gly^{high}-FSTL1 did not and even

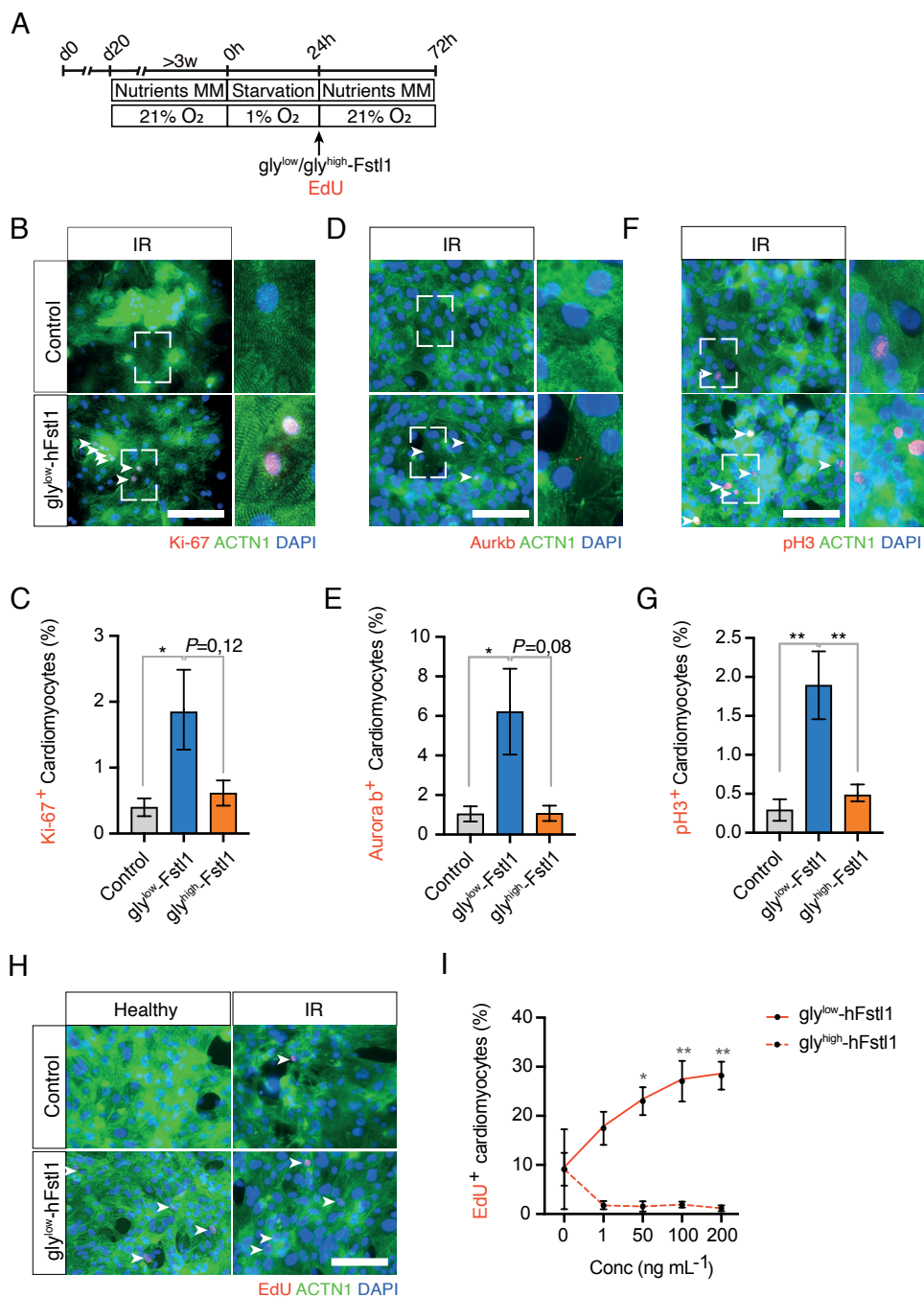


Figure 3. Gly^{low}-FSTL1 treatment after ischemia induces proliferation of iPSC-CMs

A. Schematic representation of experimental set-up. **B-G.** Representative images and quantification of Ki-67 (**B, C**), p3 (D, E), and aurora b kinase (**F, G**). **H, I.** Microscopic images of EdU, ACTN1 staining (**H**) and quantification (**I**). Arrowheads indicate EdU+ cardiomyocytes. n=3 experiments.

Figure 3 continued

Data was analysed using one-way ANOVA and Dunnett multiple comparison. * $P < 0,05$, ** $P < 0,01$, *** $P < 0,001$. Scale bar: 200 μm . Data represented as mean \pm SEM.

decreased EdU incorporation ($6,13 \pm 1,6\%$ [0ng/mL gly^{low}-FSTL1]; $19,0 \pm 1,91\%$ [gly^{low}-FSTL1]; $1,69 \pm 0,43\%$, **Figure 2k, I**). We have shown that hypo-glycosylated FSTL1 treatment induced proliferation of hypoxic CMs when CMs were supplemented with FSTL1 at the start of hypoxia. To determine potential post-hypoxic effects, iPSC-CMs were supplemented with FSTL1 after 24h hypoxia after which we treated the cells with FSTL1 and analysed for expression of proliferation markers after another 48h of non-hypoxic conditions (**Figure 3a**). Again, gly^{low}-FSTL1 induced increased expression of Ki-67 (from $0,4 \pm 0,13\%$ [control] to $1,84 \pm 0,61\%$ [gly^{low}FSTL1]), $P < 0,05$), pH3 (from $0,29 \pm 0,14\%$ [control] to $1,89 \pm 0,44\%$ [gly^{low}-Fstl1]), $P < 0,01$), and aurora b kinase (from $1,0 \pm 0,38\%$ [control] to $6,2 \pm 2,2\%$ [gly^{low}-FSTL1]), $P < 0,05$; **Figure 3b-g**) compared to control. Furthermore, incorporation of EdU was increased after treatment with gly^{low}-compared to control ($9,11 \pm 3,3\%$ [0 ng/mL gly^{low}-FSTL1]; $23,0 \pm 2,84\%$ [50 ng/mL gly^{low}-FSTL1], **Figure 3h, i**).

RNA expression profile of FSTL1 treated hypoxic mature iPSC-CMs

To assess the effect of FSTL1 on CM gene expression, we compared the transcriptional profile of gly^{low}-FSTL1 treated ischemic iPSC-CMs with gly^{high}-FSTL1 treated ischemic iPSC-CMs and control hypoxic iPSC-CMs ($n=5$) using RNA-seq. Using Limma-voom analysis³⁷ we identified 13.546 up-regulated and 2.003 downregulated genes in gly^{low}-FSTL1 treated ischemic iPSC-CMs compared to control hypoxic iPSC-CMs (**Figure 4a, b**). No significantly differentially expressed genes in gly^{high}-FSTL1 treated hypoxic iPSC-CMs compared to control hypoxic iPSC-CMs could be found (**Supplemental figure 1**). Principle component (PC) analysis showed scattering of the samples based on the largest variance between samples

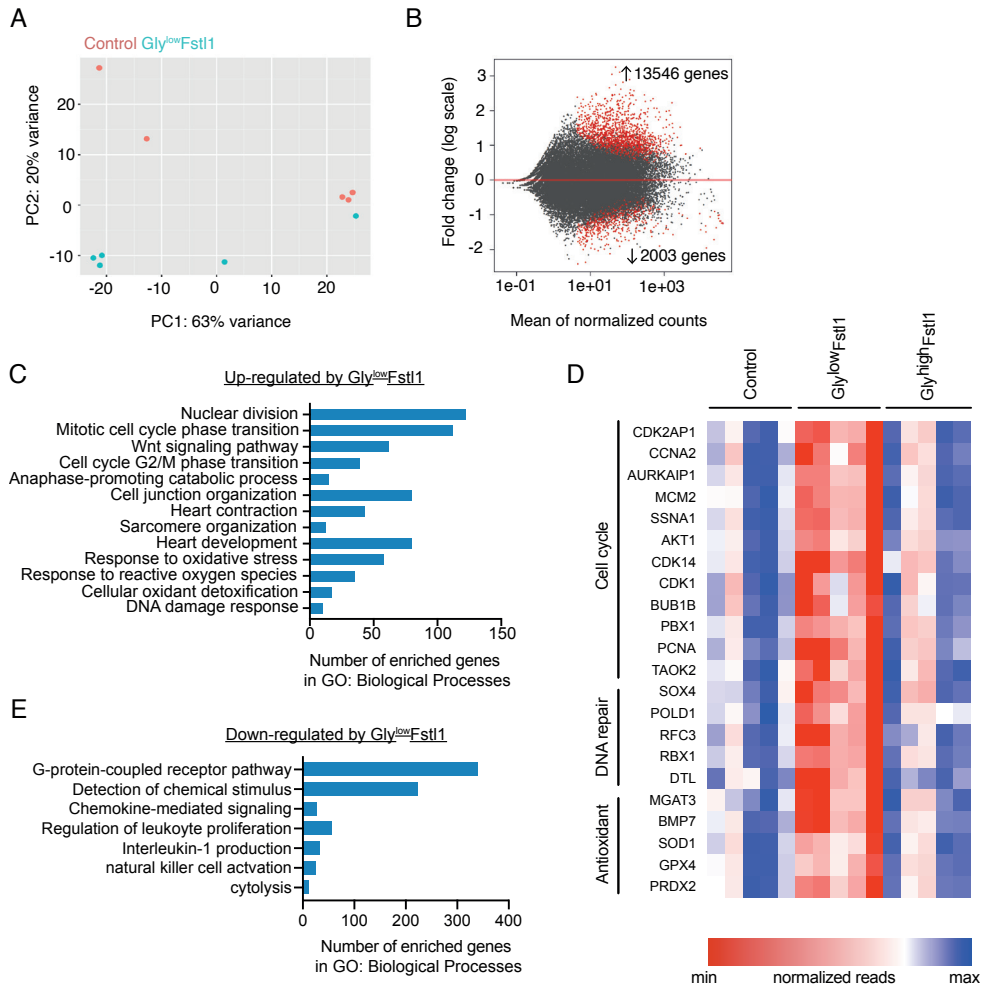


Figure 4. RNA expression profile of FSTL1 treated hypoxic iPSC-CMs

A. Principle component analysis (PCA) plots of hypo-glycosylated FSTL1 treated hypoxic iPSC-CMs and control hypoxic iPSC-CMs showing the separation between the samples based on the top differentially expressed genes using DESeq2. **B.** MA density plot of up- and down-regulated genes in hypo-glycosylated FSTL1 treated iPSC-CMs compared to control using DESeq2. The x-axis shows mean values of normalized counts of all samples and the y-axis shows log₂ Fold change in expression. **C.** Gene ontology enrichment analysis of GO term biological processes showing the top upregulated biological processes enriched after treatment with hypo-glycosylated FSTL1 compared to control. **D.** Heatmap of normalized reads of significantly upregulated cell cycle, DNA repair or antioxidant genes after hypo-glycosylated FSTL1 treatment compared to control analysed using Limma-voom differential expression analysis. Fold change compared to control is shown.

indicating clustering based on CM cell line and the experimental batches (**Figure 4b**). Gene ontology enrichment analysis indicated the top biological processes enriched in gly^{low}-FSTL1 treated hypoxic iPSC-CMs were cell proliferation and cellular response to oxidative stress (**Figure 4c**). Analysis of specifically upregulated genes after gly^{low}-FSTL1 treatment showed upregulation of cell cycle genes, DNA repair genes and antioxidant genes while treatment with gly^{high}-FSTL1 did not induce similar upregulation. Amongst downregulated biological processes after gly^{low}-FSTL1 treated were G-protein coupled receptor pathways and activation of the immune system (**Figure 4d**). Differential expression analysis between control, gly^{low}-FSTL1 and gly^{high}-FSTL1 indicated significantly increased mRNA expression of cell cycle genes, DNA damage repair genes and antioxidants after gly^{low}-FSTL1 treatment. All together, we have shown that only gly^{low}FSTL1 specifically increases activation of proliferation and the reparative response to oxidative stress and reactive oxygen species.

Human cardiac fibroblasts secrete FSTL1 and co-culture with cardiomyocytes increases FSTL1 secretion

We have shown exposure to gly^{low} FSTL1 can increase proliferation and cardioprotection of human metabolically matured CMs under hypoxic conditions. To examine whether human cFBs produce FSTL1 and if expression changes under ischemic conditions, we analysed the expression of FSTL1 by human foetal cardiac fibroblasts (hf-cFBs) and iPSC derived cardiac fibroblasts (iPSC-cFBs) (**Figure 5a**). Hf-cFBs and iPSC-cFBs were positive for vimentin and collagen 1 (**Figure 5b, c**). qRT-PCR analysis for FSTL1 revealed both CMs and cFBs expressed FSTL1 with higher basal expression levels for iPSC-cFBs compared to CMs and hf-cFBs (**Supplemental figure 1**). Comparison of FSTL1 mRNA expression levels showed a trend towards decreased FSTL1 expression in iPSC-cFBs after 24h hypoxia compared to non-hypoxia. No changes in expression of FSTL1 in hf-cFBs were observed comparing to

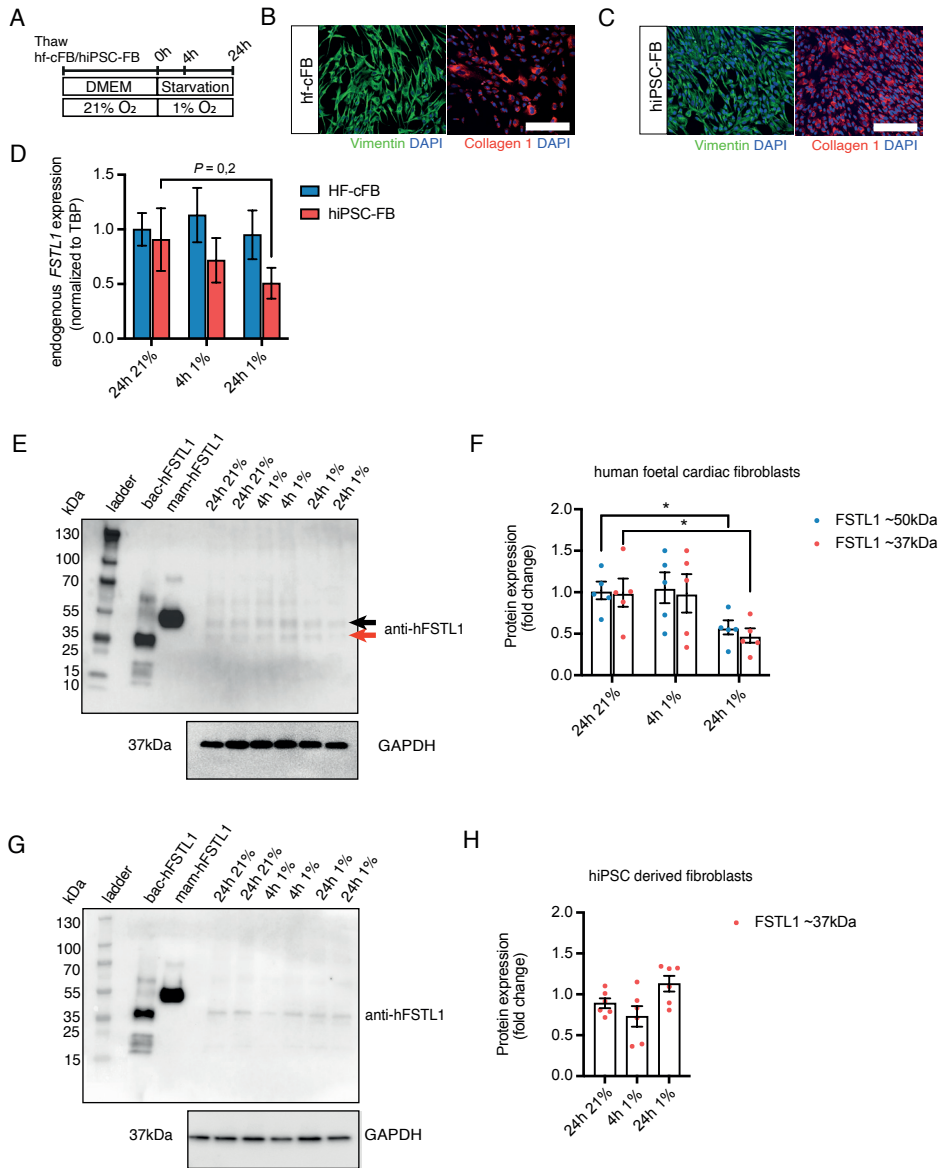


Figure 5. Healthy and hypoxic human cardiac fibroblasts produce FSTL1

A. Schematic representation of experimental set-up. **B, C.** Microscopic images of vimentin-1 and collagen 1 staining of human foetal cardiac fibroblasts (hf-cFBs) (**B**) and human iPSC-cFBs (**C**). **D.** Endogenous FSTL1 mRNA expression levels normalized to TATA binding protein (TBP) levels. **E-H.** Western blot of FSTL1 protein expression by human foetal cardiac fibroblasts (hf-cFBs) (**E**) and human iPSC-cFBs (**G**) and quantification (**F, H**). $n=3$ experiments. Data was analysed using one-way ANOVA and Dunnett multiple comparison. * $P<0,05$, ** $P<0,01$, *** $P<0,001$. Scale bar: 200 μ m. Data represented as mean \pm SEM.

Follistatin-like 1 promotes proliferation of matured hypoxic human iPSC-cardiomyocytes and is secreted by human cardiac fibroblasts

non-hypoxic cell culture conditions (iPSC-cFB: $0,9 \pm 0,3$ fold [24 hour 21%]; $0,72 \pm 0,2$ fold [4 hour 1%], $0,51 \pm 0,14$ fold [24 hour 1%], $P = 0,2$, **Figure 5d, Supplemental figure 2**). Analysis of FSTL1 protein levels showed both hf-cFBs and iPSC-cFB express FSTL1 protein at a similar intensity of bands. cFBs expressed FSTL1 of the two molecular weights: ~ 37 kDa and ~ 50 kDa (**Figure 5e, f**) while iPSC-cFB only expressed the lower molecular weight variant of FSTL1 resembling the non-glycosylated FSTL1 (gly^{low}) (**Figure 5g, h**). Under hypoxic conditions, hf-cFBs showed decreased expression of both protein isoforms (**Figure 5e, f**). Hypoxia did not significantly alter Fstl1 protein expression in iPSC-cFBs (**Figure 5g, h**).

We have shown that both, foetal and iPSC-derived cFBs, produce FSTL1 and it appears that FSTL1 production decreased in prolonged hypoxia. We next aimed to determine whether human cFBs and CMs not only express, but also secrete FSTL1 and if so whether the degree of FSTL1 secretion is affected by decreased oxygen availability. Concentrations of secreted FSTL1 into iPSC-CMs and iPSC-cFBs media after 4h or 24h of hypoxia were determined with the luminex bead-based multiplex detection system. In non-hypoxic conditions, iPSC-CMs and iPSC-cFBs secreted similar levels of FSTL1 ($6327 \pm 170,4$ pg/mL [cFBs] and $6229 \pm 163,1$ pg/mL [CMs]; **Figure 6a**). While hypoxia decreased the internal FSTL1 protein levels in iPSC-derived cFBs, media FSTL1 levels increased in hypoxia (from $6327 \pm 170,4$ pg/mL [24h 21%] to $8582 \pm 376,8$ pg/mL [24h 1%], $P < 0,01$). In iPSC-CMs, ischemia decreased FSTL1 protein secretion (from $6229 \pm 163,1$ pg/mL [24h 21%] to $5250 \pm 102,5$ pg/mL [24h 1%], $P < 0,01$). We next determined the effect of co-culturing iPSC derived CMs and cFBs of the same cell line on FSTL1 media levels in normoxia and hypoxia. To test this, CMs and cFBs were cultured at 80/20%, 70/30% or 50/50% ratio and immunofluorescence staining was used to confirm both cell types were present (**Figure 6b, c**). Non-hypoxic conditions showed highest FSTL1 secretion in a 70/30% iPSC CM/cFBs (from $6229 \pm 163,1$ pg/mL [CM] to 15404 ± 1037 pg/mL [70/30%], $P < 0,001$; **Figure 6d**) compared to cFB-only. While hypoxia decreased FSTL1 secretion in CM

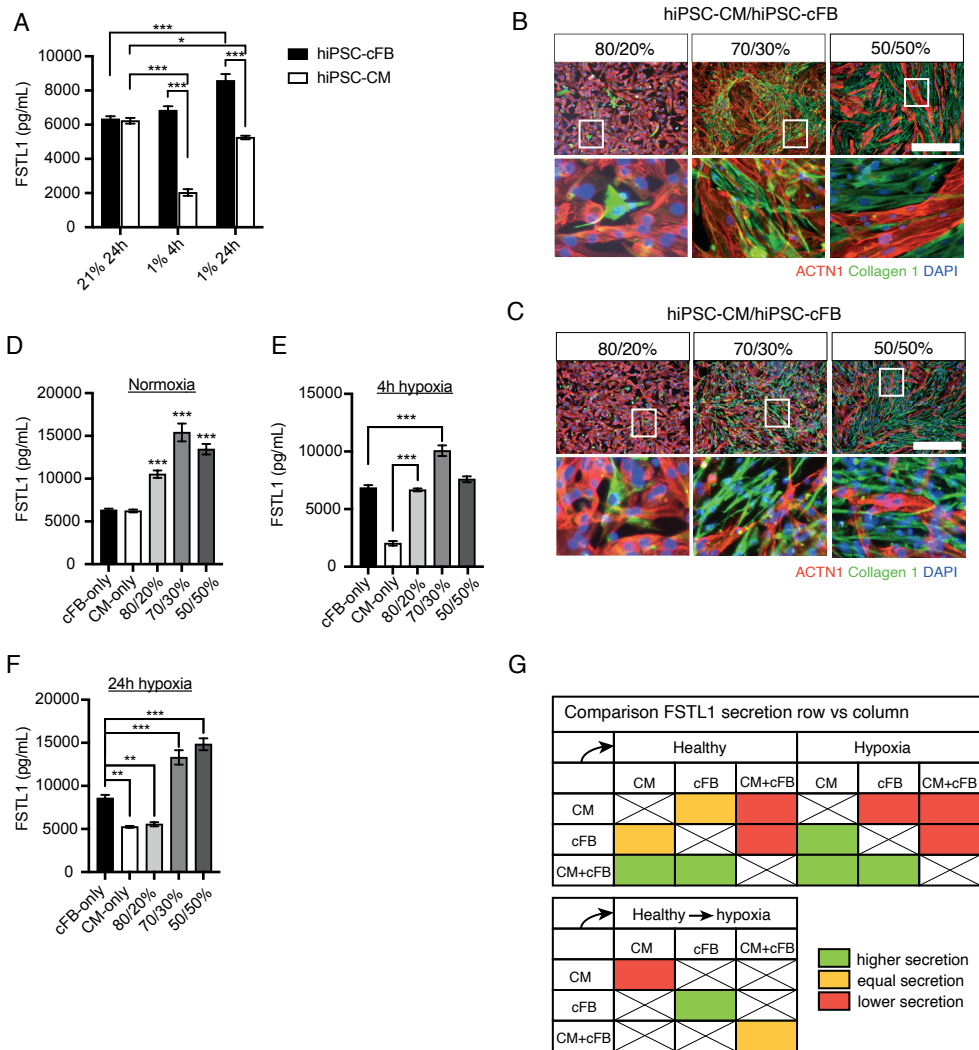


Figure 6. Hypoxia increases human iPSC-fibroblast FSTL1 secretion but decreases iPSC cardiomyocyte FSTL1 secretion.

A. Media FSTL1 protein levels of CMs or cFBs as determined by Luminex assay. **B, C.** Microscopic images of collagen 1 and α -actinin staining of CM/cFB co-cultures in normoxia (**B**) and hypoxia (**C**). **D, E.** Media Fstl1 protein levels in normoxia (**D**) or after 4h hypoxia (**E**). **F.** Media FSTL1 levels after 24h hypoxia. **G.** Comparison of FSTL1 secretion levels by the different cell types in healthy and hypoxic cells. Changes depict higher, equal or lower expression of the cell types in the rows compared with the columns. n=4 experiments. Data was analysed using one-way ANOVA and Dunnett multiple comparison. *P<0,05, ** P<0,01, ***P<0,001. Scale bar: 200 μ m. Data represented as mean \pm SEM.

monoculture, the presence of cFBs increased the FSTL1 media levels to similar levels as cFB only (**Figure 6e**). In long-term hypoxia, a ratio of 80%/20% CM/cFB did not increase FSTL1 secretion to the level of cFB monoculture while the presence of 30% or more cFB did further increase FSTL1 secretion (**Figure 6f**). At higher CM to cFB ratios, longer duration of hypoxia increased the secretion of FSTL1. However, this could also result from the accumulation of FSTL1 in the media due to a longer period of media conditioning. Compared to 24h normoxia, hypoxia increased the FSTL1 secretion in cFBs, while co-culture with CMs significantly decreased FSTL1 secretion at high CM ratio (**Supplemental figure 3**). At a higher cFB ratio, 24h hypoxia did not change FSTL1 secretion in CM-cFB co-cultures. Altogether, we report differences in FSTL1 secretion between cell types and between healthy and hypoxic culture conditions (**Figure 6g**).

DISCUSSION

In this study, we report that FSTL1 can protect human iPSC-CMs from ischemia induced cell death independent of protein glycosylation and we found hypo-glycosylated FSTL1 stimulates proliferation of metabolically matured human CMs when administered either before or after injury. Furthermore, we report both human iPSC-CMs and human cFBs secrete FSTL1 in which CMs decrease FSTL1 secretion in hypoxia and cFBs increase their FSTL1 secretion. Previously, iPSC-CMs have been reported to have an immature metabolic phenotype mainly relying on anaerobic glycolysis for ATP production instead of oxidative phosphorylation as seen in adult CMs³⁷⁻³⁹. The metabolic demand affects the CM ability to reflect the phenotype of adult CM during ischemic injury, as in the myocardium the absence of oxygen and nutrients induces a shift towards glycolytic metabolism⁴⁰⁻⁴². In this study, we used maturation media³⁵ to shift the metabolism of the CMs towards oxidative phosphorylation and therefore increase susceptibility to oxygen deprivation. As we show these metabolically matured CMs, previously shown to have limited innate cell

cycle activity, can be stimulated to proliferate, this suggests CMs in the human heart can be stimulated to proliferate using FSTL1.

Whether there is a population of cycling CMs in the adult heart remained debatable even though a turnover rate of <1% per year in human hearts has been reported via the integration of nuclear bomb test derived ^{14}C into genomic DNA⁴⁴⁻⁴⁶. If there is an innate turnover of CMs in the human heart, amplification of the degree of CM renewal could be an efficient method to mediate cardiac repair after injury. Previous studies have attempted to stimulate CM proliferation by targeting YAP1-Hippo signalling⁴⁷⁻⁴⁹, ErbB2^{50,51}, and Notch signalling^{52, 53}, but, so far, clinical translation has failed. Commonly used proliferation marker Ki-67 has been found to also be expressed in non-proliferating cells when there is overexpression of cell damage markers P53 and P21^{54, 55}, which could bias reported effects of regenerative factors. However, the reduced regenerative effect in translational studies could also be related to differences between animal models and the human heart^{56, 57} and delivery issues^{58,59}. Furthermore, with regenerative approaches the focus often lies on stimulation of CM proliferation while restoration of vascularisation and preventing extensive fibrosis are also required to enable cardiac regeneration. In light of this, studying regenerative factors that can also stimulate angiogenesis, target fibroblast behaviour and function in intercellular communication could be a promising approach. We report FSTL1 can double or triple the expression of multiple proliferation markers in human CMs to similar percentages of EdU and pH3 expression as reported in previous animal studies^{48,60} and higher aurora b kinase levels than previous studies^{47,49}. This together with previous reports of increased vascularisation and cardioprotection by FSTL1 makes it a promising target for cardiac repair. Additionally, we also report differential gene expression after hypo-glycosylated FSTL1 treatment in which all biological processes of cell proliferation (nuclear division, G2/M progression, mitosis, anaphase) and the protective response to oxidative stress and reactive oxygen species are up-regulated. Furthermore, genes involved in cytolysis and

immune cell activation were significantly down-regulated after hypoglycosylated FSTL1 treatment suggesting FSTL1 might also exert cardioprotective effects by modulating the pro-inflammatory activity of the immune system in the ischemic infarct. By decreasing both cell death and secretion of pro-inflammatory cytokines, the regenerative effect of FSTL1 treatment is more likely to lead to production of new CMs actually surviving, in a less inflammatory microenvironment of the infarct.

The secretion of cardiokines plays important roles in intercellular communication during physiology and disease both by mediating paracrine crosstalk inside the heart and by facilitating communication with peripheral organs⁶¹. To illustrate, the release of atrial natriuretic peptide (ANP) and brain natriuretic peptide (BNP) has been found to enable dynamic motion of the ventricular wall while cardiokine IL-33 released by cFBs regulated CM hypertrophy via CM soluble protein ST2¹⁹. Ischemia-inducible cardiokine secretion has been reported in the murine heart among which FSTL1 was identified as a cardioprotective cardiokine capable of preventing CM apoptosis¹⁶. Next to FSTL1, other cardioprotective cardiokines have shown altered secretion in ischemia¹⁶ among which calcitonin gene related peptide⁶², apelin⁶³, cardiotrophin-1, and FSTL1 regulated protein GDF-15⁶⁴⁻⁶⁶. Cellular FSTL1 secretion by epicardial cells⁶⁷, CMs^{27, 33, 68} and cFBs³³ has been reported in previous studies. In murine ischemic hearts, expression of FSTL1 was found to be essential in preventing cardiac rupture when expressed by cFBs^{32, 43} and expression of hypo-glycosylated FSTL1 was found to be capable of stimulating immature CMs to proliferate^{23, 27, 31, 69}. In the human heart, elevated FSTL1 plasma levels and CM FSTL1 secretion have been reported in patients with heart failure^{61, 65, 70, 71}. As ischemia impairs endoplasmic reticulum (ER) protein synthesis, protein secretion is decreased for most proteins^{16, 72}. Maintained or increased protein secretion during ER stress suggests important functions for these proteins in the post-ischemic repair response¹⁶. Our data demonstrates that ischemic conditions induce an increase of FSTL1 secretion only from cFBs while it decreases from iPSC-CMs.

Furthermore, we found differences in FSTL1 expression in hf-cFBs and hiPSC-cFBs in which hf-cFBs expressed both glycosylation variants while iPSC-cFBs only expressed hypo-glycosylated FSTL1. Glycosylation has been linked to biological activity of FSTL1 signalling^{31, 69}. Differential expression of FSTL1 glycosylation variants during differentiation has been reported in pre-adipocytes to be associated with ability of thermogenesis⁷³. As FSTL1 has been found to be important for multiple processes during cardiac development and late myocardial cell formation^{74, 75}, functions while after development, predominant expression of hypo-glycosylated FSTL1 by adult cardiac fibroblasts might be more beneficial to mediate cardiac repair. Since we show that only hypo-glycosylated FSTL1 can induce CM proliferation, it seems likely that insufficient amounts of hypo-glycosylated FSTL1 are linked to the limited innate reparative capacity of the heart. Interestingly, we found while intracellular FSTL1 expression in fibroblasts decreased under hypoxic conditions, secretion of FSTL1 increased. However, the mechanism and dynamics of intracellular and secreted FSTL1 concentrations during hypoxia remain to be elucidated. In previous studies, FSTL1 expression by fibroblasts was reported to be associated with cFB migration and proliferation in murine infarcts as part of the acute cardiac repair response³³. Furthermore, higher levels of circulating FSTL1 in dogs were reported to prevent metabolic alterations in the failing heart and improve cardiac function⁷⁶. The increased presence of fibroblasts in the infarcted myocardium and the previously described role of FSTL1 production by cFBs in preventing cardiac rupture³², suggested that hypoxic cFBs might have altered FSTL1 production and secreted FSTL1 might influence the response of hypoxic CMs.

This is the first report of FSTL1 production by human cFBs and CMs. We have shown that co-culture of both cell types increases FSTL1 secretion which indicates cellular communication related to FSTL1. Furthermore, in hypoxia the presence of cFBs even at low cell numbers is sufficient to increase FSTL1 secretion in

co-culture with CMs. Further elucidation of FSTL1 signalling between CMs and cFBs in the healthy and ischemic heart could provide insights into how we can tap into this intercellular communication to support cardiac repair.

METHODS

Cell culture. human iPSCs were kindly provided by Joseph Wu (CVI-273) and Tomo Saric (NP0141-31B) and isolation of peripheral blood mononuclear cells and reprogramming were performed as previously described^{77, 78}. human iPSCs were grown in Essential 8™ media (Gibco A1517001) until they reached 90-100% confluency. Differentiation to CMs was initiated by changing media to RPMI 1640 (ThermoFisher Scientific 11875085) and B27 minus insulin supplement (ThermoFisher Scientific A1895601) containing 7uM CHIR99021 (Selleck Chemicals S2924). After 3 days, canonical Wnt signalling was inhibited through the supplementation with Wnt-C59 (R&D systems 5148). At day 7, the media was changed to RPMI 1640 and B27 plus insulin supplement (ThermoFisher Scientific 17504001) after which the CMs were purified in RPMI 1640 no glucose (ThermoFisher Scientific 118979020) at day 9. At day 11 of differentiation, cells were re-plated in 10% KnockOut™ serum replacement (KOSR) (ThermoFisher Scientific 108280028) RPMI/B27 plus insulin. After a second purification step, media was changed to RPMI/B27 plus insulin. At day 20, media was changed to maturation media as previously described³⁶. Cells were matured in maturation media for 3 weeks before re-plating with media changes every four days.

iPSC-cFBs were differentiated from hiPSCs as previously described⁷⁹. In short, differentiation was started at 100% confluency by changing media to RPMI 1640 and B27 minus insulin supplement containing 16uM CHIR99021. After 2 days, media was changed to CFBM media supplemented with 75 ng/ml bFGF (WiCell Research Institute). Media was changed every other day with CFBM media⁸⁰ supplemented with 75 ng/ml bFGF before passaging with TrypLE express (Gibco 12604013) to a

T75 in DMEM (Gibco 11995065)/10% foetal bovine serum (Sigma Aldrich 12103C)/1% B27 plus insulin media at day 20.

Human foetal tissue for hf-cFBs was obtained following parental permission using standard informed consent procedures and fibroblasts were isolated as previously described⁸⁰.

Co-culture experiments. iPSC-CMs were plated at a density of 263 000 cells/cm². As iPSC-cFBs expand from single cell to full confluency in three days and iPSC cardiomyocytes have a basal negligible proliferation rate, iPSC fibroblasts were seeded at a three times lower density at day -3 to ensure the reported cell ratios.

Hypoxia simulation. Cells were exposed to 1% O₂ in a hypoxia workstation (Baker Ruskinn INVIVO₂ 1000) or <1% in a BD GasPak™ EZ Pouch system for 4h or 24h after a 24-h glucose starvation period during which 4 days after the previous media change, media was not changed.

Fstl1 supplementation. Recombinant human FSTL1 synthesized in *Escherichia coli* (Aviscera Bioscience) and in a mouse myeloma cell line (R&D systems) were used to include the effect of glycosylation on Fstl1 function in human iPSC-CMs. 24h prior to hypoxia or after hypoxia, cells were stimulated with bacterially or mammalian-synthesized recombinant human FSTL1 (1,0-500ng mL⁻¹) before measurement of EdU incorporation. Similarly, cells were stimulated with bacterially or mammalian-synthesized recombinant human FSTL1 (100ng mL⁻¹) for Ki-67, PH3, Aurora B kinase immunofluorescence staining, RNA expression analysis and flow cytometric analysis.

Immunofluorescence. Cells were fixed in 4% paraformaldehyde and permeabilized in 0,1% Triton-X100 before blocking in 10% normal goat serum/1% BSA (Millipore

Sigma). Cells were incubated with primary antibodies (α -actinin (Sigma-Aldrich A7811, 1:100), cardiac troponin T (Abcam ab45932, 1:100), Ki-67 (Abcam ab8330, 1:200), PHH3 (Cell Signaling Technology #9701 1:200), aurora B kinase (Abcam ab2254, 1:100) overnight and detection was mediated by incubation with secondary antibodies (Alexa Fluor® antibody conjugates (ThermoFisher Scientific)) for one hour. DAPI was used as a nuclear marker. Mounting was performed using Fluoromount-G™ medium (ThermoFisher Scientific).

To determine cell loss via pathways involving DNA fragmentation, TUNEL assays (Roche) were performed according to the manufacturer's instructions. *In vitro* proliferation after FSTL1 supplementation was assessed using Click-iT™ EdU incorporation kit (Life Technologies) according to the manufacturer's instructions. Imaging was performed using a confocal microscope (Leica Sp8x) and image analysis using ImageJ.

RNA extraction and qPCR. RNA was extracted from the cells with Tripure isolation reagent (Roche) and reverse transcribed to cDNA using qScript cDNA synthesis kit (Quantabio). Expression of target genes was determined using Perfecta™ SYBR® green super mix (Quantabio) and gene-specific primers. TATA box binding protein (TBP) mRNA expression was used as a housekeeping reference and expression levels were normalized to control using the $\Delta\Delta CT$ quantification method.

RNA sequencing. After RNA extraction, RNA quality was determined using Qubit™ RNA HS Assay Kit (ThermoFisher) and the Qubit fluorometer. The RNA library was prepared using the NEXTflex™ Rapid RNA-seq Kit (Bio Scientific) and sequenced by CEL-seq (Illumina) to determine RNA expression. The Galaxy environment⁸¹ was used to analyse differential expression between two groups with DESeq2 and Limma-voom between >two groups. Pairwise comparison between groups were conducted by applying the Wald test of the negative binomial distribution to the log2

gene counts and significance was determined by an adjusted P value <0,05.

Western blotting. Protein extraction was mediated by RIPA lysis buffer (Thermo Scientific 89901) supplemented with phosphatase inhibitors (PhosSTOP Roche) and protease inhibitors (cOmplete Roche). After determining protein concentrations with Pierce™ BCA protein assay kit (Thermo Scientific), proteins were reduced using Laemmli reagent (Biorad) supplemented with 10% β-mercaptoethanol (Gibco) and 5 minutes incubation at 95° Celcius. Proteins were loaded on 4–15% acrylamide Mini-Protean TGX gel (BioRad). After running gel electrophoreses, proteins were transferred to a PVDF membrane and blocked in 5% BSA in tris-buffered saline with Tween-20 (Thermo Scientific) (TBST). Primary antibody used was anti-Fstl1 MAB1694 (R&D systems, 1:1000) and detection was mediated by secondary anti-rat horseradish peroxidase (HRP)-conjugated antibody 31470 (Thermofisher Scientific, 1:2000) in a BioRad ChemiDoc™ Imager system.

Flow cytometry. Cells were gently dissociated with Multi Tissue Dissociation kit (Miltenyi Biotec) and incubated with LIVE/DEAD™ fixable green dead cell stain kit (Thermofisher Scientific). Cells were fixed in inside fix solution (Miltenyi Biotec) and stained with primary antibodies diluted in inside perm solution (Miltenyi Biotec). Conjugated primary antibodies used were: α-actinin-VioBlue (130-106-996 Miltenyi Biotec, 1:10), and KI67-APC (130-111-761 Miltenyi Biotec, 1:10). As a control, universal isotype control antibodies (REA Miltenyi Biotec) were used. Media and washes were collected to obtain a complete representation of cell loss. The samples were analysed using FACS Canto system (BD Bioscience) and FlowJo software.

Luminex Bead-Based Array. Media were analysed for FSTL1 protein levels using Luminex magnetic bead-based multiplex assay (R&D systems) according to the manufacturer's instructions. In short, a standard curve was generated using

calibrator diluent and the standards and samples were transferred to a microplate. The microparticle cocktail was added to the wells and the plate was incubated for 2 hours at room temperature on a horizontal orbital microplate shaker after which the plates were washed and consecutively incubated with the diluted Biotin-Antibody Cocktail and the diluted Streptavidin-PE cocktail. After resuspending the magnetic microparticles, the plates were read by a Luminex Analyzer (R&D systems).

Statistical analysis. All experiments were performed in iPSC lines from two donors. The n number depicted in the figures represents the number of independent experiments performed. Statistical analysis was performed using Prism 8 (GraphPad) software and quantifications are represented as mean \pm SEM. To compare the expression of 2 groups a normality test was performed followed by a Student's t-test. For >2 groups, one-way ANOVA was used after confirmation of normal distribution with a Shapiro-Wilk test. Post-hoc analysis was done with Dunnett multiple comparisons to determine statistically significant ($P < 0,05$) results.

Study approval. Derivation and use of human iPSCs and human foetal cardiac progenitor cells or fibroblasts were approved by the ethical committee of University Medical Center Utrecht (Utrecht, the Netherlands). All subjects provided informed consent prior to participation.

AUTHOR CONTRIBUTIONS

J.P.G, S.A.J, P.A.D., K.N and M.M.C.P. designed experiments. S.D.M, T.B. and M.M.C.P. performed all experiments. M.M.C.P. analysed data. M.M.C.P. wrote the manuscript.

ACKNOWLEDGMENTS

The authors would like to gratefully acknowledge Michal Mokry for performing the

RNA-seq library prep and CEL-seq. Tomo Šarić and Joseph Wu for providing hiPSC cell lines and Nino Chirico for providing hiPSC-derived fibroblasts.

SUPPLEMENTAL FIGURES

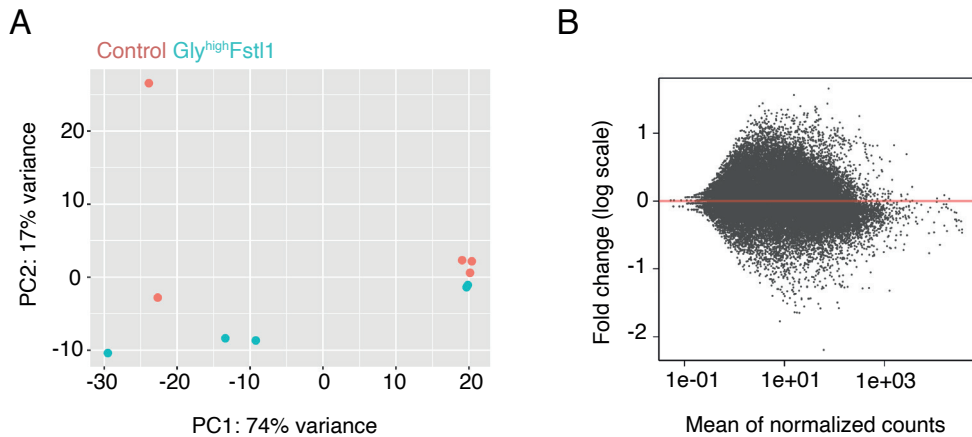


Figure S1. Differential expression analysis of hyper-glycosylated Fstl1 treated hypoxic iPSC-CMs

A. Principle component analysis (PCA) plots of hyper-glycosylated Fstl1 treated hypoxic iPSC-CMs and control hypoxic iPSC-CMs showing the variance between the samples using DESeq2. **B.** MA density plot of up- and down-regulated genes in hyper-glycosylated Fstl1 treated iPSC-CMs compared to control using DESeq2. The x-axis shows mean values of normalized counts of all samples and the y-axis shows log₂ fold change in expression

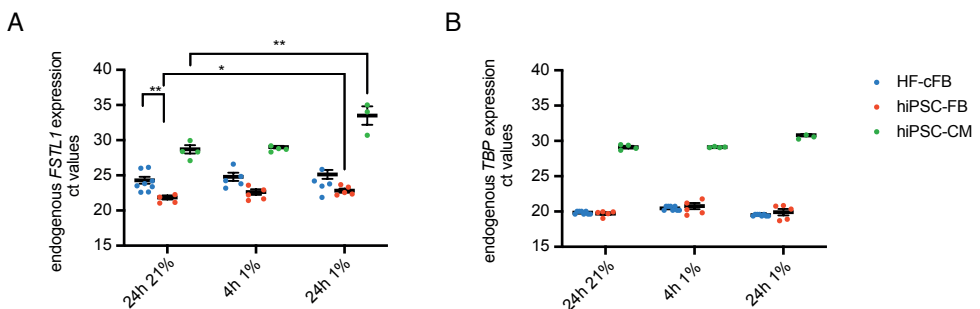


Figure S2. Fstl1 mRNA expression by human cardiac fibroblasts and human cardiomyocytes

A. Fstl1 CT values by qRT-PCR of human foetal cardiac fibroblasts (hf-cFBs), iPSC-cFBs, and iPSC-CMs. **B.** Housekeeping gene TATA binding protein (TBP) CT values. Data represented as mean ± SEM

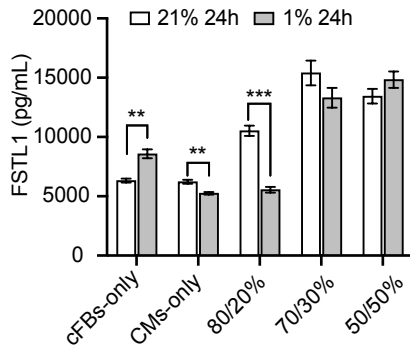


Figure S3. FSTL1 secretion in normoxia and long-term hypoxia. Media levels of FSTL1 as determined by Luminex assay in normoxia or 24 hours hypoxia in cardiomyocyte or cardiac fibroblast mono-culture of co-culture conditions (CM:cFB). Data represented as mean \pm SEM.

REFERENCES

1. Townsend N, Wilson L, Bhatnagar P, Wickramasinghe K, Rayner M, Nichols M. Cardiovascular disease in Europe: Epidemiological update 2016. *Eur Heart J*. 2016;37(42):3232-3245.
2. Mozaffarian D, Benjamin EJ, Go AS, et al. Heart Disease and Stroke Statistics — 2016 Update A Report From the American Heart Association. *AHA Stat Updat*. 2016:38-360.
3. Jopling C, Sleep E, Raya M, Martí M, Raya A, Belmonte JCI. Zebrafish heart regeneration occurs by cardiomyocyte dedifferentiation and proliferation. *Nature*. 2010;464(7288):606-609.
4. Porrello ER, Mahmoud AI, Simpson E, et al. Transient Regenerative Potential of the Neonatal Mouse Heart. *Science*. 2011;331:1078-1081.
5. Engel FB. Cardiomyocyte proliferation: A platform for mammalian cardiac repair. *Cell Cycle*. 2005;4(10):1360-1363.
6. Zhen YS, Wu Q, Xiao CL, et al. Overlapping Cardiac Programs in Heart Development and Regeneration. *J Genet Genomics*. 2012;39(9):443-449.
7. Oerlemans MIFJ, Goumans MJ, Van Middelaar B, Clevers H, Doevendans PA, Sluijter JPG. Active Wnt signaling in response to cardiac injury. *Basic Res Cardiol*. 2010;105(5):631-641.
8. Porrello ER, Olson EN. A neonatal blueprint for cardiac regeneration. *Stem Cell Res*. 2014;13(3):556-570.
9. Olson EN, Schneider MD. Sizing up the heart: Development redux in disease. *Genes Dev*. 2003;17(16):1937-1956.
10. Poss KD. Getting to the heart of regeneration in zebrafish. *Semin Cell Dev Biol*. 2007;18(1):36-45.
11. Kikuchi K, Gupta V, Wang J, et al. Tcf21+ epicardial cells adopt non-myocardial fates during zebrafish heart development and regeneration. *Development*. 2011;138(14):2895-2902.
12. Masters M, Riley PR. The epicardium signals the way towards heart regeneration. *Stem Cell Res*. 2014;13(3):683-692.
13. Schnabel K, Wu CC, Kurth T, Weidinger G. Regeneration of cryoinjury induced necrotic heart lesions in zebrafish is associated with epicardial activation and cardiomyocyte proliferation. *PLoS One*. 2011.
14. Cao J, Poss KD. The epicardium as a hub for heart regeneration. *Nat Rev Cardiol*.

- 2018;15(10):631-647.
15. Marín-Juez R, Marass M, Gauvrit S, et al. Fast revascularization of the injured area is essential to support zebrafish heart regeneration. *Proc Natl Acad Sci*. 2016;113(40):11237-11242.
 16. Doroudgar S, Glembotski CC. The cardiokine story unfolds: Ischemic stress-induced protein secretion in the heart. *Trends Mol Med*. 2011;17(4):207-214.
 17. Perbellini F, Watson SA, Bardi I, Terracciano CM. Heterocellularity and Cellular Cross-Talk in the Cardiovascular System. *Front Cardiovasc Med*. 2018;5:1-11.
 18. Zhang P, Su J, Mende U. Cross talk between cardiac myocytes and fibroblasts: From multi-scale investigative approaches to mechanisms and functional consequences. *Am J Physiol - Hear Circ Physiol*. 2012;303(12).
 19. Wu YS, Zhu B, Luo AL, Yang L, Yang C. The role of cardiokines in heart diseases: Beneficial or detrimental? *Biomed Res Int*. 2018;2018.
 20. Wei K, Serpooshan V, Hurtado C, et al. Epicardial FSTL1 reconstitution regenerates the adult mammalian heart. *Nature*. 2015;525(7570):479-485.
 21. Shimano M, Ouchi N, Nakamura K, et al. Cardiac myocyte follistatin-like 1 functions to attenuate hypertrophy following pressure overload. *Proc Natl Acad Sci*. 2011;108(43):899-906.
 22. Görgens SW, Raschke S, Holven KB, Jensen J, Eckardt K, Eckel J. Regulation of follistatin-like protein 1 expression and secretion in primary human skeletal muscle cells. *Arch Physiol Biochem*. 2013;119(2):75-80.
 23. Ogura Y, Ouchi N, Ohashi K, et al. Therapeutic impact of follistatin-like 1 on myocardial ischemic injury in preclinical models. *Circulation*. 2012;126(14):1728-1738.
 24. Chiba A, Watanabe-Takano H, Miyazaki T, Mochizuki N. Cardiomyokines from the heart. *Cell Mol Life Sci*. 2018;75(8):1349-1362.
 25. Xiao Y, Zhang Y, Chen Y, et al. Inhibition of MicroRNA-9-5p protects against cardiac remodeling following myocardial infarction in mice. *Hum Gene Ther*. 2019;30(3):286-301.
 26. Ouchi N, Oshima Y, Ohashi K, et al. Follistatin-like 1, a secreted muscle protein, promotes endothelial cell function and revascularization in ischemic tissue through a nitric-oxide synthase-dependent mechanism. *J Biol Chem*. 2008;283(47):32802-32811.
 27. Peters MMC, Meijs TA, Gathier W, et al. Follistatin-like 1 in Cardiovascular Disease and Inflammation. *Mini-Reviews Med Chem*. 2019;19(16):1379-1389.
 28. Oshima Y, Ouchi N, Sato K, Izumiya Y, Pimentel DR, Walsh K. Follistatin-like 1 is an Akt-regulated cardioprotective factor that is secreted by the heart. *Circulation*. 2008;117(24):3099-3108.
 29. Li X, Li L, Chang Y, Ning W, Liu X. Structural and functional study of FK domain of Fstl1. *Protein Sci*. 2019;28(10):1819-1829.
 30. Zwijsen A, Blockx H, Van Arnhem W, et al. Characterization of a Rat C6 Glioma-Secreted Follistatin-Related Protein (FRP): Cloning and Sequence of the Human Homologue. *Eur J Biochem*. 1994;225(3):937-946.
 31. Magadam A, Singh N, Kurian AA, Sharkar MTK, Chepurko E, Zangi L. Ablation of a Single N-Glycosylation Site in Human FSTL 1 Induces Cardiomyocyte Proliferation and Cardiac Regeneration. *Mol Ther - Nucleic Acids*. 2018;13:133-143.
 32. Kretzschmar K, Post Y, Bannier-Hélaouët M, et al. Profiling proliferative cells and their progeny in damaged murine hearts. *Proc Natl Acad Sci U S A*. 2018;115(52):E12245-E12254.
 33. Maruyama S, Nakamura K, Papanicolaou KN, et al. Follistatin-like 1 promotes cardiac fibroblast activation and protects the heart from rupture. *EMBO Mol Med*. 2016;8(8):949-966.
 34. Takahashi K, Yamanaka S. Induction of Pluripotent Stem Cells from Mouse Embryonic and Adult Fibroblast Cultures by Defined Factors. *Cell*. 2006;126(4):663-676.
 35. Feyen DAM, McKeithan WL, Bruyneel AAN, et al. Metabolic Maturation Media Improve Physio-

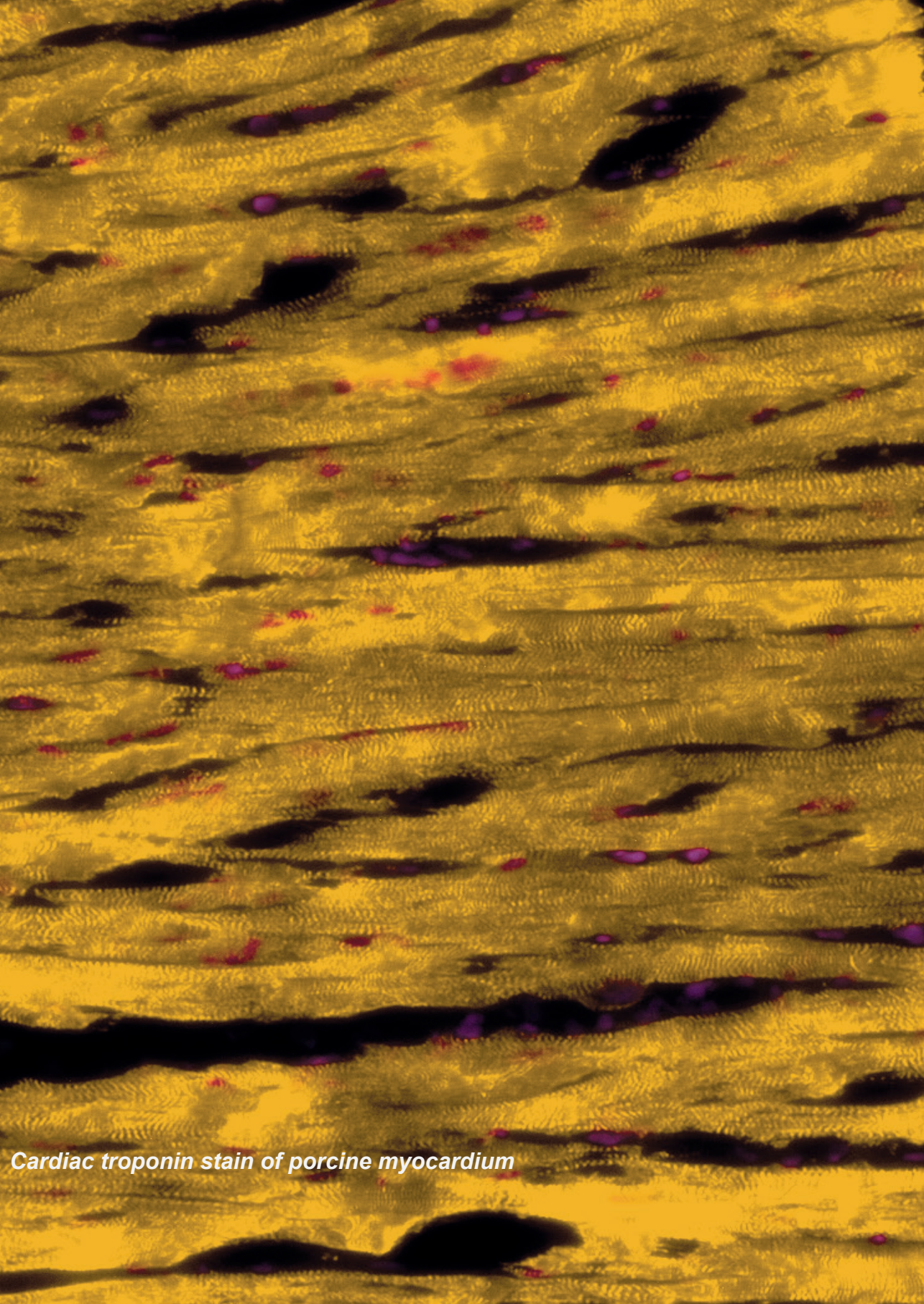
Follistatin-like 1 promotes proliferation of matured hypoxic human iPSC-cardiomyocytes and is secreted by human cardiac fibroblasts

- logical Function of Human iPSC-Derived Cardiomyocytes. *Cell Rep.* 2020;32(3).
36. Zeng X-XI, Ocorr K, Ensberg EJ, Dong PD si. Zebrafish Follistatin-like 1b regulates cardiac contraction during early development. *BioRxiv.* 2020.
 37. Hu D, Linders A, Yamak A, et al. Metabolic maturation of human pluripotent stem cell-derived cardiomyocytes by inhibition of HIF1 α and LDHA. *Circ Res.* 2018;123(9):1066-1079.
 38. Ulmer BM, Stoehr A, Schulze ML, et al. Contractile Work Contributes to Maturation of Energy Metabolism in hiPSC-Derived Cardiomyocytes. *Stem Cell Reports.* 2018;10(3):834-847.
 39. Ulmer BM, Eschenhagen T. Human pluripotent stem cell-derived cardiomyocytes for studying energy metabolism. *Biochim Biophys Acta - Mol Cell Res.* 2020;1867(3):118471.
 40. Aragonés J, Fraisl P, Baes M, Carmeliet P. Oxygen Sensors at the Crossroad of Metabolism. *Cell Metab.* 2009;9(1):11-22.
 41. Neubauer S. The Failing Heart — An Engine Out of Fuel. *N Engl J Med.* 2007;356(11):1140-1151.
 42. Sambandam N, Lopaschuk GD. AMP-activated protein kinase (AMPK) control of fatty acid and glucose metabolism in the ischemic heart. *Prog Lipid Res.* 2003;42(3):238-256.
 43. Kretzschmar K, Post Y, Bannier-Hélaouët M, et al. Profiling proliferative cells and their progeny in damaged murine hearts. *Proc Natl Acad Sci.* 2018;115(52):E12245-E12254.
 44. Mollova M, Bersell K, Walsh S, et al. Cardiomyocyte proliferation contributes to heart growth in young humans. *Proc Natl Acad Sci.* 2013;110(4):1446-1451.
 45. Bergmann O, Zdunek S, Felker A, et al. Dynamics of Cell Generation and Turnover in the Human Heart. *Cell.* 2015;161(7):1566-1575.
 46. Bergmann O, Bhardwaj RD, Bernard S, et al. Evidence for Cardiomyocyte Renewal in Humans. *Science (80-).* 2009;324:98-102.
 47. von Gise A, Lin Z, Schlegelmilch K, et al. YAP1, the nuclear target of Hippo signaling, stimulates heart growth through cardiomyocyte proliferation but not hypertrophy. *Proc Natl Acad Sci.* 2012;109(7):2394-2399.
 48. Diez-Cuñado M, Wei K, Bushway PJ, et al. miRNAs that Induce Human Cardiomyocyte Proliferation Converge on the Hippo Pathway. *Cell Rep.* 2018;23(7):2168-2174.
 49. Heallen T, Zhang M, Wang J, et al. Hippo Pathway Inhibits Wnt Signaling to Restrain Cardiomyocyte Proliferation and Heart Size. *Science.* 2011;332:458-461.
 50. D'Uva G, Aharonov A, Lauriola M, et al. ERBB2 triggers mammalian heart regeneration by promoting cardiomyocyte dedifferentiation and proliferation. *Nat Cell Biol.* 2015;17(5):627-638.
 51. Han Y, Chen A, Umansky KB, et al. Vitamin D Stimulates Cardiomyocyte Proliferation and Controls Organ Size and Regeneration in Zebrafish. *Dev Cell.* 2019;48(6):853-863.e5.
 52. Collesi C, Felician G, Secco I, et al. Reversible Notch1 acetylation tunes proliferative signalling in cardiomyocytes. *Cardiovasc Res.* 2018;114(1):103-122.
 53. Zhao L, Ben-Yair R, Burns CE, Burns CG. Endocardial Notch Signaling Promotes Cardiomyocyte Proliferation in the Regenerating Zebrafish Heart through Wnt Pathway Antagonism. *Cell Rep.* 2019;26(3):546-554.e5.
 54. Van Oijen MGCT, Medema RH, Slootweg PJ, Rijksen G. Positivity of the proliferation marker Ki-67 in noncycling cells. *Am J Clin Pathol.* 1998;110(1):24-31.
 55. Sun X, Kaufman P. Ki-67 : more than a proliferation marker. *Chromosoma.* 2018;127(2):175-186.
 56. Ge Z, Lal S, Le TYL, dos Remedios C, Chong JJH. Cardiac stem cells: translation to human studies. *Biophys Rev.* 2015;7(1):127-139.
 57. Rog-Zielinska EA, Kong CHT, Zgierski-Johnston CM, et al. Species differences in the morphology of transverse tubule openings in cardiomyocytes. *Europace.* 2018;20:III120-III124.

58. Menasché P. Cell therapy trials for heart regeneration — lessons learned and future directions. *Nat Rev Cardiol.* 2018;15(11):659-671.
59. Feyen DAM, Van Den Hoogen P, Van Laake LW, et al. Intramyocardial stem cell injection: Go(ne) with the flow. *Eur Heart J.* 2017;38(3):184-186.
60. Mohamed TMA, Ang YS, Radzinsky E, et al. Regulation of Cell Cycle to Stimulate Adult Cardiomyocyte Proliferation and Cardiac Regeneration. *Cell.* 2018;173(1):104-116.e12.
61. Shimano M, Ouchi N, Walsh K. Cardiokines: Recent progress in elucidating the cardiac secretome. *Circulation.* 2012;126(21). doi:10.1161/CIRCULATIONAHA.112.150656
62. Chai W, Mehrotra S, Jan Danser AH, Schoemaker RG. The role of calcitonin gene-related peptide (CGRP) in ischemic preconditioning in isolated rat hearts. *Eur J Pharmacol.* 2006;531(1-3):246-253.
63. Ronkainen V, Ronkainen JJ, Hänninen SL, et al. Hypoxia inducible factor regulates the cardiac expression and secretion of apelin. *FASEB J.* 2007;21(8):1821-1830.
64. Kempf T, Eden M, Strelau J, et al. The transforming growth factor- β superfamily member growth-differentiation factor-15 protects the heart from ischemia/reperfusion injury. *Circ Res.* 2006;98(3):351-360.
65. Widera C, Giannitsis E, Kempf T, et al. Identification of follistatin-like 1 by expression cloning as an activator of the growth differentiation factor 15 gene and a prognostic biomarker in acute coronary syndrome. *Clin Chem.* 2012;58(8):1233-1241.
66. Freed DH, Cunnington RH, Dangerfield AL, Sutton JS, Dixon IMC. Emerging evidence for the role of cardiotrophin-1 in cardiac repair in the infarcted heart. *Cardiovasc Res.* 2005;65(4):782-792.
67. Wei K, Serpooshan V, Hurtado C, et al. Epicardial FSTL1 reconstitution regenerates the adult mammalian heart. *Nature.* 2015;525(7570):479-485.
68. Oshima Y, Ouchi N, Sato K, Izumiya Y, Pimentel DR, Walsh K. Follistatin-like 1 is an Akt-regulated cardioprotective factor that is secreted by the heart. *Circulation.* 2008;117(24):3099-3108.
69. Wei K, Serpooshan V, Hurtado C, et al. Epicardial FSTL1 reconstitution regenerates the adult mammalian heart. *Nature.* 2015;525(7570):479-485.
70. El-Armouche A, Ouchi N, Tanaka K, et al. Follistatin-like 1 in chronic systolic heart failure a marker of left ventricular remodeling. *Circ Hear Fail.* 2011;4(5):621-627.
71. Widera C, Horn-Wichmann R, Kempf T, et al. Circulating concentrations of follistatin-like 1 in healthy individuals and patients with acute coronary syndrome as assessed by an immunoluminometric sandwich assay. *Clin Chem.* 2009;55(10)
72. Meyer BA, Doroudgar S. ER Stress-Induced Secretion of Proteins and Their Extracellular Functions in the Heart. *Cells.* 2020;9(9):1-17.
73. Fang D, Shi X, Lu T, Ruan H, Gao Y. The glycoprotein follistatin-like 1 promotes brown adipose thermogenesis. *Metabolism.* 2019;98:16-26.
74. Mattiotti A, Prakash S, Barnett P, van den Hoff MJB. Follistatin-like 1 in development and human diseases. *Cell Mol Life Sci.* 2018;75(13):2339-2354.
75. Van Den Berg G, Somi S, Buffing AAM, Moorman AFM, van den Hoff MJB. Patterns of expression of the follistatin and follistatin-like1 genes during chicken heart development: A potential role in valvulogenesis and late heart muscle cell formation. *Anat Rec.* 2007;290(7):783-787.
76. Seki M, Powers JC, Maruyama S, et al. Acute and chronic increases of circulating FSTL1 normalize energy substrate metabolism in pacing-induced heart failure. *Circ Hear Fail.* 2018;11(1):1-12.
77. Matsa E, BurrIDGE PW, Yu KH, et al. Transcriptome Profiling of Patient-Specific Human iP-SC-Cardiomyocytes Predicts Individual Drug Safety and Efficacy Responses In Vitro. *Cell*

Follistatin-like 1 promotes proliferation of matured hypoxic human iPSC-cardiomyocytes and is secreted by human cardiac fibroblasts

- Stem Cell.* 2016;19(3):311-325.
78. Hamad S, Derichsweiler D, Papadopoulos S, et al. Generation of human induced pluripotent stem cell-derived cardiomyocytes in 2D monolayer and scalable 3D suspension bioreactor cultures with reduced batch-to-batch variations. *Theranostics.* 2019;9(24):7222-7238.
79. Zhang J, Tao R, Campbell KF, et al. Functional cardiac fibroblasts derived from human pluripotent stem cells via second heart field progenitors. *Nat Commun.* 2019;10(1).
80. Bracco Gartner TCL, Deddens JC, Mol EA, et al. Anti-fibrotic Effects of Cardiac Progenitor Cells in a 3D-Model of Human Cardiac Fibrosis. *Front Cardiovasc Med.* 2019;6(April):1-11.
81. Afgan E, Baker D, Batut B, et al. The Galaxy platform for accessible, reproducible and collaborative biomedical analyses: 2018 update. *Nucleic Acids Res.* 2018;46(W1):W537-W544.



Cardiac troponin stain of porcine myocardium

Chapter 7

NON-CODING RNAs IN ENDOTHELIAL CELL SIGNALLING AND HYPOXIA DURING CARDIAC REGENERATION

Adapted from:

Biochimica et Biophysica Acta (BBA) – Molecular Cell Research 2020, 1867; 118515 doi: 10.1016/j.bbamcr.2019.07.010

Published online on 27 July 2019

*Marijn M.C. Peters*¹, Vasco Sampaio-Pinto^{2,3,4} and Paula A. da Costa Martins⁴

¹Department of Cardiology, Laboratory of Experimental Cardiology, UMC Utrecht, Regenerative Medicine Centre, University Medical Centre Utrecht, University Utrecht, Utrecht, The Netherlands.

²i3S - Instituto de Investigação e Inovação em Saúde, Universidade do Porto, Porto, Portugal & INEB - Instituto Nacional de Engenharia Biomédica, Universidade do Porto, Porto, Portugal.

³ICBAS - Instituto de Ciências Biomédicas de Abel Salazar, Universidade do Porto, Porto

⁴Department of Physiology and Cardiothoracic Surgery, Faculty of Medicine, University of Porto, Porto, Portugal.

⁵Department of Cardiology, CARIM School for Cardiovascular Diseases, Faculty of Health Medicine and Life Sciences, Maastricht University, Maastricht, The Netherlands

ABSTRACT

Heart failure (HF) as a result of myocardial infarction (MI) is the leading cause of death worldwide. In contrast to the adult mammalian heart, which has low regenerative capacity, newborn mammalian and zebrafish hearts can completely regenerate after injury. Cardiac regeneration is considered to be mediated by proliferation of pre-existing cardiomyocytes (CMs) mainly located in a hypoxic niche. To find new therapies to treat HF, efforts are being made to understand the molecular pathways underlying the regenerative capacity of the heart. However, the multicellularity of the heart is important during cardiac regeneration as not only CM proliferation but also the restoration of the endothelium is imperative to prevent progression to HF. It has recently come to light that signalling from non-coding RNAs (ncRNAs) and extracellular vesicles (EVs) plays a role in the healthy and the diseased heart. Multiple studies identified differentially expressed ncRNAs after MI, making them potential therapeutic targets. In this review, we highlight the molecular interactions between endothelial cells (ECs) and CMs in cardiac regeneration and when the heart loses its regenerative capacity. We specifically emphasize the role of ncRNAs and cell-cell communication via EVs during cardiac regeneration and neovascularisation.

1. INTRODUCTION

The non-coding part of the genome has come to light as an essential regulator in physiology and disease¹. Non-coding genes can be subdivided into different categories based on their length: short non-coding genes (<200 nucleotides (nt)) and long non-coding genes (>200 nt)². Within small non-coding RNAs (ncRNAs), microRNAs (miRNAs/miRs) received increasing attention as mediators of mRNA expression in multiple diseases. Less understood classes of ncRNAs including transcribed ultraconserved regions (T-UCRs), small nucleolar RNAs (snoRNAs), PIWI-interacting RNAs (piRNAs), large intergenic non-coding RNAs (lincRNAs) and long non-coding RNAs (lncRNAs) are also being associated with the development of human diseases¹. Among other functions, ncRNAs are known for the inhibition of mRNAs, transposon repression, DNA methylation, chromatin modification and influencing mRNA stability. High conservation of non-coding regions across phylogeny denotes an important role of ncRNAs in regulating gene expression³. Single-nucleotide polymorphisms (SNPs) in non-coding regions or disruption of ncRNA expression have been associated with the progression of cardiovascular diseases⁴. Furthermore, paracrine signalling of ncRNAs via extracellular vesicles (EVs) has recently received increasing attention as a molecular mechanism influencing pathophysiology and as a potential therapeutic target for cardiovascular diseases^{5,6}.

The human heart has limited regenerative capacity. As such, in response to myocardial infarction (MI), the injured myocardium is replaced by a fibrotic scar. Extensive remodeling of the myocardium after injury can limit the contractile capacity of the heart and lead to heart failure (HF). At steady state, cardiomyocyte (CM) renewal re-replaces apoptotic CMs at a rate of 0,5–1% per year⁷. Even though CM proliferation rate increases after injury, it remains insufficient to fully regenerate the lost myocardial tissue⁸. In contrast to the adult mammalian heart, neonatal mammal and zebrafish hearts display efficient myocardial regeneration after

injury⁹⁻¹¹. Evidence supports that the time window for mammalian heart regeneration is defined by a postnatal shift towards aerobic metabolism which promotes CM cell cycle arrest¹². Hypoxia signalling is a key mechanism for cardiac regeneration in the zebrafish heart and is achieved by the absence of endothelial cells (ECs) adjacent to CMs^{13,14}. The main strategy aiming to improve the regenerative capacity of the heart has been to stimulate CM proliferation¹⁵. However, it is important to note that the heart is not solely composed of CMs and that myocardial function also depends on other cell types and their molecular interactions. The healthy human heart consists of an estimated 2–3 billion CMs, making up to a third of the total number of cells and 70% of the cardiac volume¹⁶ whereas mesenchymal cells (e.g. cardiac fibroblasts (CFs)) were found to account to half of cardiac cells in the human heart¹⁷. The contribution of ECs and smooth muscle cells (SMCs) to the cardiac cellular composition has long been considered minor. However, a recent study combining robust genetic models and cellular markers showed that the non-myocyte population of the murine heart consists of >60% ECs and <20% CFs¹⁸. This revisited cardiac cell composition suggests that ECs are present in a much higher frequency to what was classically predicted, which might have direct implications on cardiac pathophysiology¹⁹. Hence, inducing only CM proliferation after MI may lead to defective heart regeneration as newly formed CMs are unlikely to survive the post-ischemic microenvironment in the absence of oxygen-supplying ECs²⁰. CMs interact with surrounding cells via physical contact and paracrine signalling. Upon MI, CMs in the infarcted area undergo ischemic cell death and apoptosis²¹. CMs disassemble their sarcomeres and mitochondria condense their chromatin and lose their rod-shaped morphology²². The interaction between apoptotic CMs and the microvascular network of ECs post-MI has been studied extensively²³. Both hypoxia and reperfusion disrupt the redox states in CMs leading to oxidative stress, impaired mitochondrial oxidative phosphorylation and eventually to apoptosis during the acute phase after MI, in a process mediated by activation of caspase-3²³. Unexpectedly, it

has been suggested that CMs with potential to re-enter the cell cycle proliferate due to extracellular signals present in the infarct border-zone²⁴, which correlates with a reduction in capillary density and decreased signalling from ECs. Hypoxia inducible factor 1 α (Hif1 α) stabilization in CMs located in a hypoxic microenvironment was found to be a hallmark of CM proliferation²⁵. Hif1-regulated genes are involved in O₂ delivery and consumption, glycolysis, mitochondrial function, cell survival, antioxidant defence, and angiogenesis²⁶. In fact, loss of hypoxia signalling prevented effective regeneration of the zebrafish heart¹⁴ and the small subset of cycling CMs in the adult mammalian heart was located in a hypoxic niche²⁵. Hif1 α is the main regulator of the hypoxia-induced stress response as its activity is regulated by post-translational ubiquitination and degradation under normoxic conditions^{25,27}. Under low environmental oxygen, hydroxylation and subsequent ubiquitination of Hif1 α do not take place allowing its translocation to the nucleus and activation of gene expression. Postnatal CMs lose their ability to proliferate when their metabolism changes from anaerobic glycolysis to oxidative phosphorylation¹². ROS, oxidative DNA damage, and DNA damage response (DDR) markers significantly increase during the postnatal period, which correlates with a progressive loss of cardiac regeneration. Inversely, stimulation of postnatal hypoxemia increased the proliferative time window of CMs¹². The important role of low environmental oxygen and Hif1 α stabilization in CM proliferation contradicts evidence that fast revascularisation is essential to support cardiac regeneration²⁸. Yet, the neonatal murine heart is heavily vascularised after regeneration^{9,10} and without vascularisation of the injured area, regeneration ends prematurely^{29,30}. Taken together, CM proliferation, hypoxia and neovascularization seem to be pivotal processes for cardiac regeneration that exhibit a very precise spatiotemporal regulation (**Figure 1**). Understanding the intrinsic molecular mechanisms underlying the role of hypoxia and vascularisation in CM proliferation may uncover the importance of EC-CM signalling in cardiac regeneration. Increasing evidence indicates that the molecular mechanisms involved

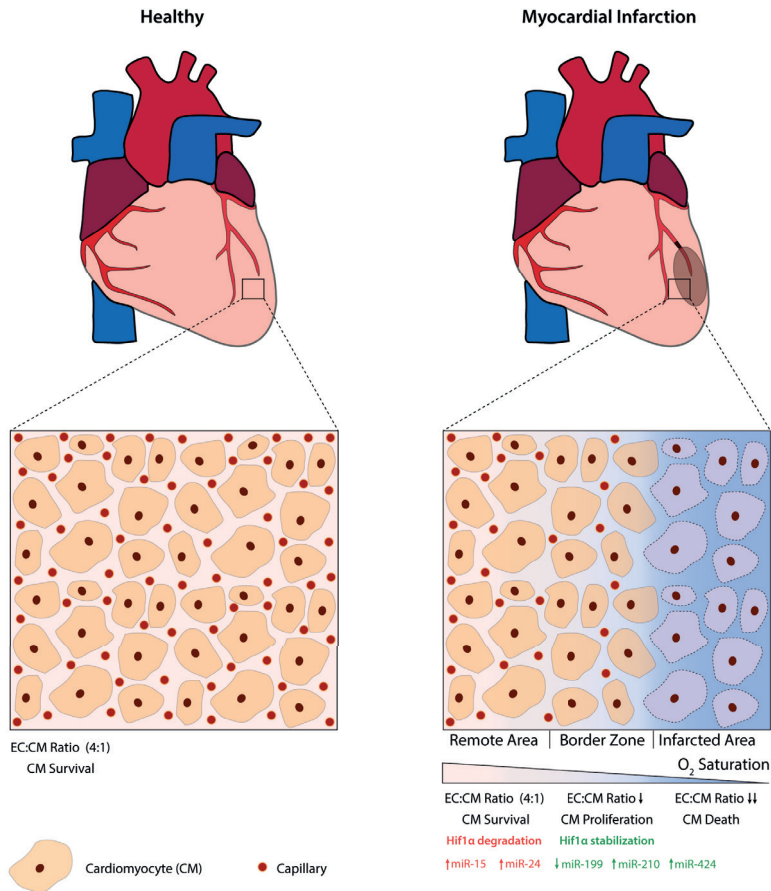


Figure 1. Hypoxia signalling is essential for cardiac regeneration.

Following an ischemic event, the myocardium is marked by extensive cell death (infarcted area). In the borderzone, lower EC:CM ratio activates a hypoxic signalling cascade (e.g. Hif1α stabilization) characterized by induction of EC and CM proliferation. Subsequent revascularization of the borderzone increases oxygen saturation, reducing hypoxia signalling (e.g. Hif1α degradation) and limiting CM proliferation. Higher oxygen levels, also found in the remote myocardium, favour CM survival. Neovascularization and neomyogenesis are tightly regulated processes and modulated by ncRNAs. In response to hypoxia, miR-199 (downregulated in CMs), miR-210 (upregulated in CMs, ECs and SMCs) and miR-424 (upregulated in ECs) favour Hif1α stabilization. In contrast, miR-15a,b (upregulated in CMs) and miR-24 (upregulated in ECs) favour Hif1α degradation.

in the heart response after MI and cardiac regeneration are also under epigenetic control of ncRNAs (**Figure 1**).

1.1. NON-CODING RNAs IN ENDOTHELIAL CELL SIGNALLING

ncRNAs are well established mediators of EC proliferation and mediate the interaction between ECs and CMs as paracrine elements. Differential expression of ncRNAs in ECs and CMs after ischemic injury indicates the potential of ncRNAs as regulators of regeneration and neovascularisation. lncRNAs and miRNAs have also been shown to be regulated by hypoxia^{31–33} and have been proposed as potential therapeutic strategies to modulate tissue vascularisation³⁴. Hence, stimulation or inhibition of ncRNA expression may be used as a therapeutic tool to induce cardiac regeneration.

1.1.1. miRNAs

miRNAs (miRs) are single stranded, small ncRNA molecules (~22nucleotides) encoded in intergenic regions of the genome that inhibit gene expression by binding to the three prime untranslated region (3'UTR) of complementary target mRNAs⁴. Binding can block the translation of the target mRNA or cause mRNA degradation depending on the degree of complementarity between the miRNA and the target mRNA. miRNAs have been found to control many cellular processes including cell survival, differentiation and proliferation³⁵. Furthermore, alterations in cardiac miRNA pathways can induce cardiomyopathies and HF^{36,37}. The discovery that miRNAs are also important in angiogenesis came from a genetic knockout of the endoRNase Dicer, an essential protein processing pre-miRNAs into mature miRNAs, as these animals displayed severely impaired angiogenesis^{38,39}. Multiple miRNAs have been found to play a pivotal role in regulating angiogenesis by impairing or inducing EC proliferation^{2,35,40}. miRNAs that influence angiogenesis can influence the expression

Table 1. NcRNAs in endothelial cell signalling during cardiac injury and regeneration

miRNA	Target	Function	Cell type	Model	References
miR-20a	TNFSF15	Inhibition of angiogenesis	EC	HUVEC	Deng (ex. 42)
miR-31	TNFSF15	Inhibition of angiogenesis	EC	HUVEC	Deng (ex. 42)
miR-199	Sirtuin-1	Master regulator of hypoxia-triggered pathways of EC apoptosis	CM	Neonatal CM	Rane (ex. 32)
miR-24	Gata2, PAK4	EC apoptosis	EC	Zebrafish, mouse	Fiedler (ex.33)
miR-210	Ptp1b, Efn3, Hif3a	CM proliferation, survival and EC proliferation	EC, SMC, CM	Mouse, rat	Arif (ex. 43) Zaccagnini (ex. 45) Ghosh *ex. 46) Hu (ex. 47)
miR-15a, b	Hif1a, Runx3, Vegf,	CM apoptosis	EC, CM	Mouse Human,	Wang Y. (ex. 48)
miR-15a, b	Arl2, Bcl2	inhibition of angiogenesis, mitochondrial degeneration, CM apoptosis	CM	Mouse	Nishi (ex. 49) Small (ex. 50)
miR-16	Vegf, Fgfr1	Negative feedback on EC proliferation and migration	EC	Mouse	Chamorro-Jorganes (ex.51)
miR-424	Vegf, Fgfr1	Negative feedback on EC proliferation and migration	EC	Mouse	Chamorro-Jorganes (ex.51)
miR-424	Cullin-2	Promoting angiogenesis	EC	Mouse, rat	Ghosh (ex. 46)
miR-195	Chek1	Inhibition CM proliferation, post-natal cell cycle arrest	CM	Mouse	Porrello (ex. 52)

Table 1 continued

miRNA	Target	Function	Cell type	Model	References
miR-26a	Smad1	Inhibition of angiogenesis	EC	Mouse	Icili (ex. 55)
miR-233-3	Rps6kb1	Inhibition of angiogenesis	EC	Ischemic MCEC	Dai (ex. 56)
miR-200c	Zeb1	EC apoptosis and senescence	EC	HUVEC	Magenta (ex. 57)
miR-101	mTor	Inhibition of angiogenesis	EC	HUVEC	Chen K. (ex. 61)
miR-101	Cullin-3	EC proliferation	EC	HUVEC	Kim (ex. 57)
miR-100	mTor	Inhibition of angiogenesis	EC, SMC	murine hind-limb	Grundmann (ex. 60)
miR-126	Spred1, PIK3R2/p85-b	EC proliferation	EC	HUVEC, murine hindlimb	Wang (ex. 62)
miR-106b-25	PTEN	EC proliferation	EC	murine hind-limb	Semo (ex. 64)
miR17-5p	Erk	Inhibition of CM proliferation and angiogenesis	EC, CM	Rat	Yang (ex. 68)
LncRNA	Target	Function	Cell type	Model	References
CARL	miR-539	CM survival	CM	Mouse	Wang (ex. 73)
miR503hg	miR-503	EC proliferation	EC	HUVEC	Fiedler (ex. 33)
MANTS	BRG1	EC proliferation	EC	HUVEC, rat, monkey, human	Leisegang (ex. 73)
NONHSAT073641	PAFAH1B1	EC proliferation	EC	HUVEC	Josipovic (ex. 75)

Table 1 continued

miRNA	Target	Function	Cell type	Model	References
MIAT	miR-150-5p	EC proliferation	EC	HUVEC, rat, human	Ishii (ex. 76) Yan (ex. 77)
PUNISHER	<i>Unknown</i>	EC maturity	EC	HUVEC, hESC, hiPSC	Kurian (ex. 78)
Linc00323	IF4A3	EC proliferation	EC	HUVEC	Fiedler (ex. 33), Hou (ex. 79)
MALAT1	CBX4	Migratory EC phenotype	EC	HUVEC, murine hindlimb	Michalik (ex. 80)
TUG1	miR-145-5p	CM apoptosis	CM	H9c2	Wu (ex. 85)
GATA6-AS	LOXL2	Inhibition of angiogenesis	EC	HUVEC	Neumann (ex. 88)
STEEL	PARP1, eNOS	EC proliferation, microvascular identity, shear stress responsiveness	EC	HUVEC	Man (ex. 66)
LEENE	eNOS	EC function, NO production	EC	HUVEC	Miao (ex. 82)
HOTTIP	β -catenin	EC proliferation	EC	Human CAD samples	Liao (ex. 83)
ECRAR	ERK1/2	EC and CM proliferation	EC, CM	Mouse, human	Chen (ex. 87)

EC; endothelial cell, CM; cardiomyocyte, SMC; smooth muscle cell

of coding genes in angiogenic signalling pathways (e.g., multiple miRNAs expressed during hypoxia were found to regulate vascular endothelial growth factor (Vegf) expression)⁴¹ (**Table 1**). Inversely, the expression of miRNAs can be influenced by coding genes involved in angiogenesis. VEGF has been shown to induce the expression of miR-20a and miR-31, two miRNAs that can bind the 3'UTR of a negative regulator of angiogenesis, tumour necrosis factor superfamily-15 (TNFSF15)⁴². Furthermore, hypoxia was also shown to affect miRNA-mediated signalling between ECs and CMs^{40,43}. miRNAs that are involved in the hypoxia signalling were recently named hypoxamiRs and were identified as crucial components to regulate cellular and molecular responses to decreased oxygen tension^{40,44}. HIF1 α is modulated by several miRNAs in ischemic heart disease^{44,45} and prevents hypoxia-induced mitochondrial damage³². Indeed, downregulation of hypoxamiR-199 in ischemic CMs led to the stabilization and upregulation of hif1 α expression. This occurs through derepression of SIRTUIN-1, a class III histone deacetylase targeted by hypoxamiR-199 which, in turn, prevents PHD2-mediated destabilization of HIF1 α ³². PHD2 downregulation by SIRTUIN-1 is mediated by NAD-dependent deacetylase activity of SIRTUIN-1. Sirtuin-1 is also targeted by the endothelial expressed miR-24, a miRNA involved in EC apoptosis through targeting of the endothelium-enriched transcription factor GATA2 and the p21-activated kinase PAK4³³. Silencing of endothelial miR-24 in mouse hearts after MI limited the infarct size and increased cardiac function. miR-210, another hypoxamiR, is ubiquitously upregulated in multiple cardiac cell types during ischemic injury including ECs, SMCs and CMs⁴⁶. During hif1 α stabilization, miR-210 expression is increased in CMs repressing its targets protein tyrosine phosphatase 1b (Ptp1b), ephrinA3 (EfnA3) and Hif3 α . Intramyocardial injections of miR-210 increased CM proliferation and survival and EC proliferation^{43,45,47}. However, another study found detrimental effects of miR-210 in mouse hearts through repression of its target hif1 α in ECs and CMs⁴⁸. The authors also suggest that miR-210 might play a different role in the mouse and human ischemic myocardium. The

exact molecular mechanisms of miR-210 signalling in the post-ischemic human heart remain to be investigated. Members of the miR-15 family (miR-195, miR-15b, miR-16-1, miR-16-2, miR-424, and miR-497) are also increased during hypoxia^{40,49}. miR-15b inhibits the translation of Vegf, therefore limiting neovascularisation of the ischemic tissue. In addition, ADP ribosylation factor-like 2 (Arl2) targeting by miR-15 has been reported to be involved in mitochondrial degeneration and resulting cardiac dysfunction⁴⁹. Moreover, miR-15 targets B-cell lymphoma 2 (Bcl-2) mRNA promoting CM apoptosis during hypoxia⁵⁰. miR-16 and miR-424 target Vegf and fibroblast growth factor receptor 1 (Fgfr1) reducing proliferation and migration of ECs⁵¹. In contrast, hypoxia increased expression of miRNA-424 in cardiac ECs was reported to promote angiogenesis by repressing Cullin2⁴⁶. Cullin2 is a scaffolding protein required to assemble the ubiquitin ligase system involved in the degradation of HIF1A and inhibition of Cullin2 led to HIF1A stabilization⁴⁶. Differential reported effects of the miR-424 might be caused by different transfection methods and efficiencies or cell autonomous/non-autonomous documented effects^{41,51}. Furthermore, cardiac specific mechanisms might explain the reported diverging effects as cardiac ECs can have a different phenotype and response to miRNA signalling.

Recent studies have demonstrated the role of the miR-15 family in regulating the postnatal CM cell cycle arrest⁵². Transfecting mouse hearts with antimiR-195 inhibited the target-binding function of miR-195 and improved cardiac function by stimulating CM proliferation⁵³. From this perspective, the miR-15 family, in preventing both CM proliferation and angiogenesis, serves as a promising target for regenerative therapy. Endogenous endothelial miRNAs (e.g., miR-26a, miR-24, miR-34c, miR-375, miR-223) are upregulated in the infarct area after MI and inhibit angiogenesis^{33,54–56}. Furthermore, miRNA-200c is upregulated in ischemic ECs and induces EC apoptosis by targeting Zeb1⁵⁷. In contrast, some miRNAs promote coronary circulation and cardiac microcirculation⁵⁸. Other pro-angiogenic hypoxamiRs like miRNA-101 and miRNA-100 express their functional properties by targeting Heme oxygenase-1 and

Cullin-3 signalling and Rapamycin, respectively⁵⁹⁻⁶¹. miR-126 has been found to be highly expressed in healthy ECs and decreased levels could predict impaired coronary vascularisation and coronary collaterals⁶². miR-126 is especially enriched in mouse embryos and regulates the response of ECs to VEGF through targeting of Sprouty-related protein SPRED1 and phosphoinositol-3kinase regulatory subunit 2 (PIK3R2/p85-b)⁶³. Likewise, the miR-106b~25 cluster has been found to be essential for EC proliferation in hindlimb ischemia in mice⁶⁴. Similar mechanisms are likely to play a role in cardiac revascularisation. miRNAs expressed by CMs can also contribute to the secretion of specific factors that influence EC behaviour and angiogenesis⁶⁵ or be transported themselves via exosomes to ECs and regulate angiogenesis^{66,67}. This allows for tight regulation of neovascularisation in the adult heart and provides multiple entry-points for possible therapeutic targets to stimulate cardiac regeneration. A recent study performed a genome-wide profiling of ncRNAs in the developing and maturing heart and identified differentially expressed miRNAs that could underlie the change in regenerative capacity including miR-17-5p, miR-122-5p and miR-20a-5p⁶⁸. Additionally, miR-17-5p was found to suppress the formation of blood vessels⁶⁹. Furthermore, RNA sequencing data of murine hearts during early stages of postnatal life, at which the regenerative capacity of the heart is gradually lost, showed a marked change in expression of miRNAs both in ECs and CMs between P3 and P570.

1.1.2. LncRNAs

LncRNAs (>200 nt) have been found to contribute to biological processes through regulating epigenetic gene silencing or by functioning as a protein scaffold². Most lncRNAs show low sequence conservation between species and most have arisen only within the primate lineage⁷¹. Interactions between lncRNAs and miRNAs also play a role in vascularisation⁷². LncRNAs can bind to the nucleotide sequence targeted

by miRNAs, circumventing their effect on mRNA targets⁷³. In addition, miRNAs can bind lncRNAs and influence lncRNA stability and induce miRNA-mediated decay⁷². Differential regulation of lncRNAs in heart development, disease and also during regeneration and repair provided an indication of the potential to target lncRNAs therapeutically (**Table 1**). Cardiac apoptosis-related lncRNA (CARL) expression was found to be increased in hypoxic CMs. Furthermore, sequestering of miR-539 by CARL lncRNA prevented mitochondrial fission and apoptosis by downregulating the miR-539 mediated inhibition of PHB2 in a mouse model of ischemia/reperfusion injury⁷⁴. Hypoxia-sensitive lncRNA miR503hg is located next to the encoding sequence of miR-424 and is involved in the pro-angiogenic response during hypoxia through cis-regulatory action on miR-424³⁴. The pro-angiogenic property of ECs was recently described to be facilitated by the expression of the lncRNA MANTIS⁷⁵ and NONHSAT073641⁷⁶. Furthermore, analysis of the expression of lncRNAs in the heart identified myocardial infarction-associated transcript (MIAT) and PUNISHER to be connected to changes in cardiac microvasculature. The presence of lncRNA MIAT after a MI suggested a role of lncRNAs in the post-ischæmic heart⁷⁷ and further investigation identified its role in regulating EC function and pathological angiogenesis⁷⁸. Through interaction with endogenous endothelial miR-150-5p, which represses Vegf translation, MIAT causes an abnormal upregulation of VEGF. The aberrant expression of VEGF leads to pathological angiogenesis and microvascular dysfunction⁷⁸. PUNISHER acts in the development of the vasculature and is expressed in mature ECs⁷⁹. Inhibition of PUNISHER is associated with severe defects in vascular branching and vessel formation⁷⁹. Furthermore, other lncRNAs have been described to modulate EC proliferation and might also be involved in regulating cardiac angiogenesis. lncRNA Linc00323 has been reported to bind IF4A3 to mediate GATA2 expression maintaining vascular structural integrity and EC proliferation^{34,80}. Moreover, pro-angiogenic lncRNA metastasis associated lung adeno carcinoma transcript 1 (MALAT1) is upregulated during hypoxia in ECs and

is involved in the balance between a proliferative and a migratory EC phenotype⁸¹. Recently, spliced-transcript endothelial enriched lncRNA (STEEL) was discovered as an important lncRNA involved in the EC angiogenic potential, microvascular identity, and shear stress responsiveness⁸². Furthermore, enhancer-associated lncRNA (LEENE) was identified as a regulator in eNOS signalling and EC function⁸³. HOTTIP expression was increased in ECs in coronary artery disease tissue and induced EC proliferation via Wnt/ β -catenin signalling⁸⁴. Mitochondrial derived lncRNA LIPCAR was identified as a biomarker of cardiac remodeling with increased expression during post-MI remodeling and chronic HF and its expression has been suggested to be related to changes in oxidative phosphorylation in CMs⁸⁵. However, much remains unknown on the role of lncRNAs in regulating cardiac angiogenesis and regeneration after MI.

The communication between CMs and ECs can also be mediated by lncRNAs and can potentially influence neovascularisation and regeneration (**Table 1**). lncRNA TUG1 expression increased during hypoxia and promoted cell apoptosis by regulating the miR-145-5p-Bnip3 axis⁸⁶. miR-145 exerts a protective effect against oxidative stress in CMs by regulating Bnip3 expression, a mitochondrial sensory of oxidative stress⁸⁶. The lncRNA AZIN2sv was identified in the rat heart to inhibit CM proliferation and loss of AZIN2sv expression promoted cardiac regeneration and attenuated adverse ventricular remodeling post MI via PTEN/AKT signalling⁸⁷. Similarly, lncRNA CAREL was found to be significantly upregulated in P7 CMs and was linked to reduced CM proliferation. CAREL acts as a competing endogenous ribonucleic acid for miR-296 and derepresses the expression of Trp53inp1 and Irf2a, both inhibitors of CM replication⁸⁸. It is still unclear whether AZIN2sv or CAREL are also expressed by ECs to mediate cardiac regeneration after injury. Interestingly the foetal lncRNA ECRAR was found to simultaneously promote cardiomyogenesis and angiogenesis post-MI⁸⁹. Even though a paracrine mechanism for increased neovascularization is proposed by the authors, further investigation is required to confirm the therapeutic

potential of ECRAR. Recently, the lncRNA GATA6-AS has been reported to silence the expression of GATA6⁸⁹. GATA6-AS is upregulated in ECs during hypoxia inhibiting proliferation of ECs. GATA6 has previously been identified to be involved in CM progenitor cell proliferation⁹⁰. Inhibition of GATA6 through miRNA-10 decreased CM progenitor cell proliferation⁹⁰. The function of GATA6 and its tight regulation through ncRNAs in both ECs and CM progenitor cells indicates the close molecular connection between both cardiac cell types. Identifying key drivers of angiogenesis after MI can shed light on the way to regenerate the heart.

1.1.3. T-UCRs

During diversion of the human and rodent genomes, 481 regions, ranging from 200 to 779 nucleotides, remained completely conserved. Known as transcribed ultraconserved regions (T-UCRs), these regions are ubiquitously expressed and contain different types of RNA species. T-UCRs are considered essential for gene regulation by acting as antisense transcriptional inhibitors of protein coding and other ncRNA genes in their proximity³. Some T-UCRs were described to be dysregulated in disease and, to some extent, have been associated with hypoxia, particularly in cancer, where the tumour microenvironment is typically hypoxic⁹¹. Moreover, in ischemic stroke, expression of noncoding ultraconserved RNAs seems to be temporally altered in spontaneously hypertensive rats, but the functional significance of these findings is yet to be evaluated⁹². Recently, uc.48+, a lncRNA from a T-UCR, was shown to be upregulated in high-fat diet induced ischemic/reperfused myocardium. Overexpression of uc.48+ enhanced CM apoptosis and myocardial ischemia/reperfusion injury while silencing it had a protective effect. Hence uc.48+ was appointed as a booster of CM apoptosis and myocardial ischemia/reperfusion injury vulnerability to high fat diet⁹³. Although the precise functions of T-UCRs are not clear, some of them are known to be modulated by microRNAs in a cross-talk

between different classes of ncRNAs⁹⁴. How these new molecular interactions are involved in regulating endothelial and cardiac cell function in pathophysiological conditions remains to be investigated.

1.1.4. Paracrine communication between ECs and CMs

The intricate network of ECs surrounding CMs in the myocardium allows for molecular interactions to take place during development and disease. The release of ROS during ischemic injury induces neuregulin-1 β protein secretion from ECs that promotes CM survival via neuregulin1 β -erbB4-phosphatidylinositol-3-kinase-Akt pathway⁹⁵. The induction of paracrine neuregulin1 β -erbB4 signalling between ECs and CMs can also induce CM proliferation via the activation of the coreceptor ERBB28. Also, the secretion of PDGF-B and angiopoietin-1 by ECs induces CM protection via the activation of the phosphatidylinositol-3-kinase-Akt pathway. Both factors stimulate EC proliferation and survival in the developing and adult heart^{96–98}. Moreover, ECs promote synchronized contraction of CMs and synthesis of the gap junction protein connexin-43 necessary for the electrophysiological coupling of CMs⁹⁹. Targeting the communication between CMs and ECs can be an effective therapeutic tool to prevent HF and mediate cardiac regeneration. In the last decade, considerable interest has been focused on EVs to explore their potential to promote intercellular crosstalk¹⁰⁰. EVs are particles that are secreted from cells and contain proteins, mRNAs, and ncRNAs. The content of EVs is released when its membrane comes into contact with the recipient cell, thereby inducing intracellular molecular changes. EVs can be subdivided into categories based on their size and subcellular origin: microvesicles (0.1–1 μ m), exosomes (20–100 nm) and apoptotic bodies (0.5–2 μ m)¹⁰⁰. All cardiac cells secrete EVs as a mechanism to communicate with recipient cells. Exosomal signalling from mesenchymal stem cells (MSCs) during hypoxia promotes EC proliferation and migration¹⁰¹. The close anatomical connection

between ECs and CMs was a reason to investigate the mechanism of crosstalk in the healthy and diseased heart¹⁰². Exosomes from CMs were found to modulate the expression of pro-angiogenic genes in ECs. Ischemic iPSC-derived CMs can produce exosomes that promote EC survival and angiogenesis via RNA-transfer of PIM-1 and VEGF-A¹⁰³. HSP70 on the surface of exosomes from cardiac cells was found to induce activation of toll-like receptor-4 and subsequent ERK1/2 and p38 MAPK signalling increasing CM survival³. Depending on the metabolic state of CMs, the miRNA content present in their exosomes is subjected to changes¹⁰². Consecutively, exosomes from ECs can affect CM contractile function. Exosomal delivery of miR-146a stimulated by an anti-angiogenic 16-kDa N-terminal prolactin fragment has been found to be associated with loss of cardiac function in patients with peripartum cardiomyopathy¹⁰⁴. A recent study focusing on brain ischemia showed that the miRNA content in exosomes derived from ECs could induce angiogenesis and neurogenesis¹⁰⁵. CD34+ cell-derived exosomes were found to induce angiogenesis and vascular protection through their ncRNA cargo especially miRNA-126¹⁰⁶¹⁰⁹. The effect could be enhanced by adding the pro-angiogenic factor Sonic Hedgehog (Shh) to the exosomes¹¹⁰. In the heart, exosomes from healthy CMs were found to contain miRNA-126 that induces proliferation of ECs whereas diabetic CMs contained less miRNA-126 and increased levels of miRNA-320 decreasing angiogenesis¹¹¹. Moreover, ischemic CM-derived exosomes were found to contain more pro-angiogenic miRNAs than exosomes released by normoxic CMs, suggesting a partial attempt to increase vascularisation in the infarct area¹⁰². A heterogeneous population of exosomes from CMs could affect the metabolism of recipient cells¹¹². Influencing the content of exosomes or stimulating ECs to produce angiogenic, cardioprotective and regenerative factors can provide scope to regenerate the injured myocardium. This highlights the importance of EC-CM communication in multiple cardiovascular diseases and the role of exosomes. Hence, several pieces of evidence suggest that ncRNAs play an epigenetic role in

controlling heart response to hypoxia. Whereas positive regulators are determinant in promoting CM proliferation and/or neovascularization, negative regulators enhance the deleterious effects of hypoxia. This modulatory role is achieved by regulation of the expression of important hypoxia signalling pathways (e.g. Hif1 α) and/or secreted molecules (e.g. VEGF). Exosome production and release added further complexity to this regulatory network. Through EVs the effects of hypoxia can be transmitted not only to neighbouring but also to more distant cells, influencing their gene expression. This knowledge was only possible due to technological advances that allowed the study of non-coding elements of the genome. Surely, a better understanding of these mechanisms and how they can be modulated to improve heart response to hypoxia is going to be pivotal for achieving heart regeneration.

1.2. Targeting ECs and extracellular vesicles as a therapeutic tool for heart failure

Revascularization has been considered as the therapeutic gold standard to treat patients with MI as endothelial dysfunction is an important aspect towards progression to HF. The growing evidence of EC-CM communication creates a window of opportunity to promote neomyogenesis while targeting ECs. Supplementation with VEGF and angiopoietin-1 was found to concomitantly induce angiogenesis and CM proliferation in a porcine model of MI¹¹³. Similarly, injection of human endothelial progenitor cells in a rat model of MI was found to increase neovascularisation and limit infarct size¹¹⁴. Furthermore, administration of neuregulin-1 to the injured myocardium, to mimic EC signalling, has been tested and found beneficial in phase 2 clinical trials¹¹⁵. Neuregulin-1 activates endothelial NO synthase in CMs and the serine/threonine kinase Akt¹¹⁶. Re-establishing EC-CM signalling has also been tested by stimulating the NO-cGMP pathway¹¹⁷. NO supplementation was found to simulate the paracrine signalling of ECs and increase CM integrity and proliferation. Likewise, treatment with serelaxin, the human recombinant form of relaxin-2

increased NO signalling from ECs¹¹⁸, also abbreviating endothelial dysfunction after MI. Ultrasound-mediated miRNA-126-3p delivery increased EC proliferation and has been since considered of therapeutic interest to treat MI¹¹⁹. Inhibition of miRNA-92a expression in a large animal model of ischemia/reperfusion injury induced EC proliferation and improved cardiac function¹²⁰. In addition, modulation of EV content and/or release might be a potential tool to mediate cardiac regeneration. Vesicular communication between cardiac cell types during cardiovascular disease can have detrimental effects on cardiac function. CM-derived TNF α -containing EVs induced inflammation and apoptosis of neighbouring CMs¹²¹. Furthermore, miR-146-loaded vesicles from ECs were found to inhibit angiogenesis of surrounding ECs and inhibit metabolic activity of CMs by targeting ErbB4, Notch1 and Irak1 in peripartum cardiomyopathy¹⁰⁴. Preventing the paracrine signalling of miR-146 loaded EVs via anti-miR-146 ameliorated disease progression. Blocking the delivery of EVs by targeting vesicle release, uptake, or formation has been considered for therapeutic purposes but might have considerable off-target effects (e.g. preventing the secretion of potentially beneficial vesicles)⁹⁹. Specifically blocking the release of miR-21-containing EVs from CFs might be beneficial as these vesicles induce cardiac hypertrophy by downregulating Sorbin and SH3 domain containing 2 (SORBS2) or PDZ and LIM domain 5 (PDLIM5)¹¹². Horizontal transfer of ncRNAs via EVs can be modulated to increase the therapeutic potential of ncRNAs and/or of injected cells. In fact, exosomal delivery of miRNA-214 secreted from ECs can induce angiogenesis of neighbouring ECs¹²². Moreover, treatment with vesicles isolated from CD34+ hematopoietic stem cells can mediate EC proliferation via the transfer of miRNA-126^{107–109,123} and vesicles from cardiomyocyte progenitor cells prevented CM apoptosis and promoted EC proliferation¹²⁴. Also, Shh enriched vesicles were found to effectively induce EC proliferation via the PI3K and ERK-dependent increase of NO¹²⁵. Overall, these findings indicate that targeting EC signalling via ncRNAs and EVs may serve as a novel therapeutic strategy to treat MI and HF.

2. CONCLUSION

Ischemic heart disease continues to lead the causes of death despite the large effort of clinicians and academia on reverting this trend¹²⁶. The discovery that the mammalian heart endows an intrinsic, yet transient, regenerative capacity propelled the cardiovascular community to explore the molecular mechanisms governing cardiac regeneration. In this quest, the role of ncRNAs in cardiovascular diseases and cardiac regeneration became evident⁶. Modulating endogenous ncRNAs and cell-to-cell transfer of ncRNAs in a cell-specific manner can serve as a therapeutic tool to induce cardiac regeneration/repair. For a long time, intergenic regions were considered disposable, however their recent discovered value generates new layers of complexity to molecular control of cardiac pathophysiology. Previous studies indicate that neovascularisation is essential for the successful regeneration of the heart. However, hypoxia signalling and hypoxia-activated ncRNAs play an important role in cardiac regeneration. The postnatal metabolic shift towards oxidative phosphorylation, generation of ROS as well as the closure of the ductus arteriosus, resulting in increased blood flow to the left ventricle correlate with the loss of cardiac regenerative capacity^{12,127}. Nonetheless, hypoxia signalling without subsequent stimulation of angiogenesis does not lead to efficient cardiac regeneration as re-establishment of blood flow to the injured myocardium is required for supporting CMs. In fact, the adult, non-regenerating, mammalian heart is not able to restore the vasculature after MI which worsens myocardial damage and patients with a lower capillary density are more likely to progress to HF^{128,129}. At present, studies on cardiac regeneration either focus on the regeneration of the myocardium or on the regeneration of the cardiac microvasculature. However, the use of single pro-angiogenic agents does not have a substantial effect on cardiac regeneration (reviewed in ²). The solution might lie in combining pro-angiogenic and neomyogenic factors as well as improving the delivery method (e.g. specific cell targeting via EVs). In fact, multiple lines of evidence suggest that to effectively regenerate the heart,

both neovascularisation and CM proliferation need to be promoted in a timely and spatially-dependent manner, as cardiac phenotypes observed in HF are not only attributed to failing CMs but to the whole cellular content.

2.1. FUTURE PERSPECTIVES

The strong specialization of the adult mammalian heart comes with the cost of low regenerative potential. This low regenerative capacity is on the basis of the heavy socio-economic burden of cardiovascular diseases. Nevertheless, encouraging reports have found ncRNAs regulating CM proliferation and neovascularization. The communication between ECs and CMs occurs at several levels and these interactions were shown to be central for neonatal cardiac regeneration in mammals. Hence, this connection represents an important opportunity for modulating heart response to injury towards regeneration or improved healing. Future studies must analyse the effect of neovascularisation on CM proliferation and explore the connection between hypoxia, CM proliferation and the timing of the angiogenic response. Moreover, studying the precise changes in the microvasculature and the molecular interaction between the CMs and the ECs during the postnatal period, when the ability to regenerate the heart is lost, can highlight the limiting elements for cardiac regeneration. Knowledge derived from these studies will be of great relevance and will contribute to the development of improved therapeutic approaches.

ACKNOWLEDGEMENTS

MMCP was supported by a Netherlands CardioVascular Research Initiative (CVON) grant (REMAIN 2014B027). VSP was supported by a Foundation for Science and Technology of Portugal (FCT) grant (SFRH/BD/111799/2015). PDCM was supported by a Dutch Heart Foundation grant (NHS2015T066) and a Foundation for Science

and Technology of Portugal (FCT) grant (PTDC/BIM-MEC/4578/2014).

REFERENCES

1. Mercer TR, Dinger ME, Mattick JS. Long non-coding RNAs: insights into functions. *Nat Rev Genet.* 2009;10:155-159.
2. Juni RP, Abreu RC, Diseases C, Sciences L, Surgery C, Martins C. Regulation of microvascularization in heart failure - The close relationship between endothelial cells, non-coding RNAs, and exosomes. *Non-coding RNA Res.* 2017;2(1):45-55.
3. Bejerano G, Bejerano G, Pheasant M, et al. Ultraconserved Elements in the Human Genome. *Science.* 2007;1321(2004):1321-1326.
4. Papageorgiou N, Tslamandris S, Giolis A, Tousoulis D. MicroRNAs in cardiovascular disease: Perspectives and reality. *Cardiol Rev.* 2016;24(3):110-118.
5. Ratajczak MZ, Ratajczak J. Horizontal transfer of RNA and proteins between cells by extracellular microvesicles: 14 years later. *Clin Transl Med.* 2016;5(1):7.
6. Kumarswamy R, Thum T. Non-coding RNAs in cardiac remodeling and heart failure. *Circ Res.* 2013;113(6):676-689.
7. Bergmann O, Bhardwaj RD, Bernard S, et al. Evidence for Cardiomyocyte Renewal in Humans. *Science.* 2009;324:98-102.
8. D'Uva G, Aharonov A, Lauriola M, et al. ERBB2 triggers mammalian heart regeneration by promoting cardiomyocyte dedifferentiation and proliferation. *Nat Cell Biol.* 2015;17(5):627-638.
9. Porrello ER, Mahmoud AI, Simpson E, et al. Transient Regenerative Potential of the Neonatal Mouse Heart. *Science.* 2011;331:1078-1081.
10. Sampaio-Pinto V, Rodrigues SC, Laundos TL, et al. Neonatal Apex Resection Triggers Cardiomyocyte Proliferation, Neovascularization and Functional Recovery Despite Local Fibrosis. *Stem Cell Reports.* 2018;10(3):860-874.
11. Poss KD, Wilson LG, Keating MT. Heart Regeneration in Zebrafish. 2002;298:2188-2191.
12. Puente BN, Kimura W, Muralidhar SA, et al. The oxygen-rich postnatal environment induces cardiomyocyte cell-cycle arrest through DNA damage response. *Cell.* 2014;157(3):565-579.
13. Jopling C, Sleep E, Raya M, Martí M, Raya A, Belmonte JCI. Zebrafish heart regeneration occurs by cardiomyocyte dedifferentiation and proliferation. *Nature.* 2010;464(7288):606-609.
14. Jopling C, Suñé G, Faucherre A, Fabregat C, Izpisua Belmonte JC. Hypoxia induces myocardial regeneration in zebrafish. *Circulation.* 2012;126(25):3017-3027.
15. Laflamme MA, Murry CE. Heart regeneration. *Nature.* 2011;473(7347):326-335.
16. Tirziu D, Giordano FJ, Simons M. Cell communications in the heart. *Circulation.*

- 2010;122(9):928-937.
17. Bergmann O, Zdunek S, Felker A, et al. Dynamics of Cell Generation and Turnover in the Human Heart. *Cell*. 2015;161(7):1566-1575.
 18. Pinto AR, Ilinykh A, Ivey MJ, et al. Revisiting cardiac cellular composition. *Circ Res*. 2016;118(3):400-409.
 19. Doll S, Dreßen M, Geyer PE, et al. Region and cell-type resolved quantitative proteomic map of the human heart. *Nat Commun*. 2017;8(1):1-13.
 20. Smart N. Prospects for improving neovascularization of the ischemic heart: Lessons from development. *Microcirculation*. 2017;24(1).
 21. Hojo Y, Saito T, Kondo H. Role of apoptosis in left ventricular remodeling after acute myocardial infarction. *J Cardiol*. 2012;60(2):91-92.
 22. Kang PM, Haunstetter A, Aoki H, Usheva A, Izumo S. Morphological and Molecular Characterization of Adult Cardiomyocyte Apoptosis During Hypoxia and Reoxygenation. *Circ Res*. 2000;87(2):118-125.
 23. Prech M, Marszałek A, Schröder J, et al. Apoptosis as a Mechanism for the Elimination of Cardiomyocytes After Acute Myocardial Infarction. *Am J Cardiol*. 2010;105(9):1240-1245.
 24. Kühn B, Del Monte F, Hajjar RJ, et al. Periostin induces proliferation of differentiated cardiomyocytes and promotes cardiac repair. *Nat Med*. 2007;13(8):962-969.
 25. Kimura W, Xiao F, Canseco DC, et al. Hypoxia fate mapping identifies cycling cardiomyocytes in the adult heart. *Nature*. 2015;523(7559):226-230.
 26. Santos CXC, Anilkumar N, Zhang M, Brewer AC, Shah AM. Redox signaling in cardiac myocytes. *Free Radic Biol Med*. 2011;50(7):777-793.
 27. Ivan M, Kondo K, Yang H, et al. HIF α Targeted for VHL-Mediated Destruction by Proline Hydroxylation: Implications for O₂ Sensing. *Science*. 2001;292(5516):464-468.
 28. Marín-Juez R, Marass M, Gauvrit S, et al. Fast revascularization of the injured area is essential to support zebrafish heart regeneration. *Proc Natl Acad Sci*. 2016;113(40):11237-11242.
 29. Lepilina A, Coon AN, Kikuchi K, et al. A Dynamic Epicardial Injury Response Supports Progenitor Cell Activity during Zebrafish Heart Regeneration. *Cell*. 2006;127(3):607-619.
 30. Das S, Goldstone AB, Wang H, et al. A Unique Collateral Artery Development Program Promotes Neonatal Heart Regeneration. *Cell*. 2019;176(5):1128-1142.e18.
 31. Kornfeld J-W, Bruning JC. Regulation of metabolism by long, non-coding RNAs. *Front Genet*. 2014;5:1-8.
 32. Rane S, He M, Sayed D, et al. Downregulation of MiR-199a derepresses hypoxia-inducible factor-1 α and sirtuin 1 and recapitulates hypoxia preconditioning in cardiac

- myocytes. *Circ Res*. 2009;104(7):879-886.
33. Fiedler J, Jazbutyte V, Kirchmaier BC, et al. MicroRNA-24 regulates vascularity after myocardial infarction. *Circulation*. 2011;124(6):720-730.
 34. Fiedler J, Breckwoldt K, Remmele CW, et al. Development of long noncoding RNA-based strategies to modulate tissue vascularization. *J Am Coll Cardiol*. 2015;66(18):2005-2015.
 35. Eulalio A, Mano M, Ferro MD, et al. Functional screening identifies miRNAs inducing cardiac regeneration. *Nature*. 2012;492(7429):376-381.
 36. Rao PK, Toyama Y, Chiang HR, et al. Loss of Cardiac microRNA-Mediated Regulation Leads to Dilated Cardiomyopathy and Heart Failure. 2009.
 37. Chen J, Murchison EP, Tang R, et al. Targeted deletion of Dicer in the heart leads to dilated cardiomyopathy and heart failure. 2008;105(6):2111-2116.
 38. Yang WJ, Yang DD, Na S, Sandusky GE, Zhang Q, Zhao G. Dicer is required for embryonic angiogenesis during mouse development. *J Biol Chem*. 2005;280(10):9330-9335.
 39. Suárez Y, Fernández-Hernando C, Pober JS, Sessa WC. Dicer dependent microRNAs regulate gene expression and functions in human endothelial cells. *Circ Res*. 2007;100(8):1164-1173.
 40. Azzouzi H el, Leptidis S, Doevendans PA, De Windt LJ. HypoxamiRs: Regulators of cardiac hypoxia and energy metabolism. *Trends Endocrinol Metab*. 2015;26(9):502-508.
 41. Hua Z, Lv Q, Ye W, et al. Mirna-directed regulation of VEGF and other angiogenic under hypoxia. *PLoS One*. 2006;1(1).
 42. Deng HT, Liu HL, Zhai BB, et al. Vascular endothelial growth factor suppresses TNFSF15 production in endothelial cells by stimulating miR-31 and miR-20a expression via activation of Akt and Erk signals. *FEBS Open Bio*. 2017;7(1):108-117.
 43. Arif M, Pandey R, Alam P, et al. MicroRNA-210-mediated proliferation, survival, and angiogenesis promote cardiac repair post myocardial infarction in rodents. *J Mol Med*. 2017;95(12):1369-1385.
 44. Greco S, Gaetano C, Martelli F. HypoxamiR Regulation and Function in Ischemic Cardiovascular Diseases. *Antioxid Redox Signal*. 2014;21(8):1202-1219.
 45. Zaccagnini G, Maimone B, Di Stefano V, et al. Hypoxia-Induced miR-210 Modulates Tissue Response to Acute Peripheral Ischemia. *Antioxid Redox Signal*. 2014;21(8):1177-1188.
 46. Ghosh G, Subramanian I V, Adhikari N, et al. Hypoxia-induced microRNA-424 expression in human endothelial cells regulates HIF-alpha isoforms and promotes angiogenesis. *J Clin Invest*. 2010;120(11):4141-4154.
 47. Hu S, Huang M, Li Z, et al. MicroRNA-210 as a novel therapy for treatment of ischemic heart disease. *Circulation*. 2010;122.

48. Wang Y, Pan X, Fan Y, et al. Dysregulated expression of microRNAs and mRNAs in myocardial infarction. *Am J Transl Res.* 2015;7(11):2291-2304.
49. Nishi H, Ono K, Iwanaga Y, et al. MicroRNA-15b modulates cellular ATP levels and degenerates mitochondria via Arl2 in neonatal rat cardiac myocytes. *J Biol Chem.* 2010;285(7):4920-4930.
50. Small EM, Frost RJA, Olson EN. MicroRNAs add a new dimension to cardiovascular disease. *Circulation.* 2010;121(8):1022-1032.
51. Chamorro-Jorganes A, Araldi E, Penalva LOF, Sandhu D, Fernández-Hernando C, Suárez Y. MicroRNA-16 and MicroRNA-424 regulate cell-autonomous angiogenic functions in endothelial cells via targeting vascular endothelial growth factor receptor-2 and fibroblast growth factor receptor-1. *Arterioscler Thromb Vasc Biol.* 2011;31(11):2595-2606.
52. Porrello ER, Mahmoud AI, Simpson E, et al. Regulation of neonatal and adult mammalian heart regeneration by the miR-15 family. *Proc Natl Acad Sci.* 2013;110(1):187-192.
53. Hullinger TG, Montgomery RL, Seto AG, et al. Inhibition of miR-15 protects against cardiac ischemic injury. *Circ Res.* 2012;110(1):71-81.
54. Meloni M, Marchetti M, Garner K, et al. Local inhibition of microRNA-24 improves reparative angiogenesis and left ventricle remodeling and function in mice with myocardial infarction. *Mol Ther.* 2013;21(7):1390-1402.
55. Icli B, Wara AKM, Moslehi J, et al. MicroRNA-26a regulates pathological and physiological angiogenesis by targeting BMP/SMAD1 signaling. *Circ Res.* 2013;113(11):1231-1241.
56. Dai GH, Ma PZ, Song XB, Liu N, Zhang T, Wu B. MicroRNA-223-3p inhibits the angiogenesis of ischemic cardiac microvascular endothelial cells via affecting RPS6KB1/hif-1a signal pathway. *PLoS One.* 2014;9(10):1-14.
57. Magenta A, Cencioni C, Fasanaro P, et al. MiR-200c is upregulated by oxidative stress and induces endothelial cell apoptosis and senescence via ZEB1 inhibition. *Cell Death Differ.* 2011;18(10):1628-1639.
58. Papageorgiou N, Zacharia E, Tousoulis D. Association between microRNAs and coronary collateral circulation: is there a new role for the small non-coding RNAs? *Ann Transl Med.* 2016;4(11):223.
59. Kim J-H, Lee K-S, Lee D-K, et al. Hypoxia-Responsive MicroRNA-101 Promotes Angiogenesis via Heme Oxygenase-1/Vascular Endothelial Growth Factor Axis by Targeting Cullin 3. *Antioxid Redox Signal.* 2014;00(00):1-14.
60. Grundmann S, Hans FP, Kinniry S, et al. MicroRNA-100 regulates neovascularization by suppression of mammalian target of rapamycin in endothelial and vascular smooth muscle cells. *Circulation.* 2011;123(9):999-1009.
61. Chen K, Fan W, Wang X, Ke X, Wu G, Hu C. MicroRNA-101 mediates the

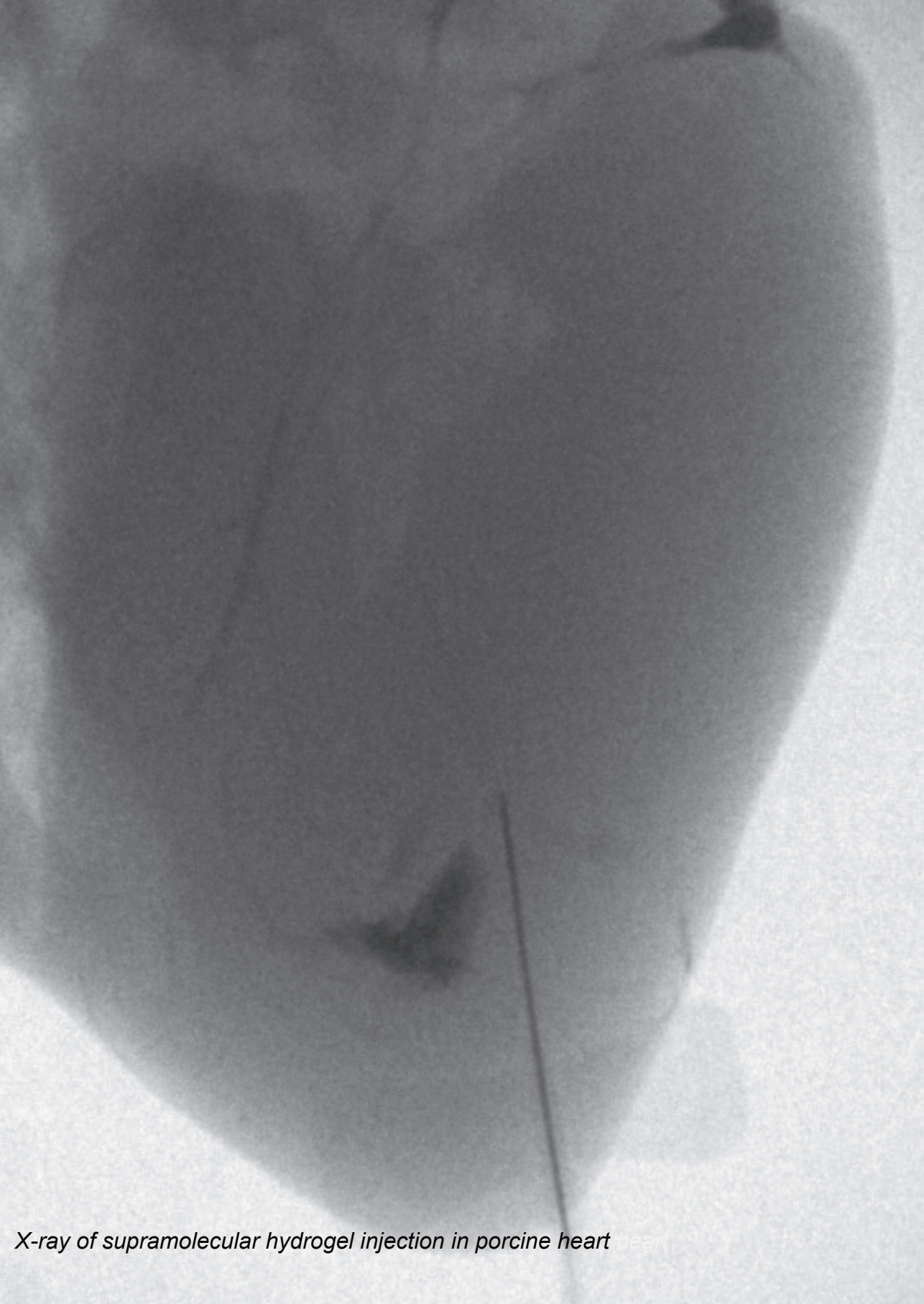
- suppressive effect of laminar shear stress on mTOR expression in vascular endothelial cells. *Biochem Biophys Res Commun.* 2012;427(1):138-142.
62. Wang S, Aurora AB, Johnson BA, et al. The Endothelial-Specific MicroRNA miR-126 Governs Vascular Integrity and Angiogenesis. *Dev Cell.* 2008;15(2):261-271.
63. Fish JE, Santoro MM, Morton SU, et al. miR-126 Regulates Angiogenic Signaling and Vascular Integrity. *Dev Cell.* 2008;15(2):272-284.
64. Semo J, Sharir R, Afek A, et al. The 106b~25 microRNA cluster is essential for neovascularization after hindlimb ischaemia in mice. *Eur Heart J.* 2014;35(45):3212-3223.
65. Haghikia A, Missol-Kolka E, Tsikas D, et al. Signal transducer and activator of transcription 3-mediated regulation of miR-199a-5p links cardiomyocyte and endothelial cell function in the heart: A key role for ubiquitin-conjugating enzymes. *Eur Heart J.* 2011;32(10):1287-1297.
66. Wang X, Huang W, Liu G, et al. Cardiomyocytes mediate anti-angiogenesis in type 2 diabetic rats through the exosomal transfer of miR-320 into endothelial cells. *J Mol Cell Cardiol.* 2014;74:139-150.
67. Ottaviani L, Juni RP, Halkein J, et al. Cardiomyocyte-derived exosomes mediate pathological cardiac microvascular remodeling. *J Mol Cell Cardiol.* 2018;120:45.
68. Sabour D, Machado RSR, Pinto JP, et al. Parallel Genome-wide Profiling of Coding and Non-coding RNAs to Identify Novel Regulatory Elements in Embryonic and Maturated Heart. *Mol Ther - Nucleic Acids.* 2018;12:158-173.
69. Yang S, Fan T, Hu Q, et al. Downregulation of microRNA-17-5p improves cardiac function after myocardial infarction via attenuation of apoptosis in endothelial cells. *Mol Genet Genomics.* 2018;293(4):883-894.
70. Adamowicz M, Morgan CC, Haubner BJ, et al. Functionally Conserved Noncoding Regulators of Cardiomyocyte Proliferation and Regeneration in Mouse and Human. *Circ Genomic Precis Med.* 2018;11(2):1-13.
71. Scheuermann JC, Boyer LA. Getting to the heart of the matter: Long non-coding RNAs in cardiac development and disease. *EMBO J.* 2013;32(13):1805-1816.
72. Ballantyne MD, McDonald RA, Baker AH. lncRNA/MicroRNA interactions in the vasculature. *Clin Pharmacol Ther.* 2016;99(5):494-501.
73. Ebert MS, Sharp PA. Emerging roles for natural microRNA sponges. *Curr Biol.* 2010;20(19):R858-R861.
74. Wang K, Long B, Zhou LY, et al. CARL lncRNA inhibits anoxia-induced mitochondrial fission and apoptosis in cardiomyocytes by impairing miR-539-dependent PHB2 downregulation. *Nat Commun.* 2015;5:1-13.
75. Leisegang MS, Fork C, Josipovic I, et al. Long Noncoding RNA MANTIS Facilitates Endothelial Angiogenic Function. *Circulation.* 2017.
76. Josipovic I, Fork C, Preussner J, et al. PAFAH1B1 and the lncRNA

- NONHSAT073641 maintain an angiogenic phenotype in human endothelial cells. *Acta Physiol.* 2016;218(1):13-27.
77. Ishii N, Ozaki K, Sato H, et al. Identification of a novel non-coding RNA, MIAT, that confers risk of myocardial infarction. *J Hum Genet.* 2006;51(12):1087-1099.
 78. Yan B, Yao J, Liu JY, et al. LncRNA-MIAT regulates microvascular dysfunction by functioning as a competing endogenous RNA. *Circ Res.* 2015;116(7):1143-1156.
 79. Kurian L, Aguirre A, Sancho-Martinez I, et al. Identification of novel long noncoding RNAs underlying vertebrate cardiovascular development. *Circulation.* 2015;131(14):1278-1290.
 80. Hou J, Zhou C, Long H, et al. Long noncoding RNAs: Novel molecules in cardiovascular biology, disease and regeneration. *Exp Mol Pathol.* 2016;100(3):493-501.
 81. Michalik KM, You X, Manavski Y, et al. Long noncoding RNA MALAT1 regulates endothelial cell function and vessel growth. *Circ Res.* 2014;114(9):1389-1397.
 82. Man HSJ, Sukumar AN, Lam GC, Turgeon PJ, Yan MS, Ha K. Angiogenic patterning by STEEL , an endothelial- enriched long noncoding RNA. 2018;115(10):2401-2406.
 83. Miao Y, Ajami NE, Huang TS, et al. Enhancer-associated long non-coding RNA LEENE regulates endothelial nitric oxide synthase and endothelial function. *Nat Commun.* 2018;9(1).
 84. Liao B, Chen R, Lin F, et al. Long noncoding RNA HOTTIP promotes endothelial cell proliferation and migration via activation of the Wnt/ β -catenin pathway. *J Cell Biochem.* 2018;119(3):2797-2805.
 85. Kumarswamy R, Bauters C, Volkman I, et al. Circulating Long Noncoding RNA, LIPCAR, Predicts Survival in Patients with Heart Failure. *Br UltraRapid Commun (Clin Track).* 2014:1569-1575.
 86. Wu Z, Zhao S, Li C, Liu C. LncRNA TUG1 serves an important role in hypoxia-induced myocardial cell injury by regulating the miR-145-5p-Binp3 axis. *Mol Med Rep.* 2018;17(2):2422-2430.
 87. Li X, He X, Wang H, et al. Loss of AZIN2 splice variant facilitates endogenous cardiac regeneration. *Cardiovasc Res.* 2018:1642-1655.
 88. Cai B, Ma W, Ding F, et al. The Long Noncoding RNA CAREL Controls Cardiac Regeneration. *J Am Coll Cardiol.* 2018;72(5):534-550.
 89. Chen Y, Li X, Li B, et al. Long Non-coding RNA ECRAR Triggers Post-natal Myocardial Regeneration by Activating ERK1/2 Signaling. *Mol Ther.* 2018;27(1):1-17.
 90. Liang D, Zhen L, Yuan T, et al. miR-10a regulates proliferation of human cardiomyocyte progenitor cells by targeting GATA6. *PLoS One.* 2014;9(7):3-10.
 91. Ferdin J, Nishida N, Wu X, et al. HINCUTs in cancer : hypoxia-induced noncoding ultraconserved transcripts. 2013:1675-1687.

92. Mehta SL, Vemuganti R. Ischemic Stroke Alters the Expression of the Transcribed Ultraconserved Regions of the Genome in Rat Brain. 2018;1024-1028.
93. Ding L, Gong C, Rao S, Wang S, Xiao W, Wang R. Noncoding transcribed ultraconserved region (T-UCR) UC.48+ is a novel regulator of high-fat diet induced myocardial ischemia/reperfusion injury. 2019;9849-9861.
94. Terreri S, Durso M, Colonna V, Romanelli A, Nigris F De, Cimmino A. New Cross-Talk Layer between Ultraconserved Non-Coding RNAs, MicroRNAs and Polycomb Protein YY1 in Bladder Cancer. *Genes (Basel)*. 2016;1-10.
95. Kuramochi Y, Cote GM, Guo X, et al. Cardiac endothelial cells regulate reactive oxygen species-induced cardiomyocyte apoptosis through neuregulin-1b/erbB4 signaling. *J Biol Chem*. 2004;279(49):51141-51147.
96. Edelberg JM, Aird WC, Wu W, et al. PDGF mediates cardiac microvascular communication. *J Clin Invest*. 1998;102(4):837-843.
97. Edelberg JM, Lee SH, Kaur M, et al. Platelet-Derived Growth Factor-AB Limits the Extent of Myocardial Infarction in a Rat Model. *J Am Coll Cardiol*. 2002;2001:608-613.
98. Dallabrida SM. Angiopoietin-1 Promotes Cardiac and Skeletal Myocyte Survival Through Integrins. *Circ Res*. 2005;96(4):e8-e24.
99. Narmoneva DA, Vukmirovic R, Davis ME, Kamm RD, Lee RT. Endothelial cells promote cardiac myocyte survival and spatial reorganization: Implications for cardiac regeneration. *Circulation*. 2004;110(8):962-968.
100. El Andaloussi S, Mäger I, Breakefield XO, Wood MJA. Extracellular vesicles: Biology and emerging therapeutic opportunities. *Nat Rev Drug Discov*. 2013;12(5):347-357.
101. Salomon C, Ryan J, Sobrevia L, et al. Exosomal Signaling during Hypoxia Mediates Microvascular Endothelial Cell Migration and Vasculogenesis. *PLoS One*. 2013;8(7):1-24.
102. Garcia NA, Ontoria-Oviedo I, González-King H, Diez-Juan A, Sepúlveda P. Glucose starvation in cardiomyocytes enhances exosome secretion and promotes angiogenesis in endothelial cells. *PLoS One*. 2015;10(9):1-23.
103. Malepu S, Renikunta H, Kraenkel N, et al. Ischemia-driven exosome release of human iPSC-CM derived cardiomyocytes increase viability of endothelial cells via pro-survival factors. *Remodel Cardioprot*. 2018:4086356.
104. Halkein J, Tabruyn SP, Ricke-Hoch M, et al. MicroRNA-146a is a therapeutic target and biomarker for peripartum cardiomyopathy. *J Clin Invest*. 2013;123(5):2143-2154.
105. Liu X, Pan W, Li C, et al. Exosomal Micrnas From Ischemic Cerebral Endothelial Cells and Neural Stem Cells Regulate Coupling of Neurogenesis and Angiogenesis. *Stroke*. 2018;49.
106. Sahoo S, Klychko E, Thorne T, et al. Exosomes from human CD34+stem cells

- mediate their proangiogenic paracrine activity. *Circ Res.* 2011;109(7):724-728.
107. Mathiyalagan P, Liang Y, Kim D, et al. Angiogenic Mechanisms of Human CD34+Stem Cell Exosomes in the Repair of Ischemic Hindlimb. *Circ Res.* 2017;120(9):1466-1476.
 108. Chen L, Wang J, Wang B, et al. MiR-126 inhibits vascular endothelial cell apoptosis through targeting PI3K/Akt signaling. *Ann Hematol.* 2016;95(3):365-374.
 109. Zernecke A, Bidzhekov K, Noels H, et al. Delivery of microRNA-126 by apoptotic bodies induces CXCL12-dependent vascular protection. *Sci Signal.* 2009;2(100):1-13.
 110. Mackie AR, Klyachko E, Thorne T, et al. Sonic Hedgehog Modified Human CD34+ Cells Preserve Cardiac Function Following Acute Myocardial Infarction. *Circ Res.* 2013;111(3):312-321.
 111. Salem, E. S., & Fan GC. Pathological Effects of Exosomes in Mediating Diabetic Cardiomyopathy. In *Exosomes in Cardiovascular Diseases.*; 2017.
 112. Bang C, Batkai S, Dangwal S, et al. Cardiac fibroblast-derived microRNA passenger strand-enriched exosomes mediate cardiomyocyte hypertrophy. *J Clin Invest.* 2014;124(5):2136-2146.
 113. Tao Z, Chen B, Tan X, et al. Coexpression of VEGF and angiopoietin-1 promotes angiogenesis and cardiomyocyte proliferation reduces apoptosis in porcine myocardial infarction (MI) heart. *Proc Natl Acad Sci.* 2011;108(5):2064-2069.
 114. Kawamoto A, Gwon H, Iwaguro H, et al. Therapeutic Potential of Ex Vivo Expanded Endothelial Progenitor Cells for Myocardial Ischemia. 2001.
 115. Gao R, Zhang J, Cheng L, et al. A phase II, randomized, double-blind, multicenter, based on standard therapy, placebo-controlled study of the efficacy and safety of recombinant human neuregulin-1 in patients with chronic heart failure. *J Am Coll Cardiol.* 2010;55(18):1907-1914.
 116. Lemmens K, Fransen P, Sys SU, Brutsaert DL, De Keulenaer GW. Neuregulin-1 Induces a Negative Inotropic Effect in Cardiac Muscle: Role of Nitric Oxide Synthase. *Circulation.* 2004;109(3):324-326.
 117. Lepic E, Burger D, Lu X, Song W, Feng Q. Lack of endothelial nitric oxide synthase decreases cardiomyocyte proliferation and delays cardiac maturation. *AJP Cell Physiol.* 2006;291(6):C1240-C1246.
 118. Dschietzig T, Brecht A, Bartsch C, Baumann G, Stangl K, Alexiou K. Relaxin improves TNF- α -induced endothelial dysfunction: The role of glucocorticoid receptor and phosphatidylinositol 3-kinase signalling. *Cardiovasc Res.* 2012;95(1):97-107.
 119. Cao WJ, Rosenblat JD, Roth NC, et al. Therapeutic Angiogenesis by Ultrasound-Mediated MicroRNA-126-3p Delivery. *Arterioscler Thromb Vasc Biol.* 2015;35(11):2401-2411.
 120. Hinkel R, Penzkofer D, Zühlke S, et al. Inhibition of microRNA-92a protects against

- ischemia/reperfusion injury in a large-animal model. *Circulation*. 2013;128(10):1066-1075.
121. Yu X, Deng L, Wang D, et al. Mechanism of TNF- α autocrine effects in hypoxic cardiomyocytes: Initiated by hypoxia inducible factor 1 α , presented by exosomes. *J Mol Cell Cardiol*. 2012;53(6):848-857.
122. Van Balkom BWM, De Jong OG, Smits M, et al. Endothelial cells require miR - 214 to secrete exosomes that suppress senescence and induce angiogenesis in human and mouse endothelial cells. *Blood*. 2017;121(19):3997-4007.
123. Jansen F, Yang X, Hoelscher M, et al. Endothelial microparticle-mediated transfer of microRNA-126 promotes vascular endothelial cell repair via spred1 and is abrogated in glucose-damaged endothelial microparticles. *Circulation*. 2013;128(18):2026-2038.
124. Barile L, Lionetti V, Cervio E, et al. Extracellular vesicles from human cardiac progenitor cells inhibit cardiomyocyte apoptosis and improve cardiac function after myocardial infarction. *Cardiovasc Res*. 2014;103(4):530-541.
125. Fleury A, Martinez MC, Le Lay S. Extracellular vesicles as therapeutic tools in cardiovascular diseases. *Front Immunol*. 2014;5:1-8.
126. Mozaffarian D, Benjamin EJ, Go AS, et al. Executive summary: Heart disease and stroke statistics-2016 update: A Report from the American Heart Association. *Circulation*. 2016;133(4):447-454.
127. Banerjee I, Fuseler JJW, Price RL, et al. Determination of cell types and numbers during cardiac development in the neonatal and adult rat and mouse. *Am Physiol*. 2007;293(3):1883-1891.
128. Coma-Canella I. Changes in myocardial function and perfusion after acute myocardial infarction. *Rev Esp Cardiol*. 2003;56(5):433-435.
129. Mohammed SF, Majure DT, Redfield MM. Zooming in on the microvasculature in heart failure with preserved ejection fraction. *Circ Hear Fail*. 2016;9(7):1-5.



X-ray of supramolecular hydrogel injection in porcine heart

Chapter 8

IN VIVO RETENTION QUANTIFICATION OF SUPRAMOLECULAR HYDROGELS ENGINEERED FOR CARDIAC DELIVERY

Adapted from:

Advanced Healthcare Materials. 2021, 2001987, doi: 10.1002/adhm.202001987

Published online on 14 February 2021

Maaïke J.G. Schotman^{*2}, Marijn M.C. Peters^{*1}, Gerard C. Krijger³, Iris van Adrichem¹, Remmert de Roos³, John L. M. Bemelmans³, Maarten J. Pouderoijen⁴, Martin G. T. A. Rutten², Klaus Neef¹, Steven A.J. Chamuleau¹, Patricia Y.W. Dankers²

¹Department of Cardiology, Experimental Cardiology Laboratory, UMC Utrecht Regenerative Medicine Centre, University Medical Centre Utrecht, Utrecht, The Netherlands

² Institute for Complex Molecular Systems, Laboratory of Chemical Biology, Department of Biomedical Engineering, Eindhoven University of Technology, Eindhoven, The Netherlands

³Department of Nuclear Medicine, University Medical Centre Utrecht, Utrecht, The Netherlands

⁴SyMO-Chem, Eindhoven, The Netherlands

* Equal contribution

ABSTRACT

Recent advances in the field of cardiac regeneration show great potential in the use of injectable hydrogels to reduce immediate flush-out of injected factors, thereby increasing the effectiveness of the encapsulated drugs. To establish a relation between cardiac function and retention of the drug-encapsulating hydrogel, a quantitative *in vivo* imaging method is required. Here, we develop our supramolecular ureido-pyrimidinone modified poly(ethylene glycol) (UPy-PEG) material into a bioactive hydrogel for radioactive imaging in a large animal model. As radioactive label we synthesized a monofunctional UPy-DOTA complexed with the radioactive isotope indium-111 (UPy-DOTA-¹¹¹In) being mixed with the hydrogel. Additionally, bioactive and adhesive properties of the UPy-PEG hydrogel were increased by supramolecular introduction of a UPy-functionalized recombinant collagen type 1-based material (UPy-PEG-RCPHC1). This method enabled *in vivo* tracking of the non-bioactive and bioactive supramolecular hydrogels and quantification of hydrogel retention in a porcine heart. In a small pilot, cardiac retention values of 8% for UPy-PEG and 16% for UPy-PEG-RCPHC1 hydrogel were observed 4 hours post injection. This work highlights the importance of retention quantification of hydrogels *in vivo*, where elucidation of hydrogel quantity at the target site is proposed to strongly influence efficacy of the intended therapy.

INTRODUCTION

Ischemic heart disease is responsible for over 9 million deaths per year worldwide as a result of blood flow deficiency in the infarcted area and through resulting adverse ventricular remodeling and contractile dysfunction¹. This adverse remodeling is caused by the inability of the heart to replace cardiomyocytes lost by ischemic damage to the myocardium. Therapeutic methods to stimulate cardiac repair remain ineffective as potential reparative drugs injected into the heart immediately flush-out through the venous microvasculature of the heart and the injection needle tract². A carrier system to protect and localize regenerative factors at the injection site, and enable sustained, slow therapeutic release might provide a solution to this delivery issue. Biomaterials are increasingly studied in the field of cardiac regeneration, where patches or injectable hydrogels are applied to aid retention and provide sustained release of drug molecules at the target site^{3,4}. Visualization of these biomaterials after injection or implantation is of high importance to assess the retention and degradation at the target site. Quantification of retention would enable correlation of drug efficacy to presence and availability at the target site, as well as monitoring the fate and distribution of the material *in vivo*. Based on this, volumes of injection or implantation could be tuned for an optimal drug release effect. Moreover, unwanted side effects at potential off-target sites could be brought to light and prevented by obtaining an enhanced understanding of the distribution. For retaining drugs at the site of injection, hydrogels are considered good candidates as biocompatible, easily injectable carrier systems for cardiac repair and regeneration⁵. Previously, it was shown that the release of miR-302 from a hyaluronic-based hydrogel promoted cardiomyocyte proliferation and regeneration after myocardial infarction (MI) in a porcine heart⁶. Furthermore, injection of a hydrogel based on decellularized extracellular matrix (ECM) in a rat MI model reduced cardiomyocyte apoptosis and neovascularization⁷. Moreover, efficacy was established in a por-

cine infarction model⁸ and currently, this decellularized ECM-based gel is in its first human-trial to examine the safety and feasibility post MI⁹. Delivery of these hydrogels is primarily performed via a minimally invasive catheter-based injection technique, where gelation occurs at the target site triggered by temperature increase¹⁰. While studying the beneficial effect of hydrogel-mediated delivery of therapeutic factors, primarily indirect parameters and the functional effect of the drugs (e.g. scar thickness, ejection fraction, and end-diastolic volume) were examined^{11–13}. Only a few studies examined the degree of hydrogel retention after injection and the potential off-target distribution of the gel, mainly in small animal models^{14–16}. A collagen matrix delivery in a mouse model with MI was assessed on its retention and distribution by PET imaging, where the hydrogel was labelled with hexadecyl-4-[(18)F] fluorobenzoate ((18)F-HFB)¹⁷. A more recent study showed *in vivo* nuclear imaging of an alginate hydrogel in which the nuclear imaging radio-metal indium-111 (¹¹¹In) was incorporated¹⁶. Intramyocardial injection in mice was performed, where a low retention was observed after one week (2-4%). To our knowledge, no study has provided quantitative numbers on the amount of cardiac retention and distribution of a supramolecular hydrogel in a large animal model.

Here, we show a first approach in performing a quantitative retention study by implementation of a radioactive tracer in our injectable pH- and temperature-responsive supramolecular poly(ethylene glycol) (PEG) hydrogel functionalized at each end with ureido-pyrimidinone (UPy) units (**Figure 1A**)¹⁸. This UPy-PEG hydrogelator is an injectable viscous liquid at a pH > 8.5 and rapidly forms a hydrogel once exposed to physiological pH¹⁹. To increase tissue adhesiveness, a UPy-functionalized recombinant peptide based on human collagen type 1 is introduced to the hydrogel (RCPHC1, **Figure 1B**), enriched with repeating amino acid sequences based on the integrin-binding peptide RGD. Supramolecular labelling of the hydrogel is performed using monofunctional UPy-labels, either for radioactive or for fluorescent

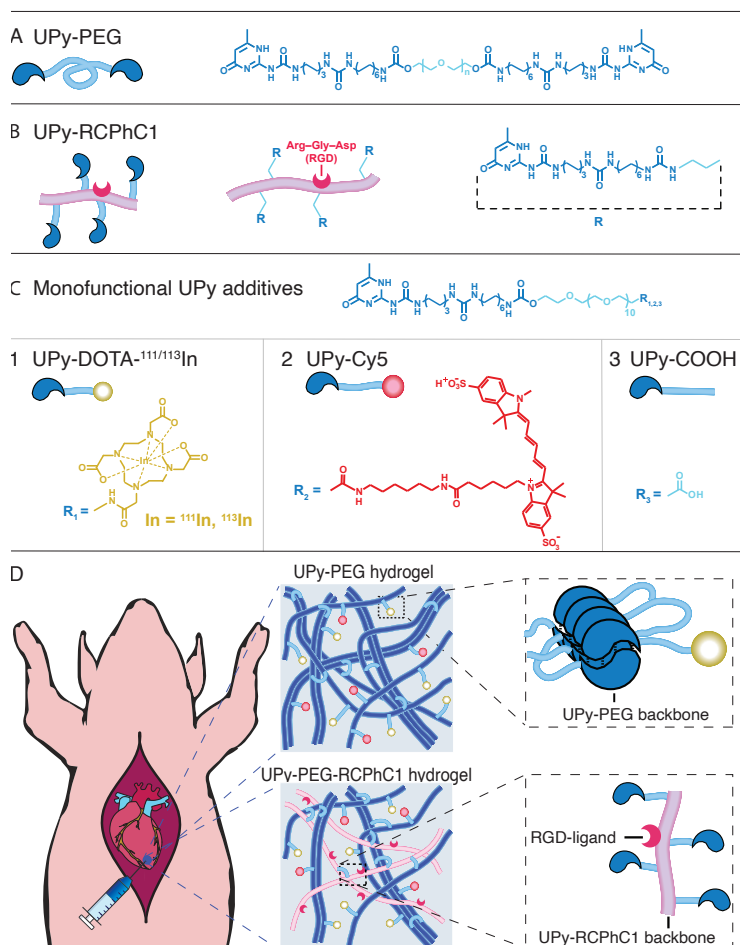


Figure 1. Hydrogel formulation and study overview

A, B. The chemical structure and schematic overview of hydrogelators UPy-PEG (**A**) and UPy-PEG-RCPhC1 (**B**). **C.** The monofunctional UPy-additives used during this study with the (non-)radioactive label UPy-111/113In (**1**), the fluorescently-labelled UPy-Cy5 (**2**), and the non-fluorescent label mimic UPy-COOH (**3**). **D.** The epicardial hydrogel injection in a porcine model, and the concept of the two different hydrogels used in this study, UPy-PEG and UPy-PEG-RCPhC1.

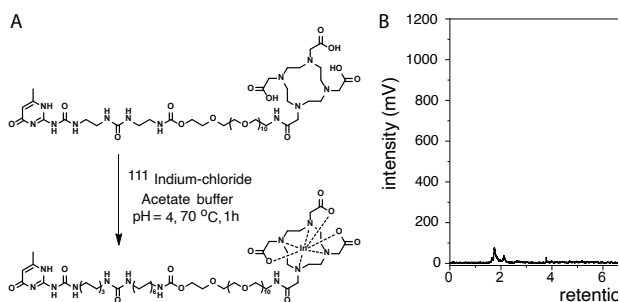


Figure 2. Chelation of the ^{111}In with the UPy-DOTA label, with the labelling method (A), and radio-HPLC after chelation of UPy-DOTA- ^{111}In at basic pH (>9) (B), with loose ^{111}In at a retention time of 1.8–2.2 minutes and labelled UPy-DOTA- ^{111}In at 9.2–9.7 minutes, showing a chelation efficiency of 97%.

visualization. The hydrogel is radioactively labelled using a 1,4,7,10-tetraazacyclododecanetetraacetic acid (DOTA) chelated with radioactive isotope ^{111}In , covalently bound to a monofunctional UPy-moiety, allowing for *in vivo* radioactive detection. In addition, a fluorescent UPy-Cy5 label was synthesized and used for *ex vivo* histological fluorescence analysis (Figure 1C). Comparative visualisation and quantification of hydrogel retention and distribution was performed for epicardial injections of UPy-PEG and UPy-PEG-RCPhC1 hydrogels in a porcine model (Figure 1D).

RESULTS AND DISCUSSION

Molecules

The UPy-DOTA was chelated with the radioactive ^{111}In label (Figure 2A). Instant-thin layer chromatography (iTLC) (Supplemental Figure 1) as well as a separation and detection of radioactive compound by high-performance liquid chromatography (radio-HPLC) (Figure 2B) showed an optimal chelation after approximately 1 hour (with a varying range of 93-98%). The chelation remained stable at basic pH (Figure 2B) for approximately 24 hours. As a reference, a non-radioactive isotope indium-113 (^{113}In) was chelated to the UPy-DOTA moiety (UPy-DOTA- ^{113}In) for *in vitro* measurements. A monofunctional UPy-moiety functionalized with the fluorescent probe cyanine-5-amine (UPy-Cy5), allowed histological staining after injection, where an

unfunctionalized monofunctional UPy-moiety (UPy-COOH) was used as a non-fluorescent reference. To introduce bioactivity and potential adhesion to the cardiac tissue UPy-RCPHC1 was added synthesized by modification of pristine RCPHC1 with UPy-units. ¹H-NMR spectroscopy showed an average number of six UPy-moieties grafted on the RCPHC1 backbone (**Supplemental Figure 3**).

Hydrogel Preparation

The hydrogels were prepared in a simple mix-and-match manner, where the hydrogel precursors were dissolved at high pH PBS (either UPy-PEG, or UPy-PEG in combination with UPy-RCPHC1). Additives were introduced after the hydrogel precursors were fully dissolved. The molar ratio of the UPy-PEG hydrogel for UPy-PEG: UPy-DOTA: UPy-Cy5 or UPy-COOH was set at 10:0.35:0.01. The additive ratio for UPy-PEG-RCPHC1 was identical, containing a 9:1 ratio of UPy-PEG and UPy-RCPHC1. The pH of the hydrogel precursor was adjusted to 9 or 8.8±0.1 for UPy-PEG and UPy-PEG-RCPHC1, respectively. The UPy-PEG-RCPHC1 hydrogelator shows similar viscosities at pH 8.8 to the UPy-PEG hydrogelator at pH 9 (**Supplemental Figure 5**), which was desired to keep the flow properties similar.

Mechanical Properties of the Hydrogels

The myocardium shows viscoelastic characteristics, which is due to a combination of cardiac cells and ECM proteins. During heart failure, collagen accumulation can affect the viscoelasticity of the myocardium significantly²⁰. A hydrogel showing viscoelastic properties and accommodating the pulsating behaviour of the heart is desired. To examine the mechanical properties of the hydrogels used in this study, UPy-DOTA was chelated in acetate buffer with non-radioactive isotope ¹¹³In, where an optimal chelation efficiency was confirmed by RP LC-MS (>95%, **Supplemental Figure 2**). A previous study reported that the release of a UPy-DOTA label complexed with Gadolinium(III) from the UPy-PEG hydrogel is in line with the rate of

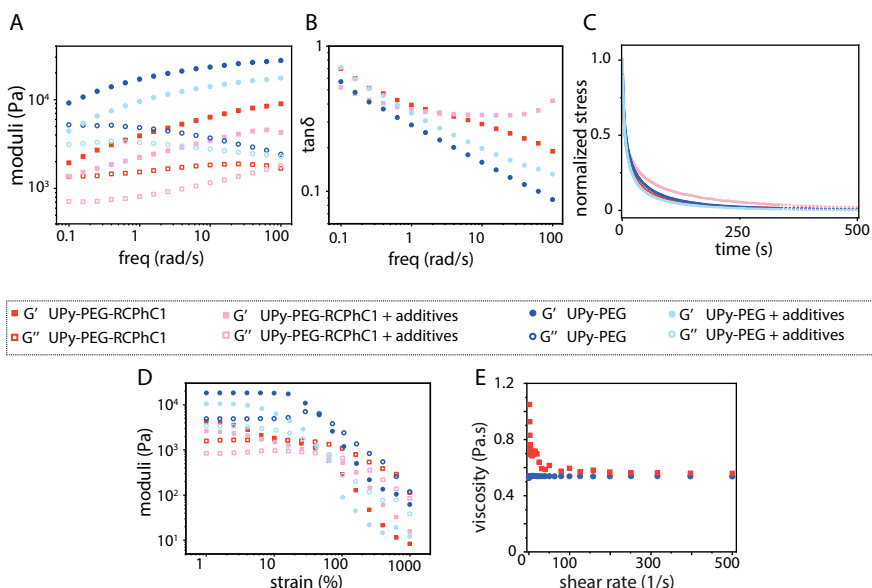


Figure 3. The mechanical properties of the hydrogels

Showing the frequency sweep (**A**) and the corresponding $\tan \delta$ (**B**) at 1% strain with frequencies between 0.1 and 100 $\text{rad}\cdot\text{s}^{-1}$ (**A**), the stress-relaxation at 1% strain, measured over a time span of 500 seconds (**C**), and the strain-sweep at 1 $\text{rad}\cdot\text{s}^{-1}$ with strains varying from 1 to 1000% (**D**), showing viscoelastic properties of the UPy-PEG, and the UPy-RCPHC1 hydrogel, measured at 37 °C.

erosion of the hydrogel itself²¹. Rheology was used to examine the influence of the additives (UPy-DOTA-¹¹³In and UPy-COOH; **Figure 1C.3**) on the mechanical properties of the hydrogels. After pH neutralization, the UPy-PEG as well as the UPy-PEG-RCPHC1 hydrogels show frequency-dependent viscoelastic behaviour, i.e. an increase of G' while frequency was increased, while G'' remains stable or decreases (**Figure 3A**). This behaviour is reflected in the $\tan \delta$ (G''/G') (**Figure 3B**), that showed a decrease for both hydrogels by a factor of 7, 5.3, 3.8, and 1.2 over the tested frequency range for the UPy-PEG, UPy-PEG with additives, UPy-PEG-RCPHC1, and UPy-PEG-RCPHC1 with additives, respectively. This indicates that the solid properties are getting more distinctive as the frequency is increased, whereas at lower frequencies more liquid-like properties are observed. This suggests that at lower frequencies (longer measuring time) there is more time for structural rearrangement, i. e. characteristic interactions in the material can relax and the material

starts to flow. At high frequencies (shorter measuring time) there is less time for re-arrangement, i. e. all interactions remain present in the structure and have no time to relax, therefore displaying a less dynamic and more solid structure. For the UPy-PEG hydrogel, the additives resulted in a weaker gel, at lower frequencies (with a G' of 9.1 kPa vs. 4.4 kPa at 0.1 rad.s⁻¹, respectively), as well as higher frequencies (with a G' of 27 kPa vs. 17 kPa at 100 rad.s⁻¹, respectively, **Figure 3A**, blue).

In a previous study, addition of monofunctional UPy-molecules to the bifunctional UPy-PEG molecule showed to decrease the dynamics of the network, influencing the stiffness of this mixture²². Addition of UPy-DOTA and UPy-COOH showed to decrease the stiffness, where the latter is added from a stock solution in DMSO, which caused a decrease in stiffness of the hydrogel. However, addition of the monofunctional UPy-molecules increase the stiffness of the hydrogel as shown in previous studies, in comparison to solely DMSO addition to the hydrogel (**Supplemental figure 6**). Both UPy-PEG hydrogels showed similar frequency dependent behaviour, with increased stiffness at higher frequencies, and the same viscoelastic properties. A significant decrease in moduli is observed for the UPy-PEG-RCPHC1 hydrogel, where the UPy-PEG hydrogel showed to be a stiffer gel (2-3 times stiffer in comparison to the UPy-PEG hydrogel). This could be explained by the lower number of UPy-moieties in this hydrogel, lowering the supramolecular cross-linking ability and therefore the stiffness of the hydrogel. Comparison of UPy-PEG-RCPHC1 with and without additives showed small differences in moduli (**Figure 3A**, red). The hydrogel with additives displayed lower storage modulus (with a G' of 1.9 kPa vs. 1.3 kPa at 0.1 rad.s⁻¹) and loss modulus (with a G'' of 1.4 kPa vs. 0.7 kPa at 0.1 rad.s⁻¹), indicating that the additives have an influence on the mechanical properties of the hydrogels. However, similar to the UPy-PEG hydrogel, the frequency dependent viscoelastic behaviour of both hydrogels is comparable. The stress-relaxation measurements show similar relaxation curves for the UPy-PEG hydrogel with and without additives,

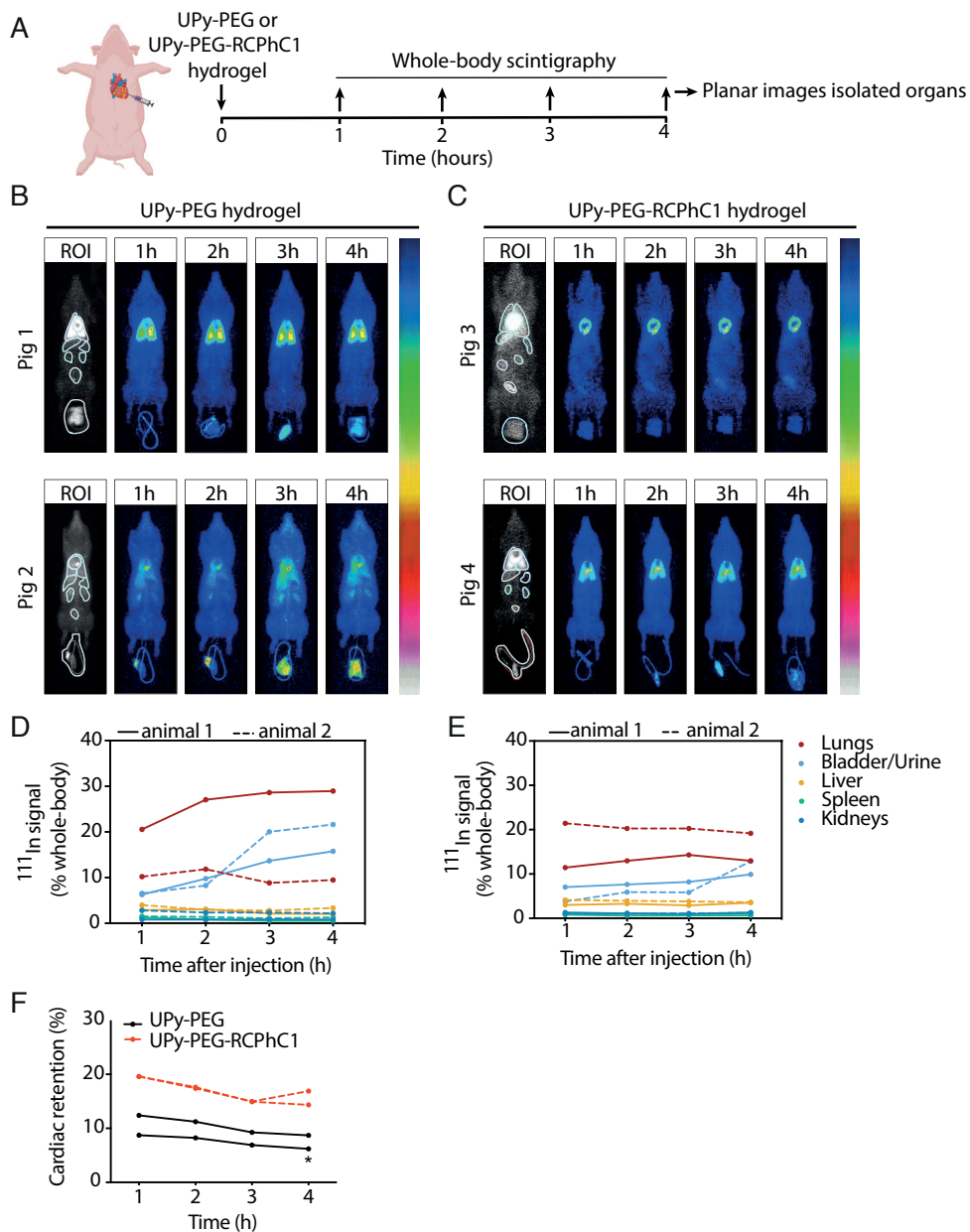


Figure 4. Scintigraphy imaging shows biodistribution of supramolecular hydrogels after epicardial injection

A. Experimental protocol. **B, C.** Whole-body scintigraphy scans 1 to 4 hours after injection of UPy-PEG (**B**) or UPy-PEG-RCPHC1 (**C**) hydrogel. Areas with high radioactive signal are identified by bright red colouration and areas with low radioactivity are identified by blue colouration. **D, E.** Quantification of distribution in indicated remote organs after epicardial injection of UPy-PEG (**D**) or UPy-PEG-RCPHC1 (**E**) hydrogel. **F.** Quantification of cardiac retention. Data are individual animals ($n=2$ per hydrogel). Differences were evaluated using paired Students-t-test. *represents $P<0.05$.

where 50% relaxation was achieved at 6.2 vs. 8 seconds, respectively (**Figure 3C**, blue). For the UPy-PEG-RCPHC1 hydrogels with and without additives, only small differences can be observed, with a time of 6.8 vs. 6.2 seconds at a 50% relaxation, respectively (**Figure 3C**, red). This indicates a minimum to no difference that is observed considering relaxation times. The UPy-PEG hydrogel without additives shows a linear course for storage as well as loss moduli until a minimum of 25% deformation, whereas the UPy-PEG hydrogel with additives shows a slight decrease in G' and G'' after a strain of approximately 5%, whilst still retaining its hydrogel properties. The hydrogels with and without additives are disrupted at 45 and 65% strain, respectively (**Figure 3D**, blue). A similar trend as the UPy-PEG with additives is observed for the UPy-PEG-RCPHC1 hydrogels with and without additives, where a small decrease in G' and G'' is observed after a strain of 6%. Here, disruption of the hydrogels with and without additives occur at approximately 25 and 40% strain, respectively (**Figure 3D**, red). UPy-PEG-RCPHC1 hydrogels with and without additives showed small variability regarding the strain and frequency sweep, where differences in stiffness were observed (**Supplemental figure 7**). This marks the variability of the UPy-functionalized RCPHC1, introduced to the system. Overall, minor differences in mechanical properties of hydrogel variants were observed between absolute moduli and stiffness of the hydrogels, which should not affect usability in envisioned applications.

In vivo injection in pig heart and scintigraphy

For the porcine experiments, one day prior to *in vivo* injection the additives (UPy-DOTA- ^{111}In and UPy-Cy5) were added to the dissolved hydrogel precursors. Per injection of 200 μL the obtained activity was 5–10 MBq. Detailed hydrogel formation can be found in the experimental section. Hydrogels (UPy-PEG or UPy-PEG-RCPHC1) were injected epicardially (6 x 200 μL) after thoracotomy into the left ventricular wall of beating porcine hearts (n=2). Scintigraphic total body scans

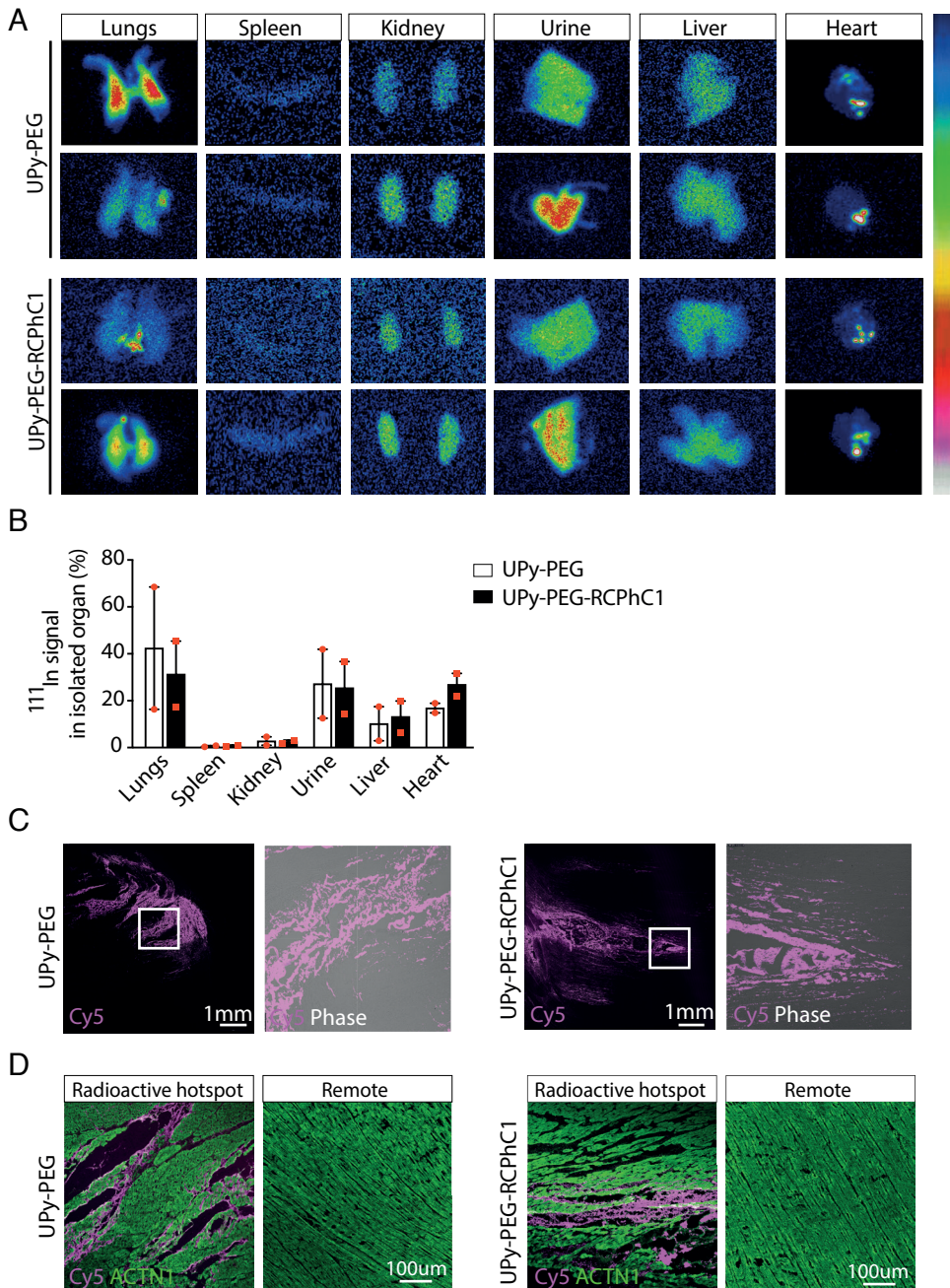


Figure 5. Scanning of isolated organs shows organ distribution of supramolecular hydrogels

A, B. Scintigraphic scans of individually isolated organs 4 hours after epicardial injection of supramolecular hydrogels (**A**) and quantification of radioactive signal as a percentage of total signal in the isolated main organs (**B**). Areas with high radioactive signal are identified by bright red colouration and areas with low radioactivity are identified by blue colouration **C.** Histology representative images of hydrogels

Figure 5 continued

by supramolecular bound fluorescent signal UPy-Cy5 in the radioactive high intensity regions of the heart.

D. Immunofluorescent staining of myocardium in radioactive hotspots and remote of radioactive hotspot. ACTN1, cardiac alpha actinin. Data is based on individual animals (n=2 per hydrogel). Differences were evaluated using a paired Students t-test.

were performed 1, 2, 3 and 4 hours after injections and biodistribution of the hydrogel was quantified as percentage of radioactive signal in each organ from total whole body radioactive signal to exclude remaining radioactive signal in the dead volume of the syringes. Areas with high radioactive signal are identified by bright red coloration and areas with low radioactivity are identified by blue coloration. The total body scans showed that the injections of the UPy-PEG led to a cardiac retention of 6.2% and 8.7% after 4 hours (**Figures 4B, F**). The remaining gel distributed to the lungs (29% and 9.5%), bladder and urine (15.8% and 21.6%), liver (2.0 and 3.4%), kidneys (0.8% and 2.2%), and spleen (0.56 and 1.28%) (**Figure 4D**). The residual activity was distributed evenly across the body without the presence of an increased and localized radioactive signal (“hotspots”). Injection of UPy-PEG-RCPHC1 showed a cardiac retention of 16.9% and 14.3% after 4 hours (**Figure 4C, F**). The remaining activity was distributed to the lungs (13.0% and 19.2%), bladder and urine (9.9% and 12.9%), liver (3.5% and 3.6%), kidneys (1.3% and 1.2%), and spleen (1.2% and 0.66%) (**Figure 4C, E**). Also, for the UPy-PEG-RCPHC1 the residual activity did not lead to hotspots. When comparing the cardiac retention of the two hydrogels at the 4 time points after injection, UPy-PEG-RCPHC1 injection showed increased retention ($P < 0.05$, $n = 4$). The ^{111}In signal in the lungs stabilized between 2 and 3 hours after injection of the UPy-PEG hydrogel in both pigs while the ^{111}In signal in the bladder and urine increased till 4 hours after injection indicating secretion (**Figure 4D**). The UPy-PEG-RCPHC1-hydrogel showed no increased in off-target distribution after 1 hour post-injection except for the ^{111}In signal in the bladder and urine (**Figure 4E**).

When comparing the off-target biodistribution at the 4 time points after injection, no significant difference was found between the two hydrogels for lung biodistribution ($P > 0.05$, $\alpha = 0.19$, $n = 2$) or bladder/urine biodistribution ($P > 0.05$, $\alpha = 0.09$, $n = 2$). During scintigraphic whole body scans, the measurement of radioactive signal from organs can be influenced by degree of tissue penetration and scattering, and by signals from overlapping organs. Therefore, 4 hours after injection, organs were isolated and scanned individually. Scanning of the explanted, isolated organs (heart, lungs, bladder/urine, liver, kidneys, spleen) indicated the retained radioactive signal in the heart was 14.8% and 18.9% for UPy-PEG and 22.1% and 31.7% for UPy-PEG-RCPHC1 as a percentage of the total combined signal in the isolated organs (**Figure 5A, B**). Furthermore, scintigraphy showed localised UPy-PEG-RCPHC1 at the individual injection sites with five to six radioactive hotspots (**Figure 5A**), corresponding to the individual injection sites. The UPy-PEG injected pig hearts showed three to four more diffuse and merged injection sites. One UPy-PEG injected heart showed increased radioactive signal at the base of the heart remote from the injection area (**Figure 5A**). To verify presence of the gel at the sites with high radioactive signal in the heart, histological analysis was performed. The heart was sliced into five slices from apex to base and individual slices were scanned to identify sites of high ^{111}In signal using a 1 MBq point source (**Supplemental Figure 10**). These revealed intense Cy5 signal in sections of tissue with high radioactivity signal, showing deposits of seemingly condensed gel in larger interstitial spaces and strings of gel in the smaller interstitial spaces between individual cardiomyocytes (**Figure 5C**). This was further confirmed by immunofluorescent staining for cardiac alpha actinin (**Figure 5D**). During the washing steps of the staining procedure, the gel in the larger interstitial space dissolved, while the gel surrounding the cardiomyocytes was retained. At the areas remote from the radioactive high intensity regions, no Cy5 signal was found (**Figure 5D**). This pattern of distribution of the gel within the myocardium is hypothesized to be due to the flexibility of the gel to distribute and adhere to the myocardium and the

extracellular matrix. It is important to note only a small sample size of merely two animals per group was used to analyze *in vivo* hydrogel biodistribution. Therefore, no significant conclusions can be drawn on the difference between the two hydrogels in the *in vivo* experiments. However, the current study does give insights into the potential use of ^{111}In labeling of injectable hydrogels for *in vivo* hydrogel retention quantification and comparison of retention and off-target distribution of multiple hydrogels. When comparing the cardiac retention of UPy-PEG and UPy-PEG-RCPHC1 in the four pigs we see a trend towards increased retention in the pigs injected with UPy-PEG-RCPHC1. This increase is likely to be caused by an increase in the adhesion of the gel to the extracellular matrix at the site of injection due to the integrin-based recombinant peptide RCPHC1. Earlier studies using biomaterials to augment factor delivery, focused on the retention of delivered cells or compounds^{12,18} or effects on functional parameters, rather than retention of the biomaterial^{23,24}. Even though these studies gave insight into the potential benefits of hydrogel mediated delivery, so far, no knowledge has been generated on the biodistribution of hydrogels in a large animal model after injection or quantitative approaches to determine the degree of retained hydrogel at the site of injection. In addition, this shows a trend towards decreased off-target distribution (lungs, bladder) and less diffuse distribution of UPy-PEG-RCPHC1 compared to UPy-PEG hydrogel at the cardiac injection sites. However, we still report relatively high values of ^{111}In signal in the lungs compared to other organs and intracardiac retention. When comparing our reported values of lung biodistribution to previous studies of labelled cells, we see that, of the small number of studies that report biodistribution after injection, similarly high levels of off-target biodistribution to the lungs were reported. In previous studies in rats. the majority of injected cells were engrafted in the lungs 48 hours after injection and cardiac retention values were reported below 1%^{25,26}. Furthermore, a previous study in pigs showed labelled cell off-target localization in the lungs of 26-47% with cardiac retention between 3 and 11% of the injected dose²⁷. Injection of an alginate hydrogel

cross-linked with radio-metal ^{111}In showed a retention in the heart of 2-4%, one week post-injection¹⁶. As a highly vascularized organ, it is likely this accumulation of ^{111}In signal reflects dissolved UPy-polymers that enter the lungs via the coronary veins or the central circulation. Previously, we have shown that the UPy-polymers do not affect biocompatibility or induce toxicity¹⁶. Further investigation into the effect of pulmonary biodistribution of intracardiac injected hydrogels is needed. The distribution of the hydrogels to the lungs did not increase within 4 hours after injection, considering the UPy-PEG-RCPhC1 hydrogel. The remaining off-target distribution of the hydrogels to the bladder indicated clearance of the hydrogel through the secretory tract which limits the risk of extracardiac accumulation. As the main cause of limited cardiac retention has been suggested to be the immediate clearing via the dense venous microvasculature and the needle track², we tracked the hydrogel biodistribution up to 4 hours after injection. The limited changes within the presence of ^{111}In signal in all organs within these 4 hours is in line with previous studies on the importance to improve acute cardiac retention rather than chronic engraftment^{27,28}.

Even though the UPy-based hydrogel gels in physiological pH of the myocardium and shows increased retention compared to previously reported values, the presence of strong cardiac contractions and the needle track remains a challenge to maintain maximal cardiac retention of hydrogels. The achieved cardiac retention of ~30% of UPy-PEG-RCPhC1 hydrogel is likely to increase effectiveness of regenerative therapies compared to non-hydrogel mediated delivery. With the method described, we were able to quantitatively compare the retention of two supramolecular hydrogels and show these hydrogels appear to be safe on short term follow-up of 4 hours.

CONCLUSION

Quantitative imaging and distribution tracking after intramyocardial injection in a large animal model was achieved via modification of a pH-switchable

supramolecular hydrogel. In a simple mix-and-match manner, two types of hydrogels were radioactively labelled in a modular approach, with limited influence on the gelation properties. This ensured radioactive imaging of the hydrogels in a porcine heart *in vivo* to quantify and compare the retention of these supramolecular hydrogels. Introduction of RCPHC1 to the hydrogel implied to increase hydrogel retention in the heart with defined deposits of hydrogel at the injection sites still visible after 4 hours. Furthermore, the distribution of the hydrogels to other organs was reduced by addition of integrin-based recombinant peptide RCPHC1.

Finally, our method allows for dose quantification, increasing understanding of dose optimization and therefore drug effectiveness, which is of great importance in the translation towards cardiac regenerative therapy. Additionally, this method enables direct visualization of potential off-target localization which can be used for efficient risk-analysis of new therapies.

EXPERIMENTAL SECTION

Materials. All starting materials and reagents were obtained from commercial sources and used as received, unless stated otherwise. Solvents from Sigma Aldrich were of p.a. quality. Deuterated chloroform and deuterium oxide were purchased at Cambridge Isotope Laboratories. Sulfo-Cyanine5 amine was purchased at Lumiprobe. FujiFilm Manufacturing Europe B.V. kindly provided us the Cellnest, a recombinant peptide based on human collagen type I (RCPHC1), which was used without further purification.

Instrumentation. ¹H-NMR spectra were recorded on a 400 MHz NMR operating at 400 MHz for functionalization analysis. Reverse-phase high-performance liquid chromatography-mass spectrometry (RP-HPLC-MS) was performed on a Thermo scientific LCQ fleet spectrometer. The purity of UPy-RCPHC1hC1 was determined

with Waters Xevo G2 Quadrupole Time-of-Flight liquid chromatography–mass spectrometry equipped with an Agilent Polaris C18A reverse-phase column (ID 2.0 mm, length 100 mm). Derivatives were dissolved in H₂O (1 mg.mL⁻¹) and flowed (0.3 mL.min⁻¹) over the column using a 15–75% water/acetonitrile gradient with 0.1% formic acid prior to analysis in the positive mode in the mass spectrometer. Purification of UPy-Cy5 was performed on a prep-RP-HPLC (using gradients of acetonitrile in water, with addition of 0.1 vol% trifluoroacetic acid), where collected fractions were freeze-dried and analyzed by RP-HPLC-MS. Chelation efficiency was analyzed with two methods: instant thin layer chromatography with a glass microfiber chromatography paper impregnated with a silica gel stationary phase (Agilent Technologies) and sodium chloride 0.9% as a mobile phase, and high performance liquid chromatography (Thermo Scientific Dionex UltiMate 3000), both with NaI(Tl) detector for gamma rays (Canberra). A relatively geometry independent dose calibrator (VDC-404, Veenstra Instruments, the Netherlands) was used to quantify the activity pre-injection.

Synthesis of UPy-DOTA. The precursors UPy-C6-U-C12-C-OEG12-NH₂ and N-hydroxysuccinimide activated DOTA (DOTA-NHS-xTFA) were synthesized as described elsewhere²⁹. UPy-C6-U-C12-C-OEG12-NH₂ (280 mg, 0.26 mmol) was dissolved in dimethylformamide (DMF, 5 mL) and DOTA-NHS-xTFA (383 mg, 0.53 mmol) and DiPEA (0.62 mL, 3.57 mmol) were added. The reaction mixture was stirred overnight and subsequently the solvent was removed under vacuum and twice co-evaporated with toluene. Eluting over reversed phase C18 column with a gradient ACN/water of 5/95 to 80/20 afforded the intermediate UPy-DOTA (360 mg, 94%) as a white powder after freeze-drying.

¹H NMR (400 MHz, CDCl₃/CD₃OD) δ 5.86 (s, 1H), 4.19 (t, J = 4.7 Hz, 2H), 3.65 (s, 44H), 3.53 (dt, J = 13.3, 6.0 Hz, 7H), 3.43–3.18 (m, 14H), 3.11 (q, J = 7.0 Hz, 13H), 2.25 (s, 3H), 1.58 (p, J = 6.8 Hz, 2H), 1.48 (p, J = 7.2 Hz, 6H), 1.37 (q, J = 5.9,

3.7 Hz, 4H), 1.34–1.17 (m, 16H) ppm. ¹³C NMR (101 MHz, D₂O-NaOD) δ 179.94, 179.72, 175.39, 173.12, 168.35, 162.77, 159.58, 157.85, 157.34, 156.42, 104.28, 71.99, 69.80, 69.52, 69.32, 68.98, 68.83, 63.74, 58.71, 58.37, 57.16, 50.45, 40.62, 39.78, 39.25, 38.69, 30.21, 30.06, 29.66, 29.48, 29.39, 29.17, 26.89, 26.72, 26.42, 22.64 ppm.

LC-MS (ESI) Rt = 5.75 min, m/z calc for C₆₆H₁₂₂N₁₂O₂₃, 1451.8 Da; found 484.83 [M+3H]³⁺, 726.6 [M+2H]²⁺, 737.5 [M+Na+H]²⁺, 1452.4 [M+H]⁺, 1473.9 [M+Na]⁺.

Synthesis of UPy-Cy5. The synthesis of the UPy-COOH has been described previously²⁹, UPy-COOH (2.36 mg, 2.08 μmol) was dissolved in DMF (2 mL). N,N-Diisopropylethylamine (2.15 mg, 16.6 μmol) was added and the solution was stirred at room temperature for 15 min. Sulfo-Cy5-NH₂ (2 mg, 27.0 μmol) dissolved in DMF (3 mL) was added to the solution and stirred for 1 hour at argon environment. H₂O (containing 0.1 v/v% formic acid, 20 mL) was added to the solution and centrifuged (4 min, 3000 rpm) followed by decantation. Ultrapure water was added (20 mL) and the product was lyophilized. The compound was purified with preparative RP-HPLC using a gradient of 40% ACN in H₂O (both containing 0.1 v/v% formic acid). Lyophilization yielded pure UPy-Cy5 (1.75 mg, 9.4 μmol, 45%) as a blue solid. This was dissolved in DMSO at 1 mg.mL⁻¹ and used from this stock solution. ESI-MS: m/z Calc. for C₉₁H₁₄₉N₁₁O₂₅S₂ 1861.37; Obs. [M+3H]³⁺ 621.33, [M+2H]²⁺ 931.17, [M+H]⁺ 1861.75.

Synthesis of hydrogelators UPy-PEG and UPy-RCPHC1. The hydrogelator UPy-PEG with mn, PEG = 10 kg.mol⁻¹, was synthesized by SyMO-Chem BV, Eindhoven, The Netherlands¹⁹. Briefly, the PEG was added to 1,1'-carbonyldiimidazole (CDI) in dichloromethane, after which excess of CDI was removed by precipitation in diethyl ether. This was coupled to 1,10-diaminododecane, followed by precipitation in diethyl ether. Solid UPy-isocyanate was added to a solution of diamine terminated-PEG in a mixture of 1:1 dichloromethane and chloroform. The UPy-RCPHC1 was

synthesized in a similar manner as previously described³⁰. In short, UPy-hexyl-urea-dodecyl-amine was dissolved in DMSO and N,N-diisopropylethylamine was added, whereafter CDI was added. The CDI functionalization was confirmed by RP-HPLC-MS, after which the solution was added to RCPHC1 dissolved in DMSO and left stirring overnight at argon environment.

Preparation of radioactively labelled hydrogel precursor. Two days prior to *in vivo* injection 20 wt% hydrogel precursors were prepared by dissolving UPy-PEG (36 μ mol, 400 mg), or UPy-RCPHC1 (2.53 μ mol, 140 mg) and UPy-PEG (23.2 μ mol, 260 mg) in 1.6 mL basic PBS (pH 11.7, adjusted with 1M NaOH) at 70 °C until fully dissolved after approximately 1h. After dissolving, the pH was adjusted to 9 and stored in the fridge until the following day. The following day, UPy-DOTA compound (1.7 μ mol, 2.5 mg) was dissolved at 2 mg.mL⁻¹ in acetate buffer (pH 4 – 5) at 50 °C for 30 min. The radioactive isotope indium-111-chloride (107 MBq, Curium, Petten, the Netherlands) was added to the UPy-DOTA dissolved in acetate buffer. This was kept at 70 °C for 1h, after which the chelation efficiency was examined. The chelation efficiency varied from 97 – 99%, determined by radio-HPLC and iTLC. After chelation, the pH was adjusted to 9 using a 5M, 1M NaOH solution. This was then added to the hydrogel precursor solutions, where fluorescently labelled UPy-Cy5 (25 nmol, 47 μ g) from a DMSO stock solution (1 mg.mL⁻¹) was added. The weight percentage was adjusted to 10wt% using basic PBS (pH 9). This was stored overnight in the fridge in the dark until injection the following morning. After loading of the six syringes (approximately 200 μ L each), the exact activity per syringe was quantified using the dose calibrator.

Preparation of non-radioactively labelled hydrogel. One day prior to measuring, the hydrogel precursor solutions were prepared by dissolving UPy-PEG (40 mg, 3.6 μ mol), or (14 mg, 0.25 μ mol) and UPy-PEG (26 mg, 2.3 μ mol) at 20 wt% in basic PBS (pH 11.7) at 70 °C until fully dissolved after approximately 1h. UPy-DOTA

compound (0.25 mg, 0.17 μmol) was dissolved in acetate buffer (2 mg.mL⁻¹, pH 4 – 5) at 50 °C for 30 min, after which indium-113-chloride (37.3 μg , 0.17 μmol) was added to the acetate buffer and kept at 70 °C for 1h. The chelation was confirmed by reversed-column LC-MS. After chelation, the pH was adjusted to 9 using 5M NaOH and 1M NaOH solutions. This was added to the hydrogel precursor solution, where UPy-COOH (4.7 μg , 2.5 nmol), the non-fluorescent reference of UPy-Cy5, was added from a DMSO stock solution (1 mg.mL⁻¹). The hydrogel precursor solution was adjusted to pH 9, at a final weight percentage of 11wt%. As control, UPy-PEG (40 mg, 3.6 μmol), or (14 mg, 0.25 μmol) and UPy-PEG (26 mg, 2.3 μmol) were dissolved in basic PBS (pH 11.7) at 70 °C until fully dissolved. The pH was adjusted to 9, and the final weight percentage was 11wt%. This was stored in the fridge until used the following morning. For the rheological measurements, the hydrogel disks were made in cylindrical Teflon molds (diameter of 8 mm, height of 2 mm). Precursor gels (100 μL , pH 9) were pipetted in the molds, where 10 μL of acidic PBS (10 μL , 13 mM HCl) was added, resulting in a final weight percentage of 10wt%. This was left to equilibrate for approximately 1.5h before measuring.

Rheological measurements. Rheological characterization of the hydrogels was performed on a discovery hybrid rheometer (DHR-3, TA Instruments), using a flat stainless-steel geometry with a diameter of 8 mm, with gap heights varying from 500 - 1000 μm . Low viscosity silicon oil (47 V 100, RHODORSIL®) was used around the hydrogel to limit evaporation during measurements at 37 °C. Frequency sweep measurements were performed at $\omega = 0.1 \text{ rad.s}^{-1}$ to 100 rad.s^{-1} , at a strain of $\gamma = 1\%$. Stress-relaxation was performed at a strain of $\gamma = 1\%$, over a time span of 500s, where the first 1s of measurement time was disregarded. This data was normalized using the highest stress generated from this point onwards. Strain-sweep measurements were performed at strains between $\gamma = 1$ and $\gamma = 1000\%$, with a frequency of $\omega = 1 \text{ rad.s}^{-1}$. Time sweeps of 60 s were performed in between measurements (data not shown), with a strain of $\gamma = 1\%$ and a frequency of $\omega = 1$

rad.s-1.

Animals and surgical procedure. Four Topigs Norsvin pigs (age ~six months, weight 60-65 kg) received care in accordance with the guide for the care and use of laboratory pigs prepared by the Institute of Laboratory Animals. Experiments were approved by the Animal Experimentation Committee of the Medicine Faculty of the Utrecht University, the Netherlands. Sedation was mediated by intramuscular infusion of ketamine (10 mg.kg⁻¹), midazolam (0.4 mg.kg⁻¹), atropine (0.05 mg.kg⁻¹), and intravenous injection of thiopental (4 mg.kg⁻¹) via the cannulated ear vein. General anaesthesia was maintained by continuous infusion of cist-atracurium (0.1 mg.kg⁻¹.hr⁻¹), midazolam (0.4 mg.kg⁻¹.hr⁻¹), and sufentanil (2.5 µg.kg⁻¹.hr⁻¹) via the cannulated ear vein. A thoracotomy was performed to gain access to the epicardium and the apex was loosely fixed with a Starfish Cardiac Positioner (Medtronic, Minneapolis, MN, USA). Six hydrogel injections, with a total volume of 1.2 mL, were performed through a 25-gauge needle. The thorax was closed prior to the first scintigraphic scan.

Short-term in vivo tracking and quantification. To detect the ¹¹¹In label serial anterior and posterior total body scans were performed with a full field of view gamma scintillation camera with a medium energy general purpose (MEGP) collimator (Philips Skylight Gamma Camera System Dual SPECT with Philips JETStream Workplace R3.0). Photopeak windows of 20% were set at 174-274 keV. With a scan speed of 10 cm.min⁻¹ total body scans were made with a matrix of 512x1024. For static scans of the isolated organs a scan time of 300 seconds per scan were used and a matrix of 256x256. The images were quantified by identifying the heart, lungs, liver, spleen, kidneys and bladder in the anterior and posterior cumulative 174 and 274 keV images as 2D regions of interest (ROI) and determining the total number of counts and pixels per ROI. The square root of the total number of counts from the ROI obtained from the anterior total body scan and the ROI obtained from the

posterior total body scan determined the geometric mean of the counts as described by Stratton et al.³¹. The geometric mean of the total body ROI was identified as the 100% value to determine the % uptake of the ¹¹¹In signal in each organ.

Histological analysis. For immunostaining, hearts were snap frozen and cut into 10 μ m sections. Fixation of the tissue was mediated by incubation in 100% acetone for 10 minutes at 4 °C for 10 minutes before permeabilization for 10 min in 1% Triton X-100 (Thermo Scientific) in PBS. Heart tissue was then blocked for 1 hour in 10% normal whole goat serum (Vector laboratories S-1000-20) in PBS. Sections were stained overnight at 4 °C with sarcomeric α -actinin (Sigma Aldrich A7811) after which 1 hour incubation with secondary antibody conjugated with Alexa Fluor 488 in combination with nuclear marker Hoechst (Life Technologies 33342) was performed. Sections were then mounted in Fluoromount-GTM (ThermoFischer Scientific 00-4958-02) before imaging with SP8x Leica confocal microscope.

Statistical analysis. The *in vivo* data were expressed as individual animals as the sample size was n=2 per group. Statistical analysis was performed per group in which the individual datapoints per scan were compared and evaluated with a paired Students t-test to compare the biodistribution values at the different time points post-injection per hydrogel. Data analysis was performed using GraphPad Prism version 8.0.0 for Mac OS X, GraphPad Software, San Diego, California USA, www.graphpad.com. P<0.05 was considered statistically significant.

SUPPLEMENTARY INFORMATION

Supplementary figures can be found at <https://doi.org/10.1002/adhm.202001987>

ACKNOWLEDGEMENTS

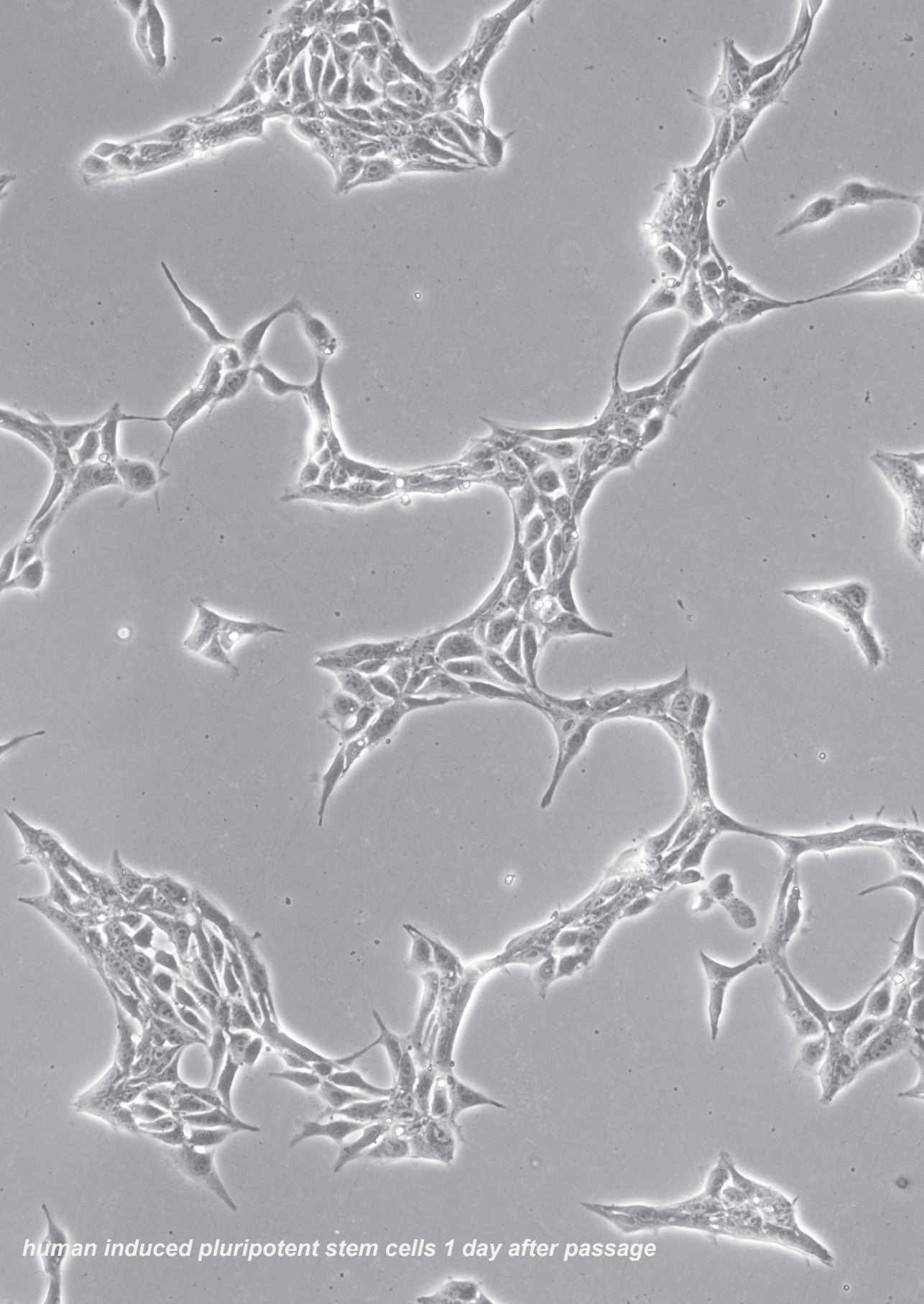
The authors would like to thank the following people for their technical assistance with the animal experiments: Marlijn Janssen, Joyce Visser, Martijn van Nieuwburg, Evelyn Velema, Ingrid Boots, Monique Jacobs, Anke Wassink, and Jeannette Wolfswinkel. The ICMS Animation Studio is acknowledged for the design of some of the cartoons. The Netherlands Cardiovascular Research Initiative: an initiative with support of the Dutch Heart Foundation, CVON2014-27 REMAIN, and the Ministry of Education, Culture and Science (Gravity Programs 024.001.035 and 024.003.013).

REFERENCES

1. Matsui Y. Role of matricellular proteins in cardiac tissue remodeling after myocardial infarction. *World J Biol Chem.* 2010;1(5):69.
2. Feyen DAM, Van Den Hoogen P, Van Laake LW, et al. Intramyocardial stem cell injection: Go(ne) with the flow. *Eur Heart J.* 2017;38(3):184-186.
3. Hasan A, Khattab A, Islam MA, et al. Injectable Hydrogels for Cardiac Tissue Repair after Myocardial Infarction. *Adv Sci.* 2015;2(11):1-18.
4. Stapleton LM, Steele AN, Wang H, et al. Use of a supramolecular polymeric hydrogel as an effective post-operative pericardial adhesion barrier. *Nat Biomed Eng.* 2019;3(8):611-620.
5. Li J, Mooney DJ. Designing hydrogels for controlled drug delivery. *Nat Rev Mater.* 2016;1(12).
6. Wang LL, Liu Y, Chung JJ, et al. Local and sustained miRNA delivery from an injectable hydrogel promotes cardiomyocyte proliferation and functional regeneration after ischemic injury. *Nat Biomed Eng.* 2018;1:983-992.
7. Wassenaar JW, Gaetani R, Garcia JJ, et al. Evidence for mechanisms underlying the functional benefits of a myocardial matrix hydrogel for post-MI treatment. *J Am Coll Cardiol.* 2016;67(9):1074-1086.
8. Seif-Naraghi SB, Singelyn JM, Salvatore MA, et al. Safety and efficacy of an injectable extracellular matrix hydrogel for treating myocardial infarction (Science Translational Medicine (2013) 5 (173ra25)). *Sci Transl Med.* 2014;6(233).

9. Traverse JH, Henry TD, Dib N, et al. First-in-Man Study of a Cardiac Extracellular Matrix Hydrogel in Early and Late Myocardial Infarction Patients. *JACC Basic to Transl Sci.* 2019;4(6):659-669.
10. Carlini AS, Gaetani R, Braden RL, Luo C, Christman KL, Gianneschi NC. Enzyme-responsive progelator cyclic peptides for minimally invasive delivery to the heart post-myocardial infarction. *Nat Commun.* 2019;10(1):1-14.
11. Dobner S, Bezuidenhout D, Govender P, Zilla P, Davies N. A Synthetic Non-degradable Polyethylene Glycol Hydrogel Retards Adverse Post-infarct Left Ventricular Remodeling. *J Card Fail.* 2009;15(7):629-636.
12. Ciuffreda MC, Malpasso G, Chokoza C, et al. Synthetic extracellular matrix mimic hydrogel improves efficacy of mesenchymal stromal cell therapy for ischemic cardiomyopathy. *Acta Biomater.* 2018;70:71-83.
13. Waters R, Alam P, Pacelli S, Chakravarti AR, Ahmed RPH, Paul A. Stem cell-inspired secretome-rich injectable hydrogel to repair injured cardiac tissue. *Acta Biomater.* 2018;69:95-106.
14. Roche ET, Hastings CL, Lewin SA, et al. Comparison of biomaterial delivery vehicles for improving acute retention of stem cells in the infarcted heart. *Biomaterials.* 2014;35(25):6850-6858.
15. Hastings CL, Roche ET, Ruiz-Hernandez E, Schenke-Layland K, Walsh CJ, Duffy GP. Drug and cell delivery for cardiac regeneration. *Adv Drug Deliv Rev.* 2015;84:85-106.
16. Patrick PS, Bear JC, Fitzke HE, et al. Radio-metal cross-linking of alginate hydrogels for non-invasive *in vivo* imaging. *Biomaterials.* 2020;243(March):119930.
17. Ahmadi A, Thorn SL, Alarcon EI, et al. PET imaging of a collagen matrix reveals its effective injection and targeted retention in a mouse model of myocardial infarction. *Biomaterials.* 2015;49:18-26.
18. Bastings MMC, Koudstaal S, Kieltyka RE, et al. A fast pH-switchable and self-healing supramolecular hydrogel carrier for guided, local catheter injection in the infarcted myocardium. *Adv Healthc Mater.* 2014;3(1):70-78.
19. Dankers PYW, Hermans TM, Baughman TW, et al. Hierarchical formation of supramolecular transient networks in water: A modular injectable delivery system. *Adv Mater.* 2012;24(20):2703-2709.
20. Wang Z, Golob MJ, Chesler NC. Viscoelastic properties of cardiovascular tissues. *Viscoelastic Viscoplastic Mater.* 2016;32:137-144.

21. Bakker MH, Tseng CCS, Keizer HM, et al. MRI Visualization of Injectable Ureidopyrimidinone Hydrogelators by Supramolecular Contrast Agent Labeling. *Adv Healthc Mater.* 2018;7(11):1-8.
22. Hendrikse SIS, Wijnands SPW, Lafleur RPM, et al. Controlling and tuning the dynamic nature of supramolecular polymers in aqueous solutions. *Chem Commun.* 2017;53(14):2279-2282.
23. Garbern JC, Minami E, Stayton PS, Murry CE. Delivery of basic fibroblast growth factor with a pH-responsive, injectable hydrogel to improve angiogenesis in infarcted myocardium. *Biomaterials.* 2011;32(9):2407-2416.
24. Chen CH, Chang MY, Wang SS, Hsieh PCH. Injection of autologous bone marrow cells in hyaluronan hydrogel improves cardiac performance after infarction in pigs. *Am J Physiol - Hear Circ Physiol.* 2014;306(7):1078-1086.
25. Bonios M, Terrovitis J, Chang CY, et al. Myocardial substrate and route of administration determine acute cardiac retention and lung biodistribution of cardiosphere-derived cells. *J Nucl Cardiol.* 2011;18(3):443-450.
26. Li SH, Lai TYY, Sun Z, et al. Tracking cardiac engraftment and distribution of implanted bone marrow cells: Comparing intra-aortic, intravenous, and intramyocardial delivery. *J Thorac Cardiovasc Surg.* 2009;137(5):1225-1233.e1.
27. Hou D, Youssef EAS, Brinton TJ, et al. Radiolabeled cell distribution after intramyocardial, intracoronary, and interstitial retrograde coronary venous delivery: Implications for current clinical trials. *Circulation.* 2005;112:150-157.
28. Menasché P. Cell therapy trials for heart regeneration — lessons learned and future directions. *Nat Rev Cardiol.* 2018;15(11):659-671.
29. De Feijter I, Goor OJGM, Hendrikse SIS, et al. Solid-Phase-Based Synthesis of Ureidopyrimidinone-Peptide Conjugates for Supramolecular Biomaterials. *Synlett.* 2015;26(19):2707-2713.
30. Spaans S, Fransen PPKH, Schotman MJG, et al. Supramolecular Modification of a Sequence-Controlled Collagen-Mimicking Polymer. *Biomacromolecules.* 2019;20(6):2360-2371.
31. Stratton JR, Ballem PJ, Gernsheimer T, Cerqueira M, Slichter SJ. Platelet destruction in autoimmune thrombocytopenic purpura: Kinetics and clearance of indium-111-labeled autologous platelets. *J Nucl Med.* 1989;30(5):629-637.



human induced pluripotent stem cells 1 day after passage

Chapter 9

GENERAL DISCUSSION AND FUTURE PERSPECTIVES

Marijn C. Peters^{1,2}

¹ Department of Cardiology, Laboratory of Experimental Cardiology, Division of Heart and Lungs, University Medical Centre Utrecht, The Netherlands.

² Regenerative Medicine Centre Utrecht, University Medical Centre Utrecht, The Netherlands.

DISCUSSION

Despite the decrease in direct mortality of a myocardial infarction by e.g. reperfusion therapies¹, the chronic burden of ischemic heart disease increases as the heart undergoes ventricular remodelling and loses contractility with the irreversible loss of cardiomyocytes. To decrease this chronic burden and improve the recovery of the heart after an ischemic insult, development of strategies that increase the cardiac reparative capacity is a key focus in the field. To move towards a reparative therapy, four steps can be taken (**Figure 1**). Firstly, we need to optimise our *in vitro* models of human ischemic heart disease to be able to better predict the effectiveness of new therapies. Secondly, additional cell death by reperfusion therapies needs to be resolved. Thirdly, the cardiomyocytes lost during an ischemic episode need to be replaced by new contractile tissue. Lastly, the implementation of new therapies (e.g. drug retention, targeted delivery) needs to be improved.

In this thesis, we show advances in these four steps of therapy development. Firstly, we improved *in vitro* disease modelling using human cardiomyocytes by testing the effect of metabolic maturation on sensitivity to hypoxia(**Chapter 3**). Secondly, we improved our current golden standard of reperfusion therapy by identifying a new tool to inhibit oxidative stress induced cardiac cell death (**Chapter 2**). Thirdly, we used our optimized *in vitro* ischemic heart disease model to test Follistatin-like 1 (Fstl1) as a tool to induce cardiomyocyte proliferation (**Chapter 6**). Lastly, we developed a method to visualize supramolecular hydrogels for cardiac delivery to improve drug retention (**Chapter 8**). In **part 1** we focused on protecting the heart from ischemia/reperfusion injury and optimised an *in vitro* model of human ischemic heart disease to test cardioprotective and reparative therapies. **Part 2** focused on cardiomyocyte proliferation to regenerate the heart in order to look into the implementation of regenerative therapies in **part 3**, focused on local and sustained delivery of non-coding RNAs to repair the heart. Several steps in the translational chain need to be

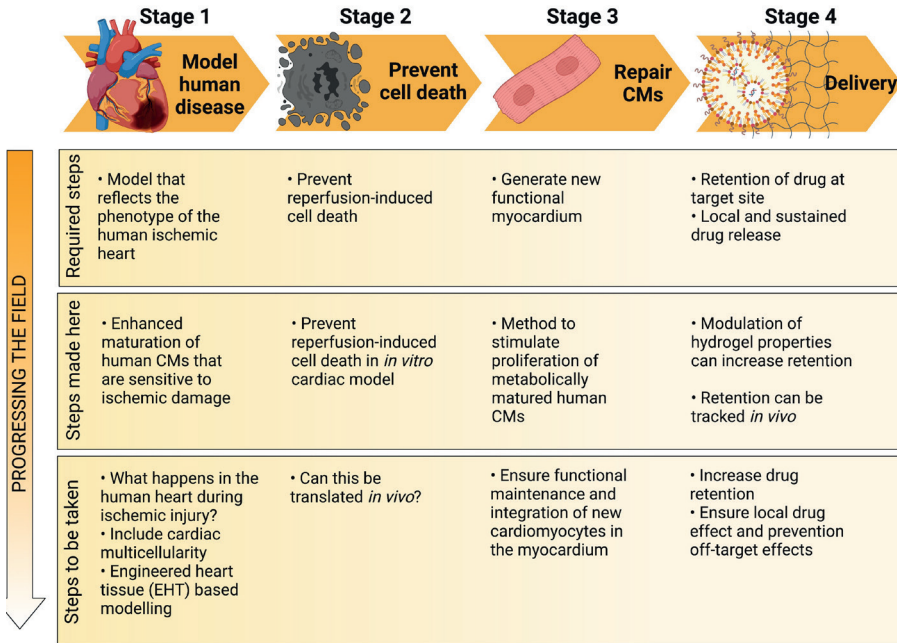


Figure 1. Stages of research towards clinical translation of cardiac reparative medicine

developed to shift the management of ischemic heart disease towards cardiac repair.

MODELING HUMAN CARDIAC ISCHEMIC INJURY

Clinically relevant disease modelling

As the field moves forward towards developing a functional regenerative therapy for patients after cardiac ischemic injury by generating large numbers of pluripotent stem cell-derived cardiomyocytes, new knowledge arises on cellular behaviour and the mechanisms underlying ischemic injury and ventricular remodelling. However, it is important to consider the models used in preclinical research might not reflect the exact characteristics of the human disease. It remains therefore challenging to efficiently model human cardiac ischemic injury. The high failure risk in clinical trials due to non-representative preclinical models needs to be overcome in order to move

towards a reparative therapy. Therefore, a therapy has to be validated in multiple experimental models². Currently, clinical trials are preceded by preclinical studies involving *in vitro* cell models of cardiac diseases using murine cardiomyocytes, neonatal rat cardiomyocytes, human induced pluripotent stem cell derived cardiomyocytes (hiPSC-CMs), or *in vivo* models using small animals (e.g. murine) and large animals (e.g. porcine). While animal models enable the study of ischemia on organ function, survival and therapy delivery, the development of *in vitro* human models of ischemic heart disease enable the study of human specific cellular responses to ischemic conditions. Especially as the physiology of the human heart differs greatly from that of the rodent heart³⁻⁵, validation of therapeutic tools in human based ischemic damage models can provide insight into responsiveness of human cardiomyocytes to drug intervention in ischemic or healthy conditions⁶. However, to generate a representative model, it is vital to study whether the cardiomyocytes differentiated from hiPSCs show similar cellular physiological characteristics and responsiveness as adult cardiomyocytes in the human myocardium.

In vivo and in vitro cardiomyocyte maturation

hiPSC-derived cardiomyocytes spontaneously contract, express sarcomeric proteins, show excitation-contraction coupling and display cardiac action potential and calcium signalling⁷. When comparing the physiology of adult cardiomyocytes and hiPSC-derived cardiomyocytes, the immature nature of hiPSC-derived cardiomyocytes is apparent. hiPSC-derived cardiomyocytes have a circular rather than rod-shaped morphology, shorter sarcomere length, no T-tubules, glycolytic energy metabolism, lower resting membrane potential and upstroke velocity, and are proliferative⁷⁻⁹, as compared to the tissue resident cardiomyocytes. Adult human cardiomyocytes take up to 10 years to mature in intracellular structure and ploidy¹⁰⁻¹², while hiPSC-derived cardiomyocytes are used for disease modelling after 20 to 40 days of differentiation^{13,14}. To accelerate the ageing of hiPSC-derived cardiomyocytes to

better mimic the phenotype of adult human cardiomyocytes, mechanisms of maturation in development were studied. The changes throughout development guide the biochemical alterations of cardiomyocyte maturation to enable cardiac growth and sustained cardiac contractility. After birth, the cardiac workload increases with the increase in hemodynamic pressure and the onset of pulmonary circulation¹⁵. To meet the increased energetic demand, cardiomyocyte metabolism switches from aerobic glycolysis of glucose to fatty acid oxidation. Evidence from murine studies show downregulation of hypoxia inducible factor 1 α (HIF1 α) mediates the metabolic switch to oxidative phosphorylation¹⁶. This shift drives myocardial differentiation and is followed by phenotypical changes in cell structure and gene expression to enable continuous contractions throughout a lifetime¹⁷. Furthermore, studies in neonatal sheep and mice showed an increase in circulating thyroid hormone (T3) as initiator of cardiomyocyte maturation by increasing cardiomyocyte width, binucleation and P21 expression and decreasing cardiomyocyte proliferation^{18,19}. Reported characteristics of cardiomyocyte maturation in the murine and human heart include sarcomere organization (e.g. assembly (e.g. isoform switching), expansion and M-line formation), T-tubule formation (e.g. sarcoplasmic reticulum expansion), physiological hypertrophy to replace hyperplasia based heart growth, and changes in electrophysiology (e.g. increase of ventricular ion channels and decrease in automaticity ion channels)^{12,17,20}. With the goal of using hiPSC-derived cardiomyocytes to model the healthy and diseased human myocardium and assess potential regenerative approaches, these differences in phenotype between adult human- and hiPSC derived-cardiomyocytes severely affect the predictive capacity of cardiomyocyte behaviour. Learning from maturation during development, biochemical methods to improve hiPSC-derived cardiomyocyte maturation have focussed on stimulating metabolic switching towards fatty acid oxidation^{8,21,22}, HIF1 α inhibition²³, and hormone mediated modulation (e.g. T3-mediated maturation)²⁴. These methods to accelerate cardiomyocyte maturation improved force generation, increased sarcomeric

organization, oxidative phosphorylation and cell size and decreased proliferation. In **chapter 3**, we showed using metabolic maturation medium for three consecutive weeks after differentiation (developed by Feyen et al. ⁸) improved hiPSC-derived cardiomyocyte susceptibility to hypoxic damage while immature hiPSC-derived cardiomyocytes without this metabolic maturation step were insensitive to hypoxic cell death. Additionally, we showed the availability of glucose in the media during hypoxia did not affect the sensitivity of immature hiPSC-derived cardiomyocytes to low oxygen concentrations. Metabolic profiling, however, did show disruption of metabolic activity in immature hiPSC-derived cardiomyocytes in hypoxia independent of media glucose availability. Older hiPSC-CMs cultured in maturation medium are metabolically reliant on oxidative phosphorylation and are more sensitive to hypoxia compared to younger cardiomyocytes cultured in glucose or lactate rich media. Therefore, we have optimized a model for human ischemic heart disease using hiPSC-derived cardiomyocytes. However, next to metabolic maturation, other factors contribute to the development of human cardiomyocytes and determine their behaviour upon ischemic insult. One of the drawbacks of two-dimensional cardiomyocyte culture is that it fails to mimic tissue architecture, cellular alignment and crosstalk²⁵.

Three-dimensional cardiac tissue engineering

Even though the maturity of hiPSC-derived cardiomyocytes has increased using biochemical methods like maturation under low glucose and fatty acid rich conditions, biophysical cues and interactions with non-cardiomyocytes are required to create adult-like cardiomyocytes¹⁷. As mentioned earlier, the increase in hemodynamic pressure with the onset of pulmonary circulation stimulates cardiomyocyte maturation to mediate increased cardiac pumping capacity¹⁵. Furthermore, mimicking the postnatal increase in stiffness of the cardiac extracellular matrix was found to improve sarcomere alignment, increase mechanical force, and calci-

um transients in rat neonatal and human embryonic stem cell derived cardiomyocytes⁷. These postnatal changes in mechanical stretch of cardiomyocytes have been found to directly influence electrophysiological maturation and changes in cellular morphology^{26–29}. Additionally, cellular alignment during myocardial patterning influences cardiomyocyte maturation⁷.

To improve *in vitro* cardiac disease modelling, researchers have attempted to recreate the structure of the myocardium in engineered heart tissue (EHT). Incorporating the three-dimensional environment with biochemically matured hiPSC-derived cardiomyocytes enables *in vitro* disease modelling to include the cardiac multicellularity, mechanical stress, cellular alignment and electrical pacing. To mimic the mechanical properties of the physiological myocardium and induce cellular alignment, biomaterials with similar rigidity as the extracellular matrix are used in bioprinting EHT constructs³⁰. Casting hiPSC-derived cardiomyocytes in polymer scaffolds and consecutively using electrical pacing and mechanical modulation could increase maturity of hiPSC-derived cardiomyocytes^{31,32}. This newly arisen field of EHT provides a promising approach to model human ischemic heart disease in an *in vitro* environment while closely resembling the myocardial *in vivo* environment.

PROTECTING AND REGENERATING THE HEART

Targeting cell death to protect the heart

In ischemic heart disease, cell death due to oxygen and nutrient deprivation and reoxygenation underlies the myocardial pathophysiology. The loss of cardiomyocytes drives fibrotic scar formation and adverse ventricular remodelling³³. Minimizing cellular death as a result of ischemic heart disease is therefore vital in improving cardiac repair. As reperfusion remains the current golden standard therapy for ischemic heart disease, it is a main focus to limit the detrimental side effect of reperfusion therapy. Ischemic postconditioning defined as rapid intermittent

interruption of coronary blood flow at the very onset of reperfusion has received attention as it could increase the expression of anti-oxidants and limit reperfusion injury^{34,35}. However, translation into the clinic fails. Additionally, inflating and deflating the balloon to mediate ischemic conditioning during percutaneous transluminal coronary angioplasty can lead to damage of the vessel wall³⁴. Therefore, pharmacological conditioning before or at the onset of reperfusion has received attention to mediate cardiac protection. **Chapter 2** evaluates the use of an innovative receptor interacting kinase 1 (RIPK1) necroptosis inhibitor (GSK'547) on reactive oxygen species induces injury to human cardiac cells.

Similar as to prior research with a less potent and specific RIPK1 inhibitor necrostatin-1, GSK'547 could prevent hydrogen peroxide-induced cell death. Analysis of underlying mechanism showed that both activation of the RIP1-RIP3-MLKL pathway and the mitochondrial RIP3-CAMKII-mPTP pathway were prevented by GSK'547. As GSK'547 is already approved by the FDA and currently in phase 2 clinical trials for inflammatory diseases, clinical application of GSK'547 for pharmacological conditioning to prevent cardiac reperfusion therapy is within reach. It remains important to test the effect of GSK'547 in *in vivo* setting to determine its efficacy in the infarcted area in the additional presence of pro-inflammatory cytokines. Nevertheless, GSK'547 showed promising results, matching previous observations with Nec-1, that could contribute to the prevention of reperfusion injury and limit infarct size.

Cardiomyocyte dedifferentiation and proliferation

If we surpass stage 1 of developing a representative model of human ischemic heart disease, we can move towards testing cardioprotective and regenerative approaches. As explained, maturity of *in vitro* human cardiomyocytes compared to adult cardiomyocytes is a major component of developing a representative disease model. The postnatal loss of cardiomyocyte proliferative capacity is directly

linked to the increased complexity of the intracellular architecture and cardiomyocyte maturation. In light of regenerative therapies, this highlights a potential hurdle. Targeting the proliferative capacity of cardiomyocyte to generate new myocardium, might push the already diseased heart into a less differentiated state. For example, sustained stimulation of cardiomyocyte proliferation via targeting the Hippo-Yap pathway in a porcine myocardial infarction model led to uncontrolled heart growth and sudden arrhythmic cardiac death³⁶. Then the question remains whether differentiated mature cardiomyocyte function and proliferation of cardiomyocytes can co-exist to mediate cardiac repair. To find an answer to this question, we can look into cardiomyocyte maturation in lower phylogenetic species that can regenerate after injury. In zebrafish hearts, complete cardiac regeneration after injury is mediated by dedifferentiation and proliferation of pre-existing cardiomyocytes³⁷. This might suggest that the zebrafish heart is less mature and differentiated than the porcine (and human) heart which would enable dedifferentiation of cardiomyocytes while maintaining sufficient cardiac contractility. When comparing zebrafish cardiomyocytes with human cardiomyocytes, zebrafish cardiomyocytes do have less structured T-tubules and a less complex sarcoplasmic reticulum³⁸, which would support this hypothesis. However, sarcomere structural organization, actin filaments and mitochondria abundance of zebrafish cardiomyocytes point towards a more mature phenotype. In fact, previous studies found sarcomere length in adult zebrafish cardiomyocytes was not significantly different from human cardiomyocytes³⁹⁻⁴¹. Therefore, understanding the balance between maturation and proliferation is important in moving towards regenerative approaches. Alternatively, studying mechanisms of hiPSC-derived cardiomyocyte maturation could in turn provide more insights into human heart development and maturation and the pathophysiology of hereditary cardiomyopathies as some cardiomyopathies are related to defective cardiomyocyte maturation^{17,42,43}. In **chapter 6**, we tested whether we could induce proliferation of hiPSC-derived cardiomyocytes after the cardiomyocytes were met-

abolically matured. With very low basal proliferation rate of 1,4% KI67-positivity compared to 5,9% KI67-positivity in immature hiPSC-derived cardiomyocytes and increased sarcomeric structural organization and reliance on oxidative phosphorylation⁸, proliferation of matured ischemic cardiomyocytes could be stimulated using non-glycosylated Follistatin-like 1 (Fstl1). While increasing the expression of cell cycle genes, Fstl1 also increased the expression of anti-oxidants and genes associated with sarcomere organization as shown by RNA expression profiling. Analysis of downregulated biological processes did not show downregulation of processes involved with cardiomyocyte maturation, such as cardiac contraction and cell junction organization (both upregulated after Fstl1 treatment). However, it is important to assess whether increased proliferation leads to the generation of functional differentiated cardiomyocytes. Therefore, functionality of Fstl1 treatment has to be examined under *in vivo* conditions. Furthermore, we assessed Fstl1 production by fibroblasts under normoxic and hypoxic conditions and found hypoxia increased Fstl1 production by fibroblasts. Conversely, we did report different Fstl1 protein production and post-translational modification between human foetal cardiac fibroblasts and hiPSC-derived cardiac fibroblasts. This further emphasizes the importance of analysing Fstl1 therapeutic potential under *in vivo* conditions where the multicellular nature of the heart is taken into account. Previously mentioned EHTs might also be a good intermediate step to investigate Fstl1 function in cardiac tissue context. This could enable the study of Fstl1 initiated mechanisms in cellular crosstalk, under mechanical strain and during electrical pacing of cardiomyocytes and cardiac fibroblasts. Nevertheless, understanding the mechanisms of *in vivo* cardiac ischemic injury are crucial in inventing reparative approaches.

Non-coding RNAs in cardiac repair

Since the discovery of the innate proliferative capacity of human cardiomyocytes and the complete cardiac regeneration in zebrafish, the field of regenerative

medicine has expanded rapidly towards defining the right target to activate the molecular switch to repair the heart. In **chapter 4 and 7**, we describe the increased interest in non-coding RNAs as tools to target cardiac repair. The majority of the transcribed genome consists of non-coding RNAs that regulate gene expression of coding RNAs⁴⁴. The large number of cardiac specific non-coding RNAs and their regulatory function in multiple cardiac developmental and disease-specific processes, emphasize their potential as therapeutic targets. As gene expression is under tight regulation of the non-coding transcriptome, targeting a regulatory non-coding RNA rather than one of its gene targets has been shown to yield beneficial effects⁴⁴. Furthermore, if a non-coding RNA is only expressed in the heart, targeting it for therapeutic purposes would prevent off target effects in distal organs. In **chapter 7**, we focussed on the role of non-coding RNAs in endothelial cell signalling during cardiac injury and regeneration. As the re-establishment of the vascular network in the infarct area is crucial in mediating cardiac repair in the zebrafish heart⁴⁵, we studied non-coding RNA mediated intercellular communication between endothelial cells and cardiomyocytes in the healthy and injured heart. Here, we identified a list of miRNAs and long non-coding RNAs that have been reported in their function in cardiac regeneration and vascularisation. The interplay between hypoxia-inducible non-coding RNA expression and their stimulation of endothelial cell function and myocardial repair guides cardiac regeneration^{46–48}. Therefore, therapeutic manipulation of non-coding RNA expression could activate the cardiac regulatory networks that turn the molecular switch towards regeneration in contrast to current fibrotic repair.

Local and sustained delivery of therapies

As discussed, promising targets have been identified that play a role in regulating the components of cardiac repair. Non-coding RNAs that can simultaneously alter behaviour of cardiomyocytes, fibroblasts and endothelial cells

in the infarcted area would therefore be the main tool for regenerative therapy. Administration of miRNA or miRNA inhibitors (antimiRs) to target cells could directly alter mRNA expression and have epigenetic effects. However, as RNAs consist of nucleotides they can be subjected to RNase-mediated degradation in the inter- and intracellular environment⁴⁹. Additionally, local delivery of RNAs is vital to prevent off-target organ effects. To ensure safe delivery of RNA therapy to the infarction site where the RNAs can exert their function, multiple delivery techniques have been investigated. miRNA stability and prevention of lysosomal degradation can be mediated by the use of extracellular vesicles to deliver miRNA therapeutics⁵⁰⁻⁵². Extracellular vesicles are released by all cells and transport bioactive molecules from one cell to another cell to mediate intercellular communication⁵¹. The membrane of extracellular vesicles is composed of a lipid bilayer which prevents miRNA degradation. Furthermore, molecules on the outside of the membrane can direct the vesicles to specific target cells enabling targeted delivery. These characteristics of extracellular vesicles makes them promising tools for cardiac delivery. While cellular uptake can be enhanced by chemical modifications that increase hydrophobicity⁵³, targeted delivery can also be mediated by scaffold-mediated delivery that encapsulate the miRNA and provide three-dimensional distribution of the miRNA at the target site⁴⁹. Supramolecular hydrogels that are thin and liquid before injection and form a rigid gel in myocardial tissue allow for minimally invasive catheter-based injection based on temperature, pH or shear stress mediated gel formation^{54,55}. In **chapter 8** we developed a method to visualize the distribution of supramolecular ureido-pyrimidinone modified poly (ethylene glycol) (UPy-PEG) based hydrogel using radioactive isotope indium-111 based labelling. With this method we could quantify the localization of the hydrogel after injection and measure differences in hydrogel retention over time. Furthermore, we showed that addition of a UPy-functionalized recombinant peptide, based on human collagen type 1, could double the retention at the injection sites in defined gel deposits. With this study, we

emphasize the importance of determining the distribution of a therapy after injection to ensure therapeutic effect and prevent off-target effects. Based on this, we advise researchers to include retention studies in their preclinical studies on regenerative therapies as a drug not maintained at the target site cannot exert its function.

FUTURE DIRECTIONS

While in this thesis we describe approaches to increase translatability of cardiac reparative studies, it is important to mention there are still steps to be taken to move to successful clinical trials. In line with the work presented in this thesis, mechanisms of Fstl1 function in fibroblasts and cardiomyocytes and the role of glycosylation in intercellular communication will be studied to further elucidate the working mechanism of Fstl1. Furthermore, a large animal study studying the regenerative effect of Fstl1 delivery after myocardial infarction is set-up to move towards clinical application. Furthermore, the RIP1 inhibitor GSK'547 will be tested for prevention of ischemia/reperfusion injury *in vivo* where both oral and intravenous delivery will be compared to measure the effect of GSK'547 on cardiac function and infarct size following reperfusion. In line with our method to visualize hydrogel distribution following injection, the gel with UPy-functionalized recombinant peptide based on human collagen type 1 is currently being tested in a porcine animal model of ischemic heart disease in combination with regenerative factor anti-miR-195.

Following these steps to further develop the advances made in this thesis, it is important the field moves towards the use of more representative models of ischemic heart disease. With the rise of technologies like hiPSC-CMs, and three-dimensional multicellular models like EHT⁵⁶ or heart-on-a-chip⁵¹, the use of murine models of myocardial infarction can be reduced to enable human-specific and even patient specific disease modelling. In contrast to *in vivo* studies in which the identification of disease mechanisms on the molecular level and level of cellular

communication is difficult, *in vitro* disease models mimicking human tissues allows for tightly controlled disease modelling and assessment of cellular behaviour. With the development of advanced imaging techniques (e.g. spinning disk, super resolution microscopy, confocal microscopy, calcium imaging) and advances in gene editing and cellular visualisation (e.g. CRISPR-Cas9), cellular communication and subcellular changes following injury can be documented before advancing to *in vivo* studies. In this case, functionality of the therapy on the human cellular level would be confirmed before translation to *in vivo* studies that test for safety and drug behaviour in the context of multi-organ systems.

Next to pushing the field towards more effective disease modelling, the development of reparative therapies should also increase in translatability. With the identification of multiple factors that can induce cardiomyocyte proliferation in pre-clinical animal studies, it still remains unclear whether adult human cardiomyocytes can be stimulated to proliferate. We have shown in this thesis, metabolically matured hiPSC-CMs can be stimulated to proliferate using Fstl1, but we haven't yet tested this in three-dimensional context or in the context of multiple cell types. It would be of interest to investigate whether human cardiomyocytes aligned in a three-dimensional construct with endothelial cells and fibroblasts can dedifferentiate and proliferate without losing contractile force. Likewise, will the cardiomyocytes after cytokinesis electrically couple to the pre-existing cardiomyocytes to contribute to contractility without leading to arrhythmias? Since the zebrafish and neonatal heart have the capacity to regenerate after injury, there seems to be a way for new cardiomyocytes to be generated from pre-existing cardiomyocytes. However, whether this exact capacity is evolutionary retained in the human myocardium and whether we can find a way to tap into this exact mechanism remains to be seen. Therefore, closely assessing the behaviour of human cardiomyocytes in tissue context during ischemic injury and in combination with proliferation inducing factors would be the next step to

understand mechanisms of cardiac repair.

For cardioprotective approaches it would be interesting to test the functionality of cardiomyocytes that survive due to the necroptosis inhibition. If the release of reactive oxygen species no longer induces necroptosis in the presence of RIP1 inhibitors and the mitochondria no longer lose their membrane potential, is there remaining damage from the sudden oxygen influx that would affect the cardiomyocyte contractility?

In terms of delivery tools, it remains crucial to test the safety and local targeting of drug delivery using retention-improving biomaterials. For example, the effectiveness of hydrogels that form a gel after injection and the effect of this gel formation on the surrounding tissue. It remains unclear whether the gel would provide support to the tissue or whether the presence of the solidifying gel would push against the already weakened myocardium. Next to development of a hydrogel capable of forming a gel in the tissue environment, hydrogel rigidity and required injection volume are also very important factors to consider. Therefore, analysis of drug-scaffold-tissue interaction should be a focus of future research to move towards translation.

CONCLUSIONS

This thesis aimed to advance our knowledge on cardiac reparative approaches. We discovered a novel tool to inhibit reactive oxygen species induced cardiac cell death. Using metabolic maturation media, we tested whether matured hiPSC-derived cardiomyocytes were sensitive to ischemia and developed an *in vitro* model of human cardiac ischemic injury. Additionally, we examined if matured hiPSC-derived cardiomyocytes could be stimulated to proliferate and we discovered the protective and regenerative capacity of hypo-glycosylated Fstl1 on human hypoxic cardiomyocytes. Furthermore, in this thesis is the first report of Fstl1 production and secretion

by human cardiac fibroblasts and altered secretion following ischemia. Lastly, we developed a method to quantify the distribution of supramolecular hydrogels using *in vivo* tracking of radioactively labelled hydrogel subunits. Altogether, in this thesis we showed progression in ischemic disease modelling and drug development to move towards regenerative therapy to treat patients with ischemic heart disease.

REFERENCES

1. Virani SS, Alonso A, Benjamin EJ, et al. *Heart Disease and Stroke Statistics—2020 Update: A Report from the American Heart Association.*; 2020.
2. Ytrehus K. The ischemic heart - Experimental models. *Pharmacol Res.* 2000;42(3):193-203.
3. Ge Z, Lal S, Le TYL, dos Remedios C, Chong JJH. Cardiac stem cells: translation to human studies. *Biophys Rev.* 2015;7(1):127-139.
4. Rog-Zielinska EA, Kong CHT, Zgierski-Johnston CM, et al. Species differences in the morphology of transverse tubule openings in cardiomyocytes. *Europace.* 2018;20:III120-III124.
5. Jung G, Bernstein D. hiPSC modeling of inherited cardiomyopathies. *Curr Treat Optrions Cardiovasc Med.* 2014;16(7).
6. Wei H, Wang C, Guo R, Takahashi K, Naruse K. Development of a model of ischemic heart disease using cardiomyocytes differentiated from human induced pluripotent stem cells. *Biochem Biophys Res Commun.* 2019;520(3):600-605.
7. Yang X, Pabon L, Murry CE. Engineering adolescence: Maturation of human pluripotent stem cell-derived cardiomyocytes. *Circ Res.* 2014;114(3):511-523.
8. Feyen DAM, McKeithan WL, Bruyneel AAN, et al. Metabolic Maturation Media Improve Physiological Function of Human iPSC-Derived Cardiomyocytes. *Cell Rep.* 2020;32(3).
9. Goversen B, van der Heyden MAG, van Veen TAB, de Boer TP. The immature electrophysiological phenotype of iPSC-CMs still hampers in vitro drug screening: Special focus on IK1. *Pharmacol Ther.* 2018;183:127-136.
10. Bergmann O, Bhardwaj RD, Bernard S, et al. Evidence for Cardiomyocyte Renewal in Humans. *Science.* 2009;324:98-102.
11. Bergmann O, Zdunek S, Felker A, et al. Dynamics of Cell Generation and Turnover in the Human Heart. *Cell.* 2015;161(7):1566-1575.
12. Peters NS, Severs NJ, Rothery SM, Lincoln C, Yacoub MH, Green CR. Spatiotemporal relation between gap junctions and fascia adherens junctions during postnatal development of human ventricular myocardium. *Circulation.* 1994;90(2):713-725.

13. Lian X, Hsiao C, Wilson G, et al. Robust cardiomyocyte differentiation from human pluripotent stem cells via temporal modulation of canonical Wnt signaling. *Proc Natl Acad Sci U S A*. 2012;109(27).
14. Karakikes I, Ameen M, Termglinchan V, Wu JC. Human Induced Pluripotent Stem Cell-Derived Cardiomyocytes: Insights into Molecular, Cellular, and Functional Phenotypes. *Circ Res*. 2015;117(1):80-88.
15. Zhu R, Blazeski A, Poon E, Costa KD, Tung L, Boheler KR. Physical developmental cues for the maturation of human pluripotent stem cell-derived cardiomyocytes. *Stem Cell Res Ther*. 2014;5(1):1-18.
16. Menendez-Montes I, Escobar B, Palacios B, et al. Myocardial VHL-HIF Signaling Controls an Embryonic Metabolic Switch Essential for Cardiac Maturation. *Dev Cell*. 2016;39(6):724-739.
17. Guo Y, Pu WT. Cardiomyocyte maturation: New phase in development. *Circ Res*. 2020;1086-1106.
18. Hirose K, Payumo AY, Cutie S, et al. Evidence for hormonal control of heart regenerative capacity during endothermy acquisition. *Science* 2019;364(6436):184-188.
19. Chattergoon NN, Giraud GD, Louey S, Stork P, Fowden AL, Thornburg KL. Thyroid hormone drives fetal cardiomyocyte maturation. *FASEB J*. 2012;26(1):397-408.
20. Li F, Wang X, Capasso JM, Gerdes AM. Rapid transition of cardiac myocytes from hyperplasia to hypertrophy during postnatal development. *J Mol Cell Cardiol*. 1996;28(8):1737-1746.
21. Hidalgo A, Glass N, Ovchinnikov D, et al. Modelling ischemia-reperfusion injury (IRI) in vitro using metabolically matured induced pluripotent stem cell-derived cardiomyocytes. *APL Bioeng*. 2018;2(2).
22. Horikoshi Y, Yan Y, Terashvili M, et al. Fatty acid-treated induced pluripotent stem cell-derived human cardiomyocytes exhibit adult cardiomyocyte-like energy metabolism phenotypes. *Cells*. 2019;8(1095):1-21.
23. Hu D, Linders A, Yamak A, et al. Metabolic maturation of human pluripotent stem cell-derived cardiomyocytes by inhibition of HIF1 α and LDHA. *Circ Res*. 2018;123(9):1066-1079.
24. Yang X, Rodriguez M, Pabon L, et al. Tri-iodo-L-thyronine promotes the maturation of human cardiomyocytes-derived from induced pluripotent stem cells. *J Mol Cell Cardiol*. 2014;72:296-304.
25. Li J, Hua Y, Miyagawa S, et al. hiPSC-derived cardiac tissue for disease modeling and drug discovery. *Int J Mol Sci*. 2020;21(23):1-32.
26. Damon BJ, Rémond MC, Bigelow MR, et al. Patterns of muscular strain in the embryonic heart wall. *Dev Dyn*. 2009;238(6):1535-1546. doi:10.1002/dvdy.21958
27. Geach TJ, Hirst EMA, Zimmerman LB. Contractile activity is required for Z-disc sarcomere maturation in vivo. *Genesis*. 2015;53(5):299-307.

28. Lindsey SE, Butcher JT, Yalcin HC. Mechanical regulation of cardiac development. *Front Physiol.* 2014;5 :1-15.
29. Scuderi GJ, Butcher J. Naturally Engineered Maturation of Cardiomyocytes. *Front Cell Dev Biol.* 2017;5:1-28.
30. Smith AST, Macadangdang J, Leung W, Laflamme MA, Kim D-H. Human iPSC-derived cardiomyocytes and tissue engineering strategies for disease modeling and drug screening. *Biotechnol Adv.* 2017;35(1):77-94.
31. Leonard A, Bertero A, Powers JD, et al. Afterload promotes maturation of human induced pluripotent stem cell derived cardiomyocytes in engineered heart tissues. *J Mol Cell Cardiol.* 2018;118:147-158.
32. Hirt MN, Boeddinghaus J, Mitchell A, et al. Functional improvement and maturation of rat and human engineered heart tissue by chronic electrical stimulation. *J Mol Cell Cardiol.* 2014;74:151-161.
33. Cokkinos D V., Pantos C. Myocardial remodeling, an overview. *Heart Fail Rev.* 2011;16(1):1-4.
34. Wu Y, Liu H, Wang X. Cardioprotection of pharmacological postconditioning on myocardial ischemia/reperfusion injury. *Life Sci.* 2021;264:118628.
35. Shen Y, Liu X, Shi J, Wu X. Involvement of Nrf2 in myocardial ischemia and reperfusion injury. *Int J Biol Macromol.* 2019;125:496-502.
36. Gabisonia K, Prosdocimo G, Aquaro GD, et al. MicroRNA therapy stimulates uncontrolled cardiac repair after myocardial infarction in pigs. *Nature.* 2019;569(7756):418-422.
37. Jopling C, Sleep E, Raya M, Martí M, Raya A, Belmonte JCI. Zebrafish heart regeneration occurs by cardiomyocyte dedifferentiation and proliferation. *Nature.* 2010;464(7288):606-609.
38. Hodgson P, Ireland J, Grunow B. Fish, the better model in human heart research? Zebrafish Heart aggregates as a 3D spontaneously cardiomyogenic in vitro model system. *Prog Biophys Mol Biol.* 2018;138:132-141.
39. Dvornikov A V., Dewan S, Alekhina O V., Pickett FB, De Tombe PP. Novel approaches to determine contractile function of the isolated adult zebrafish ventricular cardiac myocyte. *J Physiol.* 2014;592(9):1949-1956.
40. Kolanowski TJ, Antos CL, Guan K. Making human cardiomyocytes up to date: Derivation, maturation state and perspectives. *Int J Cardiol.* 2017;241:379-386.
41. Iorga B, Dan Neacsu C, Neiss WF, et al. Micromechanical function of myofibrils isolated from skeletal and cardiac muscles of the zebrafish. *J Gen Physiol.* 2011;137(3):255-270.
42. Birket MJ, Ribeiro MC, Kosmidis G, et al. Contractile Defect Caused by Mutation in MYBPC3 Revealed under Conditions Optimized for Human PSC-Cardiomyocyte Function. *Cell Rep.* 2015;13(4):733-745.

43. Pei J, Schuldt M, Nagyova E, et al. Multi-omics integration identifies key upstream regulators of pathomechanisms in hypertrophic cardiomyopathy due to truncating MYBPC3 mutations. *Clin Epigenetics*. 2021;13(1):1-20.
44. Abbas N, Perbellini F, Thum T. Non-coding RNAs: emerging players in cardiomyocyte proliferation and cardiac regeneration. *Basic Res Cardiol*. 2020;115(5):1-20.
45. Marín-Juez R, Marass M, Gauvrit S, et al. Fast revascularization of the injured area is essential to support zebrafish heart regeneration. *Proc Natl Acad Sci*. 2016;113(40):11237-11242.
46. Yin VP, Lepilina A, Smith A, Poss KD. Regulation of zebrafish heart regeneration by miR-133. *Dev Biol*. 2012;365(2):319-327.
47. Eulalio A, Mano M, Ferro MD, et al. Functional screening identifies miRNAs inducing cardiac regeneration. *Nature*. 2012;492(7429):376-381.
48. Arif M, Pandey R, Alam P, et al. MicroRNA-210-mediated proliferation, survival, and angiogenesis promote cardiac repair post myocardial infarction in rodents. *J Mol Med*. 2017;95(12):1369-1385.
49. Eulalio A, Mano M, Ferro MD, et al. Functional screening identifies miRNAs inducing cardiac regeneration. *Nature*. 2012;492(7429):376-381.
50. Xuan W, Wang L, Xu M, Weintraub NL, Ashraf M. MiRNAs in Extracellular Vesicles from iPS-Derived Cardiac Progenitor Cells Effectively Reduce Fibrosis and Promote Angiogenesis in Infarcted Heart. *Stem Cells Int*. 2019;2019.
51. De Jong OG, Kooijmans SAA, Murphy DE, et al. Drug Delivery with Extracellular Vesicles: From Imagination to Innovation. *Acc Chem Res*. 2019;52(7):1761-1770.
52. Song Y, Zhang C, Zhang J, et al. Localized injection of miRNA-21-enriched extracellular vesicles effectively restores cardiac function after myocardial infarction. *Theranostics*. 2019;9(8):2346-2360.
53. Schroeder A, Levins CG, Cortez C, Langer R, Anderson DG. Lipid-based nanotherapeutics for siRNA delivery. *J Intern Med*. 2010;267(1):9-21.
54. Pape ACH, Bakker MH, Tseng CCS, et al. An injectable and drug-loaded supramolecular hydrogel for local catheter injection into the pig heart. *J Vis Exp*. 2015;2015(100):1-8.
55. Uman S, Dhand A, Burdick JA. Recent advances in shear-thinning and self-healing hydrogels for biomedical applications. *J Appl Polym Sci*. 2020;137(25):1-20.
56. Goldfracht I, Protze S, Shiti A, et al. Generating ring-shaped engineered heart tissues from ventricular and atrial human pluripotent stem cell-derived cardiomyocytes. *Nat Commun*. 2020;11(1):1-15.



Follistatin-like 1 supplementation in hypoxia chamber

ADDENDUM

Nederlandse samenvatting

Acknowledgements

List of publications

Curriculum Vitae

Marijn C. Peters^{1,2}

¹ Department of Cardiology, Laboratory of Experimental Cardiology, Division of Heart and Lungs, University Medical Centre Utrecht, The Netherlands.

² Regenerative Medicine Centre Utrecht, University Medical Centre Utrecht, The Netherlands.

NEDERLANDSE SAMENVATTING

Hart- en vaatziekten zijn de meest voorkomende doodsoorzaak wereldwijd¹. De behandeling van patiënten met een hartinfarct (ischemische hartziekte) is verbeterd door reperfusie therapieën die de doorbloeding van het aangedane hartspierweefsel mogelijk maken^{2,3}. Echter is de chronische last van ischemische hartziekten erg hoog doordat het verlies aan hartspiercellen niet kan worden hersteld en de resulterende aanmaak van littekenweefsel zorgt voor een afname van hartfunctie en zelfs kan leiden tot hartfalen. Naast de schade van de blokkade in zuurstofvoorziening in het hart kan er ook additionele schade optreden door het heropenen van de gesloten slagader, zogenaamde reperfusie schade. Het stimuleren van natuurlijk herstel van het hartspierweefsel na een hartinfarct en het voorkomen van schade door reperfusie therapieën is hierdoor een belangrijk doel binnen cardiovasculair onderzoek.

Dit proefschrift laat zien dat we effectief reperfusie schade kunnen voorkomen en humane metabolisch-volwassen hartspiercellen zich kunnen laten herstellen in een *in vitro* model van ischemisch hartziekte. Ook geeft ons onderzoek aan hoe belangrijk het is voor klinische relevantie bij preklinisch onderzoek de toedieningsmethode en de retentie van de therapie op de beschadigde plek mee te nemen bij het bepalen van de effectiviteit van therapieën. Steeds meer, ontrafelen we de mechanismen die ten grondslag liggen aan hartschade en herstel door het in beeld brengen van zowel reacties op cellulair gebied als op functioneel gebied. Door het combineren van oplossingen voor reperfusie schade, het beperkte herstellend vermogen van het hartspierweefsel en het gelokaliseerd houden van medicijnen op de plaats van bestemming komen we steeds dichterbij een manier om het hart te kunnen herstellen en de ontwikkeling van hartfalen te voorkomen.

Hoofdstuk 1 toont aan dat een nieuwe RIP1 activatieremmer, GSK'547⁴, momenteel in fase 2 van klinische studies voor ontstekingsziektes, in humane hartspiercellen reperfusie schade kan voorkomen door het blokkeren van necroptotische celdood.

Wanneer we schade induceerde met waterstofperoxide, een zuurstofradicaal, zorgde dit voor een overleving van gemiddeld 15,6%. Toevoeging van GSK'547 voordat het waterstofperoxide werd toegevoegd, als simulering van het toevoegen van de therapie voor het openen van de geblokkeerde slagader, verhoogde de overleving naar 75,7%. GSK'547 werkte hierbij door de activatie van de eiwitten RIP1, RIP3 en MLKL te remmen. Deze eiwitten hebben een sleutelrol in het uitvoeren van necroptotisch celdood. Naast het remmen van RIP1, RIP3 en MLKL remt GSK'547 ook schade aan het mitochondriale membraan door CaMKII expressie te onderdrukken. Eerder onderzoek heeft het belang van necroptose⁵⁻⁸ en mitochondriale schade⁹⁻¹¹ in reperfusie schade beschreven wat laat zien dat het vinden en ontwikkelen van effectieve remmers van necroptose en mitochondriale schade een goede manier is om reperfusie schade te voorkomen en de infarctgrootte te beperken.

Deel 2 is gericht op het stimuleren van het herstel van hartspiercellen. In **hoofdstuk 2** ligt de focus op waarom het stimuleren van proliferatie van hartspiercellen een goede therapeutische behandeling zou zijn voor het voorkomen van hartfalen en de rol van niet-coderend RNA, miRNA-128 als mogelijk regeneratieve factor. Aangezien het hart niet alleen bestaat uit hartspiercellen en het herstel van het hart niet alleen herstel van hartspiercellen maar ook ontwikkeling van nieuwe bloedvaten en reactie van fibroblasten vergt, richt **hoofdstuk 3** zich op het glyco-eiwit Follistatin-like 1 (FSTL1) als regeneratieve factor. FSTL1 heeft diverse functies afhankelijk van spatiotemporele regulatie en post-translationele modificaties. In foetale ontwikkeling zorgt het voor remming van cel proliferatie^{12,13} en in ziekte kan het zorgen voor proliferatie van cellen^{14,15}. Ook stimuleert FSTL1 angiogenese¹⁶, onderdrukt het cel-apoptose^{14,17}, en voorkomt het de ruptuur van het infarct door expressie in fibroblasten^{18,19}. Om in hoofdstuk 5 te onderzoeken of FSTL1 een goede therapie kan zijn voor humane ischemische hartziekte ontwikkelden we in **hoofdstuk 4** een *in vitro* model. Gebruik makende van humane geïnduceerde pluripotente stamcellen stimuleerde we differentiatie tot jonge hartspiercellen of

hartspiercellen met een additionele metabolische veroudering²⁰. Door de cellen in een lage zuurstof en nutriënten-omgeving te plaatsen, modelleerde we ischemische hartziekten en bekeken we het effect van de veroudering op de overleving van de hartspiercellen. Dit liet zien dat alleen cellen met een additionele metabolische veroudering gevoelig zijn voor lage zuurstof en nutriënten terwijl ischemie in jonge hartspiercellen niet zorgde voor celdood. Analyse van de metabolische reactie van de jonge en verouderde cellen op de ischemie liet zien dat de metabolische flexibiliteit van de jonge cellen wel afneemt in ischemie maar vele maten minder dan bij de verouderde cellen. Op basis van de resultaten concludeerde wij dat alleen metabolisch verouderde hartspiercellen gevoelig zijn voor ischemie zoals we zien in de celdood van hartspiercellen tijdens ischemisch hartziekten. In **hoofdstuk 5** bekeken we of FSTL1 in dit *in vitro* model celdood kon onderdrukken en de aanmaak van nieuwe hartspiercellen kon stimuleren. Hierbij zagen wij dat FSTL1 celdood onderdrukte en dat alleen FSTL1 zonder suikergroepen proliferatie van hartspiercellen stimuleerde. Het tijdstip van toevoeging van FSTL1, voor of na schade had hierbij geen effect op de regeneratieve werking. Aangezien eerder onderzoek liet zien dat FSTL1 expressie in fibroblasten essentieel was voor het voorkomen van de ruptuur van het infarct in proefdieren^{18,19}, maar er geen eerdere studies zijn die FSTL1 expressie in humane fibroblasten bevestigen, onderzochten wij de FSTL1 expressie in humane fibroblasten. Humane fibroblasten en hartspiercellen produceerde FSTL1 en ischemie zorgde hierbij in fibroblasten voor een verhoogde eiwitsecretie en in hartspiercellen voor een verlaagde FSTL1 secretie. De combinatie van humane hartspiercellen en fibroblasten in kweek zorgde voor een cumulatief hogere FSTL1 secretie waarbij de aanwezigheid van fibroblasten in lage aantallen voldoende was om FSTL1 secretie te verhogen. Dit hoofdstuk liet zien dat proliferatie van verouderde hartspiercellen kan worden gestimuleerd in ischemische omstandigheden door FSTL1 en dat FSTL1 secretie een rol speelt bij communicatie tussen hartspiercellen en fibroblasten in ischemie. De onderliggende mechanismen

van deze FSTL1-gemedieerde communicatie tussen hartspiercellen en fibroblasten in ischemie moeten nog nader onderzocht worden.

Deel 3 is gewijd aan de vertaling van *in vitro* resultaten naar een therapie waarin er gekeken wordt naar een lokale medicijn administratie en het behoud op de plek van schade. **Hoofdstuk 6** gaat in op de rol van niet-coderende RNA's op hartregeneratie en endotheelcellen en het inspelen op extracellulaire vesicle-communicatie tussen endotheelcellen en hartspiercellen voor hartherstel. De ontwikkeling van nieuwe therapieën voor ischemische hartziekte focussen zich vooral op de aanmaak van nieuwe hartspiercellen waarbij er niet rekening wordt gehouden met de rol van endotheelcellen in het behoud van de nieuw aangemaakte hartspiercellen in het infarct. In dit hoofdstuk beschrijven we de veranderingen in endotheelcellen tijdens hartschade en de communicatie tussen hartspiercellen en endotheelcellen met behulp van niet-coderende RNA's. De rol van niet-coderende RNA's in hartschade en herstel is essentieel waarbij communicatie tussen celtypes in de gebieden rondom het infarct met behulp van deze niet-coderende RNA's bepaalt of het infarct herstelt wordt met een litteken of er volledige regeneratie plaatsvindt²¹⁻²⁶. Omdat niet-coderende RNA's bijwerkingen kunnen hebben wanneer ze terecht komen op andere locaties dan de plek van schade is het essentieel dat deze gelokaliseerd toegediend kunnen worden en dat er gecontroleerd kan worden dat ze op de plek van schade blijven na injectie. Eerder onderzoek heeft alleen laten zien dat alles wat in het hart wordt geïnjecteerd direct wordt uitgepompt via het veneuze micro vasculaire netwerk in het hart²⁷. Om de retentie van medicatie in het hart te vergroten wordt het gebruik van injecteerbare hydrogels veel onderzocht, alleen het blijft onduidelijk of deze wel zorgen voor een verhoogde retentie omdat er enkel wordt gekeken naar functioneel effect^{28,29}. In **hoofdstuk 7** ontwikkelde wij een nieuwe methode om direct na de injectie de locatie en verspreiding van de hydrogel te kunnen bepalen. Door directe labeling van de gel met radioactief-indium en visualisatie via scintigrafie is er tot vier uur na injectie bepaald waar de gel zich lokaliseert. De gel eerder gebruikt

in studies liet een vergelijkbare lage retentie van 16,9% zien terwijl het toevoegen van een extra adhesie collageengroep (RCP) de retentie verhoogde naar 26,9%. Dit hoofdstuk benadrukt dat het belangrijk is om naast functioneel effect ook te focussen op de retentie van de therapie.

Dit proefschrift voegt nieuwe inzichten toe aan het veld van hartregeneratie. De focus lag op verschillende elementen belangrijk voor hartregeneratie: Het ontwikkelen en optimaliseren van een *in vitro* humaan model van ischemisch hartziekte, het identificeren van een nieuwe factor die het hart kan beschermen tegen reperfusie schade en een factor die proliferatie van hartspiercellen kan stimuleren en het ontwerpen van een nieuwe methode om real-time lokalisatie van geïnjecteerde hydrogel te bepalen. Gebruikmakende van het werk in dit proefschrift kunnen therapieën worden getest in het geoptimaliseerde ischemisch hartziekte model en kunnen GSK'547 en FSTL1 kunnen worden getest in een varkensmodel om de laatste stap te maken voor klinische translatie. Ons onderzoek naar retentie van hydrogels na injectie in het hart benadrukt het belang van retentiestudies in de directe effectiviteit en mogelijke bijwerkingen van het medicijn. Een combinatie van cardioprotectie, hartregeneratie en verbeterde medicijnlevering en retentie op de plek van schade vormen de sleutel tot het herstel van het hart en het verbeteren van de kwaliteit van leven voor mensen na een hartinfarct.

REFERENTIES

1. Virani SS, Alonso A, Benjamin EJ, et al. *Heart Disease and Stroke Statistics—2020 Update: A Report from the American Heart Association.*; 2020.
2. Mozaffarian D, Benjamin EJ, Go AS, et al. Heart Disease and Stroke Statistics — 2016 Update A Report From the American Heart Association. *AHA Stat Updat.* 2016;38-360.
3. Townsend N, Wilson L, Bhatnagar P, Wickramasinghe K, Rayner M, Nichols M. Cardiovascular disease in Europe: Epidemiological update 2016. *Eur Heart J.* 2016;37(42):3232-3245. doi:10.1093/eurheartj/ehw334
4. Harris PA, Berger SB, Jeong JU, et al. Discovery of a First-in-Class Receptor Interacting Protein 1 (RIP1) Kinase Specific Clinical Candidate (GSK2982772) for the Treatment of Inflammatory Diseases. 1:1-42.
5. Zhu H, Sun A. Journal of Molecular and Cellular Cardiology Programmed necrosis in heart disease : Molecular mechanisms and clinical implications. 2018;116(August 2017):125-134. doi:10.1016/j.yjmcc.2018.01.018
6. Oerlemans MIFJ, Liu J, Arslan F. Inhibition of RIP1-dependent necrosis prevents adverse cardiac remodeling after myocardial ischemia – reperfusion in vivo. 2012. doi:10.1007/s00395-012-0270-8
7. Oerlemans MIFJ, Koudstaal S, Chamuleau SA, De Kleijn DP, Doevendans PA, Sluijter JPG. Targeting cell death in the reperfused heart: Pharmacological approaches for cardioprotection. *Int J Cardiol.* 2013;165(3):410-422. doi:10.1016/j.ijcard.2012.03.055
8. Koudstaal S, Oerlemans MIFJ, Spoel TIG Van Der, Janssen AWF. Necrostatin-1 alleviates reperfusion injury following acute myocardial infarction in pigs. 2014;1:150-159. doi:10.1111/eci.12391
9. Nakagawa T, Shimizu S, Watanabe T. Cyclophilin D-dependent mitochondrial permeability transition regulates some necrotic but not apoptotic cell death. 2005;434(March). doi:10.1038/nature03417.1.
10. Zhang T, Zhang Y, Cui M, et al. CaMKII is a RIP3 substrate mediating ischemia- and oxidative stress – induced myocardial necroptosis. 2016;22(2). doi:10.1038/nm.4017
11. Fang X, Wang H, Han D, et al. Ferroptosis as a target for protection against cardiomyopathy. 2019:1-9. doi:10.1073/pnas.1821022116
12. Adams D, Larman B, Oxburgh L. Developmental expression of mouse Follistatin-like

- 1 (Fstl1): Dynamic regulation during organogenesis of the kidney and lung. *Gene Expr Patterns*. 2007;7(4):491-500. doi:10.1016/j.modgep.2006.10.009
13. Prakash S, Borreguero LJJ, Sylva M, et al. Deletion of Fstl1 (Follistatin-Like 1) from the Endocardial/Endothelial Lineage Causes Mitral Valve Disease. *Arterioscler Thromb Vasc Biol*. 2017;37(9):e116-e130. doi:10.1161/ATVBAHA.117.309089
14. Wei K, Serpooshan V, Hurtado C, et al. Epicardial FSTL1 reconstitution regenerates the adult mammalian heart. *Nature*. 2015;525(7570):479-485. doi:10.1038/nature15372
15. Lara-Pezzi E, Felkin LE, Birks EJ, et al. Expression of follistatin-related genes is altered in heart failure. *Endocrinology*. 2008;149(11):5822-5827. doi:10.1210/en.2008-0151
16. Ouchi N, Oshima Y, Ohashi K, et al. Follistatin-like 1, a secreted muscle protein, promotes endothelial cell function and revascularization in ischemic tissue through a nitric-oxide synthase-dependent mechanism. *J Biol Chem*. 2008;283(47):32802-32811. doi:10.1074/jbc.M803440200
17. Shimano M, Ouchi N, Nakamura K, et al. Cardiac myocyte follistatin-like 1 functions to attenuate hypertrophy following pressure overload. *Proc Natl Acad Sci U S A*. 2011;108(43):899-906. doi:10.1073/pnas.1108559108
18. Kretzschmar K, Post Y, Bannier-Hélaouët M, et al. Profiling proliferative cells and their progeny in damaged murine hearts. *Proc Natl Acad Sci U S A*. 2018;115(52):E12245-E12254. doi:10.1073/pnas.1805829115
19. Maruyama S, Nakamura K, Papanicolaou KN, et al. Follistatin-like 1 promotes cardiac fibroblast activation and protects the heart from rupture. *EMBO Mol Med*. 2016;8(8):949-966. doi:10.15252/emmm.201506151
20. Feyen DAM, McKeithan WL, Bruyneel AAN, et al. Metabolic Maturation Media Improve Physiological Function of Human iPSC-Derived Cardiomyocytes. *Cell Rep*. 2020;32(3). doi:10.1016/j.celrep.2020.107925
21. Tao L, Bei Y, Zhou Y, Xiao J, Li X. Non-coding RNAs in cardiac regeneration. *Oncotarget*. 2015;6(40):42613-42622. doi:10.18632/oncotarget.6073
22. Yin VP, Lepilina A, Smith A, Poss KD. Regulation of zebrafish heart regeneration by miR-133. *Dev Biol*. 2012;365(2):319-327. doi:10.1016/j.ydbio.2012.02.018
23. Fish JE, Santoro MM, Morton SU, et al. miR-126 Regulates Angiogenic Signaling and Vascular Integrity. *Dev Cell*. 2008;15(2):272-284. doi:10.1016/j.devcel.2008.07.008

24. Arif M, Pandey R, Alam P, et al. MicroRNA-210-mediated proliferation, survival, and angiogenesis promote cardiac repair post myocardial infarction in rodents. *J Mol Med*. 2017;95(12):1369-1385. doi:10.1007/s00109-017-1591-8
25. Diez-Cuñado M, Wei K, Bushway PJ, et al. miRNAs that Induce Human Cardiomyocyte Proliferation Converge on the Hippo Pathway. *Cell Rep*. 2018;23(7):2168-2174. doi:10.1016/j.celrep.2018.04.049
26. Adamowicz M, Morgan CC, Haubner BJ, et al. Functionally Conserved Noncoding Regulators of Cardiomyocyte Proliferation and Regeneration in Mouse and Human. *Circ Genom Precis Med*. 2018;11(2):e001805. doi:10.1161/CIRCGEN.117.001805
27. Feyen DAM, Van Den Hoogen P, Van Laake LW, et al. Intramyocardial stem cell injection: Go(ne) with the flow Frederieke van den Akker1. *Eur Heart J*. 2017;38(3):184-186. doi:10.1093/eurheartj/ehw056
28. Ciuffreda MC, Malpasso G, Chokoza C, et al. Synthetic extracellular matrix mimic hydrogel improves efficacy of mesenchymal stromal cell therapy for ischemic cardiomyopathy. *Acta Biomater*. 2018;70:71-83. doi:10.1016/j.actbio.2018.01.005
29. Dobner S, Bezuidenhout D, Govender P, Zilla P, Davies N. A Synthetic Non-degradable Polyethylene Glycol Hydrogel Retards Adverse Post-infarct Left Ventricular Remodeling. *J Card Fail*. 2009;15(7):629-636. doi:10.1016/j.cardfail.2009.03.003

ACKNOWLEDGEMENTS

Dit proefschrift was niet mogelijk geweest zonder de ondersteuning van mijn promotieteam, mijn collega's, mijn vrienden en familie. Een aantal mensen wil ik graag in het bijzonder hieronder bedanken.

Promotieteam

Prof. Dr. Sluiter, beste **Joost**, ik wil jou ontzettend bedanken voor je openheid, betrokkenheid en alle inspirerende vergaderingen. Door het stellen van kritische vragen, het opgooien van balletjes, en het snelle leggen van connecties bracht je mij bij elke meeting weer een stuk verder op weg. Ondanks dat je zoveel mensen begeleidt, teams leidt, en veel op je bord hebt liggen, blijft je deur altijd open voor je team. Die eigenschap en je kundigheid bewonder ik enorm. Ik hoop in de toekomst nog veel van je te kunnen leren. Alles wat ik gedurende mijn PhD heb ik geleerd neem ik in ieder geval mee! Bedankt Joost!

Prof. Dr. Chamuleau, beste **Steven**, bedankt voor jou rol als promotor waarin je mij altijd steunde ondanks je drukke werkschema. Tijdens mijn PhD vertrok je naar Amsterdam voor je nieuwe baan waarin je de fusie ging leiden tussen divisie cardiologie van het VUMC en het AMC. Hierdoor werd Joost mijn eerste promotor maar bleef jij geïnteresseerd in de projecten waar we samen over gespard hebben. Tijdens onze meetings in de eerste fase van mijn PhD hebben jouw klinische blik en je overzicht mij altijd geïnspireerd om met enthousiasme onderzoek te doen. Bedankt voor je begeleiding!

Dr. Neef, dear **Klaus**, as my daily supervisor you were always there for quick questions and sparring sessions. I appreciate the way you shared your knowledge and your vision while always allowing me to develop my own style as a scientist. You taught me much in all the elements that are involved in doing research, from planning experiments to troubleshooting to data representation. I would like to thank you tremendously for the time you took to supervise me during my PhD. Thank you!

Beste Prof. Dr. Vos en Pasterkamp, **Marc** en **Gerard**, bedankt voor jullie input als aio-begeleidingscommissie. Ik heb jullie betrokkenheid erg gewaardeerd!

Leden van mijn leescommissie, **Pieter Doevendans, Jeffrey Beekman, Paula da Costa Martins, Jolanda van der Velden** en **Daniela Salvatori**, bedankt voor het zitting nemen in mijn leescommissie en het kritisch lezen van mijn proefschrift.

Lieve **Iris**, mijn paranimf, in de tijd dat ik jou heb leren kennen ben jij niet alleen een trouwe collega geweest, een luisterend oor, een sparringpartner, een geweldige analist en hulp maar ook een erg goede vriendin geworden. Alle reisjes naar London met concerten, Winter Wonderland Hyde Park en onze creatieve momentjes waar we hele wetenschappelijke projecten bedachten. Jouw hulp en vrolijke energie tijdens jouw tijd bij het RMCU gaf altijd zonneshijn aan mijn dagen en toen je wegging was dat ook zeker flink wennen. Jij hebt een erg belangrijke rol gespeeld tijdens mijn promotietraject. Ik ben ontzettend dankbaar dat jij naast mij staat bij mijn verdediging en ik had het ook niet anders voor mij gezien!

Lieve **Casper**, mijn paranimf, jij bent een echte vriend geworden tijdens onze promotietrajecten. Jij stond altijd klaar voor mij, als ik er even doorheen zat of als we gewoon allebei een Genmab-koffie/thee pauze nodig hadden. Ik waardeer al onze theetjes (nu helaas vaak Skype theetjes), etentjes, uitjes met het team, muzikale momenten dat je me meenam naar Remco in de werfkelder, wandelingen in het Gagelbos en alle mooie gesprekken.

Collega's

Beste REMAIN-consortium leden, **Eva, Patricia, Maaïke, Joep, Marta**, het was fijn om met jullie samen te werken en te leren van jullie expertise! Bedankt!

Beste Prof. Dr. Van Rooij, beste **Eva**, ik leerde je al kennen als mijn examiner tijdens mijn master stage in jouw lab waar ik mijn passie voor de moleculaire cardiologie heb gevonden. Tijdens mijn PhD heb ik met je mogen samenwerken in het REMAIN consortium en heb ik het als ontzettend fijn ervaren om bij je terecht te kunnen voor vragen en ondersteuning. Bedankt!

Beste Prof. Dr. Dankers, beste **Patricia**, bedankt voor de meetings en de sparringsessies rondom hoe we nu het beste de UPy-hydrogel konden testen in onze varkensmodellen. Het was erg fijn hoe gemakkelijk je te benaderen was voor vragen rondom plannen en het manuscript

en om gebruik te mogen maken van jouw indrukwekkende expertise.

Beste **Maaïke**, het was erg fijn om met jou samen te werken! Jij als UPy-gel expert vanaf TU Eindhoven en ik vanuit de vertaling naar grote proefdieren. Samen de handen ineen om te onderzoeken hoe we het beste de retentie van de gel konden gaan bekijken in een varkensmodel. Bedankt voor de meetings, de samenwerking met het manuscript schrijven en de gezelligheid!

Thank you to all international colleagues at the Mercola lab at Stanford University, specifically **Mark, Anna, Michelle, and Aurora**.

Dear Prof. Dr. Mercola, dear **Mark**, I am very grateful for the opportunity to work in your lab as a visiting student researcher in summer 2019. I have developed greatly as a researcher from my time in your lab, the lab meetings and the sparring session with you, **Anna** and **Pilar**. Your experience, wisdom and mentorship are truly admirable. Dear Dr. Hnatiuk, dear **Anna**, thank you for your help! Dear **Michelle**, thank you for taking me along and teaching me the iPS differentiations and maturation of the cardiomyocytes. I learned a great deal from you!

Dear **Aurora**, as the only other PhD student researcher at the Mercola lab it was great to connect with you. I appreciate how you took me along with team events and the fun we had! Thank you!

Dear **Pilar** and **Tom** of Regencor, I appreciate your help in the Delicate consortium, the meetings and your input on our experiments with FSTL1. Thank you!

Dear collaborators at Glaxo Smith Kline, **Jean-Luc, Allison**, thanks for your providing us with the GSK compound and the support with the compound preparations.

De collega's van cardiologie, **Linda, Frebus, Wouter, Steven, Timion, Thijs, Mira, Jelte, Max, Rene, Marijn, en Omayra**, bedankt voor jullie feedback en de gezelligheid!

Marish, bedankt voor je input in het GSK-project. Jouw kennis over de necroptose remming heeft ons erg geholpen tijdens de meetings! **Ingrid, Tamara, Joukje, en Ineke**, bedankt voor jullie ondersteuning vanuit het stafsecretariaat van cardiologie!

Uiteraard wil ik ook alle collega's van experimentele cardiologie bedanken! Om te beginnen **Hesther, Saskia, Suzanne, Pieter, en Zhiyong**, en voor jullie ondersteuning,

hulp en feedback. Prof. Dr. Doevendans, **Pieter**, bedankt voor je ondersteuning en de korte, doelgerichte feedback! Deze heb ik altijd erg gewaardeerd! Alle analisten van het G02 lab, in het bijzonder, **Arjan, Daniek, Hemse, Mark** voor hoe jullie er altijd waren voor hulp en het hele lab draaiende houden. **Evelyne, Marian, Emma, Patricia, Margarida, Clémence, Marieke, Nazma, Juntao, Robin, Clara**, bedankt voor alle hulp en gezelligheid! **Qiangbing**, thank you for your help with the FSTL1 plasmid prep! **Simon**, bedankt voor je hulp met de media glucose en lactaat metingen en voor alle gezelligheid bij de PhD borrels! **Michal** en **Noortje** van de sequencing faciliteit, ontzettend bedankt voor jullie hulp en flexibiliteit!

De biotechnici van proefdier groot, **Evelyn, Joyce, Marlijn, Martijn**, ontzettend bedankt voor jullie hulp bij de varkensstudie. Ik heb veel geleerd van jullie kennis. De manier waarop jullie meedenken bij alles wat komt kijken bij het opzetten van een varkensstudie heeft mij enorm geholpen! Bedankt voor alle hulp en de gezelligheid tijdens de OK dagen!

Collega's van diergeneeskunde en beeldvorming, **Jeannette** en **Anke**, bedankt voor jullie hulp bij alles wat komt kijken bij het opzetten van een studie met radioactief materiaal. Het was enorm veel werk maar zonder jullie was het nooit gelukt! **Ingrid** en **Monique**, bedankt voor alle hulp bij de SPECT! Collega's van nucleaire geneeskunde, **John, Remmert** en **Gerard**, bedankt voor jullie hulp bij het gebruik van radioactief Indium in onze varkensstudie.

Collega's van RMCU cardio, **Elise, Alain, Corina, Tom, Sandra, Jiayi, Magdalena, Vasco, Jiabin, Renee, Aoife, Aina, Nino, Christian, Laurynas, Floor, Iris, Inge** and students. You made me go to work happy every single day. The RMCU 5th floor became my second home and I feel so grateful for getting to know you! **Alain**, bedankt voor alle hulp, gezelligheid en hoe gemakkelijk het was om jou te benaderen voor vragen! **Corina**, bedankt voor de hulp en de gezelligheid als mijn eerste kamerbuddy samen met **Iris**. **Renee**, jouw werkmentaliteit en wetenschappelijke drive zijn indrukwekkend. Bedankt voor je hulp, de gezelligheid en je input! **Aoife**, thank you for your fun energy and the exciting meetings! You bring sunshine into the lab! **Aina**, you came into the lab as the second PhD student of our little team hired for the large animal part of the projects I had been working on. It was hard at the start to let my babies go but your open and feisty personality quickly made me like you a lot! I wish you all the best with your PhD and thank you so much for your input, and the fun we had! **Nino**, you have become

a good friend in a very short time. The way you come into the lab makes me smile ear-to-ear each time. Your little quirks, how you always bring food, the height of your lab chair, your self-cut hairdo, the way you are a danger on the road on your bicycle and you nearly killed me makes me like you even more. I wish you all the best and will see much more of you I'm sure! Thank you so much for being you and being my friend! **Laurynas**, thank you for helping me with the RNA isolations and qPCRs of the FSTL1 project. You took quite some work off my hands when I needed it! Your energy and joking around in the lab always made me ugly laugh! **Christian**, bedankt voor alle hulp en de gezelligheid! **Floor**, dank je voor alle goede gesprekken en de gezelligheid! Ik weet zeker dat wij elkaar nog gaan zien in de toekomst bij Jolanda of in een later stadium! Succes met je PhD! **Inge**, elke ochtend om 7 uur (of soms iets later als we niet uit bed kwamen) was jij het lichtpuntje. Hard meezingen met de radio, random geluidjes maken, zeuren over hoe druk we het hebben, de grappige momenten, ik zal ze allemaal enorm missen. Je bent goud voor het lab en onmisbaar voor zovelen. Bedankt voor je hulp, je input, en alle momenten dat je er voor me was!

The students I supervised, **Thomas, Sofia, Angela**, thanks for your help during my PhD! I am proud of how you have all grown during your internships and very grateful for your contributions to the projects (which can also be seen in the authorships of the chapters of this thesis). I wish you all the best!

Collega's van RMCU, **Joost, Anita, Diënty, Petra, Petra, Chris, Tobias, Adel, Loes, Corneliëke, Mattie, Ihsan, Elana, en Paul**. Bedankt voor de gezelligheid! **Elana**, bedankt voor alle momenten dat jij er voor me was, dat we konden sparren over het combineren van hoog niveau sport en een PhD en de smoothiebowls bij Loua! Ik weet zeker dat wij elkaar nog veel gaan zien! **Paul**, ik kon altijd bij jou terecht voor een praatje, hulp of gewoon even een theetje. Bedankt voor de gezelligheid, de hulp en het luisterend oor!

Stefan van de Hubrecht FACS faciliteit, bedankt voor al je hulp wanneer de Fortessa weer eens kuren had. Hoe druk je het ook had je nam altijd de tijd om te helpen, een praatje te maken en te brainstormen over experimentplannen. Bedankt!

Vrienden en familie

Naast al mijn geweldige collega's, heb ik veel steun ervaren aan al mijn vrienden en dierbaren tijdens mijn promotietraject. Bedankt dat jullie er altijd voor me waren terwijl ik het altijd druk had.

Lieve **Laura, Myrthe, Fleur, Lara, Marjolein**, bedankt voor jullie vriendschap. Wij kennen elkaar vanaf de middelbare school en ondanks dat wij elkaar nu minder zien is onze vriendschap nog zo sterk! Lieve **Maja** en **Kyra**, bedankt voor jullie vriendschap als mijn lieve dansvriendinnen bij DAMN, Amsterdam Dance Centre en Neva. Lieve **Elyna**, wat ben ik dankbaar dat ik jou heb leren kennen! Je bent in een korte tijd een hele goede vriendin geworden! De eer om ceremoniemeester te zijn op jouw bruiloft met **Mike** heb ik dan ook erg gewaardeerd! Dankjewel! Lieve **Keke**, elkaar teruggevonden nadat je hiphop docent op mijn dansschool was zoveel jaren terug. Nu samen dansen, filmmarathons kijken (of toch in slaap vallen?), kickboksen, lachen en huilen. Bedankt dat je er altijd voor me bent! Ik kijk uit naar de nieuwe uitdaging van het samen dansen bij Darebels! **Nina**, vanaf het moment dat jij DAMN overnam heb ik zo ontzettend veel van jou geleerd. Je creativiteit is ongelofelijk inspirerend en ik leer elke dag nog van jou!

Lieve **Lennart**, Lenbob, zoveel meegemaakt samen. Bedankt voor je steun tijdens mijn PhD. Lieve **Ed**, bedankt voor alle goede gesprekken bij de wedstrijden van **Lennart**, hoe jij mij in jullie gezin hebt verwelkomd met open armen. Lieve **Mim**, ex-schone mams, bedankt voor je warmte, je goede zorgen, alle slimme trucjes, de bananenplant, en je liefde. Ik ben ontzettend dankbaar dat ik jullie heb mogen leren kennen. Lieve **Eline**, bedankt voor de fijne gesprekken en de gezelligheid!

Lieve familie, **oma knotje, Harmen, Jessie, Ivy, Bryan, Peter-Frank, Wilmie, Romy, Ilse, Andy, Doreen, Ted, Lita, opa, oma, Esther, Leon, Kim, Sanne, Bas, Carlijn, Lisan**, en **Koen**, bedankt voor jullie warmte! Lieve **opa**, bedankt voor alles wat je voor me was, hoe je trots was en me altijd stimuleerde om te streven naar excellentie. Zonder jou had ik dit pad nooit durven kiezen.

Pap en **mam**, jullie hebben mij altijd gestimuleerd het beste uit mezelf te halen. Zonder jullie had ik hier letterlijk en figuurlijk niet gestaan! So, thanks for the brains ;-)
Pap, mijn papa kan alles, maar in mijn geval is dat dan ook echt zo. Ik wilde altijd op jou lijken en

ik lijk volgens mij ook best wel op jou. Jouw wilskracht is inspirerend en jij bent een grote reden waarom ik nooit opgeef. Want jij bent mijn vader en dan moet ik het dus wel kunnen! Onze tijd in California zal ik nooit meer vergeten en jij weet wel waarom. Bedankt voor je steun en liefde. **Mam**, ik wil je ontzettend bedanken voor alle momenten dat je er voor me was, dat je naar mijn PhD gezeur hebt geluisterd en me geholpen hebt met het maken van moeilijke keuzes. Je moet soms wel wat pushen om bij mij binnen te komen maar je geeft niet op om met je mamagevoel bij mij te komen. Ik kan niet in woorden uitdrukken hoeveel jullie voor mij betekenen want alles lijkt te weinig. Ik hou van jullie!

Lieve **Anton, Coby, Marit** en **Robin**, bedankt voor jullie warmte en steun voor mij en voor Jord.

Anniek, sestra, jij bent mijn beste vriendin, mijn steun en toeverlaat, de Michelle to my RuPaul, de Otis to my Tekenis, de Gigi to my Ria, de Damon to my Stefan, de Lafayette to my Sookie, en de Ron to my Harry. I love you to bits!

Bram, ossebam, jij en ik zijn gesneden uit hetzelfde hout en dat schuurt soms wel eens. Maar bovenal waardeer ik wie je bent want je bent een prachtmens, met je hart van goud. Ik hou zielsveel van je!

Noodle, mijn niet-geheel-onbelangrijke-afleiding tijdens mijn computer momenten of online meetings. De beste stoorzender waar iemand voor kan wensen!

Sam, voor altijd in mijn hart, ik hou van je.

En dan lieve **Jord**, the yin to my yang. Bedankt voor je liefde, je steun en hoe je me inspireert en uitdaagt om het beste uit mezelf te halen. Je wilskracht, zelfverzekerdheid, passie, creativiteit, visie en rust gronden en inspireren mij. Ik omarm elk avontuur met jou als mijn rots en mijn golven. Ik ben elke dag dankbaar dat wij elkaar hebben gevonden. Ik hou van je!

Liefs, Marijn

LIST OF PUBLICATIONS**Published**

Lei Z.*, **Peters MC.***, Sluijter, JP., Induction of cardiomyocyte proliferation, a new way forward for true myocardial regeneration? Non-coding RNA Investig 2018

Peters MC.*, Meijs TA.*, Gathier W., Doevendans PAM., Sluijter JPG., Chamuleau SAJ., and Neef K., Follistatin-like 1 in Cardiovascular Disease and Inflammation, Mini reviews in Medicinal Chemistry, 2019

Peters MC. Sampaio-Pinto V., and da Costa Martins PA., Non-coding RNAs in endothelial cell signaling and hypoxia during cardiac regeneration, BBA Molecular Cell Research, 2019

Peters MC.*, Schotman MJG.*, Krijger GJ., van Adrichem I., de Roos R., Bemelmans JLM., Pouderoijen MJ., Rutten MGTA., Neef K., Chamuleau SAJ., Dankers PYW., in vivo retention quantification of supramolecular hydrogels engineered for cardiac delivery, Advanced Healthcare Materials, 2020

Submitted

Gladka MM.*, Johansen AKZ.*, van Kampen SJ., **Peters MC.**, Molenaar B., Versteeg D., Kooijman L., Giacca M., Van Rooij E., Thymosin- β 1 and prothymosin- α 1 promote cardiomyocyte cell division and improve cardiac function post-ischemic injury in mice, JCI, 2021

Peters MC., Maas RGC., van Adrichem I., Doevendans PA., Mercola M., Šarić T., Chamuleau SAJ., Sluijter JPG., Hnatiuk AP.*, and Neef K.*, Metabolic maturation increases human iPSC-derived cardiomyocyte susceptibility to hypoxic injury, 2021

Peters MC., Di Martino S., Boelens T., Doevendans PA, Chamuleau SAJ, Sluijter JPG.*, and Neef K.*, Follistatin-like 1 promotes proliferation of matured human cardiomyocytes and is secreted by human cardiac fibroblasts, 2021

CURRICULUM VITAE

Marijn Peters was born 28 August 1993 in Nijmegen, The Netherlands. After high school at Karel de Grote College Nijmegen, she completed her University bachelor degree in Biology at Utrecht University majoring in Animal Science with a minor in Behavioural Sciences. After her bachelor, she finished her Master's programme Biology of Disease at Utrecht University with the Cardiovascular track. During this



Master programme she spend 9 months in the laboratory of Eva van Rooij at the Hubrecht Institute to focus on cardiomyocyte proliferation and clonal expansion in mice model of myocardial infarction and 6 months in the laboratory of Joost Sluijter to study applicability of regenerative therapies in large animal models. She then continued with a PhD at the group of Steven Chamuleau at the division of Cardiology and the group of Joost Sluijter at the division of Experimental Cardiology as part of the CVON REMAIN consortium. During this period, she applied for a Hofvijvergrant and REMAIN young talent grant which enabled her to spend 1,5 months at the lab of Mark Mercola at Stanford University, California, United States of America to exchange knowledge on cardiomyocyte damage models and the use of Follistatin-like 1 as a regenerative tool. The work published in this thesis has been presented at international and national conferences.

